



HAL
open science

New catalytic systems based on carbon nanotubes supported ionic liquid phase

Laura Rodriguez Perez

► **To cite this version:**

Laura Rodriguez Perez. New catalytic systems based on carbon nanotubes supported ionic liquid phase. Coordination chemistry. Institut National Polytechnique de Toulouse - INPT, 2009. English. NNT : 2009INPT049G . tel-04400818

HAL Id: tel-04400818

<https://theses.hal.science/tel-04400818>

Submitted on 17 Jan 2024

HAL is a multi-disciplinary open access archive for the deposit and dissemination of scientific research documents, whether they are published or not. The documents may come from teaching and research institutions in France or abroad, or from public or private research centers.

L'archive ouverte pluridisciplinaire **HAL**, est destinée au dépôt et à la diffusion de documents scientifiques de niveau recherche, publiés ou non, émanant des établissements d'enseignement et de recherche français ou étrangers, des laboratoires publics ou privés.



THÈSE

En vue de l'obtention du

DOCTORAT DE L'UNIVERSITÉ DE TOULOUSE

Délivré par *l'Institut National Polytechnique de Toulouse*
Discipline ou spécialité : *Chimie Organométallique et de Coordination*

Présentée et soutenue par *Laura RODRIGUEZ PEREZ*
Le 14 décembre 2009

Titre : *New catalytic systems based on carbon nanotubes supported ionic liquid phase*

JURY

Anna MASDEU
Hélène OLIVIER-BOURBIGOU
Alain ROUCOUX
Jean-Christophe PLAQUEVENT
Philippe KALCK
Montserrat GOMEZ
Philippe SERP

Ecole doctorale : *Sciences de la Matière*

Unité de recherche : *Laboratoire de Chimie de Coordination (LCC); Laboratoire Hétérochimie
Fondamentale et Appliquée (HFA)*

Directeur(s) de Thèse : *Philippe SERP-Montserrat GOMEZ*

Rapporteurs : *Anna MASDEU-Hélène OLIVIER-BOURBIGOU*

AUTEUR: RODRIGUEZ PEREZ Laura

DIRECTEURS DE THESE: SERP Philippe and GOMEZ Montserrat.

TITRE: «Nouveaux systèmes catalytiques en phase liquide ionique supportée sur nanotubes de carbone».

RESUME:

Récemment, les liquides ioniques ont attiré l'attention de la communauté scientifique de la catalyse homogène en tant que solvants répondant aux principes de la chimie verte. De par leur nature chargée, ces phases ioniques sont idéales pour des réactions biphasiques avec des substrats organiques et permettent une récupération facile du catalyseur. Leur caractère ionique leur confère une organisation spatiale à l'échelle nanométrique permettant des phénomènes de solvations particuliers et une réactivité spécifique. Néanmoins, ces solvants continuent à être onéreux et les supporter peut permettre à la fois de réduire de façon significative les quantités utilisées et de récupérer facilement le catalyseur immobilisé dans la phase liquide ionique.

Jusqu'à présent, la catalyse supportée sur liquides ioniques a mis en jeu des supports oxydes mésoporeux classiques comme la silice. Au cours de cette thèse, une étude comparative entre ces types de supports et des nanotubes de carbone multiparois a été réalisée pour différentes réactions catalytiques. Les nanotubes de carbone présentent une macrostructure très ouverte avec une mésoporosité importante. Ainsi, la limitation par transfert de masse dans la porosité du support est diminuée et la cinétique de la réaction, augmentée. Une première étape de fonctionnalisation des nanotubes de carbone a permis d'améliorer la compatibilité avec la phase liquide ionique. L'immobilisation stabilise le catalyseur (complexe métallique $[\text{Rh}(\text{nbd})(\text{PPh}_3)_2][\text{PF}_6]$ ou nanoparticules de palladium) dans la phase liquide ionique après formation d'un film autour des nanotubes. Les systèmes catalytiques supportés ont été utilisés pour différentes réactions tests : l'hydrogénation, le couplage C-C de Heck et la réaction séquentielle Heck/hydrogénation.

Des composites supports oxydes (SiO_2 ou Al_2O_3)/liquide ionique ont été préparés afin d'étudier les interactions spécifiques liquide ionique-surface et les comparer avec le liquide ionique pur.

MOTS CLES: Liquide ionique / Nanotubes de carbone / Catalyse en phase liquide ionique supportée / Complexes / Rhodium / Nanoparticules / Palladium / Hydrogénation / Couplage C-C de Heck / Réactions séquentielles.

AUTHOR: RODRIGUEZ PEREZ Laura

PhD SUPERVISORS: SERP Philippe and GOMEZ Montserrat.

TITLE: «New catalytic systems based on carbon nanotubes supported ionic liquid phase».

SUMMARY:

As catalytic support, carbon nanotubes present an open macrostructure with large mesoporosity which avoids mass transfer limitations. Ionic Liquids (ILs) have received much attention in the past years due to their importance in a broad range of applications. In catalysis, they are used to immobilize the catalyst in biphasic reactions and enable an easy separation. Their ionic character confers to these media a special organization of several nanometers that induces solvation phenomena and specific reactivity that can be linked either to confinement effects in the organized structure or to molecular interactions. However, these solvents remain expensive and the fact to support them onto carbon nanotubes as a thin film should permit to reduce significantly the volumes used.

In this PhD thesis in order to prepare carbon nanotubes-IL hybrid materials, multi-walled carbon nanotubes were covalently modified with imidazolium salt-based moieties. This functionalization allowed specific interactions between the IL thin film and the chemical moieties on the MWCNTs surface. Then, the catalyst (rhodium complex or palladium nanoparticles) was immobilized into the IL thin film. The catalytic performances have been evaluated in bench reactions: hydrogenation of 1-hexene for rhodium, and selective hydrogenation, Heck, and sequential Heck/hydrogenation process for palladium. Finally, a comparative study has been performed between carbon nanotubes and other classical mesoporous oxide supports, including silica. The carbon nanotubes based catalyst present better performances than their counterparts prepared on conventional supports.

Additionally, composites based on SiO₂/IL or Al₂O₃/IL were prepared to carry out a structural study with the aim of understanding their specific surface interactions and compare them to pure ionic liquid.

KEY WORDS: Ionic liquid / Multi-walled carbon nanotubes / Supported ionic liquid phase catalysis / Complexes / Rhodium / Nanoparticles / Palladium / Hydrogenation / C-C Heck coupling / Sequential reactions.

TABLE OF CONTENTS

GLOSSARY.....	9
INTRODUCTION AND OBJECTIVES	13
1 BIBLIOGRAPHIC INTRODUCTION.....	17
1.1 Supported ionic liquid phase catalysts: preparation and characterization.....	21
1.1.1 Supports involved in SILPC.....	22
1.1.2 Ionic Liquids used in supported ionic liquid phase catalysis.....	32
1.1.3 Nature of the catalyst involved in SILPC.....	34
1.1.3.1 Immobilized IL as catalyst.....	34
1.1.3.2 Metal complexes immobilization.....	36
1.1.3.3 Metal nanoparticles.....	37
1.2 Supported ionic liquid phase catalysis: Applications.....	41
1.2.1 Alkylation reactions.....	41
1.2.2 Hydroformylation reaction.....	42
1.2.3 Hydroamination reactions.....	43
1.2.4 Hydrogenation reactions.....	45
1.2.5 Carbonylation reactions.....	49
1.2.6 C-C coupling reactions.....	49
1.2.6.1 Suzuki-Miyaura cross-coupling.....	49
1.2.6.2 Heck reaction.....	51
1.2.6.3 Aldol condensations.....	52
1.2.7 Oxidation reactions.....	52
1.2.8 Cyclopropanation reactions.....	54
1.2.9 Phase transfer reactions.....	55
1.2.10 Carbon dioxide fixation reactions.....	55
1.2.11 Other reactions.....	56
1.3 Structured reactors: monolithes, membranes, fibers, fixed bed	58
1.4 Conclusion.....	59
2 MULTI-WALLED CARBON NANOTUBES SURFACE MODIFICATION	71
2.1 Carbon nanotubes: generalities and history	71
2.1.1 Structure of carbon nanotubes.....	71
2.1.1.1 Single-walled carbon nanotubes.....	72
2.1.1.2 Multi-walled carbon nanotubes.....	73

2.1.2	Synthesis of CNTs.....	74
2.1.2.1	Arc discharge	74
2.1.2.2	Laser ablation.....	74
2.1.2.3	Chemical vapour deposition (CVD)	74
2.1.3	Properties.....	75
2.1.3.1	Physical properties	75
2.1.3.2	Chemical properties	77
2.1.4	Potential and current applications.....	80
2.2	Results and discussion.....	81
2.2.1	Surface activation of multi-walled carbon nanotubes.....	82
2.2.1.1	Synthesis	82
2.2.1.2	Characterization	82
2.2.2	Surface functionalization of multi-walled carbon nanotubes	84
2.2.2.1	Covalent approach	84
2.2.2.1.1	Synthesis.....	84
2.2.2.1.2	Characterization.....	86
2.2.2.2	Ionic approach.....	89
3	SUPPORTED IONIC LIQUID CATALYTIC PHASE: PREPARATION AND CHARACTERIZATION	99
3.1	Immobilization of a homogeneous catalysts.....	99
3.2	Immobilization of heterogeneous catalysts	101
3.2.1	Palladium nanoparticles: generalities and history	101
3.2.1.1	Synthesis, stabilization and applications.....	102
3.2.2	Metal nanoparticles synthesized in ionic liquid medium.....	103
3.2.2.1	Synthesis of Pd nanoparticles	104
3.2.2.2	Nanoparticles from Pd(II) precursor	104
3.2.2.3	Nanoparticles from Pd(0) precursor.....	105
3.2.3	Synthesis of heterogeneous supported ionic liquid phase catalyst	108
3.3	Characterization of supported IL composites	112
3.4	Structural study of the interactions between the support and the ionic liquid	116
3.4.1	DSC analysis	117
3.4.2	XRD analysis.....	118
3.4.3	NMR analysis	120
3.4.4	Ionic Liquid surface mediated distillation	126
4	SUPPORTED IONIC LIQUID PHASE: APPLICATIONS IN CATALYSIS ...	135
4.1	homogeneous supported ionic liquid phase catalysis: applications in hydrogenation	135
4.1.1	Results and discussion.....	136

4.2	Heterogeneous supported ionic liquid phase catalysis: applications in Heck C-C coupling and selective hydrogenation.....	142
4.2.1	Hydrogenation reactions.....	145
4.2.1.1	Results and discussion	145
4.2.2	C-C cross coupling reactions.....	150
4.2.2.1	Introduction.....	150
4.2.2.2	General remarks.....	150
4.2.2.2.1	C-C cross-coupling reactions in ionic liquids and in supported catalytic liquid phase	153
4.2.2.3	Results and discussion	154
4.2.3	Sequential reactions.....	156
4.2.3.1	Results and discussion	157
5	EXPERIMENTAL SECTION.....	167
5.1	General aspects.....	167
5.2	Characterization techniques.....	168
5.2.1	Nuclear magnetic resonance spectroscopy	168
5.2.2	Infrared spectroscopy	168
5.2.3	Mass spectrometry.....	168
5.2.4	Elemental analysis.....	169
5.2.5	Differential scanning calorimetry.....	169
5.2.6	Thermogravimetric analysis	169
5.2.7	X-ray diffraction.....	169
5.2.8	Transmission electron microscopy	169
5.2.9	Gas chromatography.....	170
5.2.10	X-ray Photoelectron Spectroscopy	170
5.2.11	Raman spectroscopy	171
5.2.12	Porosimetry and specific surface area	171
5.2.13	Thermal programme desorption.....	171
5.3	Multi-walled carbon nanotubes functionalization.....	171
5.3.1	MWCNTs purification.....	171
5.3.2	MWCNTs activation	171
5.3.3	Ionic functionalization of the MWCNTs surface: CNT2-CNT9	172
5.3.3.1	Covalent approach (CNT2-CNT8).....	172
5.3.3.2	Ionic approach.....	174
5.4	Synthesis of metallic nanoparticles in ionic liquid.....	174
5.5	Synthesis of supported ionic liquid phase.....	174
5.5.1	Immobilization of $[\text{Rh}(\text{nbd})(\text{PPh}_3)_2]\text{PF}_6$ over a SILPC	175
5.5.2	Immobilization of PdNP over a SILPC	175

5.6	Distillation procedures	176
5.7	Catalytic procedures	176
5.7.1	General procedure for hydrogenation reaction using the complex $[\text{Rh}(\text{nbd})(\text{PPh}_3)_2]\text{PF}_6$ as catalytic precursor	177
5.7.2	General procedure for hydrogenation reaction using preformed nanoparticles as SILPC	177
5.7.3	General procedure for Heck coupling reaction using preformed nanoparticles as SILPC	178
5.7.4	General procedure for catalytic sequential Heck/hydrogenation procedure using preformed nanoparticles as SILPC.....	178
6	CONCLUSIONS	183
7	RÉSUMÉ	187
7.1	Introduction et objectifs	189
7.2	Modification de la surface des nanotubes de carbone multi-parois	192
7.2.1	Discussion des résultats	194
7.3	Catalyseur en phase liquide ionique supportée : Preparation et caracterisation	198
7.3.1	Immobilisation d'un catalyseur homogène.....	198
7.3.2	Immobilisation d'un catalyseur hétérogène.....	199
7.3.3	Caractérisation des composites liquide ionique supportée	204
7.3.4	Etude structurale des interactions entre le support et le liquide ionique.....	206
7.4	Phase liquide ionique supportée : Application en catalyse	207
7.5	Conclusions	211

GLOSSARY

AA	Acetic acid
Acac	Acetylacetonate
AC	Active Carbon
ACC	Active Carbon Clothe
AIBN	Azobisisobutyronitrile
Am	Maleic anhydride
ATG	Thermogravimetical analysis
BET	Physical adsorption isotherm
BINAP	2,2'-bis(diphenylphosphino)-1,1'-binaphthyl
Bmim	Butyl methyl imidazolium
CNFs	Carbon nanoFibers
CNT	Carbon nanotubes
Cod	Cyclooctadinen
Cot	Cyclooctatriene
CP/MAS NMR	Cross polarization of nuclear magnetic resonance
CVD	Chemical vapour deposition
Dbp	Dibenzylidene cetone
Dppf	1,1'-bis-(diphenylphosphino)-ferrocene
DP/MAS NMR	Direct polarization of nuclear magnetic resonance
DSC	Differential scanning calorimetry
EDX	Energy dispersive X-ray spectroscopy
<i>ee</i>	Enantiomeric excess
Emim	1-ethyl-3-methylimidazolium
FFT	Fast fourier transform
FTIR	Rourier transformade infra red

GC	Gas chromatography
GPa	Giga pascal
Hmim	1-n-hexyl-3-methylimidazolium
HREM	High resolution transition electron microscopy
IS	Ion spray
ICP	Inductively coupled plasma
ILs	Ionic liquids
IR	Infrared
MWCNTs	Multi walled carbon nanotubes
Nbd	Norbornadiene
NDEAP	Diethylaminopropylated alumina
NHC	NHC=N-heterocyclic carbene
NMP	N-methylpyrrolidone
NMR	Nuclear magnetic resonance
NPs	Metallic nanoparticles
PdNPs	Palladium metallic nanoparticles
PEG	Poly(ethyleneglycol)
PGE	Phenyl glycidyl ether
PS-DVB	Polystyrene–divinylbenzene
Psmim	Polystyrene-methylimidazolium
salen	N,N'-bis(salicylaldehyde)-ethylenediimine
SAP	Supported aqueous phase.
SAPC	Supported aqueous phase catalysis
SAXS	Small angle X-ray scattering
<i>sc</i>	Supercritical
SEM	Scanning electron microscope
SILCP	Supported ionic liquid catalytic phase
SILM	Supported ionic liquid membranes

SILP	Supported ionic liquid phase
SLPC	Supported liquid phase catalyst
SMF	Synthetic metal fibers
SWCNTs	Single walled carbon nanotubes
TEM	Transition electron microscope
(TESP)mim	N-3-(3-triethoxysilylpropyl)-3methyl imidazolium
TFA	Trifluoroacetic acid
TGA	Thermogravimetry analysis
TGA-DSC	Thermogravimetric analysis-differential scanning calorimetry
THF	Tetrahydrofurane
TMGL	1,1,3,3-tetramethylguanidinium lactate
TOF	Turnover frequencies
TPD	Temperature programme desorption
VOCs	Volatile organic compounds
XPS	X-ray photoelectron spectroscopy
XRD	X-ray diffraction

INTRODUCTION AND OBJECTIVES

The research of low cost and environmentally benign catalytic systems has become one of the main subjects of modern synthetic chemistry. In this context, developments of highly active and selective catalysts are of prime importance. Heterogeneous catalysis is preferred in industrial processes compared to homogeneous catalysis because the extraction of the product and recoveries of the catalyst are relatively easier using heterogeneous systems. However, in various examples of heterogeneous catalysis, mass or heat transfer limitations in the solid catalyst may lead to an activity decrease and lower chemo- and stereo-selectivities in relation to homogeneous catalysis. Therefore, a catalytic system, which takes the advantages of both homogeneous and heterogeneous catalysis (i.e. good activity, high selectivity, easy extraction of the product and recovery of the catalyst) would greatly enhance the interest for catalytic industrial applications.

In this context, the concept of supported ionic liquid phase catalysis (SILPC) has gained much attention. The grafting of imidazolium onto a solid surface not only favours the heterogenization of expensive ionic liquids (ILs), but also offers a lot of opportunities to investigate immobilizations of homogeneous metal complexes or metal nanoparticles. Moreover, functionalized ILs recycling by this method is also possible. On the other hand, carbon nanotubes (CNTs) as catalytic support present a very open macrostructure with large mesoporosity, avoiding mass transfer limitations in catalytic reactions; thus, the use of carbon nanotubes should offer significant advantages to the supported ionic liquid phase catalysis (SILPC). Moreover, a surface functionalization should allow specific interactions between the ionic liquid film and chemical moieties covalently anchored on the nanotubes surface.

In the past two decades, metal nanoparticles have triggered an enormous interest in catalysis due to their frontier behaviour between classical homogeneous and heterogeneous catalysts. Consequently, they can lead to new reactivity trends obtaining target compounds for medical, pharmaceutical or agrochemical purposes. In spite of promising results, from a synthesis point of view, the use of solid catalysts is still preferred because of the inherent convenience for work-up procedure. In this respect, a new strategy has been developed, that is, the preparation of solid-supported metal nanoparticles using ILs. In this case, the IL acting as a stabilizer, also plays a crucial role for the catalyst immobilization.

The combination of an ionic liquid with a solid support is applied for chromatography, supported liquid membranes and for some electrochemical applications, in addition to the SILP catalysis. The physico-chemical characteristics of the corresponding composites depend on the support-ionic liquid interactions.

In this context, the objectives of this PhD thesis could be summarized as followed:

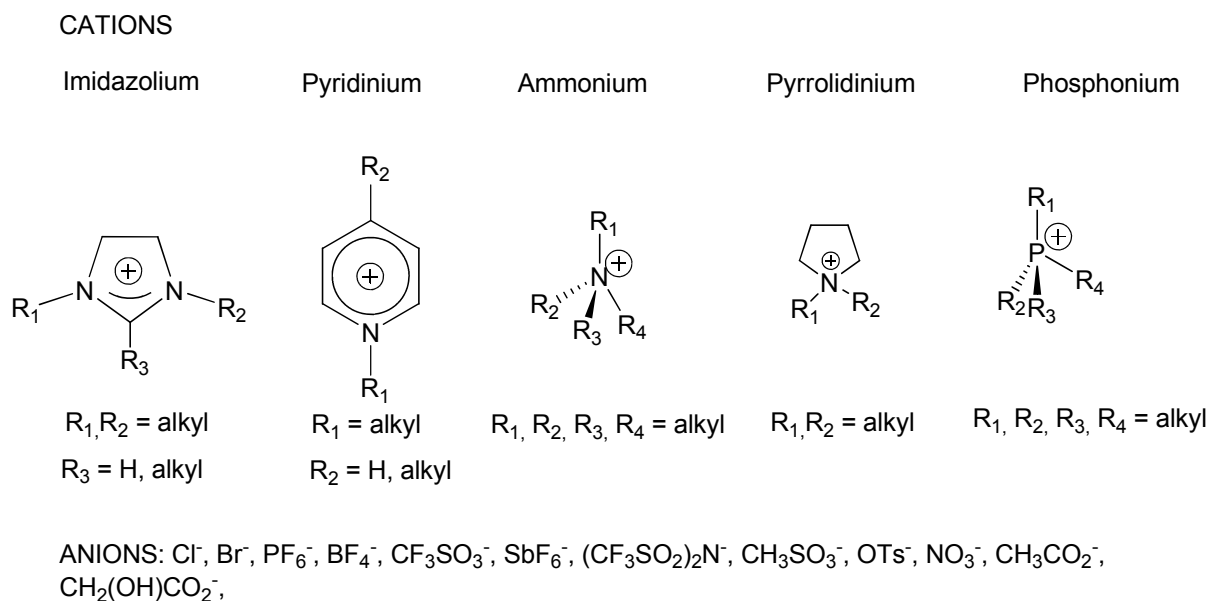
- The effective functionalization and characterization of multi-walled carbon nanotubes (MWCNTs) containing ionic moieties, and the study of their affinity for the ionic liquid medium.
- A structural study of the interactions between support and ionic liquid, including a full multi-nuclear NMR study at solid state.
- The synthesis and characterization of palladium nanoparticles starting from different metallic precursors, with or without the presence of a stabilizing ligand in different ionic liquids.
- The synthesis and characterization of supported ionic liquid phase catalysts based on functionalized MWCNTs using a Rh complex or metallic nanoparticles as catalytic active phase.
- The application of the supported ionic liquid phase catalyst in hydrogenation reactions with Rh as catalytic active phase, studying: the influence of the nature of the support, the efficiency of MWCNTs functionalization, the optimization of the ionic liquid film thickness and the recycling of the system.
- The application of SILPC with palladium nanoparticles in selective hydrogenation, Heck C-C coupling and Heck coupling/hydrogenation sequential process, studying: the palladium precursor influence, the influence of the ligand, the influence of the different ionic liquids involved and the support on the nanoparticles catalytic behaviour.

CHAPTER I

Bibliographic introduction

1 BIBLIOGRAPHIC INTRODUCTION

In the last fifteen years, ionic liquids (ILs) have gained a wide popularity from the scientific community as innovative and environmentally friendly reaction medium.^{1,2} From a chemical point of view, they are constituted of organic cations and inorganic or organic anions. For applications as solvent, the most interesting ILs are those showing low melting points, typically below room temperature, and high thermal stability.³ The melting point for a given anion-cation combination remains difficult to rationalize. However, some trends seem to emerge. Therefore, the charge delocalization over several atoms and the low symmetry showed by the cation and / or anion favour the formation of salts exhibiting low melting points.⁴ Nowadays, the 1,3-disubstituted imidazolium, pyridinium, pyrrolidinium, ammonium and phosphonium moieties are the most frequently encountered type of cation. The most common anions are $[\text{PF}_6]^-$, $[\text{BF}_4]^-$, $[\text{CF}_3\text{SO}_3]^-$, and $[(\text{CF}_3\text{SO}_2)_2\text{N}]^-$ (Scheme 1.1).



Scheme 1.1: Typical cations and anions used in ILs

These molten salts have peculiar physical properties⁴ such as:

- Low vapour pressure. ILs could be a good and green alternative to organic solvents avoiding the emission of volatile organic compounds (VOCs) in the atmosphere.
- Tunable polarities. They have the capacity to dissolved metal catalysts (salts or complexes), organic compounds, as well as gases and enzymes. Moreover, they are immiscible with many organic solvents which lead to biphasic systems.

- Thermal stability. The melting point of common ILs is below room temperature, and the decomposition temperatures are generally found at more than 250°C, offering the possibility to use them in a large variety of chemical reactions.
- Wide electrochemical window is shown by ammonium or phosphonium ionic liquids.
- Electrical conductivity and ionic stability. These properties were firstly explored for electrochemical applications and in electronic adsorption spectroscopy.
- Low toxicity for human health was reported. However the biodegradability and aquatic toxicity needs to be improved.

These properties make ILs good solvents for organic and inorganic synthesis^{1,5,6} and particularly for catalysis applications.^{2,7,4}

Concerning the inorganic synthesis the apparition of ILs has opened new lines of investigation. The reaction medium for the production of inorganic materials is usually organic solvents, aqueous systems, or gas phase.⁸ The introduction of ILs in those processes opened the way to produce new materials with different properties and structures. ILs act not only as template for the structures but they also stabilized them.⁹

For homogeneous metal-catalyzed organic processes, the separation of the products from the reaction mixture and the recovery of the catalyst constitute an important issue. Moreover, environmental constraints have become more stringent and require new solvent and processes.¹⁰ In this context, ILs appear as a green alternative to the classical homogeneous catalysis. They are used in biphasic processes as reaction solvent, or immobilizing phase on a support for transition metal catalysts or as organic catalyst.¹¹

As solvents for catalytic reactions ionic liquids have been widely used due to their polar properties. They can interact with the solute via dipolar interactions and dispersion forces and act as strong hydrogen bond bases. Not surprisingly, ILs can have presents π - π interactions with aromatic compounds.⁷ The solubility of reactive gases such as H₂, CO and O₂ in ILs, important in many catalyzed reactions, depends mainly on the ILs anion. It follows the trend: CO₂>>>C₂H₄≈CH₄>O₂>CO>H₂.^{12,13}

Taking into account their structures, ILs can be considered as polymeric superstructures stabilized by hydrogen bonds between the cations and the anions as illustrated by X-ray diffraction (XRD) structures studies.¹⁴ Therefore they can induce particular reactivity, for example in enantioselective catalysis.¹⁵ In the literature, a great number of examples using ILs as catalytic solvent can be found.⁴ The right choice of the catalyst and appropriate ionic liquid lead to high turnover frequencies and high catalyst recovery allowing its recycling.⁷

The immobilization of the catalyst in ILs is a useful strategy for recycling. Catalysts, especially cationic catalysts, remain in the ionic liquid phase upon product separation.¹⁶ Ionic liquids can also act as nanoparticles stabilizers. Even though the stabilization mechanism has not been proved, ILs seems to create an electrostatic and steric barrier between the nanoparticles,¹⁷ a stabilization type DLVO (Derjaugin-Landau-Verwey-Overbeek) has been proposed due to their polymeric structure.¹⁸ This suggestion has been corroborated by a number of analysis of these systems, HREM (High Resolution transition Electron Microscopy) showing IL-metal surface interactions,^{19,20} SAXS (Small Angle X-ray Scattering) indicating a protective layer of ionic cells around Pt and Ir nanoparticles^{19,21} and XPS (X-ray Photoelectron Spectroscopy) detecting fluor, carbon and oxygen at the surface of clusters stabilized by [bmim][BF₄] and [bmim][PF₆] (bmim: 1-n-Butyl 3-Methylimidazolium cation).^{19,21,22}

In many processes carried out in ionic liquids, these molten salts can be used simultaneously as catalyst and solvent. Chloroaluminate (III) ionic liquids allow from moderate to high yields for electrophilic substitutions and condensation reactions.²³ The adjustable nature of the Lewis acidity for those systems made them very attractive.²⁴ Unfortunately, this concept suffers many disadvantages such as their sensitivity towards H₂O and O₂ and the difficulty to separate them from product containing heteroatoms.⁷ Recent developments in organocatalysis have shown that some reactions can be advantageously performed in ILs through hydrogen bonding interactions, particularly Diels–Alder cyclo-additions and their derivatives.²⁵

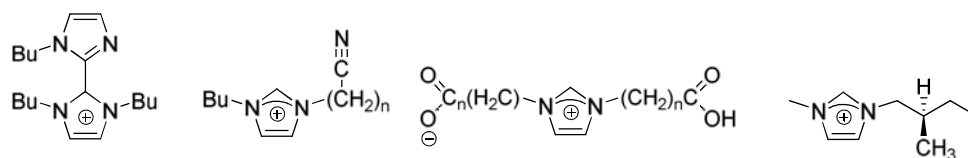
However, ILs present different drawbacks when applied in catalysis as reaction medium.

- For example, when different batches of ILs are used, the reaction yield and selectivity can vary due to the presence of impurities such as halides, and organic compounds of low volatility.²⁶ The halides contamination has been overcome with the uses of “halide free” synthesis methods of ionic liquids.²⁷
- Although ILs are usually regarded as “green solvents” it is not yet absolutely clear as many toxicological studies are still debatable.²⁸ The lack of data about biodegradability and potential toxicity of waste ILs at the end of their life cycle is a potential problem for their application.²⁹
- The use of large ILs amounts when it is used as solvent. From economical standpoint, even if being commercially available today, they remain expensive products.

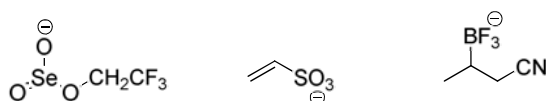
- Very pure ILs are needed to minimize the effects of impurities, and this induces heavy purification processes.³⁰
- The use of immiscible organic solvents for catalysts separation and recycling can solubilise little amounts of the ILs and the catalyst and reduce the recycling yields.
- Relatively high viscosity. The reaction that proceeds in the inter-phase or in the diffusion layer of the catalyst can be slowed down due to slow diffusion of the substrates.

The prospect to design ionic liquids (“Task ionic liquids”),³¹ by introducing functional groups to confer specific chemical properties may be the solution to overcome the limits of ionic liquids in catalysis. The imidazolium cation unit is largely used to introduce functional groups such as alcohols,³² carboxylic acids,³³ thiols,³⁴ alkynes,³⁵ alkenes,³⁶ dienes,³⁷ fluorinated chains³⁸ and chiral moieties.³⁹ Some examples of different task ionic liquids cations and anions are shown in Scheme 1.2. Less developed than functionalized cations, some functionalized anions are also shown in Scheme 1.2. The presence of a functional group may improve the catalytic reaction in all, or in one of the following aspects: favouring the activation of the catalyst, generating new catalytic species, increasing the catalyst stability and optimizing the immobilization and thus the recyclability. The task IL should stay inert with respect to the reaction medium. However, these ionic liquids exhibit higher viscosity than that shown by the non functionalized analogs. The viscosity can be reduced using asymmetrical functionalized anions in combination with the functionalized cations.⁴⁰ In this context one might control the chemical properties of an IL for a specific task but also adapt its physical properties.

CATIONS



ANIONS



Scheme 1.2: Different task ionic liquids cations and anions

In order to reduce the amounts of solvent used, an efficient strategy consists in supporting the ILs over different solids, leading to supported ionic liquid phases (SILP). This approach has already been applied in electrochemistry,⁴¹ chromatography,⁴² and elaboration of

materials as membranes for separation processes.⁴³ A large variety of supports has been used for these applications. In the catalysis field this concept has been applied also as supported ionic liquid phase catalysis (SILPC). The possibility to immobilize few amounts of ILs on the surface of a support material for catalysis applications has gained much attention in recent years.^{44,45} This concept seems to unify the advantages of both homogenous and heterogeneous catalysis. Coating ionic liquid onto a solid surface not only minimized the quantity of ILs used, but also offers a new concept of immobilization of organometallic complexes and metal nanoparticles on a solid surface. The prepared materials present the advantage of being a solid that facilitates the catalyst separation from the reaction mixtures.

1.1 SUPPORTED IONIC LIQUID PHASE CATALYSTS: PREPARATION AND CHARACTERIZATION

In the eighties, Scholten⁴⁶ and Hjortkjaer⁴⁷ describe the immobilization of a catalytic organic solution on a silica based solid catalyst, giving high efficiency and selectivity. But the concept became popular in 1989 when Davis and co-workers published a study in which a water soluble rhodium catalyst was immobilized on a thin film of water supported over a porous silica support (supported aqueous phase catalysis, SAPC).⁴⁸ Organic compounds are found in the organic phase and the reaction takes place in the water-organic inter-phase. The large interfacial area of the SAP catalyst and the fact that the catalyst remains on the support, leads to a highly efficient catalyst for organic transformation. The supported aqueous phase catalysis allows the heterogenization of homogeneous systems. But the supported liquid phase catalysis using organic solvents or water has not been applied with success in an industrial process. The main reason is the severe leaching of the immobilized liquid film. The mechanical forces of the continuous flow can physically remove the catalytic phase. In continuous gas-phase processes, evaporation of the liquid film from the support represents also an important drawback. Those disadvantages lead to short lifetime's catalysts. In this context, SILP catalyst can offers great advantages due to their low vapour pressure and tuneable polarities. Moreover the solvent can be retained on the support in its fluid state even at high temperatures. That makes SILP catalyst highly suitable for continuous process. The ionic liquid phase can be fixed by chemical bond between either the cation or the anion of the ionic liquid and the support, or by physisorption of the ionic liquid on the support. SILPC has been studied over a large variety of solid supports mainly oxide supports using different ionic liquids which can immobilize organometallic complexes or metal nanoparticles as catalytic

precursors. In the next section, the characterization and preparation of SILP catalysts are described, focusing on the support, the ionic liquid and the catalyst nature.

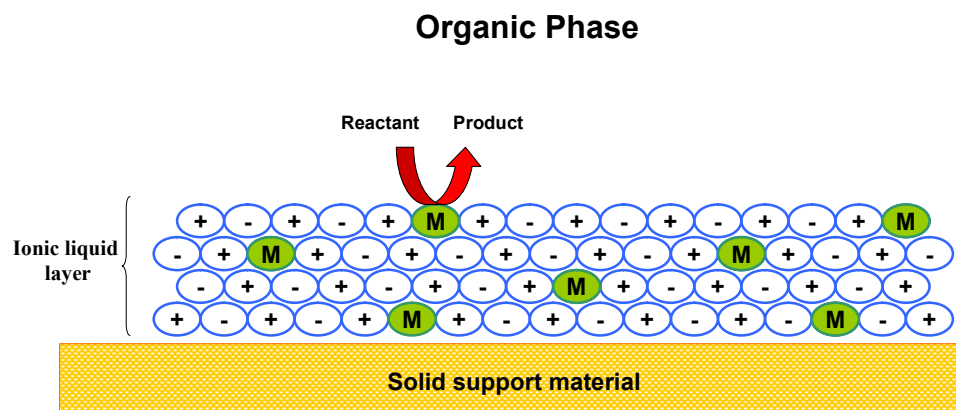


Figure 1.1: SILPC concept

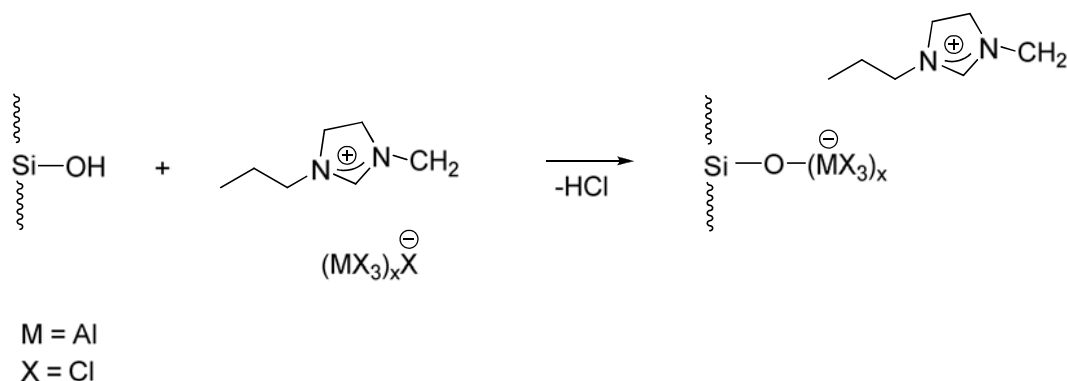
1.1.1 Supports involved in SILPC

The main supports used in SILPC are inorganic oxides, particularly silica, which has been widely studied, but also carbon based supports and organic supports such as polymers and biopolymers.

Since the apparition of SILPC, mesoporous silica gel has emerged as the most common support used. Its mesoporosity, large surface area and concentration of -OH groups on the surface as well as its low cost make silica gel the more suitable support for SILPC. Other oxide supports have been used such as MgO,⁴⁹ Al₂O₃,⁵⁰ TiO₂⁵¹ and ZrO₂.⁵¹ Active carbon,⁵² molecular sieves,⁵³ natural clays⁵⁴ and organic supports⁵⁵ have been also employed.

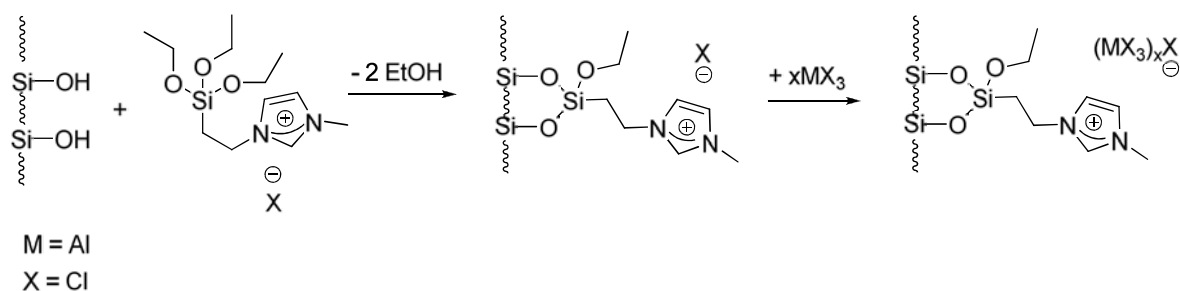
The first supported Lewis acid ionic liquid system was prepared by impregnation on a solid support surface.^{56,57} The previously dried support was treated with the minimal quantity of chloroaluminate ionic liquid (1-alkyl-3-methyl-imidazolium chloride/AlCl₃), giving a wet powder. The excess of ionic liquid was removed via Soxhlet extraction. The supports studied for this chloroaluminated catalyst were principally inorganic oxides. Mesoporous silica, acid treated montmorillonite and acid alumina were effective supports in contrast to non porous or microporous silica and neutral alumina. The treatment of these porous supports with AlCl₃ has confirmed a covalent bond between the surface and the ionic liquid.⁵⁸ The behaviour of the immobilized chloroaluminates depends on the nature of the surface. De Castro et al.⁵¹ reported the disappearance of the band at ca. 3745 cm⁻¹, assigned to the stretching vibration of the OH bond of terminal Si-OH when the chloroaluminate ionic liquid was anchored to the surface, by FT-IR analysis of SiO₂ FK700 self supported wafer. The re-appearance of this band

when removing the ILs by heat treatment at 450 °C suggests a covalent bond by the OH terminal groups with the ILs anion. A study of ^{29}Si and ^{27}Al NMR has confirmed the nature of the bonding.⁵⁹ The signals assigned to $(\text{SiO})_2\text{Si}(\text{OH})_2$ (Q_2) and $(\text{SiO})_3\text{Si}-\text{OH}$ (Q_3) groups on ^{29}Si NMR spectrum diminished in intensity after immobilization of the ionic liquid. Similar NMR analysis performed with ^{27}Al NMR showed that almost nothing of the Al_2Cl_7^- which are typical for the pure ILs, remained on the surface. Supports with lower surface area such as TiO_2 and ZrO_2 , lead to a severe leaching during the catalytic reaction resulting in low activities due to the low amount of OH groups on the surface. Moreover, X-ray diffraction analysis shows for crystalline compounds like zeolites or bidimensional silica (MCM-41) materials, a partial destruction of the surface upon reaction with chloroaluminates. The formation of hydrogen chloride during the impregnation of the chloroaluminated ionic liquids anchored via the anion is the responsible of these damages (Scheme 1.3).



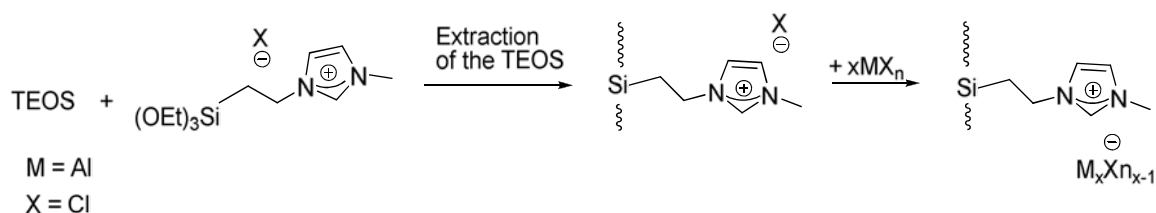
Scheme 1.3: Immobilization of an ILs on silica via the anion

The immobilization via the cation (Scheme 1.4) has been proposed to prevent the formation of HCl. Therefore, an organic anchoring group, as an imidazolium salt, was grafted on the surface and aluminium chloride was added to form the ionic complexes. NMR studies showed a strong interaction between the cation and the surface via one or two Si–O–Si bonds. This cation immobilization does not modify the crystalline structure of the silica MCM-41 support, as evidenced by X-ray diffraction analysis.⁵⁹



Scheme 1.4: Immobilization of an ILs on MCM-41 via the cation.

The formation of solid SILP catalyst by sol-gel synthesis is another approach of immobilization via the cation. The result was a solid containing 1-propyl-3-methylimidazolium chloride groups bonded to the surface silicon atoms (TEOS) from which a hexagonal mesoporous silica can be prepared (Scheme 1.5). The functionalized solid was obtained from 1-(triethoxysilylpropyl)-3-methylimidazolium chloride added to a mixture of tetraethylorthosilicate and dodecylamin. In a second step, the addition of the metal halide (AlCl_3) gave the functionalized solid (Scheme 1.5).⁶⁰ In another study, a choline hydroxide (ionic liquid = 2-hydroxyethyl)trimethylimidazolium hydroxide) was impregnated on magnesium oxide and used for aldol condensations.⁶¹

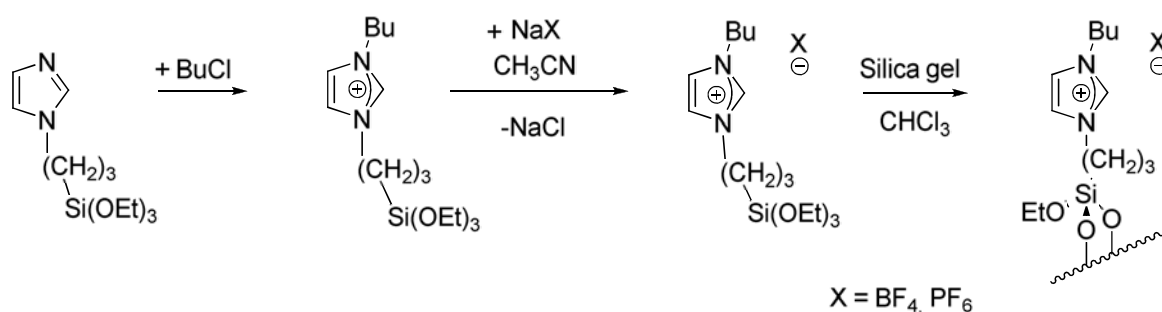


Scheme 1.5: Immobilization via the cation by a sol-gel technique.

Recently, Joni et al. reported the important leaching observed in isomerization reactions when a chloroaluminate ionic liquid is anchored to the surface via impregnation.⁶² This leaching is due to the high ionic liquid loading to obtain an acidic catalyst. They indeed reported a critical loading value of ionic liquid, necessary to observe any reactivity. They emphasized the idea of neutralization of the acid catalyst with the basic groups of the silica surface. In order to obtain an acidic catalyst without leaching, the silica support was calcinated. The chemically modified support was inactive in isomerization reactions and ready for acidic ionic liquid immobilization. TPD (temperature program desorption) of ammonia showed the disappearance of the peak related to the OH groups desorption and the appearance of another peak at high temperature indicating the acidity of the surface. Only slight leaching was observed during the reaction.

Mehnert and co-workers have reported the first example of a non acidic ionic liquid containing a rhodium-based homogeneous catalyst confined onto a heterogeneous silica gel surface.^{63,64} N-3-(3-triethoxysilylpropyl)-4,5-dihydroimidazol reacted with 1-chlorobutane to

give 1-butyl-3-(3-triethoxysilylpropyl)-4,5-dihydroimidazolium chloride (Scheme 1.6). The anion exchange was further performed using sodium tetrafluoroborate or hexafluorophosphate salts. In the immobilization step, a condensation reaction between pre-treated silica gel and the compound described above was carried out in a chloroform solution at reflux. Analysis of the surface coverage revealed *ca.* 0.4 ionic liquid fragments per nm², which corresponds to approximately 35 % of all the hydroxyl groups. Additional ILs, 1-butyl-3-methylimidazolium hexafluorophosphate ([bmim][PF₆]) or 1-butyl-3-methylimidazolium tetrafluoroborate ([bmim][BF₄]) containing the rhodium complex, was added to form the SILP catalyst. Those catalysts were used in hydroformylation and hydrogenation reactions of olefins and revealed a severe leaching when the ionic liquid concentration on the surface was over 50 %.



Scheme 1.6: Immobilization approach used by Mehnert and co-workers.^{63,64}

Riisager, Fehrmann and co-workers have prepared supported ionic liquid phase catalysts by impregnation of silica gel for hydroformylation purposes in a continuous fixed bed reactor.⁶⁵ [Rh(acac)(CO)₂], the appropriated ligand and the IL ([bmim][PF₆] or [bmim][n-C₃H₇OSO₃]) were dissolved in dry methanol. A controlled amount of silica gel was added resulting in a Rh loading of 0.2 % wt. In the literature, many examples of synthesis by impregnation via electrostatic interaction with a non acidic ionic liquid on either silica gel or aluminosilicate support (Al/MCM-41, Si/Al = 13) are described.^{66,67}

The crystalline silica MCM-41 has been reported as a suitable support for hydroformylation reactions with non acidic ionic liquids and Rh-3,3',3''-phosphinidynetris(benzenesulfonic acid) trisodium salt, P(m-C₆H₄SO₃Na)₃, (Rh-TPPTS) catalyst.⁶⁸ The ionic liquid was physisorbed on the surface by simple wet impregnation with dry methanol. Structural characterization of those Rh-SILP catalytic systems with TMGL (1,1,3,3-tetramethylguanidinium lactate) as ionic liquid have been reviewed.⁶⁹ XRD studies for different amounts of ionic liquid showed no structural changes of the MCM-41 support, the overall mesoporous hexagonal structure being maintained until 25 % wt ionic liquid loading. Nitrogen adsorption/desorption isotherms corroborated XRD results. No significant changes were observed before and after heat treatment of the supported

catalysts in toluene at 25 °C for 100 h. The loss of both pore volume and pore diameter increases with the amount of ionic liquid. The ionic liquid is dispersed in the inner walls of the mesoporous surface. SEM (Scanning Electron Microscope) images for materials up to 15 % wt ionic liquid present a smooth surface and HRTEM micrographs did not reveal remarkable differences between MCM-41 and the Rh-SILP catalyst, observing for both solids regular hexagonal arrays due to the ordered mesoporous material. These data reveal a high dispersion of the ionic liquid on the surface without modification of the solid support. Moreover, TGA-DSC (Thermogravimetric Analysis-Differential Scanning Calorimetry) for free TMGL and Rh-SILP catalyst samples showed the same temperature (227 °C) indicating no chemical transformation neither in the MCM-41 nor in the TMGL ionic liquid. Other crystalline silica supports as MCM-48 (mesoporous silica with three-dimensional channels) and SBA-15 (mesoporous silica with bi-dimensional hexagonal channels) were also recently used for SILPC.⁷⁰ Good enantiomeric excess were obtained (up to 78 % *ee*) for the acetophenone hydrogenation using ILs/MCM-48, in comparison with IL/MCM-41 (*ee* = 71 %) and for IL/SBA-15 (*ee* = 72 %). This fact might be attributed to the confinement effect of the three-dimensional channel of MCM-48 and the easy blockage of the one-dimensional channel of MCM-41 and SBA-15, which increases the diffusion resistance of the reactant to the active species in the channels.

A new concept to synthesize silica gel-immobilized ionic liquids was reported by Deng et al.⁷¹ This approach consists in physically confining an ionic liquid as [Rmim][X] (R = ethyl, butyl, decyl, cetyl; X = BF₄, PF₆) in the nanocavities of a silica gel by sol-gel methodology. The cavities act as a nanoscale reactor in which the ionic liquid behaves as catalyst or solvent. The small size of the cavities prevents the ILs leaching specially for big molecular size ionic liquids, but they are big enough to prevent mass transfer limitations. Abnormal FT-Raman spectra were observed for this silica-gel-confined ionic liquid catalysts compared to bulky ionic liquids.⁷² This behaviour was confirmed by FT-IR spectroscopy and attributed to the nano-effect (or restriction effect), as the abnormal bands on FT-Raman and FT-IR could be regulated by the particle-size of the ionic liquid (or the pore-size of the silica gel).⁷³

Microporous active carbons cloth (ACC) has been also used as support. Several ionic liquids containing a transition metal salt were dissolved in acetone. A pre-dried commercial active carbon cloth (1500 m²g⁻¹) was impregnated with the solution by capillarity. The acetone was removed in an oven at 105 °C.⁵² The structure of the applied transition metal/ACC catalyst is comparable to the SCILL (solid catalyst with ionic liquid layer) system where the solid is a real heterogeneous catalyst.⁷⁴

Recently, other carbon supports such as carbon/metal hybrid fibers have been trapped the researches interest for their application in SILPC.⁷⁵ Sintered metal fibers (SMF) show a

porosity degree up to 80–90 % with a high permeability. Their high mechanical strength, chemical and thermal stability, high conductivity and high specific surface make them suitable as supports. But, to improve the homogeneity of the ionic liquid layer on these supports, SMF were coated with carbon nano-fibbers (CNFs) and characterized by SEM. The deposition method consists in the direct growth of CNFs on the SMF by decomposition of ethane in the presence of hydrogen.⁷⁶ SILP catalyst was prepared by simple impregnation with a solution containing the ionic liquid and the rhodium homogenous catalyst in acetone (Figure 1.2). Those supports ensure the efficient use of the transition metal catalyst due to the high interface area. Moreover, their thermal conductivity avoids hot spots during exothermic hydrogenation reactions.

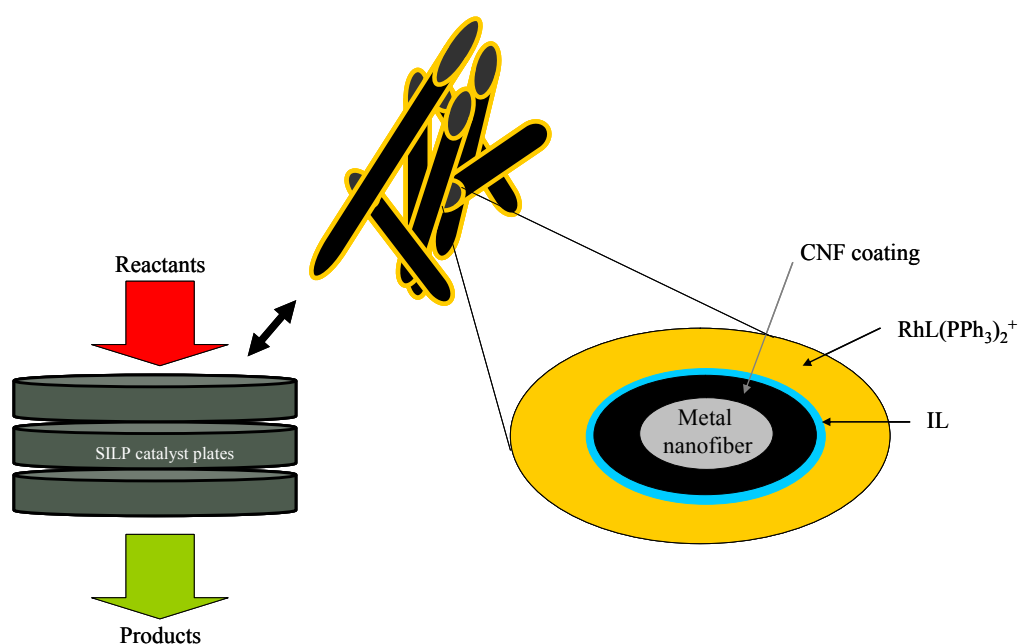


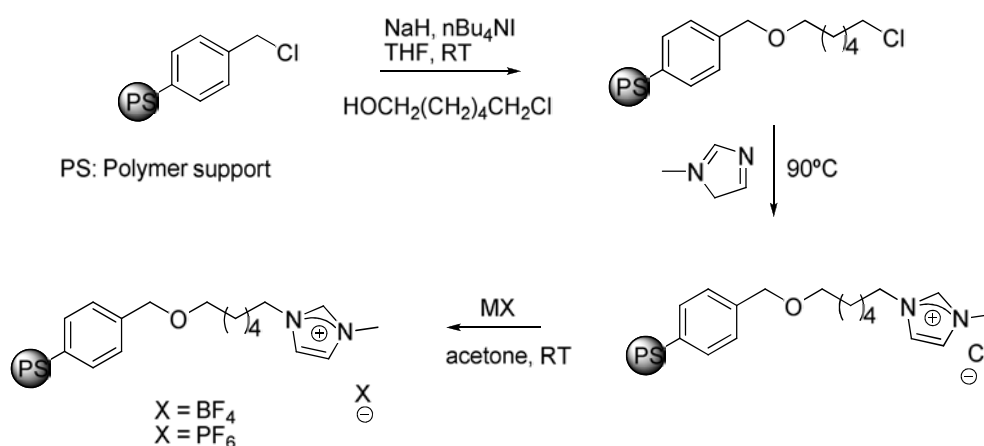
Figure 1.2: SILP catalyst combining ILs, CNFs and SMF.^{75,76}

Breitenlechner et al. used a diatomic earth (powder composed of the siliceous skeletons of diatoms, supplied by resteck: Chromosorb P, acid washed, silylated with Me_2SiCl_2) to the SILP catalysis with a homogenous catalyst immobilized in $[\text{emim}][\text{OTf}]$ (1-ethyl-3-methylimidazolium trifluoromethanesulfonate) for hydroamination reactions.⁷⁷ The diatomic earth was added to a complex solution and stirred for 5 minutes. Fast cooling followed by cold drying ensures a homogenous thin layer of ionic liquid. Diatomic earth particles from 180 to 250 μm with pores of 1 μm could be observed by SEM. An ionic liquid film of 20 nm was also observed. Mercury porosimetry studies showed a decrease on inter and intra particle pore volume and a specific surface area reduction of 66 % was observed. ^1H MAS NMR studies suggest a strong interaction between the surface and the N-C (methyl of the ethyl group) due to the lost of its free rotation.

Clays such as laponite, bentonite and K10 montmorillonite, have been also studied.⁵⁴ Laponite clay shows a lamellar structure with negative charges in the layers that can form ion pairs with ionic liquids. The free-flow powder solid is obtained by mixing the starting materials in dichloromethane, followed by drying under vacuum. The thickness of the ionic liquid film was estimated taking into account the lamellar nature of the laponite support and the measured surface area ($370 \text{ m}^2\text{g}^{-1}$) between 1.8 \AA to 10.8 \AA for different amounts of ILs. X-ray diffraction patterns of the laponite and the supported-IL film with different loading of ILs show that a part of the lamellar surface becomes accessible. It is believed that negative charges of the accessible support layers can modulate the selectivity of the catalytic process. This modulation is also due to the low mobility of the catalytic complex (prepared from CuCl, a chiral ligand and the 1-butyl-3-methylimidazolium hexafluorophosphate ionic liquid) in the thin film of ionic liquid. The authors refer to nearly two-dimensional nano-reactor behaviour with low yields but inversion of the overall selectivity reaction compared to the analogous homogeneous system.

Attapulgite, $(\text{H}_2\text{O})_4(\text{Mg,Al,Fe})_5(\text{OH})_2\text{Si}_8\text{O}_{20} \cdot 4\text{H}_2\text{O}$, formed by two bands of tetrahedral silica units connected by a continuous plane of tetrahedral basal oxygen atoms, has a dented surface leading to high surface area, moderate exchange capacity and high acidity. Attapulgite can absorb ionic liquid like TMGL to form a SILP catalyst. IR bands show the effective absorption of IL by the apparition of four peaks at 1618 cm^{-1} attributed to the stretching of C=N and at 1587 , 1650 and 1577 cm^{-1} , corresponding to -NH and -NH₂ indicating the presence of ILs. The stretching of C=N shifted to higher frequencies points to the direct coordination between the N of TMGL⁺ and the Mg²⁺ ions in the support. N₂ sorption analysis shows a decrease of the surface area from $181 \text{ m}^2/\text{g}$ in purified Atta to $164 \text{ m}^2/\text{g}$ for Attapulgite-ILs.⁷⁸

Even though inorganic materials are commonly used as support for SILPC, there are also some examples in the literature of organic materials. A polymer supported ionic liquid material [hmim][X] (hmim = 1-n-hexyl-3-methylimidazolium cation; X = BF₄, OTf) was prepared by the procedure depicted in Scheme 1.7. Its physical and chemical properties depend on the length and type of linker.⁷⁹



Scheme 1.7: Synthesis of polymer supported ionic liquid ([hmim][X])

Polystyrene-methylimidazolium [Psmim][X] ($X = \text{BF}_4^-, \text{PF}_6^-$), a polymer supported ionic liquid, was prepared by mixing the polymer and the ionic liquid (Figure 1.3).⁸⁰ A similar synthesis was previously described between poly(diallyldimethylammonium chloride) and [bmim][PF₆].⁸¹

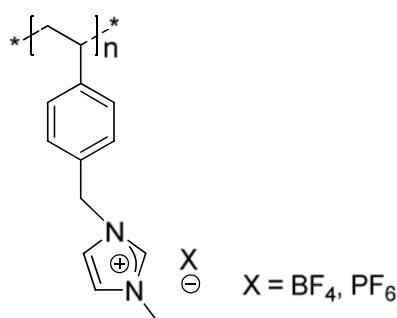
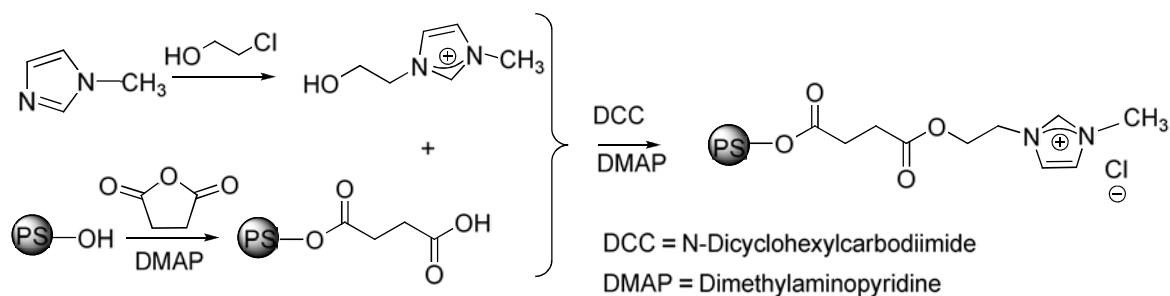


Figure 1.3: [Psmim][X], $X = \text{BF}_4^-, \text{PF}_6^-$

[PEGmim][Cl] was synthesized by anchoring the ionic liquid cation fragment to the polymer poly(ethyleneglycol) (PEG) (Scheme 1.8).⁸²



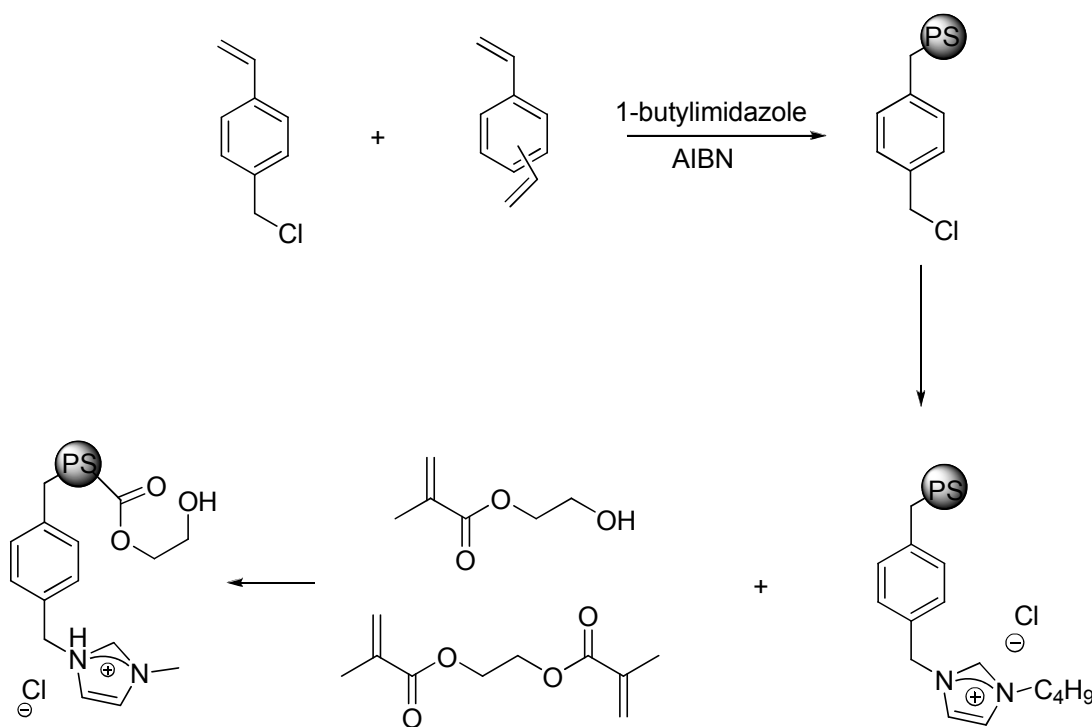
Scheme 1.8: Synthesis of [PEGmim][Cl]

Biopolymers and polysaccharides as chitosan (biopolymer derived from the shell of crustaceans) were also used as ionic liquid support. Chitosan has already been used in SAP,

because of its high sorption capacity and stabilization of metal anions (such as those coming from Pt and Pd), physical and chemical versatility and chirality.⁸³

A different approach to obtain a SILP consists in polymerizing IL monomers. Classical polymerization methodology using imidazolium monomers has been applied. A monomer/initiator mixture, with [bvim][Tf₂N] (1-Butyl-3-vinylimidazolium bis[(trifluoromethyl)sulfonyl]amide) as monomer, AIBN (2,2'-azobis(2-methylpropionitrile)) as radical initiator and [C₈(vim)₂][Tf₂N]₂ (1,1'-bis[1,8-octyl]-3-vinylimidazolium bis[(trifluoromethyl)sulfonyl]amide) as cross linker, was mixed with PVA (poly(vinylalcohol)). After thermal treatment, a dense resin was collected by filtration.⁸⁴

SILP polymeric monoliths were synthesized by covalent binding of alkyl imidazolium cations to the surface. The polystyrene–divinylbenzene (PS-DVB) resin was prepared using a solution of azobisisobutyronitrile (AIBN) in p-chloromethylstyrene, divinylbenzene, toluene, and 1-dodecanol. The subsequent alkylation with N-butylimidazole generates the SILP polymeric monolith (Scheme 1.9).⁸⁵

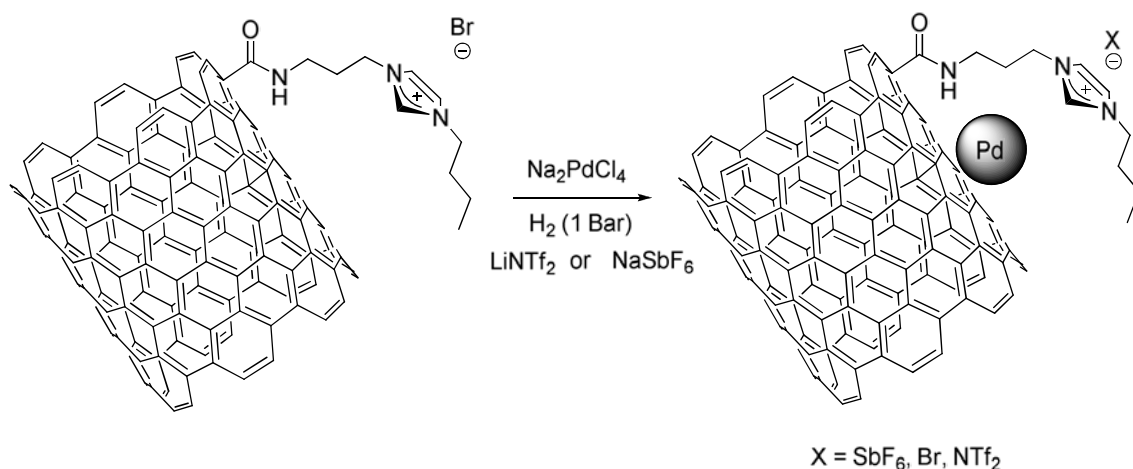


Scheme 1.9: Synthesis of SILP polymeric monolith.

FT-IR and Raman analyse of the modified monoliths show the characteristic bands of the ionic liquid and the elemental analysis indicates an ILs loading of 54.7 %wt. ILs properties are transfer to the solid phase as it can be noticed by a change in the microenvironment of the polymer monolith measured with a solvatochromic fluorescent probe. SEM images reveal a high pore size.

Supported ILs on membranes represent a different approach to prepare SILP catalyst. An air stable, room temperature ionic liquid [bmim][PF₆] and poly(vinylidene fluoride)hexafluoropropylene were copolymerized using Pd/C as catalyst.⁸⁶ Other copolymerization processes with different membrane configuration were applied in separation chemistry.⁸⁷

The functionalization of an inorganic or organic surface containing ionic liquid moieties has been carried out to give SILP catalysts. This strategy was applied with inorganic silica gel and multi-walled carbon nanotubes (MWCNTs). A thiol modified silica gel was functionalized with 1,2-dimethyl-imidazolium chloride, tetrafluoroborate or hexafluorophosphate anionic moieties, giving a monolayer of IL.⁸⁸ Those functionalized silica supports were used with and without additional ionic liquid.⁸⁹ Moreover, this catalyst can be removed from the support and replaced by fresh catalyst because it is only physisorbed. The covalent attachment of the ionic liquid decreases the specific surface area, the pore diameter and the pore volume in comparison with the unmodified silica gel. TGA analysis shows the loose of the organic part of the modified silica compounds at 400 °C, and ¹³C NMR spectra show the efficiency of the covalent attachment between the ionic liquid and the thiol linker. Lee and co-workers have functionalized MWCNTs with ionic liquid moieties. Interestingly, the change of the ionic liquid anion modulates the solubility of the nanotubes in different solvents.⁹⁰ This property makes the modified MWCNTs soluble in ionic liquid and created an IL-based catalytic system when Pd nanoparticles are immobilized on them (Scheme 1.10).⁹¹



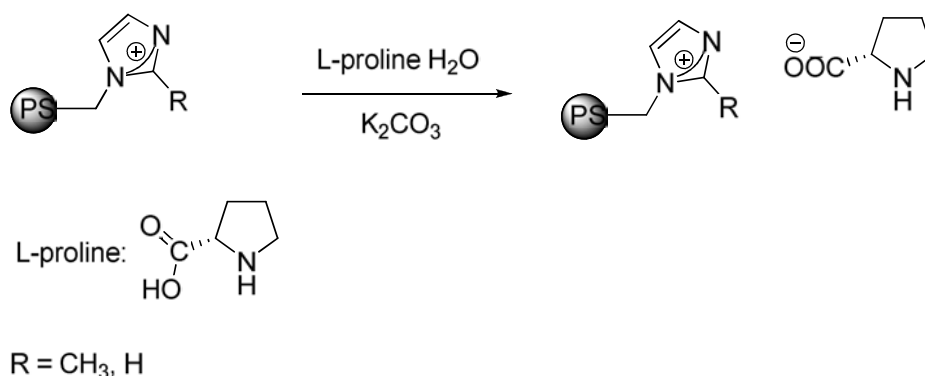
Scheme 1.10: MWCNTs-ILs catalytic system with palladium nanoparticles.

1.1.2 Ionic Liquids used in supported ionic liquid phase catalysis

In this section, the different kind of supported ILs is described: those covalently anchored on the support and those only physisorbed.

In relation to the ILs covalent anchoring, DeCastro et al.⁶⁰ have extensively studied acidic ionic liquids such as chloroaluminates ionic liquids for their application as catalyst in Friedel-Craft reaction. Chloroaluminate ionic liquid is prepared by mixing the solid Lewis acids AlCl_3 with an organic base such as a halide of imidazolium, pyridinium, sulfonium, phosphonium or ammonium salts. The acidic ionic liquid can be linked to the surface either by the anion or the cation as it has been explained earlier (section 1.1.1). The acidity of those ionic liquids can be modulated by varying the quantity of metal halide added. The control of the acidity for a wide range of values is very interesting from a catalytic point of view because the acidic strength of the catalyst can control the selectivity of some reactions. The side-chains of the ionic liquid cation can modulate the hydrophilicity or hydrophobicity of the SILP catalyst on the support. Other acidic ionic liquids are chloroferrates and chlorostanantes salts. Even though they are active in catalytic reactions, they do not react with the silanol groups when they are supported on silica, thus they experiment a severe leaching.⁹²

Ionic liquids are not always forming a layer over the solid support as can be noticed in Scheme 1.10 using MWCNTs. Ionic liquid moieties can functionalize a surface and act as linkers keeping the catalyst fixed to the support. Kume et al. reports a silica gel modified with ionic liquid moieties such as N-3-(-3-triethoxysilylepropyl)-3methyl imidazolium based ($[(\text{TESP})\text{mim}][\text{X}]$, $\text{X} = \text{Cl}, \text{NO}_3, \text{BF}_4, \text{PF}_6$) for hydrogenation reactions catalysed by palladium species. Depending on the ionic liquid anion used, the palladium precursor $\text{Pd}(\text{OAc})_2$ can exist either as palladium carbene complex ($\text{X} = \text{Cl}$) or as Pd nanoparticles (particles size in the range of 2-10 nm).⁹³ Using a similar approach, You and co-workers have prepared a novel task specific ionic liquid.⁹⁴ This novel ionic liquid was developed via anion-cation coupling of imidazolium hydroxide supported on polystyrene with L-proline. This catalyst do not need extra non-immobilized ionic liquid because it displays an efficient metal scavenging ability, which could be related to electrostatic forces and steric protection of the L-proline $-\text{COO}^-$ group and the N atom (Scheme 1.11).



Scheme 1.11: Synthesis of polymer supported task-IL.

Task specific ionic liquids containing functionalized anions (polyoxometalates and peroxometalates) were also anchored via covalent modification.^{49,95,96,97}

Neutral ionic liquids do not react with the surface because they are mainly attached by physisorption. The treatment of the surface with a substantial amount of those ILs between (5 to 50 % wt) results in the formation of a multilayer of free ionic liquid. An active catalyst can be dissolved in the inert ionic liquid phase, and act as a homogenous catalyst.^{63,64} The first ionic liquids used with this approach were 1-butyl-3-methylimidazolium hexafluorophosphate, [bmim][PF₆] or 1-butyl-3-methylimidazolium tetrafluoroborate [bmim][BF₄]. At present, those neutral ionic liquids are the more extended used. Their properties make them good solvents for metal complexes, appropriate stabilizers for metal nanoparticles and permit to be easily recycled. But the choice of the ionic liquid for a given reaction can modify the selectivity in the same reaction conditions. For example in citral hydrogenation, the higher solubility of hydrogen in [bmim][BF₄] than in [bmim][PF₆] produces different selectivity.⁹⁸

Other ionic liquids physisorbed on the surface of a solid support for SILP catalyst applications are 1,1,3,3-tetramethylguanidinium lactate (TMGL) ionic liquid and other derivatives containing TMG as a cation: [TMG][TFA] (1,1,3,3-tetramethylguanidine trifluoroacetic acid ionic liquid), [TMG][AA] (1,1,3,3-tetramethylguanidine acetic acid).⁹⁹ TMGL has been used due to its ability to coordinate to Pd nanoparticles. Palladium nanoparticles can aggregate to give bulk metal. TMGL ionic liquid has emerged as a good stabilizer avoiding PdNPs agglomeration. In this work the ionic liquid film supported over molecular sieve was estimated to 0.4 nm for an ILs loading of 20 % wt. TEM images of Pd nanoparticles show that they are in a range of 1-2 nm (Figure 1.4).⁵³

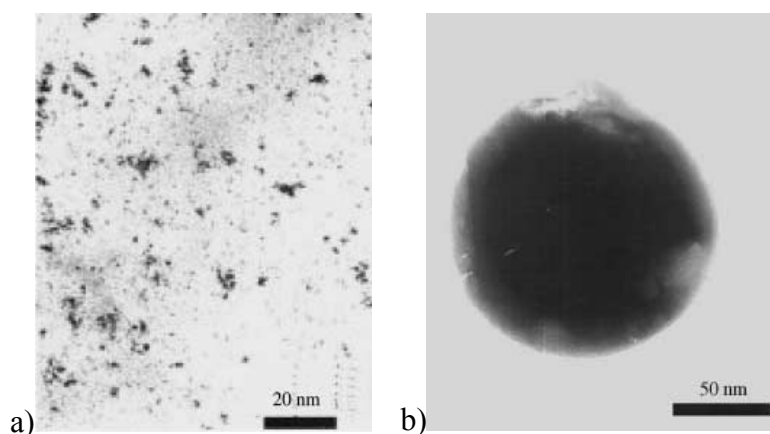


Figure 1.4: a) TEM micrograph of Pd nanoparticles dispersed in methanol/THF; b) TEM micrograph of molecular sieves with supported Pd nanoparticles. (Reproduced from ⁵³)

Non acidic ionic liquids have also been synthesized for their applications in SILP catalysis. [A336][PF₆] was prepared from Aliquat 336[®], a common phase transfer catalyst, exhibiting good hydrogen solubility which makes it suitable for hydrogenation reactions.⁹⁸

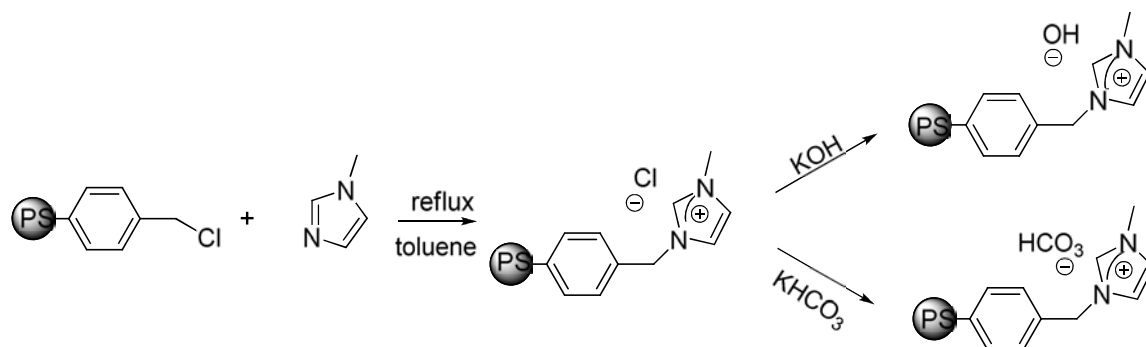
1.1.3 Nature of the catalyst involved in SILPC

1.1.3.1 Immobilized ILs as catalyst.

Not only acidic ILs, but also basic ILs have been largely immobilized onto different support materials to be used as catalyst. Acidic ionic liquids, including the well-known chloroaluminate based ionic liquids and the recently developed Brønsted acidic ones that contain trifluoromethyl sulfuric acid, proved to be effective catalysts for a variety of reactions.^{60,100} The immobilization of chloroaluminates on solid support has been described earlier in section 1.1.1. Those SILP chloroaluminate catalysts were mainly used in Friedels-Craft acylations and in alkylation reactions showing better activity and selectivity than those obtained using free ionic liquid.⁶⁰ Compared to chloroaluminate ionic liquids, Brønsted acidic ionic liquids containing trifluoromethyl sulfuric acid have emerged as powerful catalysts due to their air and water stability. They can be supported either by covalent immobilization onto a silica support,¹⁰⁰ by physical adsorption onto silica or encapsulated by sol-gel methods.¹⁰¹ These methods produce a material showing good performances in esterification of carboxylic acids with alcohols, nitration of benzene, Michael reaction of indole and condensation between indole and aromatic aldehydes.

Basic as well as acid ionic liquids have been immobilized for some catalytic studies. C. Paun et al. reported the Knoevenagel reaction mediated by a recyclable basic ionic liquid (BIL). Those basic ILs are derivatives of the Hünig's base tethered ammonium salt with the counterion bis{(trifluoromethyl)sulfonyl}imide ([NTf₂]) and are immobilized onto an acidic

silica support.¹⁰² The supported catalyst presents a good activity. No degradation of the ionic liquid was produced although the exothermicity of the reaction because the heat capacity of the silica support, and in consequence the catalyst could be recycled. The hydrolysis of propylene carbonate to 1,2-propylene glycol was also performed using a basic SILP catalyst.¹⁰³ For these purposes, a polystyrene resin was used to support a basic imidazolium hydroxide or imidazolium hydrogen carbonate (Scheme 1.12).



Scheme 1.12: Synthesis of basic ionic liquid supported on a polymer resin.

1-N-cetyl-3-methylimidazolium chloride ($[C_{16}mim]Cl$) ionic liquid, applied as template for the synthesis of MCM-48, presented good activity for Diels-Alder reactions.¹⁰⁴ Surprisingly, the homogeneous $[C_{16}mim]Cl$ system presents lower activity. Thus, a synergistic effect between the surface and the ionic liquid could be the responsible of this behaviour. Another example of ionic liquid catalyst is $[hmim][BF_4]$ supported on a polymer for phase transfer catalysis. Ammonium salts are well known for phase transfer catalysis in homogenous reactions. Chi's group has proved the catalytic activity of the supported ionic liquid in this type of reactions underlining that longer alkyl linker in the ionic liquid leads to better catalytic activity due to the better accessibility to the ILs (Figure 1.5(a)).^{79,105} They also report a synergistic effect when tert-butyl alcohol was used as solvent for fluorination reactions.¹⁰⁶ This synergy has encouraged them to synthesize a new supported ionic liquid catalyst based on a quaternary ammonium salt prepared by a solid phase quaternization of the polymer with triethylamine, N-methylimidazole and N-(2-hydroxy-2-methylpropyl)imidazole (Figure 1.5(b)).¹⁰⁷

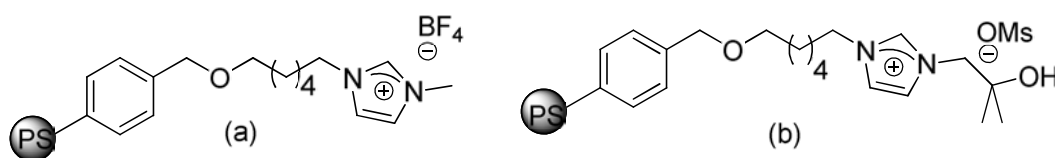


Figure 1.5: a) Polymer supported ionic liquid with long alkyl linker. b) Supported ionic liquid phase catalyst over a polymer functionalized with an alcohol moiety

The copolymerization of [bvim][Cl] and DVB leads to a polymer supported ionic liquid⁵⁵ which, as well as choline chloride/urea sieves supported ionic liquid,¹⁰⁸ is able to catalyze the cycloaddition of CO₂ with epoxides. High yields were achieved when 1-propyl-3-N-butylimidazolium bromide ILs was combined with a salt such as ZnCl₂,¹⁰⁹ in relation to butyl bromide supported on silica gel prepared by sol-gel method.¹¹⁰

Other organocatalysts are Chiral ionic liquids have been used as organocatalysts in asymmetric catalysis (Figure 1.6). The effect of supporting them onto a surface has permitted to overcome some of the drawbacks of those ionic liquids such as their high price and the difficulties to be recycled. One example is pyrrolidine-based ionic liquid, which could be recycled eight times for the Michael addition without loss of activity and selectivity.¹¹¹

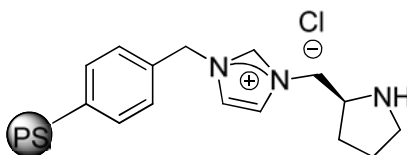
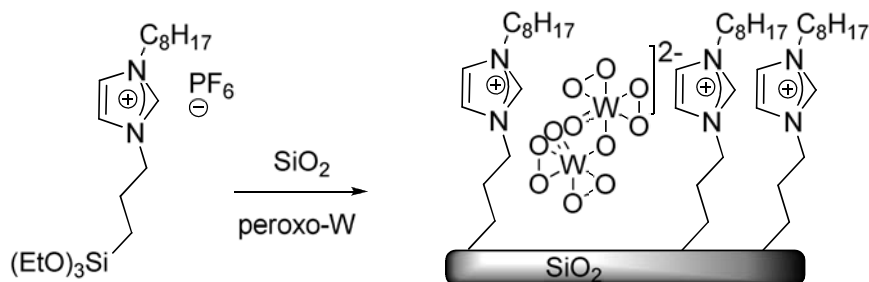


Figure 1.6: Chiral supported ionic liquid over a polymer

1.1.3.2 Metal complexes immobilization

Most of the common supported ionic liquids are based on 1,3-dialkylimidazolium cations and [PF₆] or [BF₄] anions. Their tuneable polarities make them good solvents for almost all transition metal complexes. As examples can be cited Rh and Pd complexes containing phosphines, such as triphenylphosphine or TPPTS, chiral Mn(salen) and Cr(salen) complexes (salen = N,N'-bis(salicylaldehyde)-ethylenediimine). The most popular way to immobilize a transition metal complex is to dissolve it into an appropriate ionic liquid. For this purpose the complex and the ionic liquid are dissolved in an organic solvent, which is further removed under vacuum. In the SILP concept, this ionic liquid is anchored as a thin layer onto the support surface.

[1-octyl-3-(3-triethoxysilylpropyl)-4,5-dihydroimidazolium][PF₆] ionic liquid, which is covalently anchored to silica surface can suffer an anion exchange between PF₆⁻ of the ionic liquid and a transition metal polyoxanion such as [W(=O)(O₂)₂(H₂O)₂(μ-O)]²⁻, [γ-1,2-H₂SiV₂W₁₀O₄₀]⁴⁻, [PMo₁₀V₂O₄₀]⁵⁻ or also RuO₄⁻ to be applied in olefin epoxidation reactions (W systems) and alcohol oxidation (Mo and Ru systems) (Scheme 1.13). Raman analyses confirm the maintenance of the peroxometalate structure in the anion exchange; ¹³C and ²⁹Si MAS NMR spectra revealed that the structure of the ILs was preserved.^{95, 96, 97, 49}



Scheme 1.13: SILP anion exchange between PF₆⁻ and [W(=O)(O₂)₂(H₂O)₂(μ-O)]²⁻, to give a catalyst system used in epoxidation reactions.

1.1.3.3 Metal nanoparticles

Transition metal nanoparticles (NPs) have attracted much interest from the scientific community in the last decade due to their properties lying between the bulk metal and the molecular state.¹¹² One of their major applications is in catalysis¹¹³ owing to their surface properties in the borderline between homogenous and heterogeneous catalytic behaviour. The catalytic activity of metal nanoparticles depends strongly on their size, electronic properties, surface properties and the metal oxidation state. Otherwise the main disadvantage is the difficulty to stabilize appropriate size metal nanoparticles maintaining their catalytic properties. Ionic liquids appeared as good stabilizers since the first observations of Dupont's group.¹¹⁴ Actually, ILs generate an electrostatic and steric stabilization of nanoparticles, diminishing their aggregation. Narrow size distribution of nanoparticles can be achieved with or without any other added stabilizer. The advantages of multiphase ILs/NPs systems, such as easy recovery and recycling, can be improved from a work-up point of view supporting it onto a solid support. The solid catalysts are still preferred for the easy work-up procedures. In those systems, the ionic liquid has a double function as stabilizer but also as immobilization agent of metal nanoparticles to the surface. The first study of immobilization of NPs onto a solid surface by an ionic liquid was carried out by Zhao's group in 2004.⁵³ In this work, Pd nanoparticles were immobilized on molecular sieves using 1,1,3,3-tetramethylguanidinium lactate (TMGL) as ILs. Palladium nanoparticles were preformed from Pd(OAc)₂ in THF/methanol, and then immobilized in TMGL. TEM images show particles of mean diameter 1-2 nm without any sign of agglomeration. The guanidinium ions are known to coordinate metal nanoparticles and prevent their agglomeration. Despite the fact that the ionic liquid layer makes only 0.4 nm, the authors affirm that no palladium nanoparticles are in direct contact with the support due to the strong interaction between the support and the TMGL ionic liquid. Thus, the ILs forms a layer over the solid support and coat the Pd nanoparticles at the same time. Dupont's group has preformed Rh nanoparticles from RhCl₃·3H₂O in [bmim][BF₄] under hydrogen atmosphere.¹¹⁵ Those particles were isolated and

then redispersed in [bmim][BF₄]/EtOH. The solution was used to synthesize an acidic or basic catalyzed xerogel with SiO₂ by a sol-gel technique. The solid obtained contains 70 % of Rhodium as Rh(0) nanoparticles. The acid-basic character of the xerogel does not influence the size of the Rh nanoparticles (mean diameter: 4.8 nm), but it modifies their shape. The acid catalyst gives plate like structures, while spherical nanoparticles were obtained with the basic.

Rh nanoparticles were also obtained by immobilization of a rhodium salt such as RhCl₃·3H₂O in an TMGL-based ionic liquid anchored on an attapulgite clay surface followed by reduction with hydrogen at 300 °C.⁷⁸ Rh nanoparticles of 5 nm have been observed by TEM and X-ray powder diffraction shows the effective pattern of crystalline rhodium but also some the presence of Rh(III). Rh NPs of 25 nm with high tendency to aggregation were synthesized by the same authors under the same conditions but without ILs, thus the ionic liquid plays a crucial role for NPs stabilization. Analogously, the synthesis of Ru nanoparticles supported on natural clays using [TMG][TFA] has been also reported¹¹⁶. Irregular shape Ru nanoparticles of 3 nm could be observed in the outer surface of the montmorillonite natural clay by TEM and confirmed by EDS (Energy dispersive X-ray spectroscopy) analysis, but XRD shows no crystalline Ru peaks. XPS analysis does not reveal the presence of Cl, which points to the total reduction of Ru(III) to Ru(0) species but some Ru-O species were observed which can be related to oxidation by air contact. Authors have demonstrated that Ru nanoparticles are not only in the outer surface but also in the interlayers of the montmorillonite showing a smaller size (1.2 nm).¹¹⁷ More usual is the in situ synthesis of metallic nanoparticles. Therefore, metallic precursors such as H₂[PdCl₄], [Pd(acac)₂] or Pd(OAc)₂ are immobilized in an ionic liquid and supported on a solid such as silica, carbon, polymers, clays, etc. Palladium nanoparticles are obtained by in situ reduction of these species by thermal treatment or by adding a reducing agent. The nature of the solid support and the reaction conditions influence the size of NPs, conferring them different properties (Table 1.1). For example, the smallest particles (1.2 nm) were obtained in the interlayer of a montmorillonite support with [TMG][TFA] ionic liquid (entry 11, Table 1.1). An interesting in situ preparation of Pd nanoparticles is the reduction of a Pd-N-heterocyclic carbene complex during the catalytic reaction with the aid of the ionic liquid N-3-(3-trimethoxysilylpropyl)-3-methyl imidazolium chloride (entry 2).¹¹⁸ The nanoparticles show irregular shape and 10-40 nm size distribution. [Pd(acac)₂] was reduced with H₂ at 150 °C in [bmimOH][Tf₂N] ionic liquid (entry 5).¹¹⁹ In-situ reductions of Pd(II) complexes such as Pd(OAc)₂ depend on the ionic liquid chosen for the immobilization. Thus, in N-3-(3-triethoxysilylpropyl)-3-methylimidazolium based ionic liquids ([TESP]MIm][X], X = Cl, NO₃, BF₄ or PF₆), palladium carbyne species (X = Cl) or palladium nanoparticles with size less than 10 nm (X = BF₄ or PF₆⁻) could be formed (entry 3).⁹³ An interesting result is the possibility to reduce Pd(OAc)₂ to Pd nanoparticles and not to a carbyne with 1,3-

dialkylimidazolium ionic liquids (entry 7). The complex is immobilized and decomposed on the surface by alcohol reduction. Particles of 6 nm with 1-vinyl-3-butylimidazolium based ionic liquids ([vbim]X, X = Cl, BF₄⁻ or PF₆⁻) can be observed in TEM images (Figure 1.7 a-d); electron diffraction analysis evidences an fcc structure (Figure 1.7 e).¹²⁰

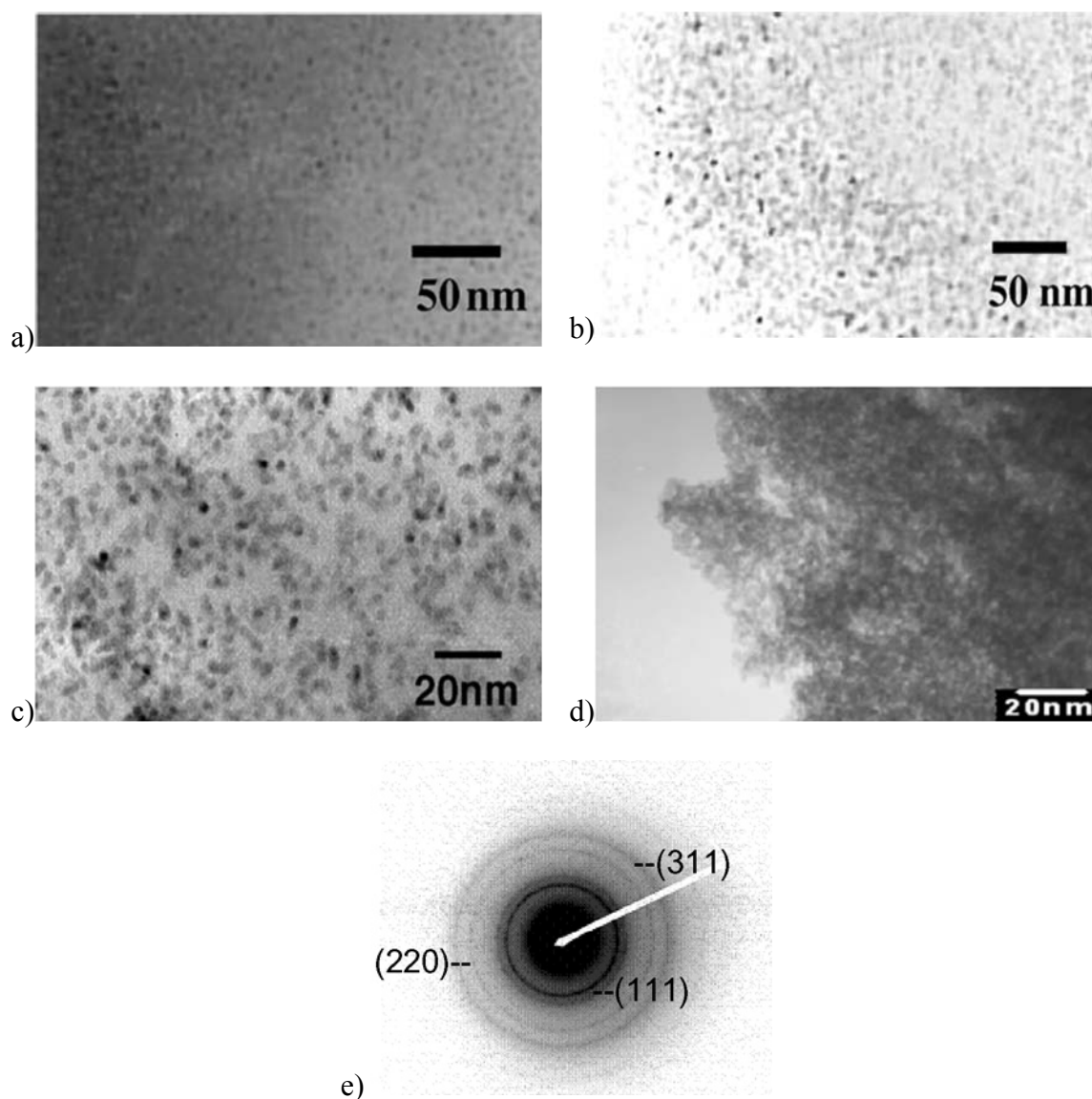


Figure 1.7: TEM and electron diffraction images of various supported Pd catalysts. (a) Pd/PS-IL[BF₄], (b) Pd/PS-IL[PF₆], (c) Pd/PS-IL[Cl], (d) Pd/SiO₂-IL[Cl], and (e) electron diffraction of Pd/PS-IL[Cl]. (reproduced from¹²⁰)

A different approach is to support Pt nanoparticles onto modified ionic liquid magnetite (Figure 1.8). The ionic liquid modification prevents aggregation of the magnetic nanoparticles in organic or aqueous solution. The platinum salt K₂[PtCl₄] is absorbed via ion exchange with the linking ionic liquid groups and then transformed onto nanoparticles with hydrazine

reduction. Other reducing agents were tested with bigger Pt nanoparticles size. When the supported ionic liquid contains the octyl group, Pt particles of 2-2.5 nm can be directly obtained attached to the surface (entry 10).¹²¹

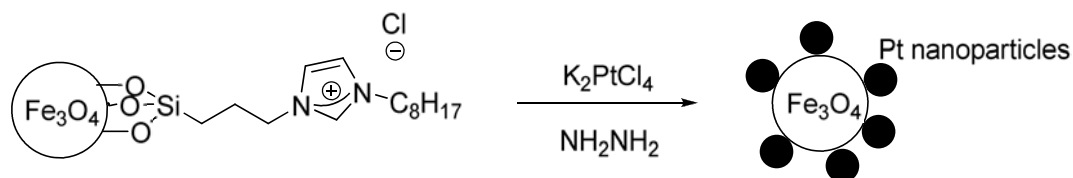


Figure 1.8: Pt nanoparticles onto modified ionic liquid magnetite nanoparticles.

Entry	Precursor	ILs	Support	Type of reduction	Size (nm)	Others species by XPS analysis
1	H ₂ PdCl ₄	[TMG][TFA]	sepiolite	H ₂ at 150°C for 4 hours	5	Oxidation of Pd ⁰
2	N-heterocyclic carbene palladium	[(TESP)mim][X]	SiO ₂	By ILs	10-40	-
3	Pd(OAc) ₂	[(TESP)mim][X]	SiO ₂	By ILs	2-10	-
				[PF ₆] ⁻	2	
				[NO ₃] ⁻	10	
				[BF ₄] ⁻		
4	Na ₂ PdCl ₄	ILs imidazolium moieties	MWCNTs	H ₂ at 1 bar, room T	10	-
5	Pd(acac) ₂	[bmimOH][Ntf ₂] [bmim][PF ₆]	CNFs/SMF	H ₂ 150°C	5 105	Pd ²⁺ species
6	Pd(OAc) ₂	[(TESP)mim][X]	SiO ₂	In-situ	3.1	-
7	Pd(OAc) ₂	Imidazolium-styrene copolymer [vbim][Cl]-styrene		Alcohol	6	-
8	RhCl ₃ ·3H ₂ O	TMGL	Attapulgit	H ₂ at 300°C	5	Rh ³⁺
9	RhCl ₃ ·3H ₂ O Rh/C	[bmim][BF ₄]	SiO ₂	Preformed 4 bar of H ₂ at 75°C	4.8	-

Entry	Precursor	ILs	Support	Type of reduction	Size (nm)	Others species by XPS analysis
10	K ₂ PtCl ₄	[(TESP)mim][X]	Fe ₂ O ₃	Hydrazine	2-2.5	-
11	RuCl ₃	[TMG][TFA]	Montmorillonite	H ₂ at 220°C	3 outer surface 1.2 interlayers	-
12	RuCl ₃	Choline	MgO	H ₂ at 280°C	<2	Ru ³⁺

Table 1.1: Nanoparticles used in SILPC.

1.2 SUPPORTED IONIC LIQUID PHASE CATALYSIS: APPLICATIONS

Since its apparition, SILPC has been extended to a great number of catalytic reactions. In this section, SILPC catalytic performances and the comparison with the corresponding biphasic, homogeneous and heterogeneous systems are discussed.

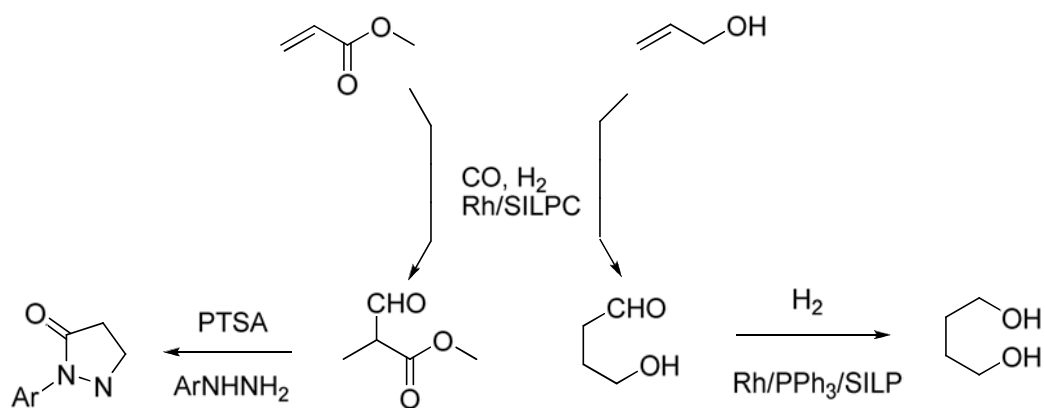
1.2.1 Alkylation reactions

Friedel-Craft alkylation reactions are catalyzed at industrial scale by homogeneous aluminium(III) chloride salts. During the work-up treatment, aluminium oxide waste, toxic and corrosive HCl gas and large amounts of water contaminated with organic impurities are produced, though the process becomes problematic from an environmental point of view. As an alternative, zeolites or metal oxides are used as heterogeneous catalysts, but they are usually less active. SILP catalysts have emerged as an alternative route for these alkylations. The first example of a SILP-type catalyst based on acidic chloroaluminate ionic liquids has been reported in 2000 by Hölderich et al.^{51,59} The authors combined acidic chloroaluminate ionic liquids to various supports such as silica,⁶⁰ alumina, TiO₂ or ZrO₂. The formed solids were tested for the alkylation of benzene, toluene, naphthalene and phenol with 1-dodecene. The catalytic activities of the supported ionic liquids have been found to be higher than those obtained by conventional H-β zeolite under similar reaction conditions. AlCl₃ leaching is not reported, but a slight loss in conversion over time in the continuous liquid-phase reaction is observed.

1.2.2 Hydroformylation reaction

The first tentative to heterogenize an olefin hydroformylation catalyst has been carried out by Mehnert's group.⁶³ The system consists on a Rh(I) complex containing monophosphine ligands (PPh₃ or TPPTS) dissolved in an ionic liquid, and consecutively immobilized on a modified silica support. The SILP catalyst was found to have higher activity than that observed with biphasic systems but severe leaching of both the ionic liquid layer and the metal complex was noticed. The introduction of TMGL as ionic liquid using MCM-41 as support palliated this problem and the catalytic system could be recycled up to eleven times.⁶⁸ The strong interaction between the TMGL ionic liquid and the complex could be the reason for this high stability. Data given in this work prove the high dispersion of the ionic liquid phase on the surface.⁶⁹ Riisager et al. has reported the continuous gas-phase hydroformylation of propene with a SILP catalyst.¹²² A rhodium(I) complex with mono- or biphosphines as ligands has been chosen for this process. The biphosphine ligand 2,7-bis-(SO₃Na)-4,5-bis(diphenylphosphino)-9,9-dimethylxanthene (sulfoxantphos) shows moderate activity but high selectivity up to 95 % towards linear aldehydes. Monophosphines show high activity but lower selectivity under the same conditions.⁶⁵ The system composed of the previous complex (rhodium(I) with sulfoxantphos ligand) with [bmim][n-C₈H₁₇OSO₃] immobilized onto dehydroxilated silica support presents 200 hours life time-on-stream. After this time, the activity decreases due to high boiling by-products, remaining anchored to the ionic liquid and poisoning the Rh catalyst. A treatment under vacuum for 10 min at 100 °C can increase the catalyst lifetime up to 700 h.^{123,124} Long term stability was found when 1-butene was used as feedstock for the reaction under the same conditions.¹²⁵

Hydroformylation of unsaturated esters such as acrylates to the corresponding branched aldehydes was performed with Rh/PPh₃ complexes dissolved in [bmim][PF₆] and further anchored to a silica gel (Scheme 1.14). High chemoselectivity and regioselectivity was achieved when controlling the temperature, Rh/P ratio and Rh concentration. [Rh(H)(CO)(PPh₃)₃]/7PPh₃ showed the best performances for hydroformylation of unsaturated esters. Water was used as solvent with the hydrophobic ionic liquid phase catalyst in order to avoid catalytic phase leaching. The resulting branched aldehydes can react with phenylhydrazine in the presence of a mild Lewis acid in a sequential two-step process with the same SILP catalyst to obtain the corresponding condensation product.¹²⁶ Hydroformylation of allyl alcohols has been performed under the same conditions giving good regioselectivity towards C₄O₂H₈. The subsequent hydrogenation of the branched aldehydes led to the formation of 1,4-butanediol.¹²⁷



PTSA: p-toluenesulfonic acid

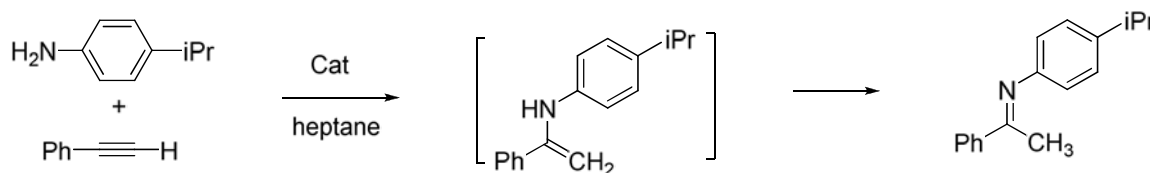
Scheme 1.14: Hydroformylation of methyl acrylate and allylic alcohol over SILP-Rh catalyst.

When supercritical CO₂ (scCO₂) was used in a gas-flow reactor, fast hydroformylation of 1-octene was achieved with a SILP catalyst. The catalyst prepared from [Rh(acac)(CO)₂] remains active for 40 h without significant leaching from the supported ionic liquid [c₃mim][Ph₂P(3-C₆H₄SO₃)] phase catalyst over SiO₂. That can be related to the greater diffusion of the substrate and gases in the supported ionic liquid due to the scCO₂ high solubility in ILs.¹²⁸

1.2.3 Hydroamination reactions

Cationic organometallic complexes are commonly used in the homogeneous hydroamination reaction. [Rh(dppf)(nbd)]ClO₄ (nbd = 2,5-norbornadiene), [Pd(dppf)](CF₃SO₃)₂, [Cu₂(C₆H₅CH₃)](CF₃SO₃)₂ and [Zn(CF₃SO₃)₂] cationic complexes were dissolved in 1-ethyl-3-methylimidazolium trifluoromethanesulfonate ionic liquid and further supported on diatomic earth.⁷⁷ The catalyst was tested in a model reaction, the direct addition of 4-isopropylaniline to phenylacetylene (Scheme 1.15). The initial reaction rate with the supported Pd complex was higher (4.3 h⁻¹) than that observed using Rh and Zn complexes (0.72 and 0.58 h⁻¹ respectively), but all three supported systems exhibit higher TOF than that obtained using analogous non-supported homogeneous catalysts (Pd = 2.10 h⁻¹, Rh = 0.34 h⁻¹, Zn = 0.10 h). Lower TOF were obtained under supported condition than in homogeneous conditions due to strong complexation of the copper(I) centre by the ILs which competes with coordination of the substrate. The selectivity towards (4-isopropyl-phenyl)-(1-phenylethylidene)-amine was found to be higher with the supported systems. No by-product arising from oligomerization of phenylacetylene was found contrary to the homogeneous catalyst.

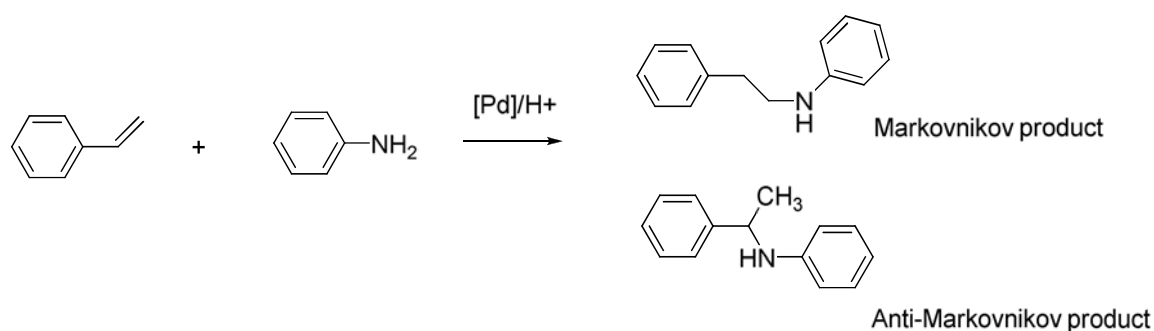
Biphasic catalytic systems show activities comprised between the corresponding homogeneous and supported catalysts.



Scheme 1.15: Direct addition of 4-isopropylaniline to phenylacetylene.

Recent studies reveal that ionic liquid not only dissolves homogeneous catalysts but also stabilizes the ionic catalytic intermediates because of its high polarity.¹²⁹

SILP concept was also used to prepare a catalyst by immobilization of $[\text{Pd}(\text{CF}_3\text{CO}_2)_2(\text{dppf})]$, a soft Lewis acid, and $\text{CF}_3\text{SO}_3\text{H}$, a strong Brønsted acid, in imidazolium salts ($[\text{emim}][\text{OTf}]$, $[\text{bmim}][\text{OTf}]$ or $[\text{hmim}][\text{OTf}]$) supported on silica, for hydroamination reactions. The catalysts show good catalytic activity for the addition of aniline to styrene, providing the Markovnikov product under kinetically conditions and mainly the anti-Markovnikov product under thermodynamic regime (Scheme 1.16). These results can be explained by the formation of ionic liquid cages around the metal complexes.¹³⁰ Authors affirm that during the dissolution of the metal complex, the inter-ionic interactions between the cations and the anions of the ionic liquid are disrupted leading to a structure perturbation. To minimize the potential energy, the ionic liquid forms small cages around the metal complex. These cages limit the metal complex mobility and entrapped the high ionic liquid soluble reactants like aniline in high concentrations, favouring metal-substrate interactions giving the anti-Markovnikov product. At high temperatures, ILs gain mobility, consequently the cages are destroyed. The ionic liquid stabilizes the polar transition state of the Markovnikov product, which occurs via π -coordination of the styrene to the Pd metal centre, favouring the nucleophilic attack with the electron pair of the nitrogen atom. The SILP catalyst gives higher performances than those obtained using homogeneous catalysts. The catalytic results were similar with all the ionic liquids tested, but at lower temperatures the activity depends on the ionic liquid nature, increasing with the polarity of the ionic liquids: $\text{emim} > \text{bmim} > \text{hmim}$. Those ionic liquid cages are also responsible of the enantio-selectivity in the hydrogenation of acetophenone.¹³¹



Scheme 1.16: Addition of aniline to styrene catalyzed by palladium systems.

1.2.4 Hydrogenation reactions

The concept of SILP was fast extended to hydrogenation reactions. Menhert and co-workers studied the hydrogenation of some olefins using $[\text{Rh}(\text{nbd})(\text{PPh}_3)_2]\text{PF}_6$ as catalytic complex.⁶⁴ The system exhibits higher activity than that obtained with homogeneous and biphasic catalytic systems. The SILP catalyst shows long stability and could be reused up to 18 cycles without activity loss; no Rh species were detected from ICP analyses. Ruta et al. used another Rh catalytic species such as $[\text{Rh}(\text{H})_2\text{Cl}(\text{PPh}_3)_3]$ immobilized in ionic liquid and supported over CNF/SMF for the selective gas-phase hydrogenation of 1,3-cyclohexadiene to cyclohexene. High turnover frequencies (>96 %) were observed. The addition of an acid in the ionic liquid phase increases the catalytic activity and enhances the stability of the supported catalyst in the continuous process.⁷⁵ A modified styrene support with L-proline shows high catalytic activity under free solvent conditions for hydrogenation of styrene with Pd.⁹⁴

Asymmetric hydrogenation was also subject of study with SILP catalysts. The chiral Ru catalyst, $[\text{RuCl}_2(\text{PPh}_3)_2(\text{S,S-DPEN})]$ (DPEN = 1,2-diphenylethylenediamine), was immobilized in a thin film of $[\text{bmim}][\text{BF}_4]$ anchored to a crystalline support. Silica MCM-48 as support shows higher selectivity in the asymmetric hydrogenation of acetophenone to phenethyl alcohol than silica supports such as MCM-41 and SBA-15, due to the presence of defined channels. The activity of this catalyst was comparable to the homogeneous system but it could be recycled 4 times without significant loss of activity. Moreover the heterogeneous catalyst without ionic liquid constituted by the Ru complex and MCM-48 presents similar activity but leaching was observed after the first run.⁷⁰ The asymmetric hydrogenation of acetophenone was also carried out using chiral complexes $[\text{Rh}(\text{BINAP})\text{L}_2]\text{X}$ (L = weakly coordinating ligand such as cod (cyclooctadiene); X = non-coordinating anion: ClO_4^- , CFSO_3^-) immobilized on a silica supported phosphonium-based ionic liquid.¹³¹ 1-cyclohexylethanol was enantioselectively formed after full reduction of the carbonyl and

phenyl groups. Compared to the corresponding homogeneous catalyst, similar activities were observed but higher enantioselectivities (30-74 % versus less than 4 % using homogeneous catalyst) were achieved using methanol as solvent. Formation of ILs cages around the complex as explained in section 1.2.4 could be the responsible of the different selectivity.

Hydrogenation reactions are widely catalyzed by Rh nanoparticles under homogeneous conditions using ionic liquids. The possibility to immobilize rhodium complexes on a supported layer of ionic liquid onto a support has opened researches using Rh nanoparticles instead of complexes in those systems. The cyclohexene hydrogenation was catalyzed with high activity in a molar ratio substrate/Rh of 15,000. Recycling up to 5 runs were carried out without any sign of nanoparticles aggregation remaining the nanoparticles firmly attached to the surface.⁷⁸ Another example of hydrogenation of cyclohexene and 1-dodecene was described by Dupont's group.¹¹⁵ Interesting is the comparative study realized. The Rh nanoparticles supported catalyst with ionic liquid on silica is more active than the same non-supported catalytic system and also more active than the commercial heterogeneous catalyst, Rh/C.

Benzene hydrogenation to cyclohexane was carried out with Ru nanoparticles immobilized on a SILP catalyst using montmorillonite as support and [TMG][TFA] as ILs, giving slightly higher activity than that obtained using the Ru-cluster-based catalysts in ionic liquid, but the SILP catalytic system could be reused 5 times. Additionally, the SILP catalyst shows higher activity compared to classical heterogeneous catalysts such as Ru/C and Ru/Al₂O₃.¹¹⁶

SILP catalyst containing palladium nanoparticles can also catalyze hydrogenation reactions giving good activity and selectivity. Solvent free hydrogenation of olefins has been carried out by preformed palladium nanoparticles immobilized in TMGL and supported onto molecular sieves.⁵³ Better activity was obtained with SILP nanocatalyst than that observed under biphasic conditions. Hydrogenation of alkadienes was also studied with high conversion and selectivity towards alkanes (entry 2, Table 1.2). That suggests a stronger interaction of the Pd alkadienes surface than that occurred with alkenes. The same results were obtained using in-situ formed palladium nanoparticles immobilized in [TMG][TFA] and supported on a sepiolite natural clay.⁹⁹ The catalyst phase was recycled up to 5 times without loss of activity, but no data concerning leaching nor palladium agglomeration is reported.

Entry	Catalyst	Olefin	Olefin/Catalyst molar ratio	T (°C)	P (MPa)	T (h)	Conversion (%)	TOF (h ⁻¹)
1	Sieves/(TMGL)/Pd	cyclohexene	12000	20	-	10	100	1200
2	Sieves/(TMGL)/Pd	cyclohexadiene	12000	20	-	3	98	3918
3	Sieves/(TMGL)/Pd	1-hexene	12000	20	-	3	100	4002

Entry	Catalyst	Olefin	Olefin/Catalyst molar ratio	T (°C)	P (MPa)	T (h)	Conversion (%)	TOF (h ⁻¹)
9	Phenanthroline/Pd	1-hexene	120	20	-	6	100	18
5	[bmim][PF ₆]/Pd	cyclohexene	500	40	-	5	100	100.2
6	Sepioline/[TMG][TFA]/Pd	1-hexene	5000	60	2	0.5	>99	10000
7	Sepioline/[TMG][TFA]/Pd	Styrene	5000	60	2	0.5	>99	10000
8	Sepioline/[TMG][TFA]/Pd	cyclohexene	5000	60	2	1	>99	5000
9	Sepioline/[TMG][TFA]/Pd	cyclohexadiene	5000	60	2	3.5	>99	1428

Table 1.2: Some examples of hydrogenation reactions with SILPC.

Ruta et al. described the hydrogenation of acetylene towards ethylene with high selectivity using Pd nanoparticles immobilized on CNF/SMF-ILs (Carbon nanofibbers/Synthetic metal fibers-ILs).¹¹⁹ Actually, the lower solubility of ethylene compared to acetylene in the ILs can be the responsible of this behaviour. No oligomerization of acetylene was detected with this system compared to the IL free system where catalyst poisoning by the oligomers takes place. Both the low solubility of H₂ in ILs and the nanoparticles surface hindered access due to the supramolecular structures created around them by the ionic liquid, can be the main reasons to avoid oligomers formation. These systems present high efficiency and long term stability. Similar selective hydrogenation results have been obtained for the hydrogenation of conjugated diene with Pd nanoparticles in a SILP catalyst.¹³²

Taking advantages of the ionic liquid anion tunable properties, Lee's group has studied the hydrogenation of trans-stilbene.⁹¹ Change the ionic liquid counter anion of the ionic liquid has no influence on the size or on the distribution of Pd nanoparticles deposited on ILs modified MWCNTs. Even more, supported catalyst can be dissolved in ionic liquid without Pd leaching. Thus, the influence of the counter anion could be studied with the best result obtained for SbF₆ with a TOF 2820 h⁻¹, using either ⁱPrOH or ⁱPrOH/[bmim][SbF₆] as solvents. When using NTf₂ as counter anion for the ILs moieties anchored to the surface, an enhancement in the activity could be observed when MeOH/[bmim][NTf₂] was used instead of MeOH highlighting an effect of the ILs. Palladium nanoparticles agglomeration was observed during the reaction, but the system was still active up to 50 runs.

Selective hydrogenation of α,β -unsaturated aldehydes, ketones, and esters is generally a versatile method to obtain many interesting products for the fragrances industry. Citral hydrogenation catalyzed by Pd nanoparticles was obtained with different selectivity depending on the ILs coated onto an ACC.⁵² The plausible explanation could be the different

solubility of hydrogen in the different ILs used. As it is known, H₂ is three times more soluble in [bmim][BF₄] than in [bmim][PF₆].¹³³ This fact explains the formation of citronella with immobilized ILs having PF₆ as anion, [bmib][PF₆] and [A336][PF₆], and the dihydrocitronella with the counter anion BF₄, [bmim][BF₄], [A336][BF₄] and [NB₄MPy][BF₄]. The latter was recycled 50 times.⁶⁶ Selective hydrogenation of cinnamaldehyde to hydrocinnamaldehyde was selectively obtained with Pd nanoparticles.⁹³ A complete conversion to hydrocinnamaldehyde could be achieved at 80 °C in 20 min for the Pd/[(tesp)mim][X]/SiO₂ system while under the same condition the biphasic [bmim][PF₆] ionic liquid needs 6 hours to reach a complete conversion. The authors explain this high activity by the high surface area of the silica gel which leads to a great enhancement of the contact of substrates and H₂ over the surface of the Pd nanoparticles, while in the bulk ionic liquid H₂ is poorly soluble. This activity presents also great dependence of the counter anion nature of the ionic liquids. Therefore for PF₆, the reaction is completed in 20 min with 100 % conversion and selectivity at 80°C and 5 MPa of H₂ pressure. But under the same conditions the activity decreases in the order PF₆⁻ > NO₃⁻ > BF₄⁻ > Cl⁻. This dependence of the ionic liquid can be also observed in biphasic systems where the activity order is [bmim][Cl] < [bmim][BF₄] < [bmim][NO₃] < [bmim][PF₆]. Recycling experiments were done without loss of activity for 9 runs and without catalytic phase leaching, in contrast to commercial heterogeneous Pd/Al₂O₃ catalyst, which, under the same conditions, presents deactivation after the third run.

Pt nanoparticles supported on an ionic liquid modified magnetite nanoparticles were used as catalyst for the hydrogenation of α,β -unsaturated alkynes and aldehydes.¹²¹ The reaction was found to be selective in the hydrogenation of alkynes to cis-alkenes and α,β -unsaturated aldehydes to the corresponding alcohols. The authors explain the high selectivity towards cis-alkenes on the basis of a support effect. The magnetic support can act as bulky ligand avoiding the access of alkenes to the metal nanoparticles surface. The magnetite nanosupport can also polarize the Pt nanoparticles, making them partially positive and thus activate the polar functional group of the α,β -unsaturated aldehydes, giving alcohols. The system acts like a homogeneous catalyst being dissolved in a solvent, but it exhibits a catalytic heterogeneous behaviour and in consequence can be separated by an external magnetic field and thus recycling.

Due to safety problems of gaseous H₂, transfer hydrogenation is applied in the industrial production of fine chemicals. Ru nanoparticles immobilized in the ionic liquid choline and supported on a crystalline MgO material catalyze this reaction.¹¹⁷ The reduction of various carbonyl compounds using KOH as a base with this catalyst to give the corresponding alcohols was nearly completed in 6-10 h and it could be recycled up to 5 times.

1.2.5 Carbonylation reactions

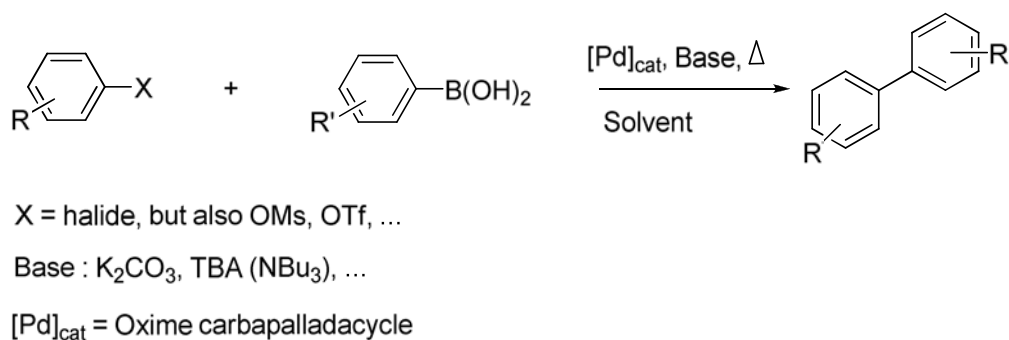
Shi et al. described the catalyzed carbonylation reaction of amines and nitrobenzene to form urea derivatives using SILP catalysts.⁷¹ The authors maintain that the high TOF (11000 h⁻¹) achieved is related to the high concentration of ionic liquid [dmim][BF₄] (dmim = 1-decyl-3-methyl imidazolium) and Rh complex, confine in the porous structure of a silica gel matrix.

The alcohol carbonylation with CO has been studied for Riisager et al.^{112,134} The silica supported catalyst was immobilized by impregnation of the ionic liquid [bmim][I] containing [Rh(CO)₂I₂]. The Monsanto type catalyst cis-[Rh(CO)₂I₂]₂ is formed in situ and characterized by IR spectroscopy. The SILP Monsanto catalyst system provided complete methanol conversion with a TOF of 76.5 h⁻¹ and selectivities up to 98 % towards the formation of acetyl products (dimethyl ether is the only by-product). Compared to the results obtained in an analogous bubble column reactor system with large amount of ILs, the reaction rate is almost the same.

1.2.6 C-C coupling reactions

1.2.6.1 Suzuki-Miyaura cross-coupling

The palladium-catalyzed Suzuki–Miyaura cross-coupling reaction is a powerful methodology for C-C bond formation, being widely used in synthetic organic chemistry. The reaction coupling occurs principally between an aryl boronic acid and halobenzene derivatives (Scheme 1.17).



Scheme 1.17: Suzuki-Miyaura cross-coupling reaction catalyzed by palladium systems.

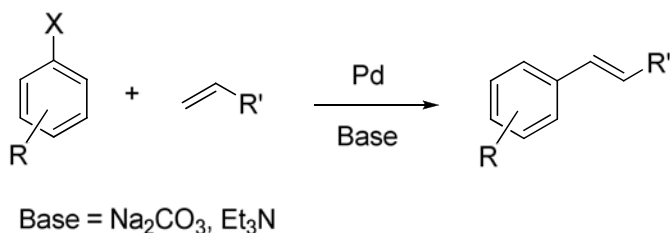
Pd-SILP catalyst has been reported by Corma's group to catalyze the Suzuki reaction between halobenzenes and phenyl boronic acid.⁶⁶ The supported catalyst was constituted by an oxime carbapalladacycle supported on an aluminosilicate support (Al/MCM-41). Catalytic

activity was favoured by polar solvents showing no homocoupling product of the phenyl boronic acid. Recycling experiments were not satisfactory due to the instability of the carbapalladacycle, which decomposed to give Pd nanoparticles leading to an important leaching. Pd(OAc)₂ has been used as catalyst for the Suzuki reaction when it is immobilized on diethylaminopropylated alumina (NDEAP) with the aid of [bmim][PF₆].¹³⁵ A mixture of alcohol and water was revealed as the best solvent with a TOF of 3000 h⁻¹. Low loading of Pd was used to avoid leaching and Pd aggregates. An analogous result was published by Han et al. with a SILP catalyst based on PdCl₂ deposited over a SBA-15 modified with chloroaluminatesilane.⁶⁷ In this case, a mixture of ⁱPrOH/H₂O or EtOH/H₂O gave the best results in relation to other solvents. Noticeably, the good solubility of organic reactants and inorganic salts in the solvent mixture could be the responsible of a TOF up to 84000 h⁻¹, in the reaction between p-bromoanisole and phenylboronic acid. The SILP catalyst shows the same activity than that observed using homogeneous PdCl₂ and heterogeneous Pd/SBA-15 catalysts. On the contrary, the SILP catalyst exhibits good stability at low Pd loadings without loss of Pd active species, while Pd/SBA-15 suffers leaching. XPS analysis shows the characteristic peak of Pd (0) after the first run. The authors suggests that ligand-free palladium(II) is reduced in situ to Pd(0) and enters into the catalytic cycle, but at the end of the reaction Pd(0) species are redeposited on the silica pore walls. The absence of agglomeration is controlled by the stabilization effect of the imidazolium salt contained in the inner walls of the mesoporous support.

Trilla et al. immobilized Pd(OAc)₂ on an hybrid materials prepared from monosilylated imidazolium and disilylated dihydro-imidazolium salts in acidic conditions using NaBF₄ and 1-cetyl-3-methylimidazolium chloride ([cmim]Cl) for Suzuki coupling reactions.¹³⁶ The catalyst presents good performances starting from activated systems as p-bromoacetate in 0.5-1 hour. No formation of biphenyl product resulting from the homocoupling reaction of the phenylboronic acid was observed. This reactivity was retained upon recycling. Moreover, C-Cl bonds could be activated using this catalyst. The high porosity of the support should facilitate the diffusion of the reactants. TEM images of the catalyst after 5 runs revealed a reduction of the Pd(II) species to aggregates of Pd(0), which was also confirmed by electron diffraction (ED). A hot filtration of the catalyst from the reaction was performed in order to determine whereas the catalysis beneath in a homogenous or heterogeneous phase. A 79 % conversion in 30 minutes time (95 % was obtained without hot filtration) was observed, which evidenced that a homogenous pathway is operating with this catalyst. Not activated arylhalides were also studied giving modest yields and a decrease of activity was observed in 5-24 h of reaction time.

1.2.6.2 Heck reaction

The Heck reaction has been one of the most largely studied Pd-catalyzed carbon-carbon coupling reactions. The wide range of application in the production of pharmaceutical intermediates, fine chemicals or polymer synthesis justifies the numerous efforts in its development. The coupling between an aryl halide and an olefin has been mainly catalyzed by palladium species such as palladium complexes containing phosphine ligands (Scheme 1.18).



Scheme 1.18: Heck coupling reaction catalyzed by palladium systems.

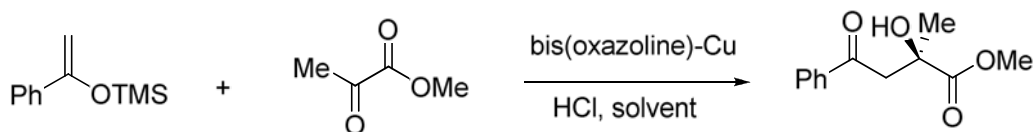
The use of SILPC for this reaction has been reported by Hagiwara and co-workers using starting precursor like Pd(OAc)₂, [Pd(PPh₃)₄], and Pd black immobilized in [bmim][PF₆] and supported over a silica gel.⁶⁷ A TOF of 8000 h⁻¹ was obtained using Pd(OAc)₂ for the reaction between iodobenzene and cyclohexyl acrylate, exhibiting higher activity than other heterogeneous Pd catalysts (such as Pd/SiO₂). Recycling experiments show a deactivation in the third run due to Pd leaching. Qiao et al. have introduced an imidazolium-styrene copolymer with immobilized Pd(OAc)₂ for the reaction of iodobenzene and ethylacrylate in water.¹²⁰ The reaction exhibited higher activity (86 %) than other Pd catalysts under the same conditions, such as homogeneous Pd(OAc)₂ (34 %), biphasic Pd(OAc)₂-[vbim][Cl] catalyst (10 %) and Pd/SiO₂ (11 %). The system was reused three times without activity loss.

Solvent free reactions are environmentally benign and economically advantageous, that is the reason the arylation of olefins with aryl halides is so interesting under these conditions. Preformed Pd nanoparticles immobilized in TMG ionic liquid and supported on a modified molecular sieves or SBA-15 were reported to display high activity and selectivity. For the reaction between iodobenzene and methyl acrylate, 93 % of (E)-methyl cinnamate was reached only using 0.001 % of Pd. The system is recyclable more than 6 times without loss of activity in contrast to the heterogeneous SBA-15/Pd system which is deactivated after two runs. During the reaction, leaching of palladium species occurred, but they are redeposited on the surface at the end of the reaction with the help of TMG, excellent stabilizer for metallic nanoparticles.¹³⁷ Other palladium nanoparticles were used for the Heck reaction, resulting from the in-situ reduction of Pd-N-heterocyclic carbene, where the catalyst behaves as a heterogeneous catalyst (proved by hot filtration test).¹¹⁸

1.2.6.3 Aldol condensations

Choline hydroxide supported on MgO was used in aldol condensation reactions using various ketones and aldehydes. The basic ionic liquid acts as catalyst with better performances than those obtained using the analogous homogeneous system in the synthesis of various carbonyl compounds used in the pharmaceutical, flavour and fragrance industries. No data was supplied about recycling experiences and catalyst leaching.⁶¹

The asymmetric Mukaiyama aldol reaction between methyl pyruvate and 1-methoxy-1-trimethylsilyloxypropene has been catalyzed by Cu(II) complexes containing bis(oxazolines) under homogeneous, biphasic and heterogeneous (supported) conditions (Scheme 1.19).¹³⁸ Despite the better activity achieved with an imidazolium-tagged bis(oxazoline)-Cu biphasic system compared to the homogenous corresponding system in CH₂Cl₂, by-product formation from the reaction between 1-phenyl-1-trimethylsilyloxyethene and acetophenone was observed. Surprisingly, the supported catalyst on silica exhibited higher chemoselectivity without loss of enantioselectivity, but decreasing in activity.



Scheme 1.19: Aldol condensation reaction between methyl pyruvate and 1-methoxy-1-trimethylsilyloxypropene catalyzed by Cu(II) complexes containing bis(oxazolines).

L-proline, acting as an organocatalyst, has been applied in the SILPC catalysis for the aldol reaction between ketones and several substituted benzaldehydes.⁸⁹ An ionic liquid modified silica support was coated with additional ionic liquid. Better yields and *ee* than those obtained with homogeneous catalysts were achieved using the appropriate linker between the surface and the ionic liquid layer, but the results remained comparable to those obtained under biphasic conditions. Recycling experiments were carried out up to nine times without activity loss. The same group introduced other organocatalysts, such as the tripeptide H-Pro-Pro-Asp-NH₂, in the analogous SILP catalytic system. The synergistic effect between the peptide and the ionic liquid surface linker 4-methylpyridinium led to better yields and *ee* at -20 °C than those obtained with the analogous homogeneous catalyst and supported L-proline.⁸⁸

1.2.7 Oxidation reactions

Oxidation reactions are applied in the preparation of intermediates in fine chemicals. For this type of processes, recycling remains the major drawback. The use of SILP catalyst might help to solve this problem.

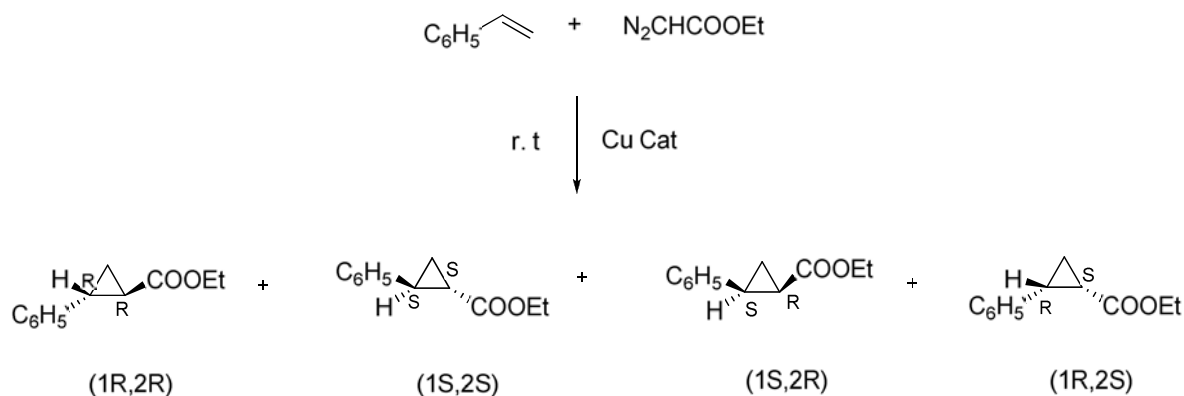
Tungsten catalysts have been widely used in the oxidation of olefins with H₂O₂ in homogeneous phase catalysis. Polyoxometalates and peroxometalates have been used for the first time in the SILPC catalysis by Mizuno et al.⁹⁵ Immobilized peroxotungstate in hydroimidazolium-based ionic liquid-modified SiO₂ was used for epoxidation reactions with H₂O₂. The catalyst was employed with good results in the epoxidation of various alkenes. The cis-trans configuration around the double bond was retained suggesting no radical intermediates. The regio- and diastereo-selectivity presented with this catalyst was similar to that obtained by the corresponding homogeneous catalyst. Moreover, the catalytic activity of the supported catalyst was comparable with the analogous [(n-C₁₂H₂₅)N(CH₃)₃]₂-[W(=O)(O₂)₂(H₂O)]₂(μ-O)] homogeneous systems but it could be recycled three times without metal leaching. Similar epoxidation SILP catalysts were synthesized with a polyoxometalate anion [γ-1,2-H₂SiV₂W₁₀O₄₀]⁴⁻. As previously described, the stereospecificity, diastereoselectivity and regioselectivity of the supported catalyst are very similar to those of the homogeneous system under the same reaction conditions. Recovery of this catalyst is performed by a simple filtration step and it can be easily recycled without loss of its catalytic performance.⁹⁶ Asymmetric epoxidation was carried out with a chiral (S,S)-Mn(III) salen complex immobilized in [bmim][PF₆], which is supported on an ionic silica modified support with N-octyldihydroimidazolium cation fragments. The supported catalyst presents comparable activity and higher selectivity than the homogeneous catalyst used under the same conditions for the α-methylstyrene and 1-phenylcyclohexene. Recycling studies could be carried out up to three runs.¹³⁹ NMR and ICP-AES analyses showed no leaching of neither Mn(III) salt nor the ionic liquid.

Alcohols oxidation into the corresponding aldehydes and ketones is catalyzed by Ru species. A modified TEOS silica with [1-methyl-3-(triethoxysilylpropyl)imidazolium][RuO₄] was applied in the aerobic oxidation of alcohols using scCO₂ as a reaction medium.⁹⁷ The full conversion of different alcohols gives no sight of over oxidation of aldehydes to carboxylic acids. The catalyst has been reused three times with minor loss of activity (<3 %) and no leaching was detected over the detection limit. Another example with Ru species stabilized by a basic ionic liquid, choline, anchored to a monocristalline MgO showed good performances for the oxidation of benzylalcohol with 100 % conversion upon one hour time, being recycled up to 7 times.⁴⁹ Good results were also achieved with an analogous heterogeneous system in the absence of choline, a deactivation in the first cycle was observed due to the leaching of Ru species, which confirms the synergy between the choline and the surface to stabilize Ru(III). In this system primary alcohols were oxidized faster than secondary ones, when using air instead of O₂; CO₂ do not poison the reaction and it can be carried out without solvent but in low yields. Recently, a heteropolyacid (H₅[PMo₁₀V₂O₄₀]·32.5H₂O) modified supported ionic

liquid was synthesized for application in oxidation reactions of alcohol to aldehydes and ketones.¹⁴⁰ The acidic and redox properties of polyoxometalates based compounds make them suitable catalysts for this type of reaction. Benzylic, allylic and aliphatic alcohols were oxidized under mild conditions using air as oxidant. The activity of the supported catalyst was analogous to the homogeneous one, being reused 5 times without metal loss. Even more, no over oxidation reaction to alcohol was detected.

1.2.8 Cyclopropanation reactions

Mayoral's group reported a SILP catalyst based on a bis(oxazoline)-copper complex immobilized in [bmim][PF₆] supported on a laponite clay for enantioselective cyclopropanation reactions (Scheme 1.20). As previously explained (section 1.1.1), these negative charged multilayer clays can modify the enantioselectivity of a reaction by the formation of ion pairs. With the influence of the support and the ionic liquid film thickness, the reaction can change its enantioselectivity from (1*S*,2*S*)-*trans* isomer in bulk solution to the (1*R*,2*S*)-*cis* isomer in the cyclopropanation of styrene (Table 1.3). The authors affirm that the system acts essentially as a bidimensional nanoreactor.⁵⁴



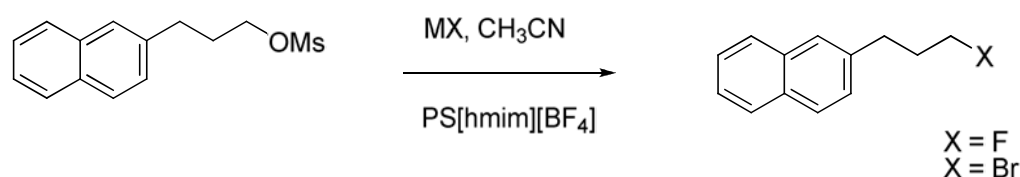
Scheme 1.20: Enantioselective cyclopropanation reactions catalyzed by copper systems.

Entry	Type of catalyst	Yield (%)	<i>trans/cis</i>	<i>ee trans</i> (%)	<i>ee cis</i> (%)
1 ^a	Homogeneous	42	67/33	54	45
2 ^{a,b}	SILPC	3	41/59	27	-53
3 ^b	SILPC	37	33/67	25	-56

Table 1.3: Effect of the catalyst in the cyclopropanation of styrene.^a 1 % catalyst, ^c 3 % catalyst, ^b ILs Film thickness per grame 0.067 mL/g

1.2.9 Phase transfer reactions

Polymer supported ionic liquids can be used as catalyst under phase transfer conditions in nucleophilic substitution reactions. Kim et al. (Scheme 1.21) have reported the use of ionic liquids as efficient catalysts in nucleophilic fluorination and other nucleophilic substitutions such as bromination of 2-(3-methanesulfonyloxypropyl)-naphthalene using alkali metal fluorides (CsF, RbF, KF) (Scheme 1.21).^{79,105}

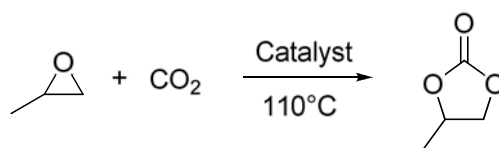


Scheme 1.21: Nucleophilic fluorination catalyzed by ionic liquids.

Actually, a longer linker between polystyrene backbone and the ionic liquid portion, such as 1-N-hexadecyl-3-methylimidazolium tetrafluoroborate ($[\text{hmim}][\text{BF}_4]$), permits an easier access to the ionic liquid. The tetrafluoroborate anion led to the best results. The ionic liquid loading is another important factor; high ILs loading favours fluorination reactions and low loading, bromination ones. Moreover, this catalyst showed high activities when used in tert-alcohols. Tertiary alcohols act as a non polar reaction medium, having a synergistic effect with the supported ILs and good performances with alkali metal fluorides.¹⁰⁶ The system enhances the reactivity of the alkali metal fluorides, forming tight ion pairs, and the reactivity of the leaving group reduces the by-products formation. Additionally, functionalization of the ionic liquid giving a quaternary ammonium salt, $[\text{him}^+\text{OH}][\text{OMs}]$, was tested in this reaction using acetonitrile as a solvent. The results could be compared to those obtained under homogeneous conditions (50 min, 97 % yield, without by-products formation). As stated before, the synergy between the imidazolium salt and the tertiary hydroxyl groups is supposed to be the responsible of the high activity.

1.2.10 Carbon dioxide fixation reactions.

For the development environmental benign processes, the chemical fixation of CO_2 is of great importance. In fact, there are many possibilities for using CO_2 as a safe and cheap C_1 source in organic synthesis. One example is the cyclo-addition of CO_2 to epoxides to produce cyclic carbonates (Scheme 1.22).



Scheme 1.22: Cyclo-addition of CO₂ to epoxides to produce cyclic carbonates.

This reaction has been already studied using homogeneous catalysts with ionic liquids and under heterogeneous conditions using alkali salts and MgO, but in both processes the need of solvent implies a separation step via distillation. The SILPC catalysis was also tested for this reaction. A green, cheap and biodegradable sieves supported choline, chloride/urea ionic liquid has displayed good activity and selectivity in a solvent free reaction with low CO₂ amount.¹⁰⁸ Comparable activity was observed with an imidazolium ILs supported on MCM-41. Higher yields were obtained by Han and co-workers.⁵⁵ They reported a supported ionic liquid polymer (copolymer of [bvim][Cl] and DVB) which shows catalytic activities higher (70 h⁻¹) than those obtained with analogous homogeneous systems [bmim]Cl or [vbim]Cl (54 h⁻¹).

Using silica immobilized ionic liquid catalyst in conjunction with extra metallic salts as zinc chloride has improved the chemical fixation of carbon dioxide with epoxides to form cyclic carbonates without addition of organic solvents. The ionic liquid 1-propyl-3-N-butylimidazolium bromide was immobilized over silica by the sol-gel technique. The zinc salt opens the propyleneoxide ring. SiO₂-ILs-ZnCl₂ can operate at low CO₂ pressures giving high TOF (2712 h⁻¹). They exhibit lower activity than heterogeneous systems but the solvent free conditions as well as the easy recuperation make them very interesting from an environmental point of view.¹⁰⁹

Another solvent free procedure was carried out with a silica supported ionic liquid via the sol-gel technique. Oligomers with carbonate and ether units obtained from phenyl glycidyl ether (PGE) and CO₂, were applied giving very high conversion. This ionic liquid has a linkage composed of four CH₂ groups anchored to the silica surface and gave a conversion of 94 % of PGE with 92 % of carbonate content depending on CO₂ pressure, and the average of monomers units was 712.¹¹⁰

1.2.11 Other reactions

Chen et al. have introduced a task-specific ionic liquid synthesized by pair coupling between the imidazolium cation and L-proline. This ionic liquid was immobilized on a polymer support. The material showed efficient metal scavenging ability and was used in CuI-catalyzed N-arylation of nitrogen-containing heterocycles (Figure 1.9).⁹⁴ Higher catalytic activity was reached with this system compared to L-proline with CuI in [bmim][BF₄] or in

organic solvent. The system was recycled 9 times without loss of activity. An excess of ILs led to an activity loss during the recycling, due to ILs solubility in the reaction medium.

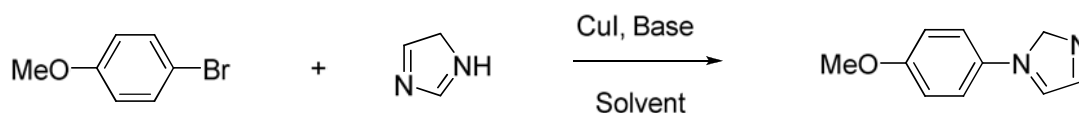
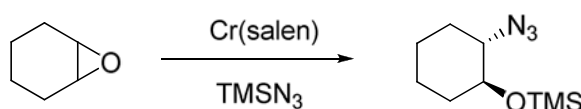


Figure 1.9: CuI-catalyzed N-arylation of nitrogen-containing heterocycles

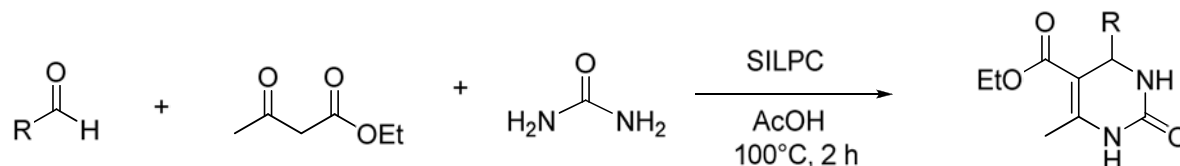
The asymmetric ring opening of epoxides was investigated by Dioos et al. with the chiral Cr(salen) complex in a SILP catalyst with TMSN₃ (Scheme 1.23). Compared with the impregnated dimeric complex, the SILP system permitted an increasing of the reactivity from a TOF of 1.9 h⁻¹ to 11.5 h⁻¹ and in selectivity 87 % vs 66 % for the 1,2-epoxy hexane. Both systems could be recycled 4 times with the same leaching (3.1 % after the 4 cycles) but in the case of “Cr(salen)”, SILP catalyst favoured the catalyst recuperation, in contrast to what was observed for the impregnated supported system.¹⁴¹



TMSN₃: Trimethylsilyl azide

Scheme 1.23: Asymmetric ring opening of epoxides catalyzed by chromium systems.

The Lewis acid catalyzed Biginelli reaction was studied with a supported polymeric ionic liquid phase catalysis with polystyrene-methylimidazolium [Psmim][X] (X = BF₄, PF₆) (Scheme 1.24).⁸⁰ The reaction between aromatic aldehydes, ethyl acetoacetate and urea to obtain the corresponding tetrahydropyrimidine-5-carboxylates was obtained in good yield, up to 99 % and could be recycled 5 times.



R = Ph, Pr, 2-Cl-C₆H₄, 4-Cl-C₆H₄, 2,4-Cl-C₆H₄, 4-NO₂-C₆H₄, 2-MeO-C₆H₄, 4-MeO-C₆H₄,

Scheme 1.24: Biginelli reaction

1.3 STRUCTURED REACTORS: MONOLITHES, MEMBRANES, FIBERS, FIXED BED

One of the main drawbacks of reactions in bulk ionic liquid is the mass transport limitations who make difficult the use of those systems in fixed bed reactors. A theoretical calculation study in the hydrogenation of citral using Pd nanoparticles on active carbon cloth has proved that the internal mass transfer of the substrates and products in the ionic layer is negligible regardless of the ILs quantity.¹⁴² Thus, SILPC is suitable for experiences in a fixed bed reactor, especially advantageous for applications with gas substrates where there is not product separation and catalyst recycling. Moreover, the combination of high solvent polarity and non volatility ensures the catalytic species to remain in the ionic liquid phase of the catalyst even in continuous operation reactions. On the contrary, of the SLP concept, this combination also facilitates the separation of the organic product phase from the catalyst. The high dispersion of the ionic liquid on the support assures a high dispersion of the immobilized catalyst in it, reducing the amount of ionic liquid needed compared to biphasic systems.

Despite all this advantages, SILP catalysts have some limitations in the liquid phase reactions. The minor solubility of ionic liquid in a liquid feedstock/product mixture can be enough to cause the catalyst death by removing the active species in the recycling process. One of the first examples of severe leaching was reported by Mehnert and co-workers in the hydroformylation of 1-hexene in a batch autoclave. Three-times better activity with SILP Rh catalyst than with the biphasic system was achieved, but the loss of the catalyst from the support make this system unrecyclable. Even worst for thin layers only mechanical forces can remove physically the ionic liquid layer. Many studies have focused in the recyclability of SILP catalysts varying the support, the ionic liquid anchored and the catalyst. Riisager et al. reported a SILP catalyst with a life time of 700h for the hydroformylation of propene in a gas phase reaction.¹²³

In separation reactions the ionic liquid was used combined with membranes to create high selective ionic liquid membranes. They usually contains [rmim][X] (R = butyl, octyl, decyl and X = PF₆ and BF₄) as ionic liquid. For the separation of organic compounds the nature of the membrane is very important. Propylene and nylon membranes give the best transport rates, but without control of the selectivity; however the used of supported ionic liquid membranes (SILM) has increased the selectivity of the permeability. For example, [bmim][PF₆] in a polyvinylidene fluoride membrane exhibits an extremely highly selective transport of secondary amines over tertiary ones. The explanation is the stronger hydrogen bonding of the secondary amine to the slightly acidic C-2 positioned hydrogen in the ionic liquid imidazolium cation. The separation of saturated hydrocarbons from the corresponding unsaturated alkenes by SILMs has also been claimed, using polymeric membrane materials.

The supported membranes containing 40 mol % solution of silver nitrate in [Rmim][NO₃] (R = ethyl or butyl). The selectivity was 69 % for alkanes towards alkenes. In polyvinylidene fluoride membranes containing [Rmim][X] (R = butyl, hexyl and octyl, X = PF₆) and [Et₂Me(MeOEt)N][(CF₃SO₂)₂N] ionic liquids, the permeation rates followed the order of the increasing hydrophobicity of the ionic liquids [bmim][PF₆] < [hmim][PF₆] < [omim][PF₆] < [Et₂Me(MeOEt)N][(CF₃SO₂)₂N]) for the selective separation of aromatic hydrocarbons benzene, toluene and p-xylene in polyvinylidene.¹⁴³ Although the permeation rates through the membrane, based on the ionic liquids, were less than those of water, the selectivity of aromatic hydrocarbons was greatly improved. Transport of tritiated water and water-soluble solutes in various membranes with [Rmim][X] (R = butyl, octyl, decyl and X = PF₆ and BF₄) ionic liquids have also been studied.^{144,145} The SILM transport properties for acid gas separations of CO₂ from nitrogen and methane, with water were also studied. The membranes were constituted by water stable ionic liquids [emim]M[X] (X = (CF₃SO₃)₂N, CF₃SO₃, (CN)₂N) and [Hex3TetradecylP]Cl and porous, hydrophilic polyethersulfone. Although water was partially soluble in ionic liquids, the displacement of the ionic liquid from the membranes did not occur and they exhibit high operational stability.¹⁴⁶

SILP polymeric monoliths with an immobilized biocatalyst were used as bioreactors. Anchoring ionic liquid moieties to the monolith has induced peculiar ionic liquid properties to the system. Those monoliths were able to adsorb the enzyme *Candida antarctica* lipase B (CALB) by strong interaction with the ionic liquid phase. The bioreactor was tested for the continuous flow synthesis of citronellyl propionate in supercritical carbon dioxide (scCO₂) by transesterification. The catalytic activity remained practically unchanged for seven operational cycles of 5h, each one performed under different supercritical conditions.⁸⁵

1.4 CONCLUSION

The concept of SILPC systems has been rapidly developed in the last years, resulting in new applications in various reactions. The heterogeneization of homogeneous catalysts by immobilization of complexes or stabilization of NPs without loss of efficiency of the catalyst has not only helped to minimize the quantities of the ionic liquid used, but also opening the scope of an easy and efficient recycling of the catalyst. Additionally, the high stability of NPs in the ILs leads to a good dispersion and no agglomeration of the bulk metal helping to increase the activity and selectivity as well as minimizing the quantities of metal employed. The lack of mass transfer limitations and the good performances exhibited in continuous gas-phase reactions make those systems suitable for industrial applications and could help to

accelerate their introduction in commercial processes. Even though, the synergistic effects between the cation-anion pair of the ILs and the catalyst need further studies, since they can influence the selectivity of a reaction and might be an effective way to improve the performances of a reaction. The understanding of how ILs affects the surface support, their synergy and their influence on the catalytic activity is another research to be performed in this area.

-
- ¹ P. Wasserschied, T. Welton, (Eds.), *Ionic Liquids in Synthesis*, VCH–Wiley, Weinheim **2002**, ISBN 3-527-30515-7.
- ² H. Olivier-Boutbigou, L. Mogna, *J. Mol. Catal. A: Chem.* **2002**, 419, 182.
- ³ K.R Seddon, (Eds.), *Ionic Liquids as Green Solvents*; ACS symposium Series 856; American Chemical Society Washington, DC **2003**.
- ⁴ P.J. Dyson, T.J. Geldbach, (Eds.) *Metal catalyzed reactions in ionic liquids*, Series: *Catalysis by Metal Complexes*, Vol. 9, Springer, Dordrecht **2005**.
- ⁵ (a) M.A.P. Martins, *Chem. Rev.* 2008, 108, 2015; (b) S.M.S. Chauhan, N. Jain, A. Kumar; S. Chauhan, *Tetrahedron* **2005**, 61, 1015.
- ⁶ A. Taubert, *Acta. Chim. Slov.* **2005**, 52, 183.
- ⁷ T. Welton, *Coord. Chem. Rev.* **2004**, 248, 2459.
- ⁸ M. Antonetti, B. Smarsly, Y. Zhou, *Angw. Chem., Int. Ed.* **2004**, 43, 4988.
- ⁹ (a) Y. Zhou, M. Antonietti, *Adv. Mater.* **2003**, 15, 1452. (b) Y. Zhou, M. Antonietti, *Chem. Commun.* **2003**, 2564. (c) Y. Zhou, M. Antonietti, *Chem. Mater.* **2004**, 16, 544.
- ¹⁰ I.F.J. Vankelecom, P.A. Jacobs, (Eds.), *Chiral catalyst immobilization and recycling*, VCH, Weinheim **2000**, chap. 2, pp 19–42.
- ¹¹ J. Dupont, R.F. de Souza, P.A.Z. Suarez *Chem. Rev.* **2002**, 102, 3667.
- ¹² U. Domanska, A. Marciniak, *J. Chem. Eng. Data* **2003**, 48, 451. (b) J.L. Anthony, J.L. Anderson, E.J. Brennecke, *J. Phys. Chem. B* **2005**, 109, 6366.
- ¹³ L.A. Blanchard, D. Hancu, E.J. Beckman, J.F. Brennecke, *Nature* **1999**, 399, 28.
- ¹⁴ J. Dupont, *J. Braz. Chem. Soc.* **2004**, 15, 341.
- ¹⁵ J. Durand, E. Teuma, M. Gómez, *C.R. Chimie* **2007** 10, 152.
- ¹⁶ Y. Chauvin, L. Mussmann, H. Olivier, *Angew. Chem. Int. Ed. Engl.* **1996**, 34, 2698.
- ¹⁷ C.W. Scheeren, G. Machado, J. Dupont, P.F.P. Fichtner, S.R. Teixeira, *Inorg. Chem.* **2003**, 42, 4738.
- ¹⁸ L. Starkey Ott, R.G. Finke, *Coord. Chem. Rev.* **2007**, 251, 1075.
- ¹⁹ C.W. Scheeren, G. Machado, S.R. Teixeira, J. Morais, J.B. Domingos, J. Dupont, *J. Phys. Chem. B* **2006**, 110, 13011.
- ²⁰ P. Migowski, J. Dupont, *Chem. Eur. J.* **2007**, 13, 32.

-
- ²¹ G.S. Fonseca, G. Machado, S.R. Teixeira, G.H. Fecher, J. Morais, M.C.M. Alves, J. Dupont, *J. Colloid Interface Sci.* **2006**, 301, 193.
- ²² A.P. Umpierre, G. Machado, G.H. Fecher, J. Morais, J. Dupont, *Adv. Synth. Catal.* **2005**, 347, 1404.
- ²³ A. Kumar, S.S. Pawar, *J. Org. Chem.* **2004**, 69, 1419.
- ²⁴ Y. Chauvin, A. Hirschauer, H. Olivier, *J. Mol. Catal.* **1994**, 92, 155.
- ²⁵ P.R. Schreiner, *Chem. Soc. Rev.* **2003**, 32, 289.
- ²⁶ P.J. Dyson, *Transit. Met. Chem.* **2002**, 27, 353.
- ²⁷ (a) P. Bonhôte, A.P. Dias, N. Papageorgiou, K. Kalyanasundaram, M. Grätzel, *Inorg. Chem.* **1996**, 35, 1168; (b) R.F. de Souza, V. Rech, J. Dupont, *Adv. Synth. Catal.* **2002**, 344, 153; (c) M. Picquet, I. Tkatchenko, I. Tommasi, P. Wasserscheid, J. Zimmermann, *Adv. Synth. Catal.* **2003**, 345, 959.
- ²⁸ J.S. Wilkes, *Green Chem.* **2002**, 4, 73; a) V.I. Parvulescu, C. Hardacre, *Chem. Rev.* **2007**, 107, 2615.
- ²⁹ (a) M.T. Garcia, N. Gathergood, P.J. Scammells, *Green Chem.* **2005**, 7, 9; (b) K.M. Docherty, C.F. Kulpa, *Green Chem.* **2005**, 7, 185; (c) C. Pretti, C. Chiappe, D. Pieraccini, M. Gregori, F. Abramo, G. Monni, L. Intorre, *Green Chem.* **2006**, 8, 238.
- ³⁰ T. Welton, *Green Chem.* **2008**, 10, 483.
- ³¹ (a) Z. Fei, T.J. Geldbach, D. Zhao, and P.J. Dyson, *Chem. Eur. J.* **2006**, 12, 2122; (c) H. Xue, R. Verma, J.M. Shreeve, *J. Fluorine Chem.* **2006**, 127, 159.
- ³² J. Fraga-Dubreuil, J.P. Bazureau, *Tetrahedron Lett.* **2001**, 42, 6097.
- ³³ Z. Fei, D. Zhao, T.J. Geldbach, R. Scopelliti, P.J. Dyson, *Chem. Eur. J.* **2004**, 10, 4886.
- ³⁴ H. Itoh, K. Naka, Y. Chujo, *J. Am. Chem. Soc.* **2004**, 126, 3026.
- ³⁵ Z. Fei, D. Zhao, R. Scopelliti, P.J. Dyson, *Organometallics*, **2004**, 23, 1622.
- ³⁶ D. Zhao, Z. Fei, T.J. Geldbach, R. Scopelliti, G. Laurency, P.J. Dyson, *Helv. Chim. Acta* **2005**, 88, 665.
- ³⁷ T.J. Geldbach, P.J. Dyson, *J. Am. Chem. Soc.* **2004**, 126, 8114.
- ³⁸ T.L. Merrigan, E.D. Bates, S.C. Dorman, J.H. Davis, *Chem. Commun.* **2000**, 2051.
- ³⁹ W.L. Bao, Z.M. Wang, Y.X. Li, *J. Org. Chem.* **2003**, 68, 591.
- ⁴⁰ D. Zhao, Z. Fei, C.A. Ohlin, G. Laurency, P.J. Dyson, *Chem. Commun.* **2004**, 21, 2500.
- ⁴¹ *Electrochemical Aspects of Ionic Liquids*, Hiroyuki Ohno (Ed.), Wiley Interscience: Hoboken, NJ **2005**.
- ⁴² (a) C.F. Poole, *J. Chromatogr. A.* **2004**, 1037, 49; (b) S. Pandey, *Anal. Chim. Act.* **2006**, 556, 38.
- ⁴³ A.P. de los Ríos, F.J. Hernández-Fernández, F. Tomás-Alonso, J.M. Palacios, D. Gómez, M. Rubio, G. Villora, *J. Membrane Sci.* **2007**, 300, 88.

-
- ⁴⁴ A. Riisager, R. Fehrmann, *Ionic Liquids in Synthesis*, 2nd edn., (Eds.: P. Wasserscheid, T. Welton), Wiley-VCH, Weinheim **2008**, Vol. 2, pp 527 – 558.
- ⁴⁵ C.P. Mehnert, *Chem. Eur. J.* **2005**, 11, 50.
- ⁴⁶ (a) L.A. Gerritsen, A. van Meerkerk, M.H. Vreugdenhil, J.J.F. Scholten, *J. Mol. Catal.* **1980**, 9, 139. (b) L.A. Gerritsen, J.M.Herman, W. Klut, J.J.F. Scholten, *J. Mol. Catal.* **1980**, 9, 157; (c) L.A. Gerritsen, J.M. Herman, J.J.F. Scholten, *J. Mol. Catal.* 1980, 9, 241; (d) L.A. Gerritsen, W. Klut, M.H. Vreugdenhil, J.J.F. Scholten, *J. Mol. Catal.* **1980**, 9, 257; (e) L.A. Gerritsen, W. Klut, M.H. Vreugdenhil, J.J.F. Scholten, *J. Mol. Catal.* **1980**, 9, 265.
- ⁴⁷ J. Hjortkjaer, M.S. Scurell, P. Simonsen, *J. Mol. Catal.* **1979**, 6, 405.
- ⁴⁸ J.P.Arhancet, M.E. Davis, J.S. merola, B.E. Hanson, *Nature*,**1989**,339,454
- ⁴⁹ M.L. Kantam, U. Pal, B. Sreedhar, S. Bhargava, Y.Iwasawa, M. Tada, B.M. Choudary, *Adv. Synth. Catal.***2008**, 350, 1225 – 1229
- ⁵⁰ H. Hagiwara, N. Okunaka, T. Hoshi, T. Suzuki, *Synlett* **2008**, 1813
- ⁵¹ C. deCastro, E. Sauvage, M. H. Valkenberg, W. F. Hölderich, *J. Catal.* **2000**, 196, 86
- ⁵² J.P. Mikkola, P.P. Virtanen, K. Kordas, H. Karhu, T.O. Salmi, *Appl. Catal., A*, **2007**, 328, 68
- ⁵³ J. Huang, T. Jiang, H. Gao, B. Han, Z. Liu, W. Wu, Y. Chang, G. Zhao, *Angew. Chem. Int. Ed.* **2004**, 43, 1397
- ⁵⁴ M.R. Castillo, L. Fousse, J.M. Fraile, J.I. Garcia, J.A. Mayoral *Chem. Eur. J.* **2007**, 13, 287
- ⁵⁵ Y. Xie, Z. Zhang, T. Jiang, J. He, B. Han, T. Wu, K.Ding, *Angew. Chem.* **2007**, 119, 7393 ; *Angew.Chem. Int. Ed.* **2007**, 46, 7255
- ⁵⁶ Akzo Nobel Inc. (F. G. Sherif, L.-J. Shyu), WO 99/03163, **1999**.
- ⁵⁷ (a) IFP (E. Benazzi, A. Hirschauer, J.-F. Joly, H. Olivier, J.-Y. Bernhard), EP 0553 009, **1993**; (b) E. Benazzi, H. Olivier, Y. Chauvin, J. F. Joly, A. Hirschauer, *Abstr. Pap. Am. Chem. Soc.* **1996**, 212, 45.
- ⁵⁸ (a) J.H. Clark, K. Martin, A.J. Teasdale, S.J. Barlow, *Chem. Commun.* **1995**, 2037. (b) J.H. Clark, P.M. Price, K. Martin, D.J. Macquarrie, T.W. Bastock, *J. Chem. Res. Synop.* **1997**, 430. (c) S. Sato, G.E. Maciel, *J. Mol. Catal. A* **1995**, 101, 153.
- ⁵⁹ M.H. Valkenberg, C. deCastro, W.F. Hölderich *Top. Catal* **2001**, 14, 1.
- ⁶⁰ M.H. Valkenberg, C. deCastro, W.F. Hölderich, *Green Chem.* **2002**,4, 88.
- ⁶¹ S. Abelló, F. Medina, X. Rodríguez, Y. Cesteros, P. Salagre, J.E. Sueiras, D. Tichit and B. Coq, *Chem. Commun.* **2004** 1096.

-
- ⁶² J. Joni, M. Haumann, P. Wasserscheid *Adv. Synth. Catal.* **2009**, 351, 423
- ⁶³ C.P. Mehnert, R.A. Cook, N.C. Dispenziere, M. Afeworki, *J. Am. Chem. Soc.* **2002**, 124, 12932; b) ExxonMobil (C. P. Mehnert, R. A. Cook), US 6673 737, **2004**.
- ⁶⁴ C.P. Mehnert, E.J. Mozeleski, R.A. Cook, *Chem. Commun.* **2002**, 3010.
- ⁶⁵ A. Riisager, P. Wasserscheid, R. van Hal, R. Fehrmann, *J. Catal.* **2003**, 219, 452.
- ⁶⁶ A. Corma, H. García, A. Leyva, *Tetrahedron* **2004**, 60, 8553.
- ⁶⁷ H. Hagiwara, Y. Sugawara, K. Isobe, T. Hoshi and T. Suzuki, *Org. Lett.* **2004**, 6, 2325
- ⁶⁸ Y. Yang, H.Q. Lin, C.X. Deng, J.R. She, Y.Z. Yuan, *Chem. Lett.* **2005**, 34, 220
- ⁶⁹ Y. Yang, C. Deng and Y. Yuan, *J. Catal.* **2005**, 232, 108
- ⁷⁰ L. Lou, X. Peng, K. Yu, S. Liu, *Catal. Commun.* **2008**, 9, 1891
- ⁷¹ F. Shi, Q. Zhang, Y. Gu and Y. Deng, *Adv. Synth. Catal.* **2005**, 347, 225
- ⁷² F. Shi, Q. Zhang, D. Li and Y. Deng, *Chem. Eur. J.* **2005**, 11, 5279
- ⁷³ F. Shi and Y. Deng, *Spectrochim. Acta A* **2005**, 62, 239
- ⁷⁴ Y. Gu, C. Ogawa, J. Kobayashi, Y. Mori, S. Kobayashi, *Angew. Chem.* **2006**, 118, 7375 – 7378; *Angew. Chem. Int. Ed.* **2006**, 45, 7217 – 7220
- ⁷⁵ M. Ruta, I. Yuranov, P.J. Dyson, G. Laurenczy, L. Kiwi-Minsker, *J. Catal.* **2007**, 247, 269
- ⁷⁶ P. Tribolet, L. Kiwi-Minsker, *Catal. Today* **2005**, 102, 15
- ⁷⁷ S. Breitenlechner, M. Fleck, T.E. Müller and A. Suppan, *J. Mol. Catal. A Chem.* **2004**, 214, 175
- ⁷⁸ S.D. Miao, Z.M. Liu, B.X. Han, *J. Phys. Chem. C*, **2007**, 111, 2185.
- ⁷⁹ D.W. Kim, D.Y. Chi *Angew. Chem. Int. Ed.* **2004**, 43, 483
- ⁸⁰ Z.T. Wang, S.C. Wang, L.W. Xu, *Helv. Chim. Acta*, **2005**, 88, 986.
- ⁸¹ A. Wolfson, I.F.J. Vankelecom, P.A. Jacobs, *Tetrahedron Lett.*, **2003**, 44, 1195
- ⁸² L. Wang, Y. Zhang, C. Xie, Y. Wang, *Synlett*, **2005**, 12, 1861.
- ⁸³ J. Baudoux, K. Perrigaud, P.J. Madec, A.C. Gaumont, I. Dez, *Green Chem.* **2007**, 9, 1346
- ⁸⁴ M.J. Muldoon and C.M. Gordon, *J. Polym. Sci., Part A: Polym. Chem.* **2004**, 42, 3865
- ⁸⁵ P. Lozano, E. GarcKarbass, T.D. Diego, M.I. Burguete, S.V. Luis, J.L. Iborra, *Adv. Synth. Catal.* **2007**, 349, 1077
- ⁸⁶ R.T. Carlin, J. Fuller, *Chem. Commun.* **1997**, 15, 1345
- ⁸⁷ L.C. Branco, J.G. Crespo and C.A.M. Afonso, *Chem. Eur. J.*, **2002**, 8, 3865

-
- ⁸⁸ C. Aprile, F. Giacalone, M. Gruttadauria, A.M. Marculescu, R. Noto, J.D. Revell, H. Wennemers *GreenChem.* **2007**, *9*, 1328
- ⁸⁹ M. Gruttadauria, S. Riela, C. Aprile, P. Lo Meo, F. D'Anna, R. Noto, *Adv. Synth. Catal.*, **2006**, *348*, 82
- ⁹⁰ M.J. Park, J.K. Lee, B.S. Lee, Y.W. Lee, I.S. Choi, S.G. Lee, *Chem. Mater.* **2006**, *18*, 1546.
- ⁹¹ Y.S. Chun, J.Y. Shin, C.E. Song, S.G. Lee, *Chem. Commun.* **2008**, 942.
- ⁹² M.H. Valkenberg, C. DeCastro, W.F. Holderich, *Appl.Catal. A* **2001**, *215*, 185
- ⁹³ Y. Kume, K. Qiao, D. Tomida, C. Yokoyama *Catal. Commun.* **2008**, *9*, 369
- ⁹⁴ W. Chen, Y. Zhang, L. Zhu, J. Lan, R. Xie, J. You, *J. Am. Chem. Soc.* **2007**, *129*, 13879.
- ⁹⁵ K. Yamaguchi, C. Yoshida, S. Uchida, N. Mizuno, *J. Am.Chem. Soc.*, **2005**, *127*, 530
- ⁹⁶ J. Kasai, Y. Nakagawa, S. Uchida, K. Yamaguchi, N. Mizuno, *Chem.–Eur. J.*, **2006**, *12*, 4176
- ⁹⁷ R. Ciriminna, P. Hesemann, J.J.E. Moreau, M. Carraro, S.Campestrini, M. Pagliaro, *Chem.–Eur. J.*, **2006**, *12*, 5220
- ⁹⁸ J.P. Mikkola, P. Virtanen, H. Karhu, T. Salmi, D.Y. Murzin, *Green Chem.*, **2006**, *8*, 197
- ⁹⁹ R. Tao, S. Miao, Z. Liu, Y. Xie, B. Han, G. An, K. Ding, *Green Chem.* **2009**, *11*, 96.
- ¹⁰⁰ K. Qiao, H. Hajiwara, C. Yokoyama, *J. Mol. Catal. A: Chem.* **2006**, *246*, 65
- ¹⁰¹ Y. Fang, X. Lao, Y. Li, B. Zhou, B. Huang, K. Zhang, *Faming Zhuanli Shenqing Gongkai Shuomingshu*, **2008**, CN 2007–10031101.5
- ¹⁰² C. Paun, J. Barklie, P. Goodrich, H.Q.N. Gunaratne, A. McKeown, V.I. Pârvulescu, C. Hardacre, *J. Mol.Catal. A: Chem.* **2007**, *269*, 61.
- ¹⁰³ L.F. Xiao, Q.F. Yue, C.G. Xia, L.W. Xu, *J. Mol.Catal. A: Chem.* **2008**, *279*, 230.
- ¹⁰⁴ H. Kaper, M. Antonietti, F. Goettmann, *Tetrahedron Lett.* **2008**, *49*, 4546
- ¹⁰⁵ D.W. Kim, D.J. Hong, K.S. Jang, D.Y. Chi, *Adv.Synth. Catal.* **2006**, *348*, 1719.
- ¹⁰⁶ D.W. Kim, H.J. Jeong, S.T. Lim, M.H. Sohn, D.Y. Chi, *Tetrahedron* **2008**, *64*, 4209
- ¹⁰⁷ S.S. Shinde, B.S. Lee, D.Y. Chi, *Tetrahedron Lett.* **2008**, *49*, 4245.
- ¹⁰⁸ A. Zhu, T. Jiang, B. Han, J. Zhang, Y. Xie, X. Ma, *Green Chem.* **2007**, *9*, 169 .
- ¹⁰⁹ L.F. Xiao, F.W. Li, J.J. Peng, C.G. Xia, *J. Mol.Catal. A: Chem.* **2006**, *253*, 265
- ¹¹⁰ H.L. Shim, M.K. Lee, K.H. Kim, D.W. Park, S.W. Park, *Polym. Adv. Technol.* **2008**, *19*, 1436
- ¹¹¹ P. Li, L. Wang, M. Wang, Y. Zhang, *Eur. J. Org. Chem.* **2008**, 1157.

-
- ¹¹² J. D. Aiken III, R.G. Finke, *J. Mol. Catal. A: Chem.* **1999**, 145, 1.
- ¹¹³ P.J. Dyson, *Coord. Chem. Rev.* **2004**, 248, 2443.
- ¹¹⁴ J. Dupont, G.S. Fonseca, A.P. Umpierre, P.F.P. Fichtner, S.R. Teixeira, *J. Am. Chem. Soc.* **2002**, 124, 4228
- ¹¹⁵ M.A. Gelesky, S.S. X. Chiaro, F.A. Pavan, J.H.Z. dos Santos, *J. Dupont Dalton Trans.*, **2007**, 5549
- ¹¹⁶ S.D. Miao, Z.M. Liu, B.X. Han, *Angew. Chem. Int. Ed.*, **2006**, 45, 266.
- ¹¹⁷ M.L. Kantam, R.S. Reddy, U. Pal, B. Sreedhar, S. Bhargava, *Adv. Synth. Catal.* **2008**, 350, 2231.
- ¹¹⁸ B. Karimi, D. Enders, *Org. Lett.* **2006**, 8, 1237
- ¹¹⁹ M. Ruta, G. Laurency, P.J. Dyson, L. Kiwi-Minsker, *J. Phys. Chem. C* **2008**, 112, 17814 .
- ¹²⁰ K. Qiao, R. Sugimura, Q. Bao, D. Tomida, C. Yokoyama, *Catal. Commun.* **2008**, 9, 2470.
- ¹²¹ R. Abu-Reziq, D. Wang, M. Post, H. Alper, *Adv. Synth. Catal.* **2007**, 349, 2145
- ¹²² A. Riisager, P. Wasserscheid, R. van Hal, R. Fehrmann, *J. Catal.* **2003**, 219, 452
- ¹²³ A. Riisager, R. Fehrmann, S. Flicker, R. van Hal, M. Haumann, P. Wasserscheid, *Angew. Chem.* **2005**, 117, 826; *Angew. Chem. Int. Ed.* **2005**, 44, 815
- ¹²⁴ A. Riisager, R. Fehrmann, M. Haumann, B.S.K. Gorle, P. Wasserscheid, *Ind. Eng. Chem. Res.* **2005**, 44, 9853
- ¹²⁵ M. Haumann, K. Dentler, J. Joni, A. Riisager, P. Wasserscheid, *Adv. Synth. Catal.* **2007**, 349, 425
- ¹²⁶ A.G. Panda, M.D. Bhor, S.R. Jagtap, B.M. Bhanage *App. Catal. A: General* **2008**, 347, 142
- ¹²⁷ A.G. Panda, S.R. Jagtap, N.S. Nandurkar, B.M. Bhanage *Ind. Eng. Chem. Res.* **2008**, 47, 969
- ¹²⁸ U. Hintermair, G. Zhao, C.C. Santini, M.J. Muldoon, D.J. Cole-Hamilton, *Chem. Commun.* **2007**, 1462
- ¹²⁹ O. Jimenez, T.E. Muller, C. Sievers, A. Spirkel, J.A. Lercher, *Chem. Commun.*, **2006**, 2974
- ¹³⁰ C. Sievers, O. Jimenez, R. Knapp, X. Lin, T.E. Muller, A. Turler, B. Wierczinski, J.A. Lercher *J. Mol. Catal. A* **2008**, 279, 187
- ¹³¹ K.L. Fow, S. Jaenicke, T. E. Muller, C. Sievers *J. Mol. Catal. A* **2008**, 279, 239
- ¹³² J.C. Chang, J.C. Lin, C.Y. Lee, G.T. Wei, J.C. Wu, U.S. Patent 20080269533, **2008**.
- ¹³³ A. Berger, R.F. de Souza, M.R. Delgado, J. Dupont, *Tetrahedron: Asymmetry*, **2001**, 12, 1825.
- ¹³⁴ A. Riisager, R. Fehrmann, WO2006122563, **2006**.
- ¹³⁵ H. Hagiwara, K.H. Ko, T. Hoshi, T. Suzuki, *Chem. Commun.* **2007**, 2838 .
- ¹³⁶ M. Trilla, G. Borja, R. Pleixats, M.W.C. Man, C. Bied, J.J.E. Moreau, *Adv. Synth. Catal.* **2008**, 350, 2566
- ¹³⁷ X. Ma, Y. Zhou, J. Zhang, A. Zhu, T. Jiang, B. Han, *Green Chem.* **2008**, 10, 59

-
- ¹³⁸ S. Doherty, P. Goodrich, C. Hardacre, V. Pârvulescu, C. Paun, *Adv. Synth. Catal.* **2008**, 350, 295
- ¹³⁹ L. Lou, K. Yu, F. Ding, W. Zhou, X. Peng, S. Liu, *Tetrahedron Letters* **2006**, 47, 6513
- ¹⁴⁰ A. Bordoloi, S. Sahoo, F. Lefebvre, S.B. Halligudi, *J. Catal.* **2008**, 259, 232–239
- ¹⁴¹ B.M.L. Dooos, P.A. Jacobs, *J. Catal.* **2006**, 243, 217
- ¹⁴² J.P. Mikkola, J. Warna, P. Virtanen, T. Salmi, *Ind. Eng. Chem. Res.* **2007**, 46, 3932
- ¹⁴³ M. Matsumoto, Y. Inomoto, K. Kondo, *J. Membr. Sci.* **2005**, 246, 77
- ¹⁴⁴ R. Fortunato, C.A.M. Afonso, M.A.M. Reis, J.G. Crespo, *J. Membr. Sci.* **2004**, 242, 197.
- ¹⁴⁵ R. Fortunato, C.A.M. Afonso, J. Benavente, E. Rodriguez-Castellón, J.G. Crespo, *J. Membr. Sci.* **2005**, 256, 216.
- ¹⁴⁶ P. Scovazzo, J. Kieft, D.A. Finan, C. Koval, D. DuBois, R. Noble, *J. Membr. Sci.* **2004**, 238, 57.

CHAPTER II

Multi-walled carbon nanotubes surface modification

2 MULTI-WALLED CARBON NANOTUBES SURFACE MODIFICATION

2.1 CARBON NANOTUBES: GENERALITIES AND HISTORY

Carbon nanotubes (CNTs) represent one of the earliest materials related to nanotechnologies. They can be defined as an ultra strong 1-D nanoscale material showing chemical stability, excellent mechanical properties, high surface area and thermal conductivity.¹ Due to their specific properties and potential applications, a wide number of research fields involve CNTs such as physics and materials.

Until 1985, the only known natural allotropes of carbon were diamond, with sp^3 hybridization, showing 3D covalent arrangement and graphite, with sp^2 hybridization, exhibiting stacked graphene sheets of linked hexagonal rings. At that time, Kroto, Curl and Smalley discovered the fullerenes.² Fullerenes are considered as graphitic sheets composed of hexagonal and pentagonal rings rolled up into a spherical shape.³ There are different types of fullerenes depending on the number of carbon atoms. The smallest and the most common fullerene is C_{60} constituted by 60 carbons. Nanotubes are considered as fullerenes like structure. Even though it is commonly considered that CNTs were discovered by S. Iijima in 1991 during his work involving fullerenes,⁴ TEM researches of Hillert in 1958 showed nanocarbon filaments produced by catalytic cracking.⁵

2.1.1 Structure of carbon nanotubes

Nowadays, CNTs can be classified in three different families depending on graphene sheets number or their arrangement: single-walled carbon nanotubes (SWCNTs), multi-walled carbon nanotubes (MWCNTs) and carbon nanofibers (CNFs). CNFs do not exhibit inner cavity, and they have been in particular studied to understand the CNTs growth process. Their quite variable external diameter can reach 500 nm. The different types of CNFs are classified according to the orientation of the graphene layers with respect to the growth catalytic axis. They can be grouped in three different families: ribbon like structure (CNF-R), where the graphite platelets are aligned parallel to the fiber axis; platelet-like structure (CNF-P), where the graphite platelets in the carbon material are oriented perpendicular to the fiber axis; herringbone type structure or fishbone nanofibers (CNF-H), where the graphitic layers are orientated at an angle to the fiber axis (Figure 2.1).⁶

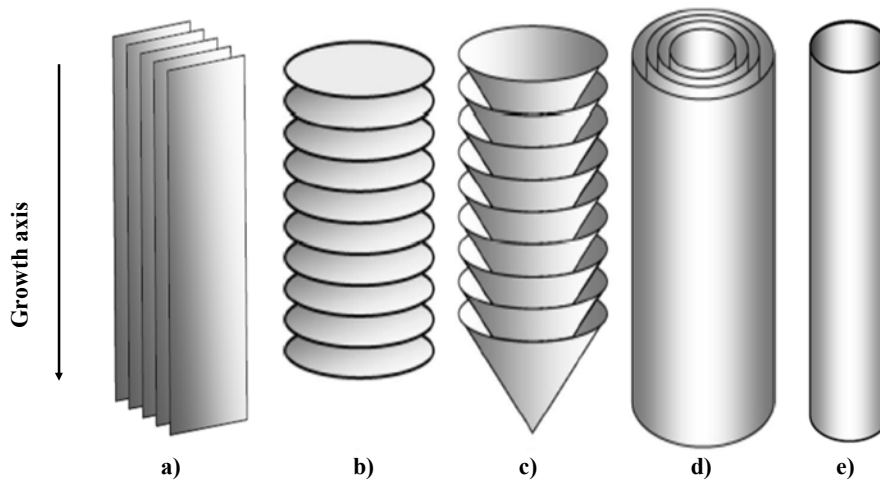


Figure 2.1: Representation of CNTs and CNF. (a) CNF-R, (b) CNF-P, (c) CNF-H, (d) MWCNTs, (e) SWCNTs

2.1.1.1 Single-walled carbon nanotubes

The structure of a SWCNTs can be described by wrapping a one-atom-thick layer of graphite called graphene into a seamless cylinder. These cylindrical carbon structures exhibit a number of novel properties.⁷ They show noteworthy strength and unique electrical properties being also efficient conductors of heat. The way that the graphene sheet is wrapped, is represented by a pair of indices (n,m) , called chiral vector. The n and m integers denote the number of unit vectors along two directions in the hexagonal crystal lattice of graphene. If $m = 0$, the nanotubes are called "zigzag". If $n = m$, the nanotubes are called "armchair". Otherwise, they are named "chiral" (Figure 2.2). SWCNTs have a diameter close to 1 nanometre, with a tube length that can arise more than one centimetre.⁸

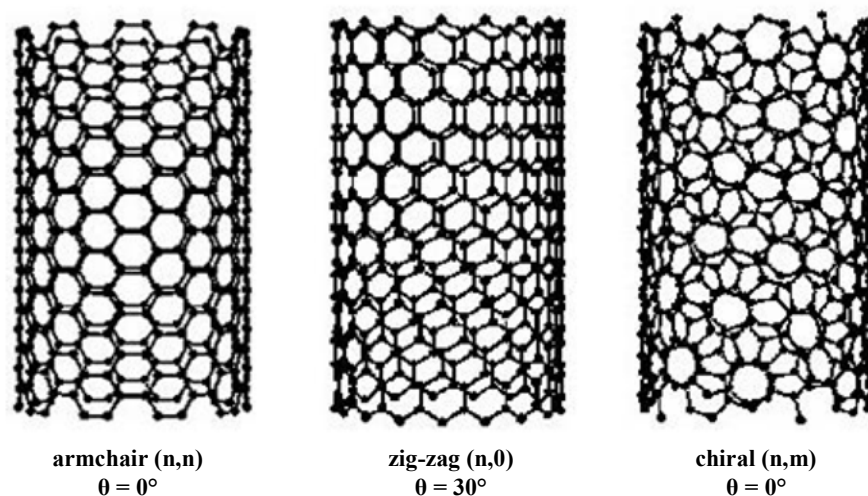


Figure 2.2: Different types of SWCNTs

2.1.1.2 Multi-walled carbon nanotubes

MWCNTs consist of multiple rolled layers (concentric tubes) of graphene. There are two models which can describe their structures. The “Russian doll” model consisting in graphite sheets arranged in concentric cylinders and the “parchment” model where a single sheet of graphite is rolled up around itself. The interlayer distance (\AA_{002}) in CNTs is around 0.340 nm, a bit more than for graphite (0.335 nm). This difference can be caused by the rolled structure of the graphene plans and the π -electronic interactions. The diameter of a multi-walled nanotube depends on the number of walls involved. Typically, the internal average diameter goes from 5 to 20 nm, while the external one varies between 10 and 50 nm. The tube length can come up to several micrometers.

Three types of MWCNTs have been particularly studied, the double-walled carbon nanotubes (DWCNTs), the bamboo like and the coiled nanotubes. The morphology and properties of DWCNTs are similar to those showed by SWCNTs. Nevertheless, their resistance to chemical modifications is improved, an important aspect for surface functionalization in order to modulate CNTs properties. A covalent functionalization of the SWCNTs surface breaks C-C double bonds creating holes and thus modifying their mechanical and electrical properties. DWCNTs show small external diameter that can vary from 1 to 3 nm.⁹ Bamboo-like CNTs consist in a linear chain of hollow segments. Perpendicular graphite sheets to the growing axis close up the tube making regular compartments showing nearly the same length.¹⁰ Coiled nanotubes have heptagons or pentagons regularly distributed in their structure conferring a regular helicity.¹¹

A constant in all types of CNTs is the lip-lip interaction between the graphene layers, favouring the stabilization of these structures.

2.1.2 Synthesis of CNTs

Different synthetic methodologies exist to produce CNTs. They can be classified in two categories: physical techniques at high temperature such as arc discharge or laser ablations and chemical techniques at moderate temperatures, mainly catalytic chemical vapour deposition (C-CVD).

2.1.2.1 Arc discharge

The arc discharge method used for the synthesis of fullerenes¹² has permitted the discovery of CNTs.⁴ When an electrical current is applied and the graphite electrodes are close enough, an electric arc discharge takes place. The temperature rises up to 3,000-4,000 °C. During this process, the carbon of the negative electrode sublimates, due to the high temperature, and it is then deposited on the cathode.¹³

Because nanotubes were initially discovered using this technique, for some time it has been the most widely-used method of nanotube synthesis, especially for MWCNTs. In 1993, Iijima and Bethune also produced SWCNTs with the arc discharge approach adding iron or cobalt in the anode acting as catalysts, giving low selectivities.¹⁴ Further optimization of this methodology has led to better selectivity but it remains low.¹⁵

2.1.2.2 Laser ablation

The laser ablation is another high temperature method to prepare carbon nanotubes, it was developed for the first time by Smalley.¹⁶ In this method, a pulsed laser vaporizes graphite in a reactor at high temperature (1,000 to 2,000 °C) in a reactor, while an inert gas is bled into the chamber. The gas flow transports the product resulting from the reorganization of the carbon vapour to the cooler zone where it can be recovered.^{15,17} The laser ablation mainly leads to the production of SWCNTs, but it is more expensive than the arc discharge approach (see section 2.1.2.1) and chemical vapour deposition (see section 2.1.2.3)

2.1.2.3 Chemical vapour deposition (CVD)

The catalytic vapour deposition of carbon was first reported in 1959,¹⁸ but it was not until 1993¹⁹ that carbon nanotubes were produced by this process. Currently, this is the most interesting method for a large scale and continuous industrial production of CNTs.

A carbon source, generally a hydrocarbon (methane, ethane, ethylene or acetylene), carbon monoxide²⁰ or ethanol,²¹ is decomposed over a metal nanocatalyst (nickel, cobalt, iron, or a mixture of them). The catalyst can be prepared in-situ, during the growth of CNTs (homogeneous phase) or in a previous step (heterogeneous phase). The versatility of the synthetic method allows the production of CNFs, SWCNTs and MWCNTs at relative low temperatures (700 °C).

The diameters of the produced carbon nanotubes are generally related to the size of the metal particles used as catalysts. The hydrocarbon gas is decomposed at the surface of the catalyst particle, and the carbon atoms diffuse and precipitate to the edges of the particle to form nanotubes. The catalyst particles can stay at the tips of the growing nanotube during the synthetic process, or remain at the nanotube base, depending on the metal support interaction.

For commercial purposes, the metallic nanoparticles are generally supported over MgO or Al₂O₃, which increases the surface area leading to high yields and the CNTs remain anchored to the support. An acid treatment may be needed to eliminate the catalyst that sometimes can destroy the original surface of the nanotubes. Alternative water soluble catalyst supports (alkali chloride such as CaCl₂) have also been used for nanotubes growth.²²

CVD growth of multi-walled carbon nanotubes is used worldwide by several companies, such as Arkema, Bayer, Hyperion Catalysis, Mitsui, Nanocyl, NanoLab, Nanothinx and Showa Denko, to produce materials on the ton scale.

2.1.3 Properties

2.1.3.1 Physical properties

Although CNTs are close in structure to graphite, their intrinsic properties are different and of high interest. Their mechanical and electrical properties are particularly remarkable.

Carbon nanotubes are the strongest and stiffest discovered materials in terms of tensile strength and elastic modulus. This strength results from the covalent sp² bonds formed between the individual carbon atoms.²³ Table 2.1 summarizes the Young's modulus and the tensile strength of CNTs compared to other materials. It should be noted that Young's modulus varies from 11050 GPa (SWCNTs²⁴) to 1250 GPa (MWCNTs²⁵), higher than those observed for CNFs. Under excessive tensile strain, the tubes undergo permanent plastic deformation. Both properties make CNTs attractive for the synthesis of nanocomposites materials.

Material	Young's Modulus (GPa)	Tensile strength (GPa)
SWCNTs	1050	150
MWCNTs	1260	150
CNFs	230	3.5
Stainless steel	208	0.4
Epoxide resin	3.5	0.005
Wood	16	0.008

Table 2.1: Young's modulus and the tensile strength (in giga pascal units) of CNTs and other materials.

The structure of a nanotube strongly affects its electrical properties because of the symmetry and unique electronic structure of graphene.¹⁵ In SWCNTs, for a given (n,m) vector the nanotube shows a metallic character ($n = m$), or a semiconductor behaviour with a very small band gap (n,m is a multiple of three); otherwise the nanotube behaves as a moderate semiconductor. A conductivity of 3×10^4 S/cm was determined for a SWCNTs bundle beam.²⁶ The electronic properties for MWCNTs are more complex. At high temperatures, they act like CNFs or graphite, but at low temperature they show a similar comportment than that exhibit by 2D quantum conductors.²⁷

The temperature stability of single-walled carbon nanotubes is estimated to be up to 2800 C under vacuum and about 750 °C at air atmospheric pressure.²⁸ CNTs present similar thermal conductivity than that observed for graphite, showing values of *ca.* 3000 W/mK.²⁹ Theoretical predictions for one isolated SWCNTs can reach 6600W/mK.³⁰

The adsorption energies of small molecules or organic compounds on CNTs are lower than those exhibited by graphite due to the sp^2 non planar carbon bonds, but the binding energy between CNTs and the adsorbed species are higher.³¹

In general, the measured experimental values for the CNTs physical properties are lower than theoretical predictions due to the presence of structural defects. In fact, the presence of heptagons and pentagons instead of hexagons and encapsulated metal nanoparticles diminish those properties. On the contrary, the structural defects increase the surface reactivity, a great advantage for their chemical modifications.

2.1.3.2 Chemical properties

The chemistry of CNTs is a current subject of intense research, which produces continuous advances and novel materials. Several approaches for the functionalization of CNTs have been developed, in both molecular and supramolecular chemistry. These approaches include functionalization of defects, covalent functionalization of the side-walls, non-covalent exohedral functionalization like the formation of supramolecular adducts using surfactants or polymers, and endohedral functionalization using fullerenes (Figure 2.3).³²

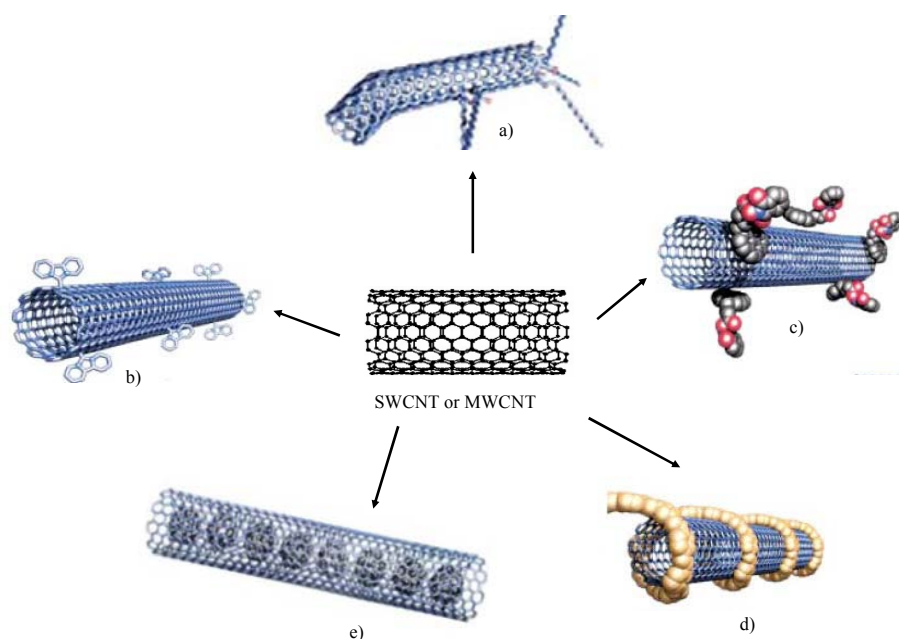


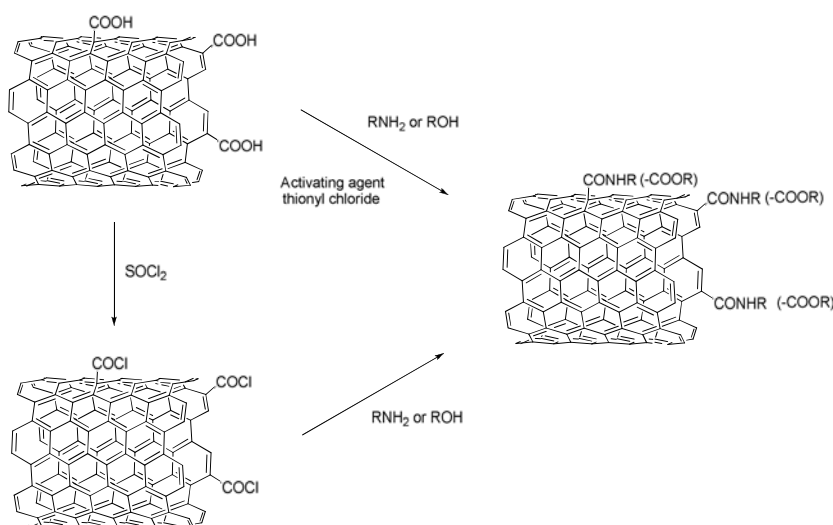
Figure 2.3: Different functionalization for CNTs: a) defect-group functionalization, b) covalent side-wall functionalization, c) non-covalent exohedral functionalization with surfactants, d) non-covalent exohedral functionalization with polymers, and e) endohedral functionalization

Acid treatment, used for CNTs purification or their functionalization, attacks penta- and hepta-rings of the tubes decorating them with oxygenated functionalities, mainly carbonyl and carboxylic groups. Defects are therefore a promising starting point for the development of a covalent chemistry and they are mainly located on the side-walls edges closing the tubes as semi-fullerenes.

The procedure was initially developed to remove the metal catalyst impurity present in the raw nanotube samples. Nanotubes were sonicated/refluxed either in concentrated nitric acid or in a mixture of sulphuric and nitric acid. This method was employed mainly for carbon nanofibers,^{33,34,35} but also for multi-walled^{36,37} or single-walled carbon nanotubes.^{38,39,40} A

prolonged reflux induces the opening of MWCNTs tips, damages the walls and slightly increases the BET surface area.⁴¹ Carboxyl, hydroxyl and carbonyl groups formed can be identified by IR spectroscopy^{37,42,43} or XPS.^{37,39,44} Other liquid phase oxidations have been successfully employed; for example, using potassium permanganate⁴⁵, osmium tetroxide, hydrogen peroxide and ozone as oxidants.⁴⁶ Alternative gas phase oxidation under air can be also used, but contrarily to liquid-phase oxidation, this method is employed to generate phenolic or carbonyl groups.^{44,47} A hydrothermal method has also been reported.⁴⁸ Additionally, the ball-milling of CNTs under reactive atmosphere such as acetylene/nitrogened to the formation of short and functionalized nanotubes.^{49,50,51}

Chen et al. activated CNTs via acylation of carboxylic acid groups in order to introduce long chain alkylamines.⁵² The resulting material is soluble in organic solvents. Bundles of CNTs break up into individual tubes and allow the uptake of solvent molecules. Esterification reactions resulted also in soluble functionalized nanotubes.⁵³ Polymers and dendrimers with terminal amino or hydroxyl groups have been coupled to activated tubes to give amide or ester functionalization (Scheme 2.1).⁵⁴

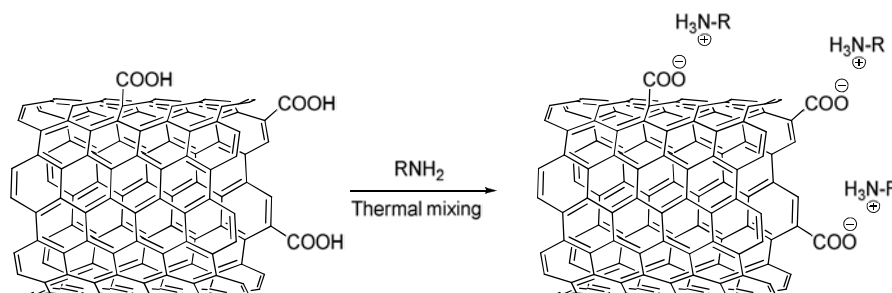


Scheme 2.1: Functionalization of carbon nanotubes starting from oxidized surfaces through the defect sites.

The amidation or esterification of oxidized nanotubes has become one of the most popular ways to produce soluble materials either in organic solvents or in water. Solid-state reaction between oxidized nanotubes and 2-aminoethanesulfonic acid afforded a water soluble material.⁵⁵ Other functionalities giving water soluble materials are glucosamine,⁵⁶ galactose⁵⁷ and mannose,⁵⁸ covalently attached to the nanotubes.

The functionalization of MWCNTs with ionic moieties increases the CNTs solubility in ionic liquids. The relative solubility of the functionalized MWCNTs in ILs, water and organic solvents could be varied by the anion exchanges.^{59,60}

Direct thermal mixing of oxidized carbon nanotubes and alkylamines produces functional materials containing ammonium salts (Scheme 2.2).^{52,61,62}



Scheme 2.2: Direct thermal mixing between CNTs and long chain amines

Other modifications such as silylations of CNT surface with silanes and carboxylate salts under basic conditions have also been reported⁶³

Attaching the acidic moieties of the CNTs to a graphitic surface can control the deposition and alignment of the tubes on a surface. Important progress concerning the controlled deposition of CNTs on gold surfaces has been achieved by introduction of thiol groups at the CNTs surface starting from carboxyl-terminated CNTs.⁶⁴

CNTs grown by the arc-discharge or laser ablation methods have been fluorinated using elemental fluorine at relative low temperatures (<600 °C).⁶⁵ The fluorination reaction is very useful because further substitution can be accomplished,⁶⁶ using Grignard⁶⁷ or organolithium⁶⁸ reagents containing alkyl groups. Several diamines⁶⁹ and diols⁴⁶ have also been reported to react with fluoronanotubes via nucleophilic substitution reactions.

Other covalent functionalizations such as hydrogenation, cycloadditions, radical addition, electrophilic additions, addition of inorganic compounds, ozonolysis, mechano-chemical functionalizations, nucleophilic additions, plasma activation and grafting polymers have been reviewed.⁶³

Non-covalent functionalization of CNTs is very attractive because it offers the possibility to link chemical handles without affecting the electronic network of the tubes. The non-covalent interactions are mainly based on Van der Waals forces or π - π stacking interactions. Polymers, polynuclear aromatic compounds, surfactants and biomolecules can be anchored following this approach.⁶³

Endohedral filling of CNTs is of high interest to produce nanowires or for efficient storage of liquid fuels. Thus fullerenes derivatives,⁷⁰ inorganic species,⁷¹ biomolecules such as DNA,⁷² ionic liquids⁷³ and bimetallic nanoparticles have been encapsulated selectively in the CNTs inner cavity.⁷⁴

2.1.4 Potential and current applications

The strength, flexibility and thermal stability of carbon nanotubes make them suitable to control other nanoscale structures, opening an important role in nanotechnology engineering.^{75,76} Although they can show good mechanical properties,⁷⁷ The main drawback in the synthesis of these nanocomposites is the non-homogeneous dispersion of the nanotubes in the matrix.⁷⁸

Due to their dimensions and unusual electric conduction, CNTs are appropriate for electrical components.⁷⁹ They are used for polymer and conducting materials design, the electronically properties of which are interesting for field emission and make them suitable for flat screens.⁸⁰ Carbon nanotubes are also used for constructing organic solar cells from polymers in renewable energy. Solar cells developed at the New Jersey Institute of Technology use a mixture of carbon nanotubes and fullerenes to form snake-like structures. Actually, buckyballs trap electrons in their structure but they cannot produce electrons flow. On the other hand, nanotubes, behaving like copper wires can then induce the electrons or current flow. Therefore, the light of the sun excites the polymers making buckyballs capturing the electrons and carbon nanotubes inducing the current flow.⁸¹ Solar cells base on C₆₀ derivatives are also reported.⁸²

Their chemical properties such as high adsorbent capacity and thermal conductivity make CNTs promising materials for catalytic applications. Even more, CNTs should offer significant advantages such as: (i) high catalytic activities arising from the mesoporous nature of these supports which avoids mass transfer limitations;⁸³ (ii) high activities and/or selectivities due to the possibility to operate in the inner cavity of carbon nanotubes (confinement effect); a recent report has shown an increase in activity of more than one order of magnitude when CNTs are used as a support;⁸⁴ (iii) well-defined and tunable structure,⁸⁵ and (iv) the possibility to build a micro-reactor by selective growth of nanocarbons by catalytic chemical vapour deposition (C-CVD) on defined substrates.⁸⁶ The best results have been obtained for hydrogenation, dehydrogenation of alcohols, hydroformylation and catalytic decomposition of hydrocarbons.⁸⁵

One major drawback of CNTs is their difficult processability and/or dispersibility linked to the inert and apolar character of their surface; covalently modified CNTs can overcome this disadvantage. Our group has studied activation procedures of MWCNTs⁸⁷ and their external functionalization in order to obtain a selective deposition of nanoparticles either in the inner cavity or on the external surface.⁷⁴ In the present work, the preparation of functionalized MWCNTs by ionic moieties covalently linked to the surface in order to immobilized ionic liquid catalytic phases is described. High purity multi-walled carbon nanotubes were

functionalized with ionic moieties to improve their compatibility and dispersion in ionic liquid medium.

2.2 RESULTS AND DISCUSSION

Multi-walled Carbon Nanotubes used in this work were synthesized by CVD using Fe/Al₂O₃ as catalyst at 650 °C. Some pictures of these MWCNTs at human and micro and nanometric scales (TEM images) are presented in Figure 2.4.

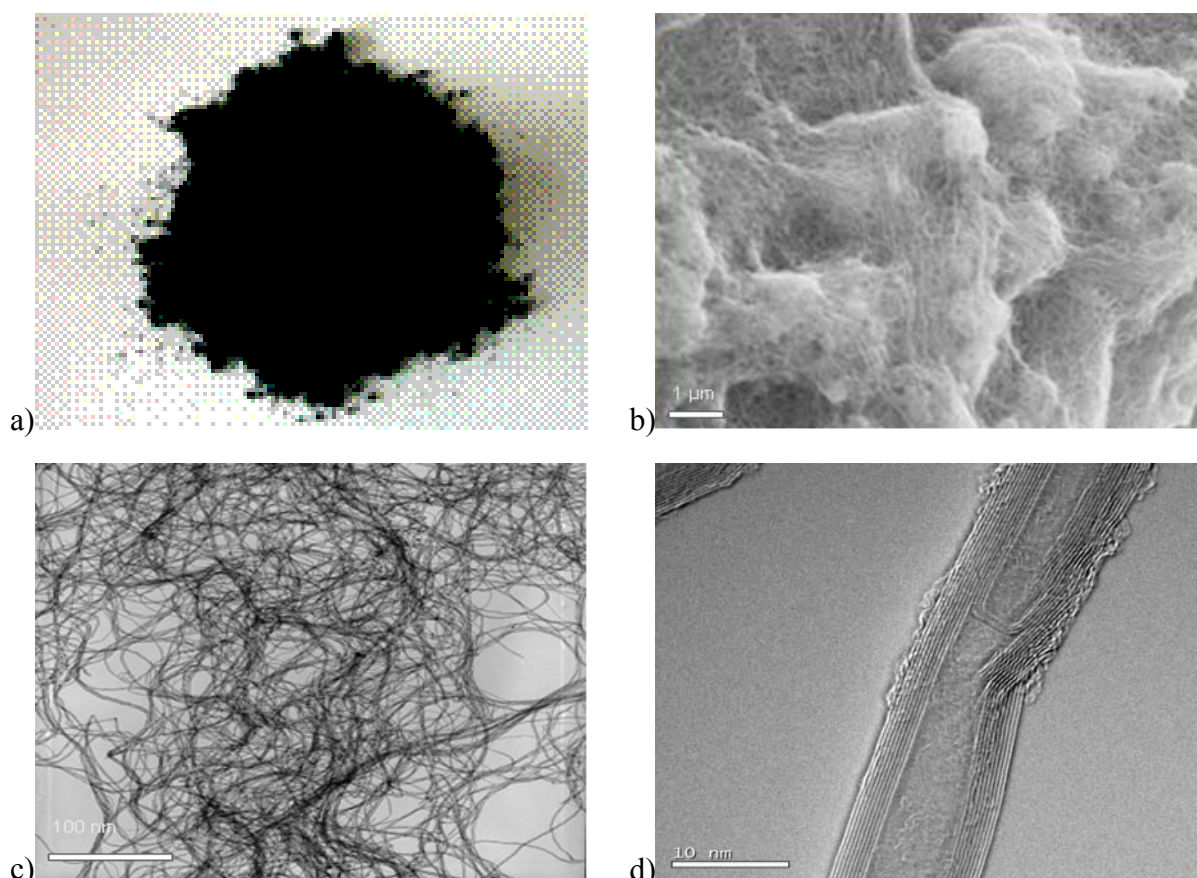


Figure 2.4: MWCNTs picture at human scale (a) and three micrographs at micro (SEM) and nanometric TEM scales (b, c, d).

Even if high purity MWCNTs are obtained, a first step of purification is required in order to eliminate amorphous carbon and remaining catalyst by a sulfuric acid treatment at 140 °C. TPD analysis (Temperature-Programme Desorption) evidences that this treatment quantitatively removes the impurities without oxidizing the external surface. Some iron nanoparticles, used as catalyst, remain inside the tubes; ATG analyses, after the purification step, reveals a purity of 98 % with 2 % of Fe, this sample is named CNT0. A BET analysis of

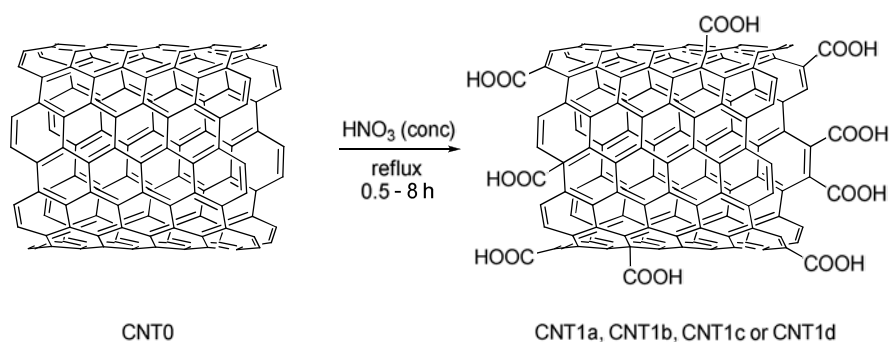
the surface shows an active surface of 227 m²/g. These MWCNTs are mesoporous with a pore volume of 0.66 cm³/g and an average pore diameter of 6-20 nm, determined by BET porisimetry. They can attain 10 μm in length and most of them exhibit closed ends. As observed by TEM analysis (Figure 2.4 d), the internal diameter varies between 4 and 12 nm, while the external goes from 8 to 21 nm. A Raman spectroscopy study has provided valuable structure information concerning the C-C bond. Two characteristic bands of MWCNTs are observed: the D mode (sp³ carbon), the defect band, located at frequencies between 1330 and 1360 cm⁻¹, and the G mode or MT-tangential mode, corresponding to the stretching mode in the graphite (sp² carbon), located at 1580 cm⁻¹ (I_D/I_G = 1.45).

2.2.1 Surface activation of multi-walled carbon nanotubes

In order to introduce covalent functionalities on MWCNTs, an activation surface step is required. The most common method to introduce surface carbonyl and carboxylic acid groups, is the chemical oxidation using nitric acid as oxidative agent.

2.2.1.1 Synthesis

The procedure used consists in the treatment of CNT0 with concentrated nitric acid to introduce mainly carboxylic acid functions (Scheme 2.3). The reaction was carried out at reflux during different reaction times (0.5, 1, 3 and 8 hours), giving different amount of functionalities (samples named CNT1a, CNT1b, CNT1c and CNT1d respectively).



Scheme 2.3: MWCNTs surface oxidation

2.2.1.2 Characterization

The acid reacts with the defects such as the penta- and hepta-rings. Those structures are principally located in the borders of the CNTs closing them and giving fullerene-like arrangement. A BET analysis after the activation treatment reveals an increase of the specific surface from 227 to 244 m²/g, due to the opening of some tubes (Table 2.2).⁸⁷

Entry	Support	BET(m ² /g)	CO ^a (μmol/g)	CO ₂ ^b (μmol/g)
1	CNT0	227	211	62
2	CNT1d	244	2132	1296

Table 2.2: Specific surface area and TPD of CNTs (8 h). ^a CO desorption of MWCNTs determined TPD analysis, ^b CO₂ desorption of MWCNTs determined by TPD analysis

Besides the carboxylic acid functions, the acid treatment introduces other polar oxygen groups at the MWCNTs surface. The results of a temperature programmed desorption (TPD) analysis of MWCNTs (CNT1d) are summarized in Table 2.3. The rising amount of oxygen groups is evidenced by the increase of the CO and CO₂ desorption. MWCNTs are mainly functionalized with carboxylic functions, as shown by the CO₂ evolution at ca. 300 °C (entry 1), although there are also other oxygen groups such as lactones, phenols, carbonyls, anhydrides, ethers and quinones (entries 2-5). The results are in agreement with those obtained by other authors.⁸⁸ The oxidation occurs on the CH_n groups at MWCNTs defects, firstly giving alcohol groups, then carbonyl C=O and finally carboxylic acid groups.^{33,89}

Entry	Chemical group	Temperature (°C)	CO (μmol/g)	CO ₂ (μmol/g)
1	Carboxylic acid	287-427	120	1017
2	Lactone	662	-	108
3	Anhydrids	517	163	163
4	Phenol	612	917	-
5	Carbonyl/quinone	777	920	-

Table 2.3: Functional groups introduced on the CNT1d surface after the activation treatment.

The efficiency of the treatment is easily evidence by infrared spectroscopy (Figure 2.5). In addition to the band due to CNT skeletal in-plane vibration at 1570 cm⁻¹ and C-H stretching at 2910 cm⁻¹ associated to defects, other new bands are observed: at 1717 cm⁻¹ (C=O vibration) and at 1200 cm⁻¹ (C–O stretching), two bands associated to carboxylic acid functions; and also at 3300 cm⁻¹, attributed to the hydroxyl groups.^{37,59}

The composition of the prepared MWCNTs (CNT0 and CNT1d) was determined by XPS and elemental analysis (Table 2.4). As expected, oxygen content elemental analysis of

oxidized CNTs increases up to 5.3 % compared to the CNT0, moreover the XPS analysis of those activated tubes detects an oxygen atom percentage of 7.6 %, demonstrating the effective grafting of oxygen surface groups. The concentric arrangement of the graphene layers does not allow reaching surface atomic oxygen percentages higher than 7–8 %, in contrast to CNFs, for which 30 % atomic oxygen at the surface can be reached.³³

MWCNTs	% wt elemental analysis				% atomic (XPS)	
	C	H	N	O	C	O
CNT0	95	0.16	-	0.64	100	-
CNT1d	87.3	0.3	0.15	5.3	92.4	7.6

Table 2.4: XPS and elemental analysis of purified (CNT0) and oxidized MWCNTs (CNT1d)

The amount of acidic functions on the MWCNTs surface is 0.85 COOH/nm² for CNT1d (activation treatment for 8 h), determined by chemical titration.⁹⁰ The titration method used (see section 5.3.2) permit to quantify only the carboxylic acid functions presented on the carbon nanotubes surface, in contrast to Boehm^{91,92} method where all the acidic functions are analysed (lactones, anhydrides, phenols, carbonyl, quinones, carboxylic acids).

2.2.2 Surface functionalization of multi-walled carbon nanotubes

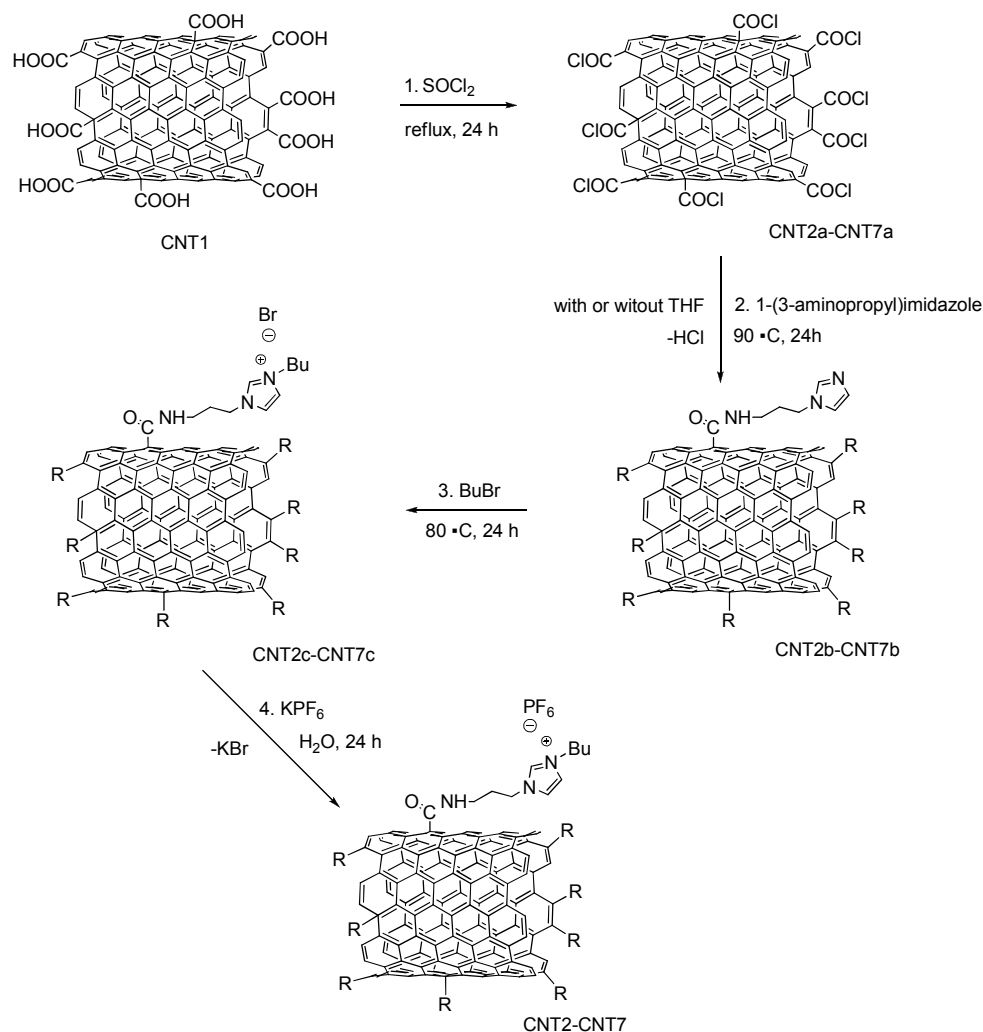
In order to improve the affinity between the carbon nanotubes and ionic liquid, activated MWCNTs (CNT1a, b, c, and d) were further functionalized with ionic imidazolium moieties to obtain different functionalized carbon nanotubes CNT2-CNT9. Two approaches were used to introduce ionic functionalities: the covalent and the ionic methodology.

2.2.2.1 Covalent approach

2.2.2.1.1 Synthesis

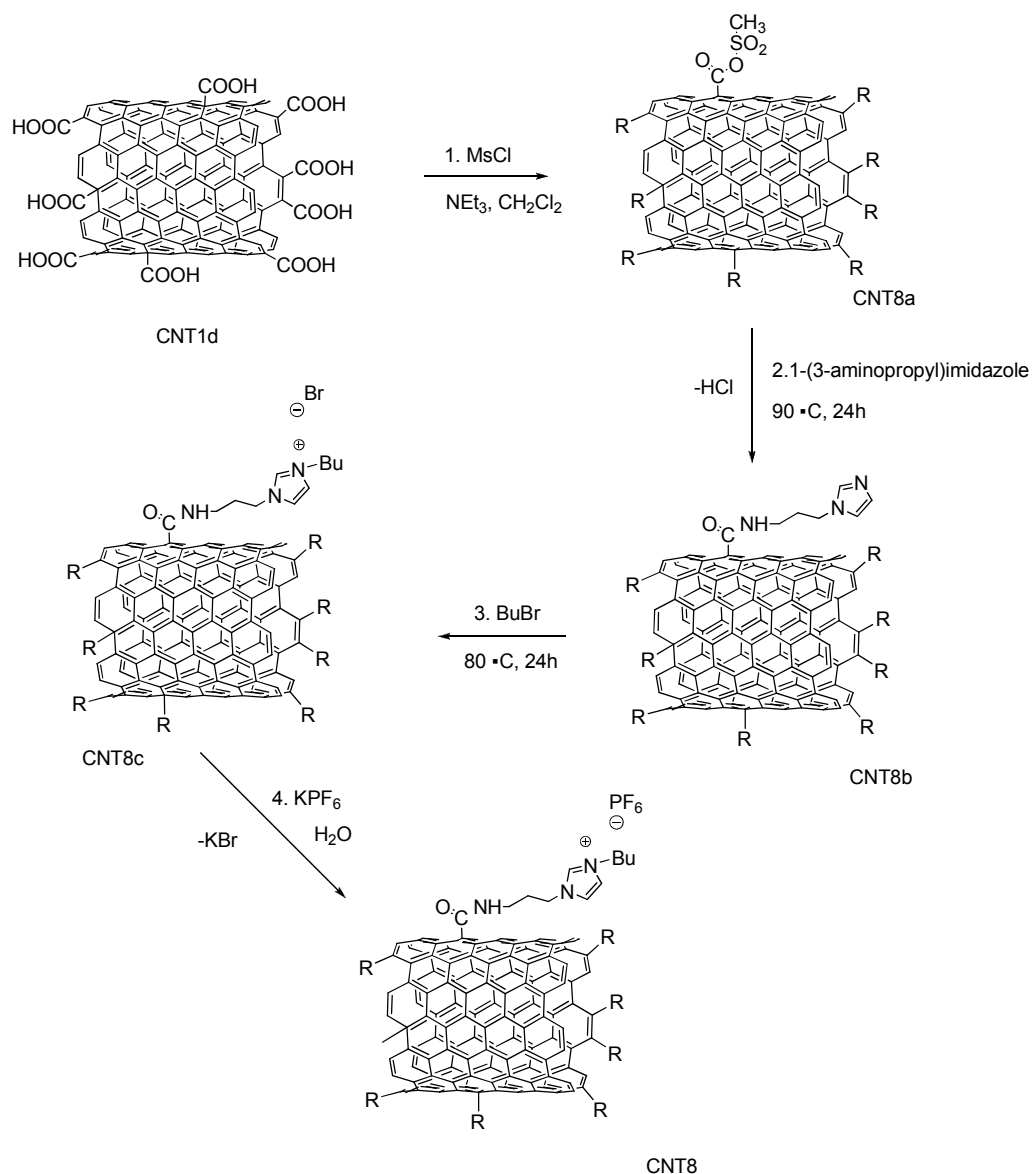
In the covalent approach, carboxylic functionalities were modified in four steps as detailed in Scheme 2.4. The first step consists in the conversion of the carboxylic acid group to acid chloride using an excess of thionyl chloride. These carbon nanotubes react with an excess of 3-(aminopropyl)imidazole at 120 °C for 24 h under nitrogen atmosphere. The resulting MWCNTs were purified by THF washing. Later, the resulting (3-aminopropyl)imidazole-functionalized MWCNTs were treated with an excess of n-butyl bromide, to obtain the N-butylimidazolium bromide-functionalized MWCNTs. Finally, an exchange reaction with

potassium hexafluorophosphates led to the imidazolium-like ionic functionalized MWCNTs samples, CNT2-CNT7 (CNT-([C₈N₃OH₁₁]⁺PF₆⁻)).



Scheme 2.4: Multi-step covalent modification of CNT1d to give functionalized CNT2-CNT7.

The major difficulty in this synthetic pathway is the second step due to the easy hydrolysis of the acid chloride functionalities. For that reason, an alternative route using methane sulfonyl acid instead of thionyl chloride was tested (Scheme 2.5). The reaction was carried out in the presence of triethylamine at room temperature. But this methodology gave a low functionality degree (see 2.2.2.1.2)



Scheme 2.5: Covalent modification of oxidized CNT (CNT1d) using methanesulfonyl acid.

2.2.2.1.2 Characterization

The efficiency of surface functionalization has been checked by IR and XPS spectroscopies, elemental analysis and TGA.

The IR spectrum of (3-aminopropyl)imidazole-functionalized MWCNTs obtained via thionyl chloride, shows the amide band at 1641 cm^{-1} , the aliphatic C–H stretching bands located between 2850 and 2950 cm^{-1} , and bands at 1250 – 1500 cm^{-1} assigned to C–H bendings.⁹³ The apparition of the intense P–F stretching band of PF_6^- anion at 830 cm^{-1} confirms the formation of the ionic N-butylimidazolium hexafluorophosphate-functionalized MWCNTs (Figure 2.5). When amide functionalization was carried out in THF (CNT2-

CNT4), the band at 1717 cm^{-1} of carboxylic acid group is still observed, indicating the presence of COOH groups. However, when the reaction was performed in the absence of solvent (CNT5-CNT6), the functionalization degree depends only on the activation time to give CNT1 (a, b, c, d) (section 2.2.1) and the carboxylic acid band (1717 cm^{-1}) due to the carboxylic acid groups that remains on the surface is almost inexistent for these samples.

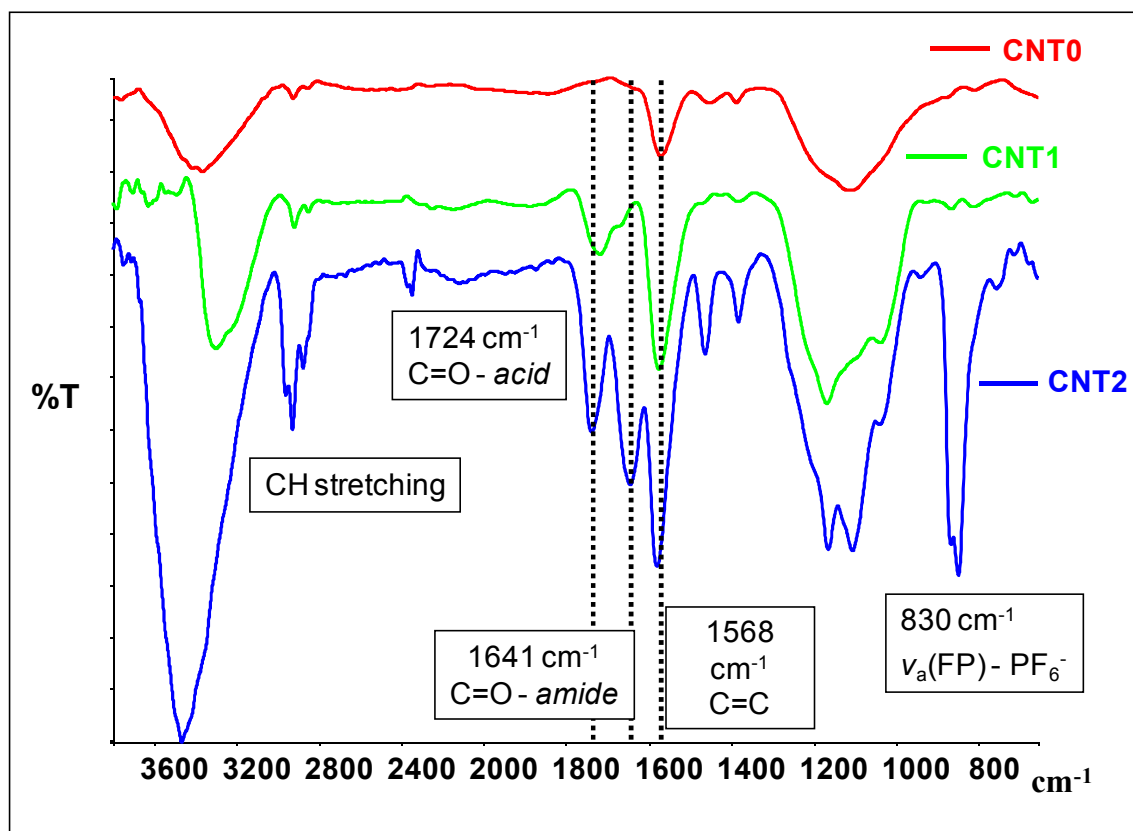


Figure 2.5: IR spectra (KBr pellets) of purified MWCNTs (CNT0), activated MWCNTs (CNT1d) and covalent functionalized MWCNTs (CNT2)

The elemental analysis and surface-semiquantitative XPS analysis confirmed the CNT functionalization (Table 2.5). Different oxidation times in the activation of the surface imply different degrees of functionalization. As it is expected, higher numbers of functionalities were obtained with longer activation times as could be observed in the Table 2.5 between entries 6 and 8. Actually, for a same activation time (8 h), when 3-(aminopropyl)imidazole was used in excess in the absence of solvent large amount of functionalities could be observed from the atomic 7.3 % of F measured by XPS, (entry 5). The use of THF in the second step of the functionalization leads to lower amount of grafted moieties (entries 3 and 4).

Entry	MWCNTs	% wt elemental analyze				% atomic XPS			
		C	H	N	O	C	O	N	F
1	CNT0	95	0.16	-	0.64	100	-	-	-
2	CNT1	87.03	0.3	0.15	5.3	92.4	7.6	-	-
3	CNT2	88.66	0.7	1.51	-	89.5	4.2	1.8	4.9
4	CNT3	82.6	1.5	1.85	7.5	82.7	10.3	1.8	5.2
5	CNT4	80.85	1.26	2.69	-	82.5	7.2	3.0	7.3
6	CNT5	70.37	0.68	1.53	-	80.8	14.2	-	5.0
7	CNT6	85.70	0.16	1.85	-	88.8	3.5	2	5.8
8	CNT7	79.70	0.65	2.31	-	84.1	6.8	3.1	6.0
9	CNT9 ^a	88.42	0.52	0.62	-	93.6	6.4	-	-

Table 2.5: Different degrees of surface functionalization of MWCNTs analyzed by elemental analysis and XPS. ^a MWCNTs obtained by ionic liquid approach (see section 2.2.2.2)

TGA analyses under air show that the imidazolium-based ionic functionalities are less stable than neat [bmim][PF₆], the decomposition temperature of which is 425 °C and 310 °C for the grafted species. Moreover, the surface functionalization has an effect on MWCNTs thermostability for functionalized (3-aminopropyl)imidazole-functionalized MWCNTs (CNT2-CNT7): the temperature of maximum gasification rate is 750 °C whereas for purified (CNT0) it is 640 °C.

The dispersibility of MWCNTs in [bmim][PF₆] ionic liquid has clearly improved after covalent ionic functionalization as can be observed in Figure 2.6. A homogeneous dispersed solution could be obtained when mixing the ILs and the ionic functionalized MWCNTs. The dispersibility follows the trend: functionalized (CNT2) > activated (CNT1) >> purified (CNT0); for CNT2 the stable suspension remains after 24 h.

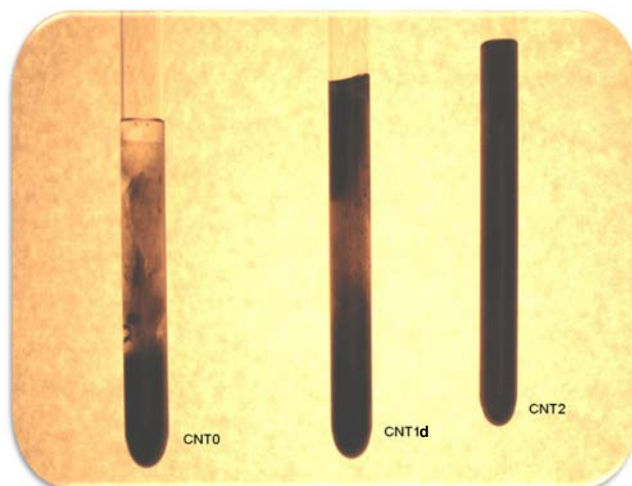


Figure 2.6: Photographs corresponding to MWCNTs (CNT0, CNT1d and CNT2) dispersion in [bmim][PF₆] ionic liquid.

Although the high toxicity and the difficulties during the work-up with thionyl chloride, this is the best reagent to activate the carboxylic acid groups. Actually, in the IR spectrum of ionic functionalized MWCNTs using methane sulfonyl acid, the characteristic amide band at 1641 cm⁻¹ does not appear. Elemental analysis performed after the second step to verify the formation of the mesylate did not exhibit the presence of sulphur species, and the amount of nitrogen was related to the surface adsorbed NEt₃ used in the synthetic route (Table 2.6 and Scheme 2.5).

Entry	MWCNTs	% wt elemental analysis			
		C	H	N	O
1	CNT8a	80.75	1.12	1.32	6.04
2	CNT8	88.38	0.64	1.63	4.19

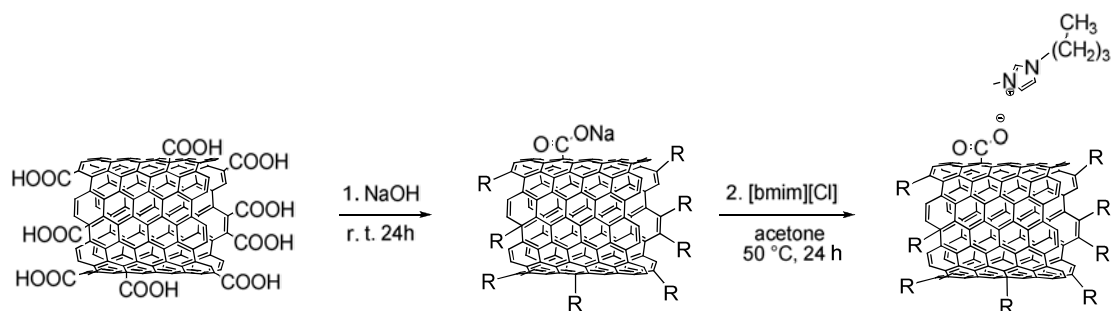
Table 2.6: Elemental analysis of the mesylate functionalized MWCNTs (CNT8a) and the covalent functionalized MWCNTs (CNT8) via methane sulfonyl acid.

Taking into account these results, we can conclude that methane sulfonyl acid is not a suitable reagent to activate the carboxylic acid groups in the covalent functionalization of multi-walled carbon nanotubes.

2.2.2.2 Ionic approach

In this approach, purified multi-walled carbon nanotubes CNT0 were modified with sodium hydroxide to produce the sodium salt of the acidified nanotubes. In order to introduce

the ionic functionality, [bmim][Cl] was mixed to the sodium salt of MWCNTs to carry out the cation exchange (Scheme 2.6).



Scheme 2.6: Ionic functionalization approach of MWCNTs.

The IR spectrum of the modified sodium salt of MWCNTs showed the carboxylate band between 1413 and 1423 cm^{-1} in addition to the classical bands of MWCNTs at 1568 and at 2850 cm^{-1} .⁹⁴ The formation of sodium carboxylate groups on the outer surface of MWCNTs makes this material highly hydrophilic, and it can easily be dispersed in water.

The elemental analysis revealed small amount of nitrogen in this ionic approach for CNT9 (entry 9, Table 2.5). No nitrogen was observed in XPS analysis. It can be supposed that the nitrogen presented on the surface is below the detection limit of this technique.

Therefore the ionic synthetic route used to functionalize MWCNTs with an ionic liquid presents lower performance than that obtained following the classical covalent approach (see section 2.2.2.1). This result is probably due to the low amount of sodium carboxylate functions on the surface after the acid-base reaction.⁹⁵ Indeed, a washing step with water is performed after base treatment in order to remove the excess of sodium hydroxide, which can dissolve small amounts of the MWCNTs sodium salts formed. The carboxylic acid groups remaining at the MWCNTs surface could be observed by IR spectroscopy, with the observation of a band at 1724 cm^{-1} corresponding to the C=O of COOH.

-
- ¹ (a) Science and Application of Nanotubes, D. Tomànek R.J. Enbody, (Eds.), Kluwer Academic/Plenum Publishers, New York, **2000**. (b) J.P. Issi, J.C. Charlier in The Science and Technology of Carbon Nanotubes, K. Fukui, K. Tanaka, T. Yamabe, (Eds.), Elsevier, **1999**. (c) M. Monthieux, P. Serp, E. Flahaut, C. Laurent, A. Peigney, M. Razafinimanana, W. Bacsa, J.M. Broto. Introduction to Carbon Nanotubes. In “Springer handbook of nanotechnology” Second revised and extended Edition B. Bhushan (eds.), Springer-Verlag, Heidelberg, Germany, **2007**, 43-112.
- ² H.W. Kroto, J.R. Heath, S.C. O’Brien, R.F. Curl, R.E. Smalley, *Nature* **1985**, 318, 162.
- ³ J. Roques, F. Calvo, F. Spiegelman, C. Mijoule, *Phys. Rev. Lett.* **2003**, 90, 075505.
- ⁴ S. Iijima, *Nature*, **1991**, 354, 56.
- ⁵ M. Hillert, N. Lange, *Zeitschr. Kristall.* **1958**, 111, 24.
- ⁶ C. Park, R.T.K. Baker, *J. Phys. Chem. B.* **1998**, 102, 5168.
- ⁷ C.Q. Sun, H.L. Bai, B.K. Tay, S. Li, E.Y. Jiang, *J. Phys. Chem. B.* **2003**, 107, 7544.
- ⁸ H. Zhu, B. Jiang, C. Xu, D. Wu, *Chem. Commun.* **2002**, 1858.
- ⁹ (a) R. Bacsa, Ch. Laurent, A. Peigney, W.S. Bacsa, Th. Vaugien, A. Rousset, *Chem. Phys. Lett.* **2000**, 323, 566. (b) E. Flahaut, R. Bacsa, A. Peigney, C. Laurent, *Chem. Commun.* **2003**, 12, 1442.
- ¹⁰ Y. Saito, *Carbon* **1995**, 33, 979.
- ¹¹ J. Xie, K. Mukhopadhyay, J. Yadev, V.K. Varadan, *Smart Mater. Struct.* **2003**, 12, 744.
- ¹² W. Krätschmer, L.D. Lamb, K. Fostiropoulos, D.R. Huffman. *Nature* **1990**, 347, 353.
- ¹³ Y. Ando, *Jpn. J. Appl. Phys.* **1993**, 32, L1342.
- ¹⁴ S. Iijima, T. Ichihashi, *Nature* **1993**, 363, 603.
- ¹⁵ D.S. Bethune, C.H. Klang, M.S.D. Vries, J. Gorman, *Nature* **1993**, 363, 605.
- ¹⁶ A. Thess, R. Lee, P. Nikolaev, H. Dai, P. Petit, J. Robert, C. Xu, Y.H. Lee, S.G. Kim, A.G. Rinzler, D.T. Colbert, G.E. Scuseria, D. Tomanek, J.E. Fischer, R.E. Smalley, *Science* **1996**, 273, 483.
- ¹⁷ P. Schützenberger, L. Schützenberger, *C.R. Acad. Sci. Paris* **1890**, 111, 774.
- ¹⁸ P.L. Walker Jr, *J. Phys. Chem.* **1959**, 63, 133.
- ¹⁹ M. José-Yacamán, *Appl. Phys. Lett.* **1993**, 62, 657.
- ²⁰ R.E. Smalley, J.H. Hafner, D.T. Colbert, K. Smith, US patent US 19980601010903.

-
- ²¹ Y. Murakami, S. Chiashi, Y. Miyauchi, M. Hu, M. Ogura, T. Okubo, S. Maruyama, *Chem. Phys. Lett.* **2004**, 385, 298.
- ²² A. Eftekhari, P. Jafarkhania, F. Moztaizadeha, *Carbon* **2006**, 44, 1343.
- ²³ D.H. Robertson, D.W. Brenner, J.W. Mintmire, *Phys. Rev. B* **1992**, 45, 12592.
- ²⁴ A. Krishnan, E. Dujardin, T.W. Ebbesen, P.N. Yianilos, M.M.J. Treacy, *Phys. Rev. B.* **1998**, 58, 14013
- ²⁵ E.W. Wong, P.E. Sheehan, C.M. Lieber, *Science* **1997**, 277, 1971.
- ²⁶ T. White, T.N. Todorov, *Nature* **1998**, 393, 240.
- ²⁷ M. Ouyang, J.L. Huang, C.M. Lieber, *Acc. Chem. Res.* **2002**, 35, 1018.
- ²⁸ E. Thostenson, *C. Tsu-Wei Composites Science and Technology* **2005**, 65, 491.
- ²⁹ P. Kim, L. Shi, A. Majumdar, P.L. MacEuen, *Phys. Rev. Lett.* **2001**, 87, 215502.
- ³⁰ S. Berber, Y.K. Kwon, D. Tomanek, *Phys. Rev. Lett.* **2000**, 84, 4613.
- ³¹ S. Talapatra, A.Z. Zambano, S.E. Weber, A.D. Migone, *Phys. Rev. Lett.* **2000**, 85, 138.
- ³² A. Hirsch, *Angew. Chem. Int. Ed.* **2002**, 41, 1853.
- ³³ T.G. Ros, A.J. van Dillen, J.W. Geus, D.C. Koningsberger, *Chem Eur J*, **2002**, 8, 1151.
- ³⁴ P.V. Lakshminarayanan, H. Toghiani, C.U. Pittman Jr. *Carbon* **2004**, 42, 2433.
- ³⁵ J. Li, M.J. Vergne, E.D. Mowles, W.H. Zhong, D.M. Hercules, C.M. Lukehart. *Carbon* **2005**, 43, 2883.
- ³⁶ C.N.R Rao, A Govindaraj, B.C. Satishkumar. *Chem Commun* **1996**, 1525.
- ³⁷ B.C. Satishkumar, A. Govindaraj, J. Mofokeng, G.N. Subbanna, C.N.R. Rao. *J Phys B At Mol Opt Phys* **1996**, 29, 4925.
- ³⁸ A. Kuznetsova, I. Popova, J.T. Yates, M.J. Bronikowski, C.B. Huffman, J. Liu, et al. *J Am Chem Soc* **2001**, 123, 10699.
- ³⁹ T.I.T. Okpalugo, P. Papakonstantinou, H. Murphy, J. McLaughlin, N.M.D. Brown. *Carbon* **2005**, 43, 153.
- ⁴⁰ Z. Yu, L.E. Brus, *J. Phys. Chem. A* **2000**, 104, 10995.
- ⁴¹ I.D. Rosca, F. Watari, M. Uo, T. Akasaka, *Carbon* **2005**, 43, 3124.
- ⁴² M.S.P. Shaffer, X. Fan, A.H. Windle. *Carbon* **1998**, 36, 1603.
- ⁴³ T. Saito, K. Matsushige, K. Tanaka., *Physica B* **2002**, 323, 280.
- ⁴⁴ H. Ago, T. Kugler, F. Cacialli, W.R. Salaneck, M.S.P. Shaffer, A.H. Windle, et al. *J Phys Chem B* **1999**, 103, 8116.
- ⁴⁵ N. Zhang, J. Xie, V.K. Varadan, *Smart Mater Struct* **2002**, 11, 962.

-
- ⁴⁶ L. Zhang, V.U. Kiny, H. Peng, J. Zhu, R.F.M. Lobo, J.L. Margrave, V.N. Khabashesku, *Chem. Mater.* **2004**, 16, 2055.
- ⁴⁷ K. Behler, S. Osswald, H. Ye, S. Dimovski, Y. Gogotsi, *J Nanopart Res* **2006**, 8, 615.
- ⁴⁸ G.S. Duesberg, R. Graupner, P. Downes, A. Minett, L. Ley, S. Roth, et al. *Synth Met* **2004**, 142, 263.
- ⁴⁹ K. Niesz, A. Siska, I. Vesselenyi, K. Hernadi, D. Méhn, G. Galbacs, et al. *Catal Today* **2002**, 76, 3.
- ⁵⁰ N. Pierard, A. Fonseca, Z. Konya, I. Willems, G. Van Tendeloo, J.B. Nagy. *Chem Phys Lett* **2001**, 335, 1.
- ⁵¹ G. Maurin, I. Stepanek, P. Bernier, J.F. Colomer, J.B. Nagy, F. Henn, *Carbon* **2001**, 39, 1273.
- ⁵² (a) J. Chen, M.A. Hamon, H. Hu, Y. Chen, A.M. Rao, P.C. Eklund, R.C. Haddon, *Science* **1998**, 282, 95; (b) M.A. Hamon, J. Chen, H. Hu, Y. Chen, M.E. Itkis, A.M. Rao, P.C. Eklund, R.C. Haddon, *Adv. Mater.* **1999**, 11, 834.
- ⁵³ M.A. Hamon, H. Hui, P. Bhowmik, H.M.E. Itkis, R.C. Haddon, *Appl. Phys. A* **2002**, 74, 333.
- ⁵⁴ (a) Y.P. Sun, W. Huang, Y. Lin, K. Fu, A. Kitaygorodskiy, L.A. Riddle, Y.J. Yu, D.L. Carroll, *Chem. Mater.* **2001**, 13, 2864; (b) K. Fu, W. Huang, Y. Lin, L.A. Riddle, D.L. Carroll, Y.P. Sun, *Nano Lett.* **2001**, 1, 439.
- ⁵⁵ B. Li, Z. Shi, Y. Lian, Z. Gu, *Chem. Lett.* **2001**, 30, 598.
- ⁵⁶ F. Pompeo, D.E. Resasco, *Nano Lett.* **2002**, 2, 369.
- ⁵⁷ K. Matsuura, K. Hayashi, N. Kimizuka, *Chem. Lett.* **2003**, 32, 212.
- ⁵⁸ L. Gu, T. Elkin, X. Jiang, H. Li, Y. Lin, L. Qu, T.R.J. Tzeng, R. Joseph, Y.P. Sun, *Chem. Commun.* **2005**, 874.
- ⁵⁹ M.J. Park, J.K. Lee, B.S. Lee, Y.W. Lee, I.S. Choi, S.-G. Lee, *Chem. Mater.* **2006**, 18, 1546.
- ⁶⁰ B. Yu, F. Zhou, G. Liu, Y. Liang, W.T.S. Huck, W.Liu, *Chem. Commun* **2006**, 2356.
- ⁶¹ J. Chen, A.M. Rao, S. Lyuksyutov, M.E. Itkis, M.A. Hamon, H. Hu, R.W. Cohn, P.C. Eklund, D.T. Colbert, R.E. Smalley, R.C. Haddon, *J. Phys. Chem. B* **2001**, 105, 2525.
- ⁶² M.G. Kahn, S. Banerjee, S.S. Wong, *Nano Lett.* **2002**, 2, 1215.
- ⁶³ D. Tasis, N. Tagmatarchis, A. Bianco, M. Prato, *Chem. Rev.* **2006**, 106, 1105.
- ⁶⁴ (a) Z. Liu, Z. Shen, T. Zhu, S. Hou, L Ying, Z. Shi, Z Gu, *Langmuir* **2000**, 16, 3569; (b) J.K. Lim, W.S. Yun, M.H. Yoon, S.K. Lee, C.H. Kim, K. Kim, S.K. Kim, *Synth. Met.* **2003**, 139, 521.
- ⁶⁵ (a) A. Hamwi, H. Alvergnat, S. Bonnamy, F. Beguin, *Carbon* **1997**, 35, 723; (b) H. Touhara, F. Okino, *Carbon* **2000**, 38, 241.
- ⁶⁶ V.N. Khabashesku, W.E. Billups, J.L. Margrave, *Acc. Chem. Res.* **2002**, 35, 1087.

-
- ⁶⁷ P.J. Boul, J. Liu, E.T. Mickelson, C.B. Huffman, L.M. Ericson, I.W. Chiang, K.A. Smith, D.T. Colbert, R.H. Hauge, J.L. Margrave, R.E. Smalley, *Chem. Phys. Lett.* **1999**, 310, 367.
- ⁶⁸ R.K. Saini, I.W. Chiang, H. Peng, R.E. Smalley, W.E. Billups, R.H. Hauge, J.L.J. Margrave, *J. Am. Chem. Soc.* **2003**, 125, 3617.
- ⁶⁹ J.L. Stevens, A.Y. Huang, H. Peng, I.W. Chiang, V.N. Khabashesku, J.L. Margrave, *Nano Lett.* **2003**, 3, 331.
- ⁷⁰ O. Vostrowsky, A. Hirsch, *Angew. Chem., Int. Ed.* **2004**, 43, 2326.
- ⁷¹ J. Sloan, J. Hammer, M. Zwiefka-Sibley, M.L.H. Green, *Chem. Commun.* **1998**, 347.
- ⁷² T. Ito, L. Sun, R.M. Crooks, *Chem. Commun.* **2003**, 1482.
- ⁷³ S. Chen, G. Wu, M. Sha, S. Huang, *J. Am. Chem. Soc.* **2007**, 129, 2416.
- ⁷⁴ E. Castillejos, P.J. Debouttière, L. Roiban, A. Solhy, V. Martinez, Y. Kihn, O. Ersen, K. Philippot, B. Chaudret, P. Serp, *Angew. Chem. Int. Ed.* **2009**, 48, 2529.
- ⁷⁵ H. Zhang, T. Liu, T. Sreekumar, S. Kumar, V. Moore, R. Hauge, R.E. Smalley, *Nano Lett.* **2003**, 3, 285.
- ⁷⁶ J.N. Coleman, M. Cadek, R. Blake, K.P. Ryan, V. Nicolosi, A. Fonseca, J.B. Nagy, C. Belton, W.J. Blau, *Adv. Funct. Mater.* **2004**, 14, 791.
- ⁷⁷ (a) M. Cadek, J.N. Coleman, K.P. Ryan, V. Nicolosi, G. Bister, A. Fonseca, J. B. Nagy, K. Szostak, F. Beguin, W.J. Blau, *Nano Lett.* **2004**, 4, 353; (b) M. Cadek, J.N. Coleman, V. Barron, K. Heidecke, W.J. Blau, *Appl. Phys. Lett.* **2002**, 81, 2503.
- ⁷⁸ E.T. Thostenson, Z. Ren, T.W. Chow, *Compos. Sci. Technol.* **2001**, 61, 1899.
- ⁷⁹ A. Akturk, *Phys. Rev. Lett.* **2007**, 98, 166803.
- ⁸⁰ Y.S. Choi, J.H. Kang, Y.J. Park, W.B. Choi, C.J. Lee, S.H. Jo, C.G. Lee, J.H. You, J.E. Jung, N.S. Lee, J.M. Kim, *Diamond and Relat. Mater.* **2001**, 10, 265.
- ⁸¹ C. Li, Y. Chen, Y.B. Wang, Z. Iqbal, M. Chhowalla, S. Mitra, *J. Mater. Chem.* **2007**, 17, 23, 2406.
- ⁸² I. Riedel, E. von Hauff, J. Parisi, N. Martín, F. Giacalone, V. Dyakonov, *Adv. Funct. Mater.* **2005**, 15, 1979.
- ⁸³ H. Vu, F. Gonçalves, R. Philippe, E. Lamouroux, M. Corrias, Y. Kihn, D. Plee, P. Kalck and P. Serp, *J. Catal.* **2006**, 240, 18.
- ⁸⁴ X. Pan, Z. Fan, W. Chen, Y. Ding, H. Luo and X. Bao, *Nature Mater.* **2007**, 6, 507.
- ⁸⁵ P. Serp, M. Corrias, P. Kalck, *Appl. Catal. A* **2003**, 253, 337.
- ⁸⁶ M. Ruta, I. Yuranov, P.J. Dyson, G. Laurenczy, L. Kiwi-Minsker, *J. Catal.* **2007**, 247, 269.
- ⁸⁷ A. Solhy, B.F. Machado, J. Beausoleil, Y. Kihn, F. Gonçalves, M.F.R. Pereira, J.J.M. Órfão, J.L. Figueiredo, J. L. Faria, P. Serp, *Carbon* **2008**, 1194.

-
- ⁸⁸ M.F.R. Pereira, J.L. Figueiredo, J.J.M. Orfão, P. Serp, P. Kalck, Y. Kihn, *Carbon* **2004**, 42, 2807.
- ⁸⁹ D.Q. Yang, J.F. Rochette, E. Sacher, *J. Phys Chem B* **2005**, 109, 7788.
- ⁹⁰ M.L. Toebes, J.M.P. van Heeswijk, J.H. Bitter, A. Jos van Dillen, K.P. de Jong, *Carbon* **2004**, 42, 307.
- ⁹¹ H. Boehm, *Carbon* **2002**, 40,145.
- ⁹² H. Boehm, *Carbon* **1994**, 32(5), 759.
- ⁹³ J. Wu, M.J. Wang, J.P.W. Stark, *J. Quant. Spectrosc. Radiat. Transf.*, **2006** 102, 2285.
- ⁹⁴ U. Zielke, K.J. Huttinger, W.P. Hoffman, *Carbon* **1996**, 34, 983.
- ⁹⁵ R. Giordano, P. Serp, P. Kalck, Y. Kihn, J. Schreiber, C. Marhic, J.-L. Duvail, *Eur. J. Inorg. Chem.* **2003**, 610

CHAPTER III

Supported ionic liquid catalytic phase:
preparation and characterization

3 SUPPORTED IONIC LIQUID CATALYTIC PHASE: PREPARATION AND CHARACTERIZATION

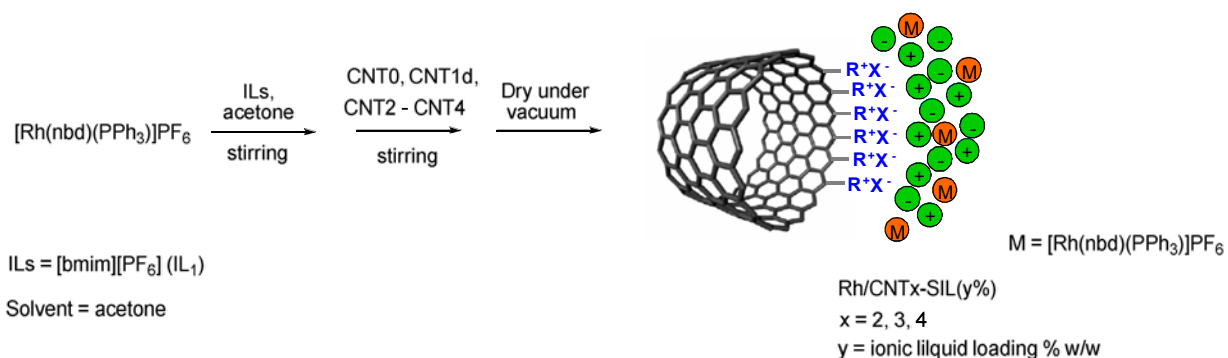
SILPC is a very attractive concept where a thin film of ionic liquid is immobilized within the pores of a solid support combining advantages of both materials.¹ A homogeneous (metal complex) or a heterogeneous (metal nanoparticles) catalytic precursor could be dispersed in the ionic liquid and further immobilized on a solid support to constitute the SILP catalyst. When non volatiles ionic liquids are used as supported phase, long-term reactions have shown promising results.² Compared to conventional supported homogeneous catalysis, this approach permits to recover by simple filtration the catalyst no without metal leaching.³ The use of SILPC (supported ionic liquid phase catalysis) is thus one of the most efficient ways to solve the problem of catalyst recovery,⁴ avoiding energy consumption (via distillation) and diminishing the use of organic solvents that contribute considerably to volatile organic compounds' emissions. Until now, most of the SILPCs have been prepared on oxide supports as SiO₂, Al₂O₃, MgO or ZnO; carbonaceous supports as active carbon cloth and graphite nanofibers; natural clays as attapulgite or laponites; and polymeric supports (see section 1.1.1). The use of carbon nanotubes should offer significant advantages such as: (i) increasing catalytic activities due to their mesoporous nature that avoids mass transfer limitations,⁵ (ii) high activity and/or selectivity due to the possibility to operate in the inner cavity of carbon nanotubes (confinement effect),⁶ (iii) well-defined and tunable structure,⁷ and (iv) the possibility to build a micro-reactor by selective growth of carbon nanotubes by catalytic chemical vapour deposition on defined substrates.⁸

In our work, 1-butyl-3-methylimidazolium hexafluorophosphate [bmim][PF₆] and pure multi-walled carbon nanotubes (described in chapter 2) were used to prepare the SILP catalysts. To improve the compatibility and dispersion of the ionic liquid on the nanotubes surface, MWCNTs were functionalized with ionic moieties (see section 2.2). A rhodium complex [Rh(nbd)(PPh₃)₂][PF₆] (nbd = norbornadiene) and preformed palladium nanoparticles were immobilized in the ionic liquid phase to further act as catalytic precursors in hydrogenation of olefins (Rh), C-C coupling (Pd) and selective hydrogenation (Pd) reactions.

3.1 IMMOBILIZATION OF A HOMOGENEOUS CATALYSTS

Immobilization of homogeneous organometallic complexes in a SILP catalytic system constitutes a well-established method because of its effective separation and recycling of the catalyst. An ionic rhodium catalyst, [Rh(nbd)(PPh₃)₂][PF₆], synthesized as previously described

in the literature (section 5.5.1),⁹ was immobilized following the Scheme 3.1. Multi-walled carbon nanotubes, purified (CNT0), oxydized (CNT1d) or functionalized (CNT2-CNT4), were added to a solution of a given amount of $[\text{Rh}(\text{nbd})(\text{PPh}_3)_2]\text{PF}_6$ in acetone in the presence of $[\text{bmim}][\text{PF}_6]$ ionic liquid. The volatile components were evaporated under reduced pressure. The resulting material contains an ionic liquid loading of 20, 37, 55 or 64 % w/w. Almost all the CNT supported ionic liquid phase composites ($\text{Rh}/\text{CNT}_x\text{-SIL}(y\%)$, where $x = 0-4$ and $y =$ ionic liquid loading amount) were obtained as black free flowing powder except $\text{Rh}/\text{CNT}_4\text{-SIL}(64\%)$, which showed a gel aspect because of the high amount of ionic moieties anchored on the CNT surface ($0.85 \text{ COOH}/\text{nm}^2$) and the large amount of ionic liquid loading.



Scheme 3.1: Immobilization of $[\text{Rh}(\text{nbd})(\text{PPh}_3)_2]\text{PF}_6$ in $[\text{bmim}][\text{PF}_6]$ on a functionalized MWCNTs

Other supports such as $\gamma\text{-Al}_2\text{O}_3$, ZrO_2 , TiO_2 , SiO_2 , ZnO , MgO and Active Carbon (AC) were also used to prepare SILP catalyst following the same procedure than that described for MWCNTs. The specific surface area of these supports is given in Table 3.1.

Support	CNT0	SiO_2	Al_2O_3	TiO_2	ZrO_2	MgO	AC	ZnO
BET Surface (m^2/g)	227	310	155	35-65	15-35	130	>100	20

Table 3.1: BET specific surface.

Ionic liquid loadings of 37, 55 and 64 % w/w were used to prepare the composites $\text{Rh}/\text{S-SIL}(y\%)$ ($\text{S} = \text{Al}_2\text{O}_3, \text{ZrO}_2, \text{TiO}_2, \text{SiO}_2, \text{ZnO}, \text{MgO}, \text{AC}$) giving different aspects, from pates to flow powder, summarized in Table 3.2. A critical ILs loading for each support could exist, for which the powder aspect is lost. This critical ILs loading should be related with the specific surface area and pore volume of the support; increasing amounts of ILs induce a pasty aspect.

ILs loading (%)	SiO ₂	Al ₂ O ₃	TiO ₂	ZrO ₂	MgO	AC	ZnO
37	powder	powder	powder	powder	powder	powder	powder
55	powder	agglomerates	agglomerates	agglomerates	agglomerates	powder	agglomerates
64	powder	pate	pate	Pate	agglomerates	agglomerates	pate

Table 3.2: Different aspects of composites Rh/S-SIL (y %) (S = Al₂O₃, ZrO₂, TiO₂, SiO₂, ZnO, MgO, AC)

3.2 IMMOBILIZATION OF HETEROGENEOUS CATALYSTS

In order to synthesize SILP composites with an immobilized heterogeneous catalyst, palladium nanoparticles were performed in ionic liquid medium.

3.2.1 Palladium nanoparticles: generalities and history

Nanometric size species have evidenced an ever-increase interest in the last two decades, which comes from the wide variety of applications where they are involved.¹⁰ Among them, the use of metallic nanoparticles in photochemical,^{11,12} optical¹³ and nanoelectronic applications,^{14,15,16} and also in quantum computers,¹⁷ chemical sensors^{18,19} and as catalysts for fuel cells²⁰ could be mentioned. From a chemical point of view, however, one of the main applications of the transition metal nanoparticles is in the field of catalysis.^{21,22,23}

Metallic nanoparticles are defined as entities formed by association of metallic atoms showing a size in the nanometric scale (1-100 nm), which places them between molecular compounds and bulk metal.

Other terms such as “nanocluster” or “colloid” have been recurrently employed as synonym of “nanoparticle”, although their use remains controversial. Some authors dislike the use of “nanocluster” instead of “nanoparticle”, preferring the exclusive application of this term to the traditional molecular clusters constituted by a few number of metallic centers. However, the similarity of both concepts makes the use of “nanocluster” to refer to metallic nanoparticles quite safe. In contrast, the term “colloid” can refer to any species whose size is in the nanometric scale, independently of its properties, being its use, therefore, inaccurate.

Thus, nanoparticles can be divided in nanoclusters, with small size distribution in the solid state (1-10 nm), and colloids, with large size distribution and average diameter higher than 10 nm.^{24,25} R. G. Finke summarized some criteria to distinguish between colloids and nanoparticles, including control over the composition, size, shape and control of the desired properties.²⁶

3.2.1.1 *Synthesis, stabilization and applications*

The interest to use metallic nanocatalysts comes from their intermediate situation between molecular complexes and bulk metal, which confers them new properties that may induce novel effects compared to classical homogeneous or heterogeneous catalysts. For example, one of the main advantages in this field would be the achievement of high activities and high selectivities attained with homogeneous catalysts with the possibility of an easier catalyst recycling.

Metal nanoparticles used as catalytic precursors present some specific characteristics. When nanoparticles are the real catalytic active species, the interactions substrate-catalyst take place on their surface. Thus, the number of superficial metal atoms should be as large as possible in order to increase the catalytic activity. Consequently, nanoparticles should be as small as possible (1-10 nm) to increase the number of surface atoms.²¹ Moreover nanoparticles should prove a reproducible synthetic route, a well-defined superficial composition, a narrow size distribution and constant physical and chemical properties.

Concerning the synthesis of nanoparticles,^{25,27} two different approaches have been developed: the “top-down” methodology based on physical ways involving mechanical, thermal or even chemical decomposition of bulk metals,^{28,29} and the “bottom-up” strategy based on chemical methodologies consisting in a slow continuous nucleation, starting from metal atoms, which are obtained from decomposition of salts or molecular compounds, followed by fast autocatalytic surface growth after the formation of the metallic critical nucleus size.^{30,31,32} Clusters with a “Magic number” size (clusters of a defined number of atoms, usually forming stable geometric structures giving large binding energies) achieve thermodynamic stability associated with a maximum metal-metal bonds.

The “bottom up” preparative method is more suitable to obtain small and uniform nanoparticles in size, shape and composition than the “top down” approach which usually gives large size distribution of nanoparticles showing low composition control^{33,34} and making them less suitable for catalytic applications.³⁵ In the “bottom up” strategy, control of the atom aggregation is the most important step to control the size and shape of metal nanoparticles.³⁶ The most common chemical methods involved in the bottom-up method include electrochemical^{37,38} or chemical reduction of metallic salts with alcohols,³⁹ molecular

hydrogen,⁴⁰ carbon monoxide⁴¹ or hydrides⁴², and thermal,⁴³ photochemical⁴⁴ or sonochemical decomposition,^{45,46,47} and ligand displacement^{48,49} of organometallic precursors. The last method is in particular appropriate for low-oxidation state precursors.

Because of metallic nanoparticles are not thermodynamically stable, they show a trend to agglomerate to form bulk metal, losing their specific properties.²⁶ In order to avoid this agglomeration, stabilizing agents should be present, independent of the synthetic way. Therefore, stabilizers can provide an electrostatic and/or steric barrier between the particles to prevent agglomeration, generating three possible ways to stabilize the nanoclusters: electrostatic, steric or electrosteric stabilization.^{22,50}

In general, electrostatic stabilization consists in the coordination of anionic species⁵¹ and their interaction with the corresponding cations, forming a double charged layer that prevents particles proximity approach, due to the repulsion between the external charged layers.²¹ Salts are largely used as electrostatic stabilizers; more recently, ionic liquids have been introduced for this purpose.^{19,52,53} Metal nanoparticles preparation in ionic liquids has been extensively discussed,^{54,55} since the first work described by Dupont's group.⁵⁶ In particular, palladium nanoparticles dispersed in ionic liquids have been prepared in our group from different precursors ([Pd(nbd)(ma)], ma = maleic anhydride; [PdCl₂(cod)], cod = cyclooctadiene; PdCl₂ and [Pd₂(dba)₃], dba = dibenzylideneacetone).^{57,58} The electrostatic stabilization of PdNPs by the ionic liquid depends on the palladium precursor as showed by TEM analysis. Those nanoparticles proved good activity in the Suzuki-Miyaura cross-coupling reaction, the system was reused ten times without major loss of activity.⁵⁹

The steric stabilization is based on the use of macromolecules such as dendrimers^{57,60} or polymers,^{36,61} or also by coordination of bulky ligands^{62,63} to isolate the particles, avoiding their agglomeration. Finally, the electrosteric stabilization combines both electrostatic and steric effects by the use of charged molecules containing long chains, like ionic surfactants.^{64,65}

The importance of the choice of the stabilizing agent must be underlined, because they play a crucial role in the control of both size and shape of nanoparticles.⁶⁶

3.2.2 Metal nanoparticles synthesized in ionic liquid medium

In the present work, palladium nanoparticles have been synthesized in two different ionic liquids [bmim][PF₆] and [emim][HPO(OMe)O] (emim = 1-ethyl-3-methylimidazolium) and from [Pd₂(dba)₃] and [PdCl₂(cod)] precursors under hydrogen atmosphere in the presence of a ligand (4-(3-phenylpropyl)pyridine), following the methodology previously described in our

group.⁵⁹ This ionic liquid phase has been immobilized on the surface of SiO₂ or functionalized carbon nanotubes CNT2-CNT7, to be further applied in catalytic reactions.

In order to discuss the size, shape, organization and dispersion of the palladium nanoparticles and taking advantage of the non-measurable vapour pressure of ILs,⁶⁷ TEM analyses were carried out on suspensions of nanoparticles in ionic liquid ([bmim][PF₆] or [emim][HPO(OMe)O]).

3.2.2.1 Synthesis of Pd nanoparticles

The synthetic way chosen for the formation of the nanoparticles is based on Chaudret group's methodology. Organometallic precursors allow the synthesis of metal nanoparticles under mild conditions, giving particles of uniform and small size with a clean surface.⁶⁸ These nano-objects display an interesting surface chemistry appropriated to catalytic purposes.^{69,70}

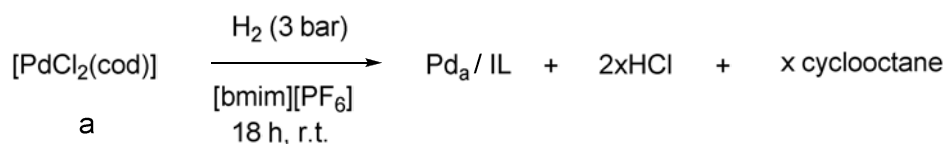
Synthesis involves organometallic precursor decomposition at room temperature and low pressure of hydrogen (3 bar) in the presence of stabilizing agents.

The synthetic method challenges, such as absence of surface oxidation, nature of the surface species, cluster growth control and surface reactivity, are related to the precise control of the reaction conditions. The organometallic precursor's ligands should be replaced by the stabilizing agent. The ideal case is the reduction of an olefinic precursor, which leads to the production of alkanes unable under these conditions to interact strongly with the growing metal surface. Examples of this kind of precursors are [Ni(cod)₂]⁷¹ and [Ru(cod)(cot)] (cod = cyclooctadiene; cot = cyclooctatriene).⁷⁰ Complexes with allylic groups also easily decompose under mild conditions, such as [Rh(η³-C₃H₅)]. Other complexes such as [M₂(dba)₃] (M = Pd, Pt)^{72,73} or [PdCl₂(cod)] have been also used.⁷²

In our study, two different types of organometallic precursors were used based on Pd(II), [PdCl₂(cod)] and Pd(0) [Pd₂(dba)₃] species. The nanoparticles were synthesized using ionic liquid acting as both reaction medium and stabilizer. 4-phenylpropylpyridine was also used as stabilizer in ionic liquid.⁷⁴

3.2.2.2 Nanoparticles from Pd(II) precursor

[PdCl₂(cod)] was used in the synthesis of nanoparticles by chemical decomposition under hydrogen atmosphere as described in Scheme 3.2.



Scheme 3.2: Pd nanoparticles synthesis from [PdCl₂(cod)]

The synthesis was carried out in a Fisher Porter bottle under 3 bar of hydrogen pressure. The yellow solution turned black at room temperature after stirring for 18 h.

TEM analysis revealed the presence of palladium nanoparticles (Figure 3.1). The spherical particles were not homogeneous in size, with an average size distribution of 2.15 ± 0.72 nm. Compared with results reported by our group using $[\text{PdCl}_2(\text{cod})]$ as precursor in the absence of ligand, no star-like-shaped superstructures were observed.⁵⁹ The nanoparticles size and the different shape observed can be related with the high precursor concentration used that favours a rapid nucleation leading to small particles not allowing their organization in a special geometrical shape.

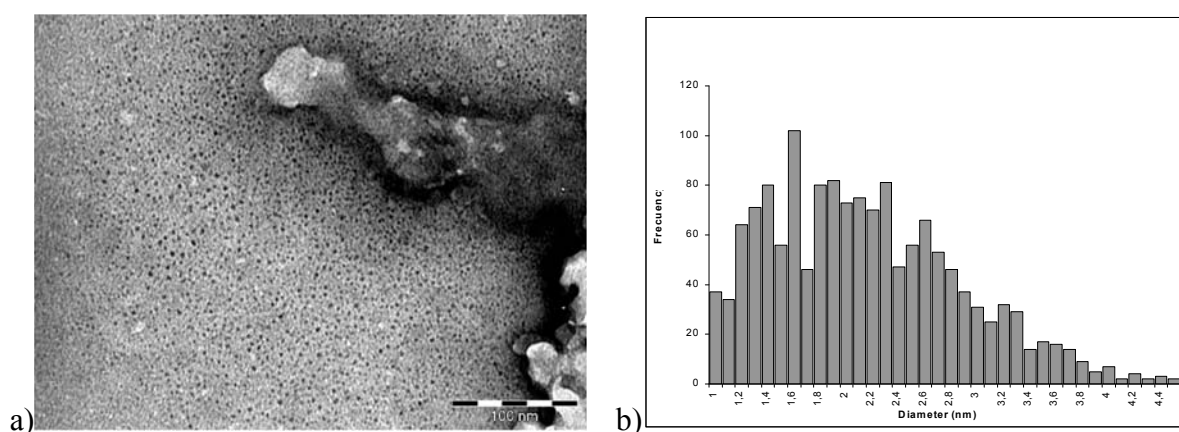
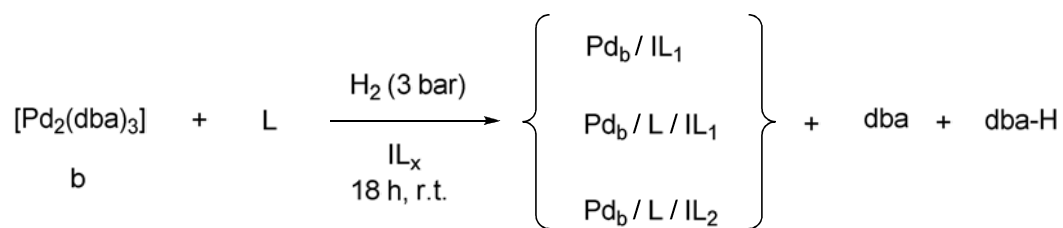


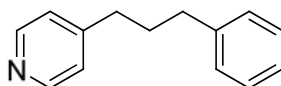
Figure 3.1: a) TEM photograph of Pd_a/IL (scale bar = 100 nm), b) particle size distribution histogram (1468 counted particles).

3.2.2.3 Nanoparticles from Pd(0) precursor

With the purpose to obtain palladium nanoparticles in a reproducible manner and with homogeneous shapes and sizes, $[\text{Pd}_2(\text{dba})_3]$ was chosen as Pd(0) precursor. The reaction took place in the absence and also in the presence of 4-(3-phenylpropyl)pyridine. Two different ionic liquids $[\text{bmim}][\text{PF}_6]$ and $[\text{emim}][\text{HPO}(\text{OMe})\text{O}]$ were used as solvents in order to observe the electrostatic stabilization influence (Scheme 3.3).



L = 4-(3-phenylpropyl)pyridine

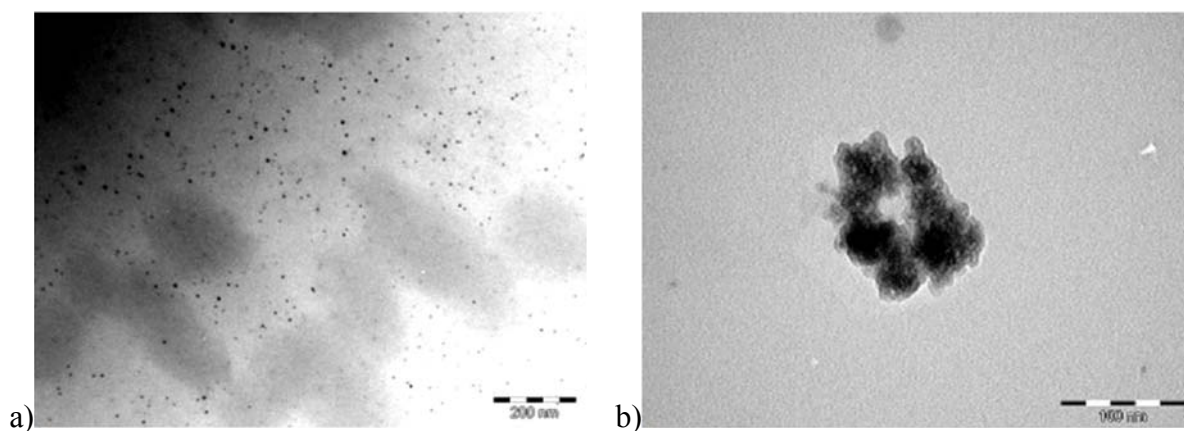


IL_x: IL₁ = [bmim][PF₆]
 IL₂ = [emim][HPO(OMe)O]

dba-H = reduction subproduct

Scheme 3.3: Pd nanoparticles synthesis in presence or absence of the ligand L from [Pd(dba)₃].

TEM analysis of Pd_b/IL₁ mainly revealed aggregates (Figure 3.2, b) and also some areas showing well-dispersed palladium nanoparticles (Figure 3.2, a). These palladium nanoparticles only stabilized by ionic liquid [bmim][PF₆] without ligand on the metallic surface (Pd_b/IL₁) shows particles with average size diameter of 5.25 nm ± 2.31 with very wide size distribution as can be observed in Figure 3.2, c.



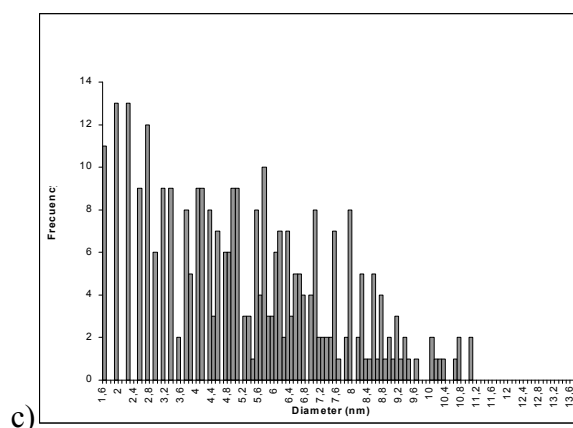


Figure 3.2: a) TEM photographs of Pd_b/IL₁ without ligand (scale bar 200 nm); b) nanoparticles aggregates (scale bar 100 nm); and c) particle size distribution histogram (317 counted particles).

On the contrary, when 4-(3-phenylpropyl)pyridine was used as ligand in a Pd:L ratio = 1:0.3, TEM micrographs revealed well-dispersed nanoparticles with no agglomerations (Figure 3.3 a). A mean diameter of 4.34 ± 1.33 nm was calculated for the particles (255 counted particles), meaning that nanoparticles are formed, but with a relatively large size distribution. In fact, two populations of particles can be proposed from the size distribution histogram (Figure 3.3 b): at ca. 4.0 nm and at ca. 5.1 nm. The better nanoparticles dispersion can be related to the positive stabilizing effect of the 4-(3-phenylpropyl)pyridine. The ligand coordination at the metallic surface has been previously evidenced by ¹H NMR study for ruthenium NPs.⁷⁵

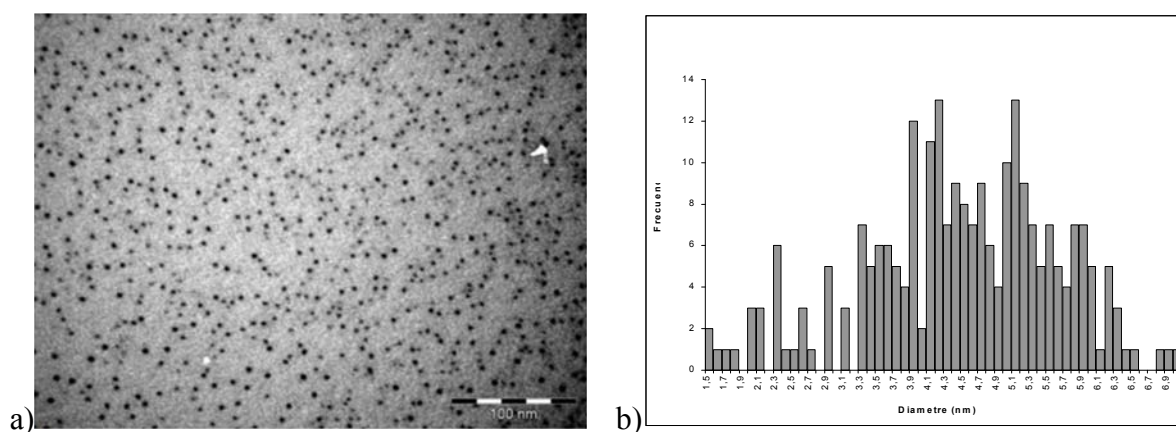


Figure 3.3: a) TEM micrograph of nanoparticles Pd_b/L/IL₁, stabilized by 4-(3-phenylpropyl)pyridine in [bmim][PF₆] (scale bar 100 nm). b) The corresponding size distribution diagram (255 counted particles).

The nanoparticles obtained in [emim][HPO(OMe)O] and the ligand 4-(3-phenylpropyl)pyridine shows homogeneous size distribution as observed in their TEM

micrographs (Figure 3.4 a, b) and confirmed by the Gaussian like particle size distribution (Figure 3.4 c). Their average size is 4.47 ± 0.78 nm. Besides the ligand positive influence in the nanoparticles stabilization, the peculiar organization of palladium nanoparticles (Figure 3.4, a) should be related to the ionic liquid counteranion.

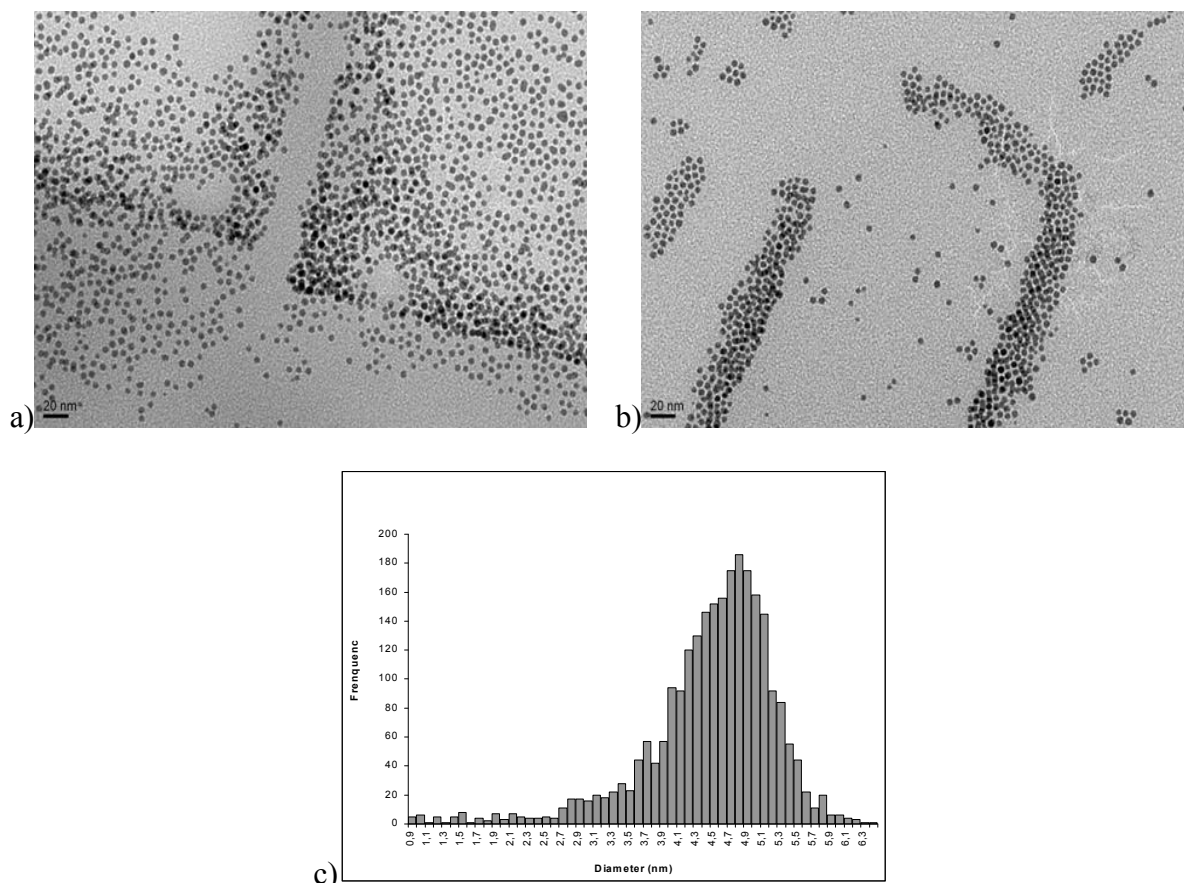


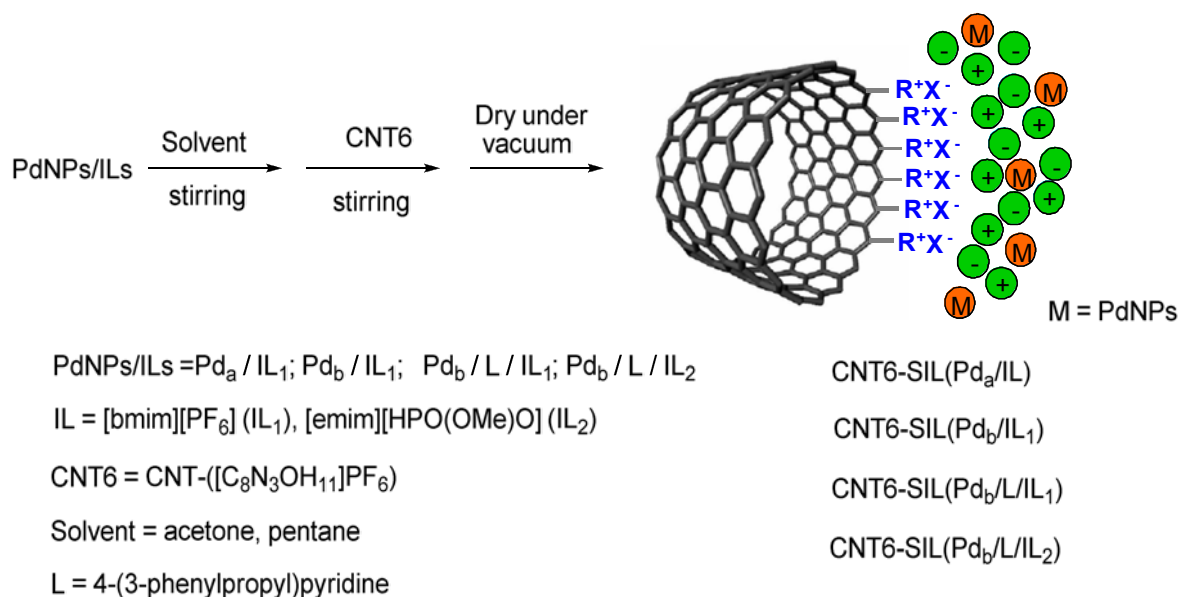
Figure 3.4: a) and b) TEM micrographs of nanoparticles $\text{Pd}_b/\text{L}/\text{IL}_2$, stabilized by 4-(3-phenylpropyl)pyridine in $[\text{emim}][\text{HPO}(\text{OMe})\text{O}]$ (scale bar 20 nm); and c) The corresponding size distribution diagram (2527 counted particles).

3.2.3 Synthesis of heterogeneous supported ionic liquid phase catalyst

The simultaneous use of metal nanoparticles as well as ILs solvent offers a multiphase system, which allows an easy recovery and reuse of the catalyst. In spite of the good results in the reactions catalysed with this type of systems,⁵⁵ the use of solid catalysts is still preferred because of the inherent convenience for the work-up procedure and effective recycling. In this respect, the preparation of solid supported metal nanoparticles using ILs is the strategy that we have adopted in this work.

In this section, palladium nanoparticles preformed in ionic liquid (see section 3.2.2) were immobilized on a solid support (Scheme 3.4). Functionalized carbon nanotubes CNT3, CNT6 were added to a solution of organic solvent containing the metallic nanoparticles in ionic

liquid. The solvent was removed under reduced pressure in order to obtain a free flowing powder. The resulting material contains 0.35 % w/w of palladium nanoparticles and an ionic liquid loading of 34 % w/w.



Scheme 3.4: Immobilization of PdNPs dissolved in ILs over CNT.

TEM and EDX (Energy Dispersive X-ray Spectroscopy) (Figure 3.5) analyses of $\text{CNT6-SIL}(\text{Pd}_b/\text{L}/\text{IL}_2)$ showed the presence of Pd nanoparticles in the catalyst, as well as the presence of C, O, N, P, from the ionic liquid used ($[\text{emim}][\text{HPO}(\text{OMe})\text{O}]$). Fe, Al and Cr were also observed, due to the remaining impurities from the carbon nanotubes synthesis. The relative big size of the metal nanoparticles (4.9 nm) compared to the small external diameter of the carbon nanotubes used (between 8-21 nm) is the main reason for the configuration of those structures around the metal particles. As can be observed in Figure 3.6a, nanoparticles are enclosed by several nanotubes. The ionic liquid is probably adsorbed on the functionalized MWCNTs surface and also coating the metal nanoparticles, avoiding the direct contact between both MWCNTs and the nanoparticles surface. Similar results have been reported by Zhao's group with Pd nanoparticles stabilized in 1,1,3,3-tetramethylguanidinium lactate ionic liquid supported onto molecular sieves.⁷⁶ More over, the image FFT (Fast Fourier Transform) corresponding to one particle shows, in addition to the characteristic planes corresponding to the fcc palladium structure (3,1,1), (2,2,0), (2,0,0) and (1,1,1) (Figure 3.6c), two other unknown planes ($d = 1.48 \text{ \AA}$ and 1.73 \AA) were observed. The inverse FFT calculating treatment of these planes (Figure 3.6d and e) shows they belong to a crystalline compound

placed around the metal nanoparticle (Figure 3.6d), probably due a crystalline form of the ionic liquid.

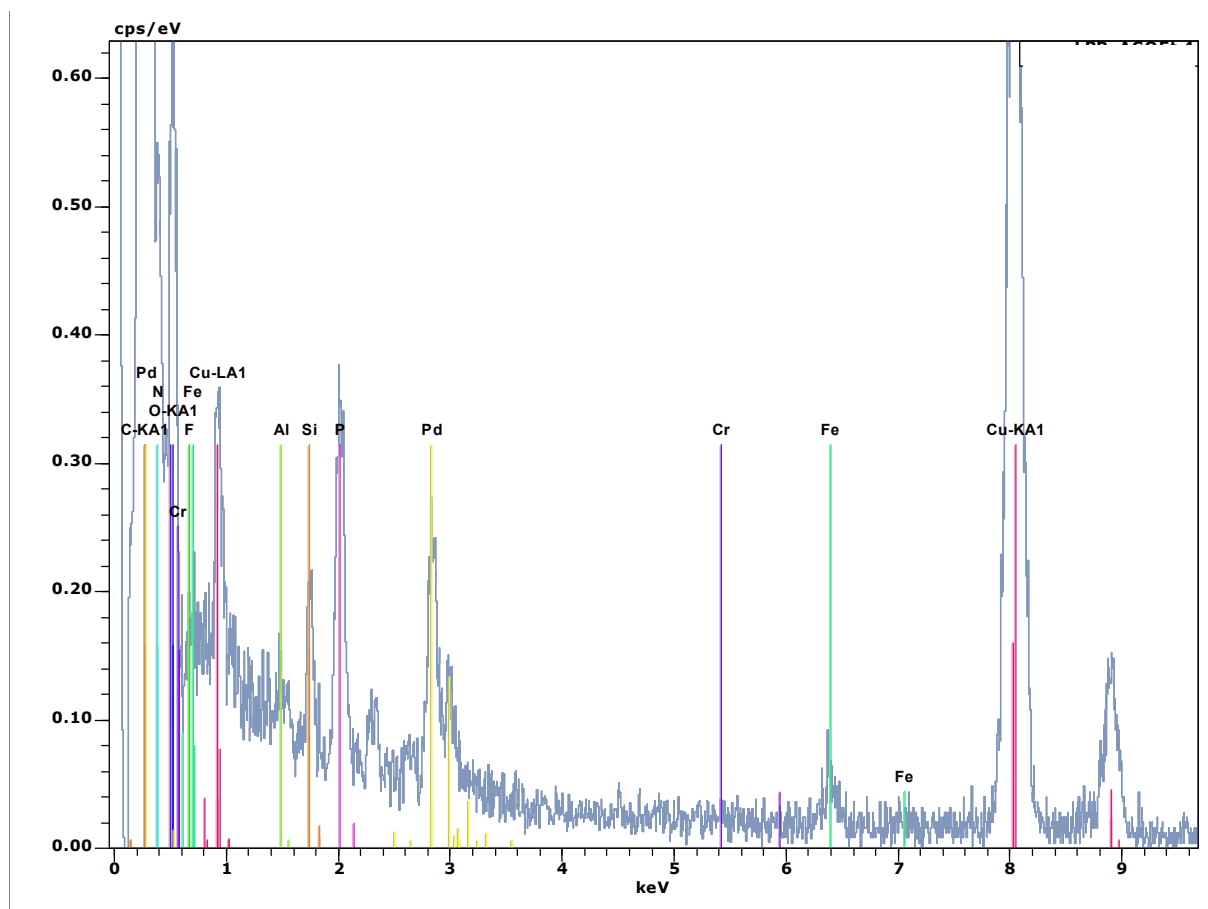
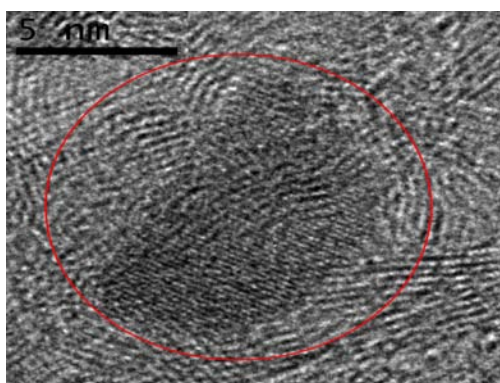


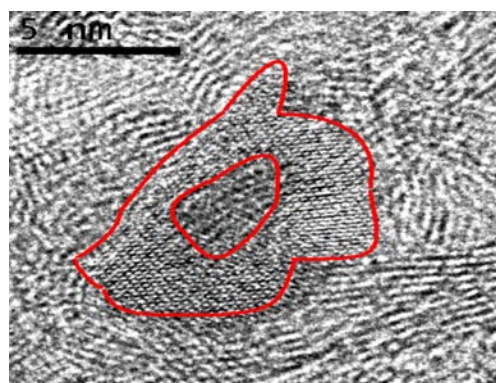
Figure 3.5: EDX analysis of CNT6-SIL(Pd_v/L/IL₂)



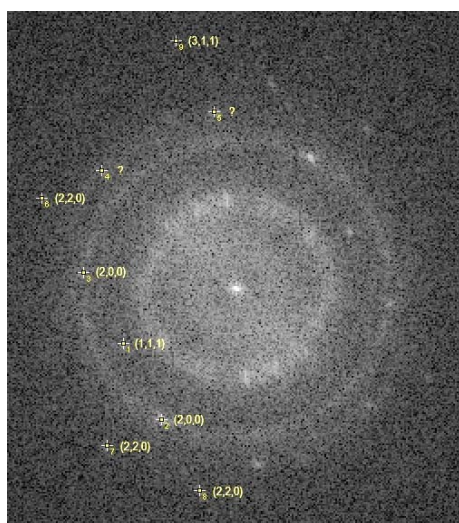
a)



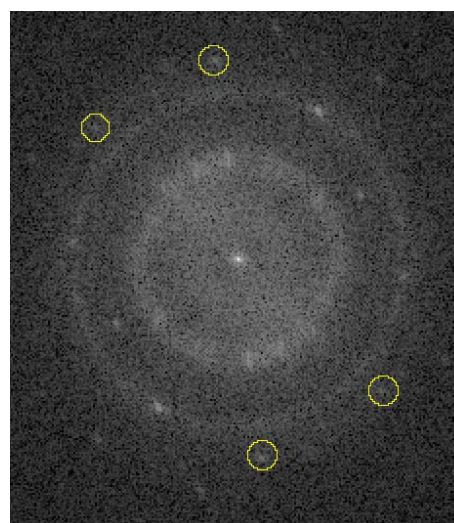
b)



d)



c)



e)

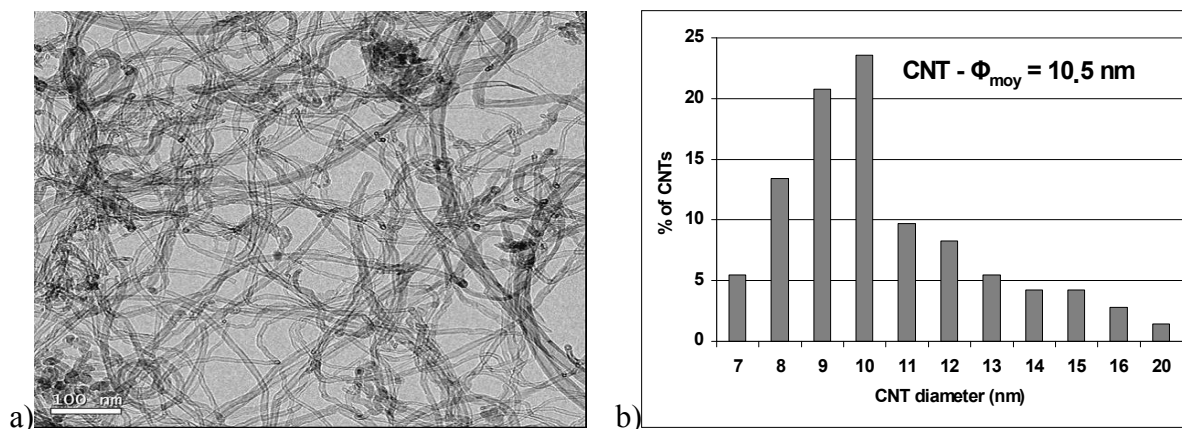
Figure 3.6: a) TEM micrograph of CNT6-SIL(Pd/L/IL₂) (scale bar 10 nm); b) One isolated palladium nanoparticle (scale bar 5 nm); c) FFT of the nanoparticle with the corresponding fcc palladium planes; d) Inverse FFT showing the unknown planes; e) calculated TEM image coming from the FFT calculating treatment of d) image.

With the aim of studying the positive influence of functionalized multi-walled carbon nanotubes on the catalytic activity, the same procedure was applied using SiO₂ as support for comparison purposes. The SILP catalyst was obtained as a grey flowing powder with 0.35 % w/w of palladium content and an ionic liquid loading of 34 % w/w.

3.3 CHARACTERIZATION OF SUPPORTED IL COMPOSITES

CNT supported ionic liquid phase composites (CNT_x-SIL(y% w/w)), prepared as described in section 3.1 using [bmim][PF₆] but without metallic species, have been characterized by TEM, TGA and XRD techniques.

The effective grafting of an ionic liquid film on ionic functionalized multi-walled carbon nanotubes walls (CNT2-CNT7), producing CNT-SIL composites, could be confirmed by TEM and HREM micrographs. The thickness of the [bmim][PF₆] film depends on the amount of ILs. For CNT3-SIL(55%), the film shows a mean thickness of 3.3 nm (1 nm < thickness < 10 nm) (Figure 3.7 e). Therefore, the mean MWCNTs external diameter shifts from 10.5 nm for CNT0 (Figure 3.7 microphotograph a, histogram b) to 19 nm for CNT3-SIL(55%) (Figure 3.7 c, histogram d). It should be noted that in the nanotubes size distributions, two different populations are observed: at 10 nm corresponding to CNT0 and at 19 nm for the CNT-SIL composites (Figure 3.7, histogram d). The non homogeneity of the sample could be related to the different degree of surface functionalization, which depends on the surface concentration of defaults.



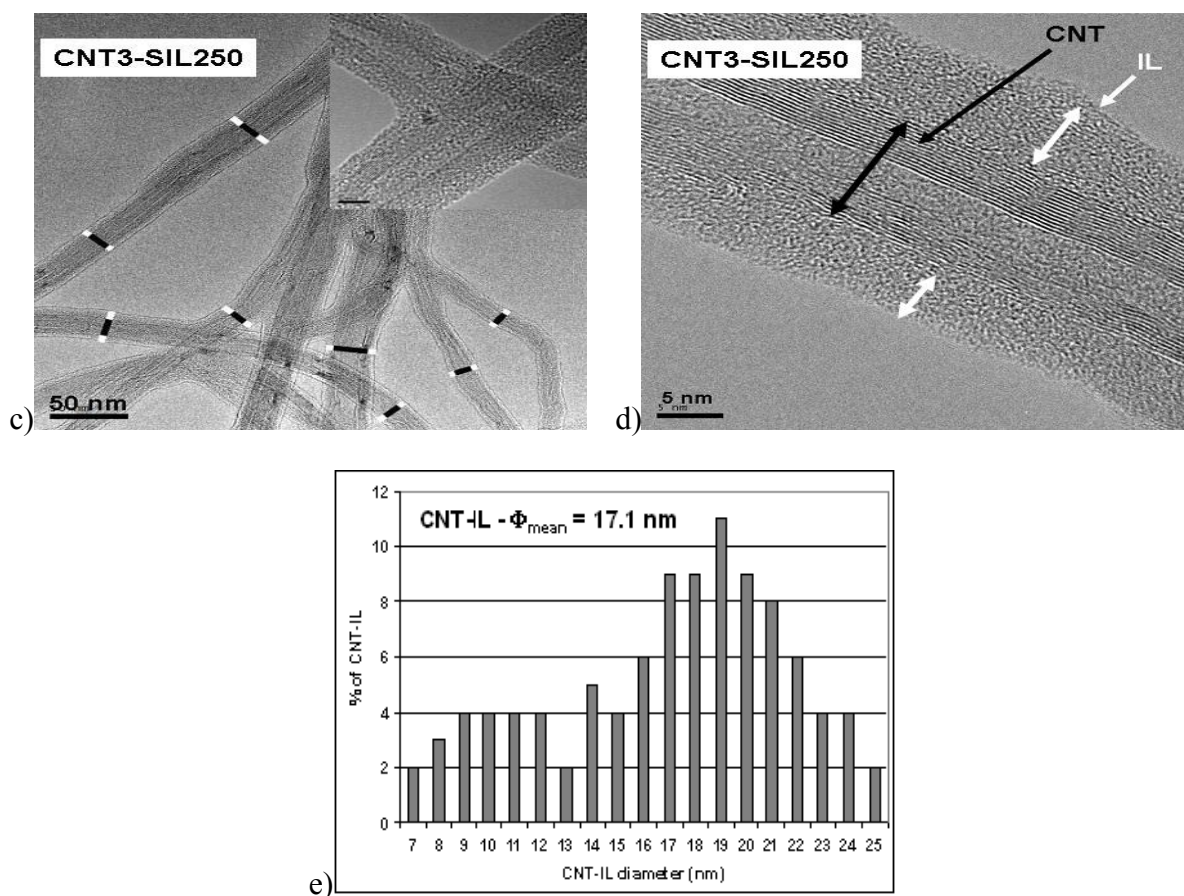


Figure 3.7: TEM photographs of a) CNT0, b) CNT0 average external diameter histogram c) and d) CNT3-SIL(55%), e) CNT3-SIL(55%) average external diameter histogram.

The XRD diffractograms of CNT_x-SIL samples show the peaks of MWCNTs at $2\theta = 30.37^\circ$ ($d_{002} = 3.37 \text{ \AA}$) and 50.21° ($d_{100} = 2.09 \text{ \AA}$) (Figure 3.8) and broad peaks at $2\theta = 16.54^\circ$, 22.28° and 24.30° distinctive of the amorphous ILs phase. No peaks corresponding to the transition of [bmim][PF₆] from liquid to high melting point crystal due to the confinement in the CNTs cavity, were observed.⁷⁷

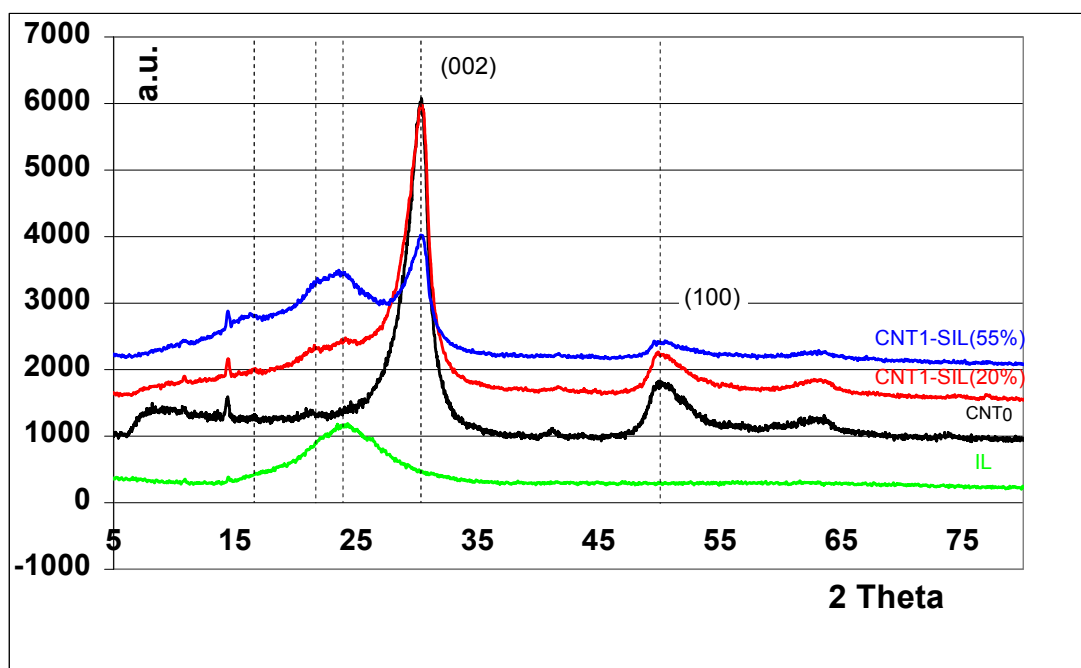


Figure 3.8: XRD patterns of CNT_x-SIL samples compared to CNT₀ and pure ILs

The degree of functionalization of the MWCNTs surface by ionic moieties has also an influence on the texture of the CNT-SIL produced. Actually, CNT₂ and CNT₃ in the presence of different ILs loading amounts are always obtained as powders. In contrast, CNT₄, which presents the highest concentration of ionic groups, containing 55 % w/w of ionic liquid [bmim][PF₆] (CNT₄-SIL(55%)), is a gel. This phenomenon has already been reported for CNT mixed with imidazolium-based ILs, leading to gel, often called bucky gels of ILs.⁷⁸ The gels can be formed either by physical CNT bundles cross-linking, mediated by local molecular ordering of the ILs or by CNT entanglement. If such gels can find promising applications as soft materials for electrochemical applications,⁷⁹ for catalytic purposes their formation should be avoided since it induces low catalytic activity, due to a poor contact between the catalyst and/or support, gas and liquid phases.

TGA analysis confirms the presence of the [bmim][PF₆] film on the MWCNTs surface; the thermostability of these films is lower than that of pure ILs, since the [bmim][PF₆] film decomposes between 340 °C and 360 °C, depending on the film thickness, in contrast to 425 °C for pure [bmim][PF₆] (Figure 3.9). Increasing the amounts of ILs leads to an increase of the decomposition temperature of the ionic liquid film.

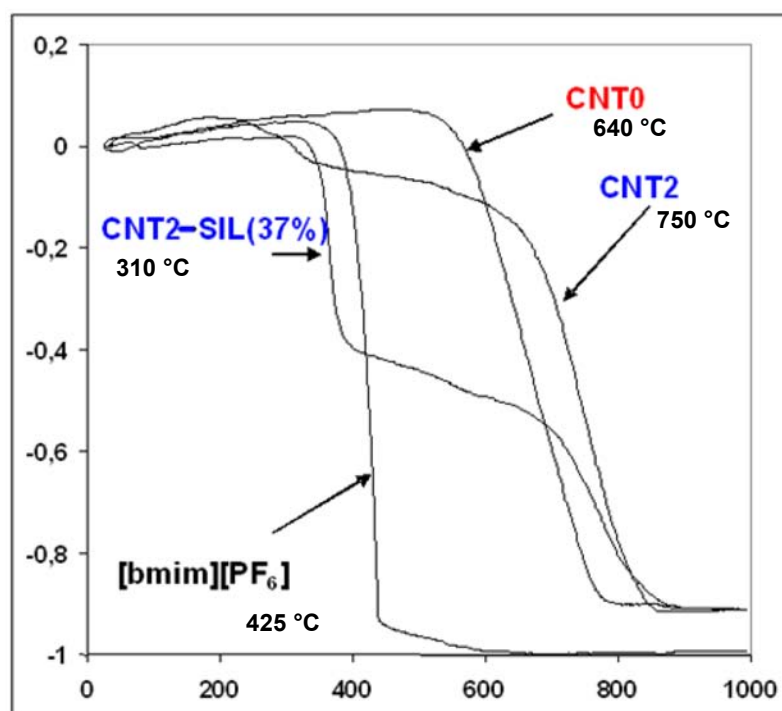


Figure 3.9: TGA analysis of neat ILs, CNT0, CNT2 and CNT2-SIL(37%).

Composites S-SIL(37 % w/w) (S = Al₂O₃, ZrO₂, TiO₂, SiO₂, ZnO, MgO, AC) (see section 3.1) were also analyzed by TGA. As exhibited in Figure 3.10, a strong support influence on the ionic liquid thermal decomposition is observed. SiO₂-SIL(37%), MgO-SIL(37%), AC-SIL(37%), ZnO-SIL(37%) and CNT_x-SIL(37%) show lower ILs film thermostability than pure [bmim][PF₆]. Al₂O₃-SIL(37%), TiO₂-SIL(37%) and ZrO₂-SIL(37%) have the same or even higher ILs film thermostability than that observed for pure ILs.

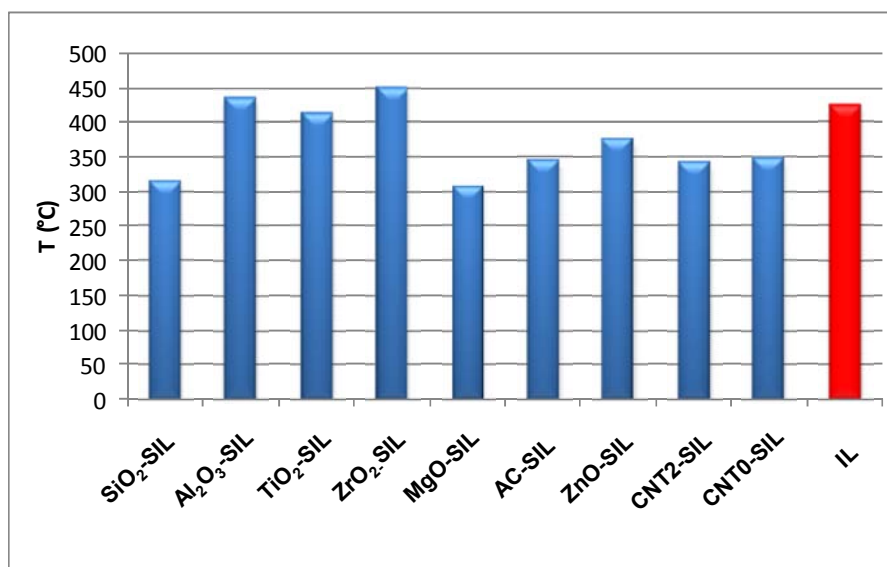


Figure 3.10: Thermal decomposition (TGA analysis) of composites S-SIL(37% w/w) corresponding to the ionic liquid layer

To the best of our knowledge, the influence of IL–support interaction on ILs film thermostability has not yet been reported. As the ILs support interaction may also have an impact on catalytic performances, we decided to carry out a structural study of two composites showing a very different behaviour: SiO₂-SIL with lower thermal stability compared to that for pure ILs and Al₂O₃-SIL with a thermal stability close to the one of pure ILs.

3.4 STRUCTURAL STUDY OF THE INTERACTIONS BETWEEN THE SUPPORT AND THE IONIC LIQUID

With the aim of studying the interactions of the ionic liquid with the supports, we have been interested in carrying out a full structural study mainly by NMR of ILs supported on SiO₂ and Al₂O₃. In SILPC, a thin film of ionic liquid is immobilized on the surface pores of a solid support. Nevertheless, it has been reported that, if an appropriate amount of ILs is combined with silica⁸⁰ or carbon nanotubes,^{81,79} confined ionic liquids gel are formed. Specific interactions of ILs with solid supports are scarcely studied in the literature. Depending on these interactions, some physico-chemical characteristics of the composites may differ from those of pure ILs. Thus, XRD and differential scanning calorimetry (DSC) analyses of ILs/CNTs gels have revealed different profiles compared to those exhibited for the pure ionic liquid.⁸¹

In the present study, we have observed different catalytic behaviour depending on the nature of the support (see later section 4.1.1 and Table 4.3). Thus, we were interested in

studying the nature of these interactions choosing SiO₂-SIL and Al₂O₃-SIL composites (prepared as described in section 5.5), due to their pronounced difference in their catalytic behaviour. In this section, a detailed characterization by TGA, DSC, XRD, IR and solid NMR analyses of [bmim][PF₆] thin films immobilized on amorphous silica gel and γ -alumina supports compared to pure [bmim][PF₆] is reported. While SiO₂-SIL reveals strong interactions between the ILs and the solid support, the Al₂O₃-SIL composite shows weak contacts.

3.4.1 DSC analysis

DSC analyses (heating from -120 °C to +40 °C) revealed remarkable differences between SiO₂-SIL(37 % w/w) and Al₂O₃-SIL(37 % w/w). Even though in both cases a glass transition point was observed at similar temperature (-79.5 ° and -76 °C for SiO₂-SIL and Al₂O₃-SIL respectively), a completely different profile was observed at higher temperatures. Hence, Al₂O₃-SIL, showed one broad exothermic (at -27.8 °C) and two sharper endothermic (at -4.6 °C and +9.1 °C) peaks close to those observed for pure [bmim][PF₆] (Figure 3.11). The endothermic peak observed at ca. +9.1 °C corresponds to the melting point of the ILs used (10.5 °C for the pure ILs),⁸² while the broad exothermic one at -27.8 °C corresponds to the transition phase between two crystalline phases of [bmim][PF₆] (for pure ILs, at -19.5 °C), as recently reported in the literature for neat [bmim][PF₆].⁸³ On the contrary, no significant peaks were observed for the SiO₂-SIL composite.

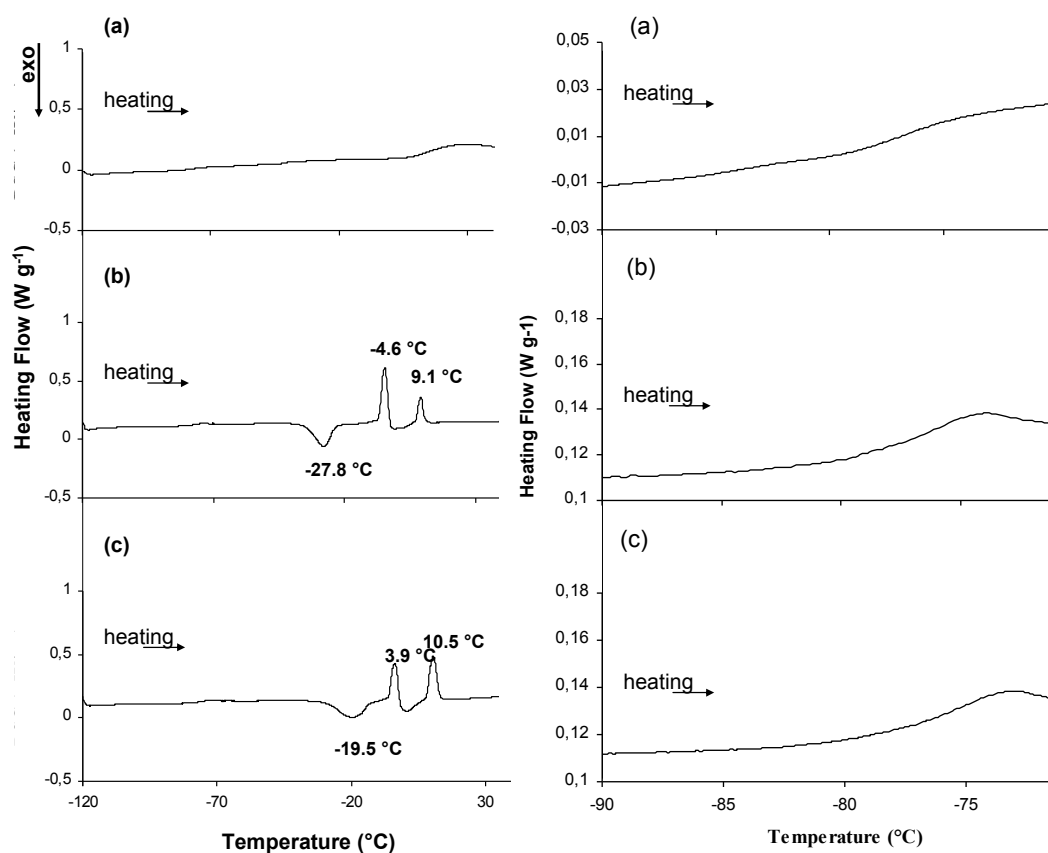


Figure 3.11: DSC analyses on heating (left) and expansion plot (right) to indicate the glass transition temperature: a) pure [bmim][PF₆]; b) Al₂O₃-SIL composite and c) SiO₂-SIL composite.

3.4.2 XRD analysis

XRD diffractograms were recorded at -100 °C, below the glass transition temperature (Figure 3.12). While Al₂O₃-SIL composite showed many weak diffraction peaks revealing its polycrystalline structure similar to [bmim][PF₆] pattern, SiO₂-SIL showed only a broad signal.

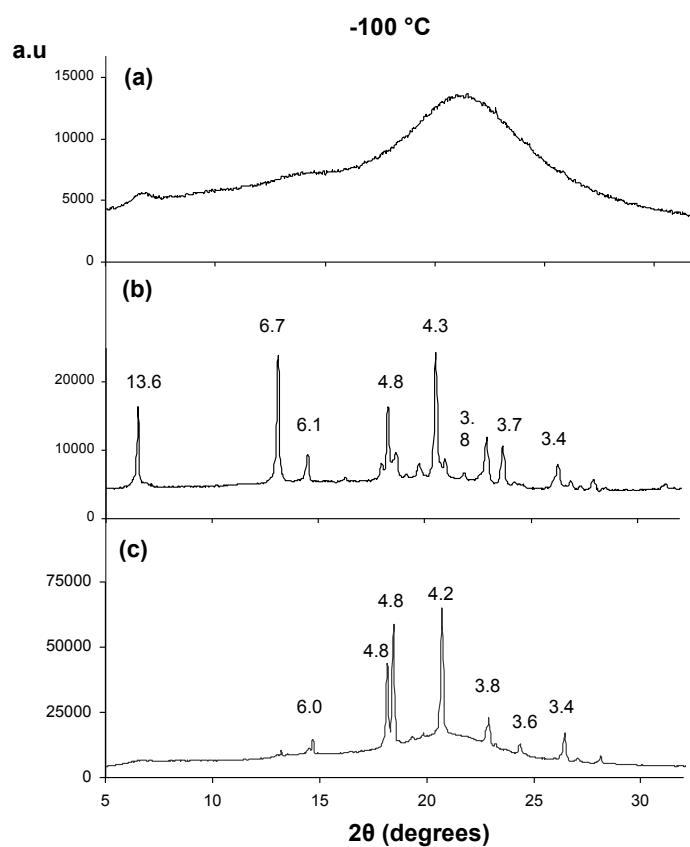


Figure 3.12: Low temperature (-100 °C) XRD diffractograms (d spacing, in Å, is indicated on each sharp peak): a) SiO₂-SIL, b) Al₂O₃-SIL and c) pure [bmim][PF₆].

At -20 °C, over the exothermic transition phase, polycrystalline patterns were observed for pure ILs as well as for Al₂O₃ composite, in contrast to SiO₂-SIL which remained amorphous. At room temperature, [bmim][PF₆] and both composites presented amorphous diffractograms.

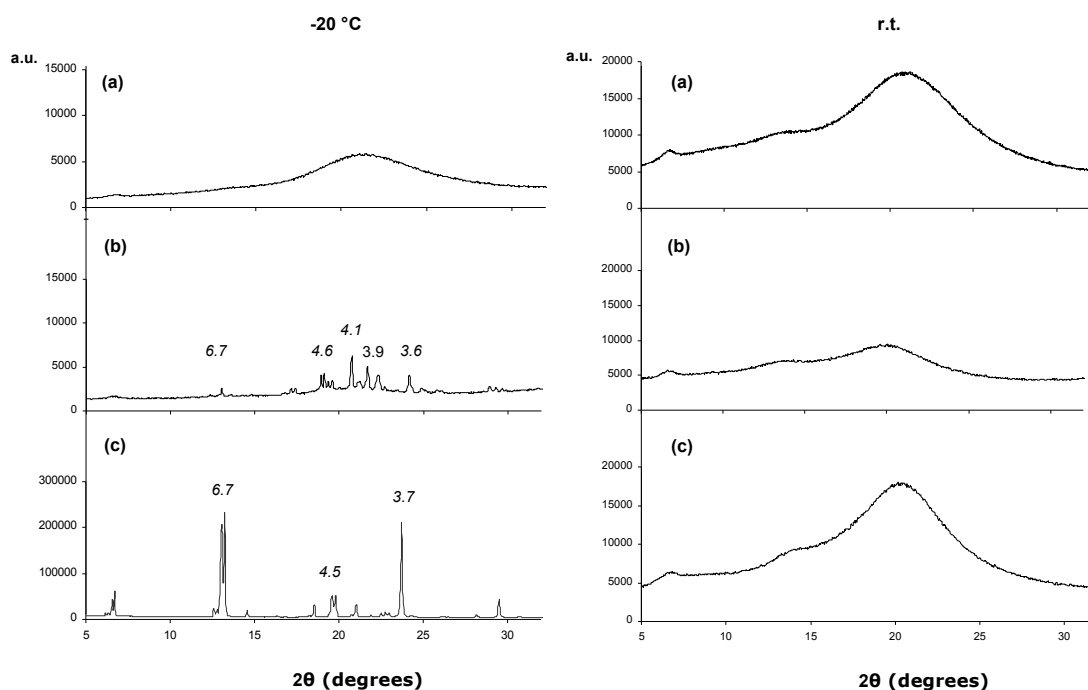


Figure 3.13: XRD diffractograms (d spacing, in Å, is indicated on each sharp peak) at -20°C (left) and room temperature (right): a) SiO₂-SIL, b) Al₂O₃-SIL and c) pure [bmim][PF₆].

These observations evidence a different effect of the solid support on the structure of the ionic liquid thin film. Whereas alumina slightly modifies the ILs structure, silica induces important changes.

3.4.3 NMR analysis

In order to obtain further details about the structural modification induced by the support, we have carried out a solid state NMR study. ¹H and ¹³C NMR experiments were recorded to study the ionic liquid cation modifications induced by the support. ¹H MAS NMR spectra of SiO₂-SIL and Al₂O₃-SIL composites showed the corresponding signals of the ILs without important changes in chemical shifts in relation to the pure [bmim][PF₆], only signal broadening was evidenced (Figure 3.14, left). Nevertheless for silica and the corresponding SiO₂-SIL composite, high field shift was observed for the hydroxyl groups (peak at ca. 5 ppm). But, no changes were detected when compared γ -alumina and Al₂O₃-SIL (Figure 3.14, right).

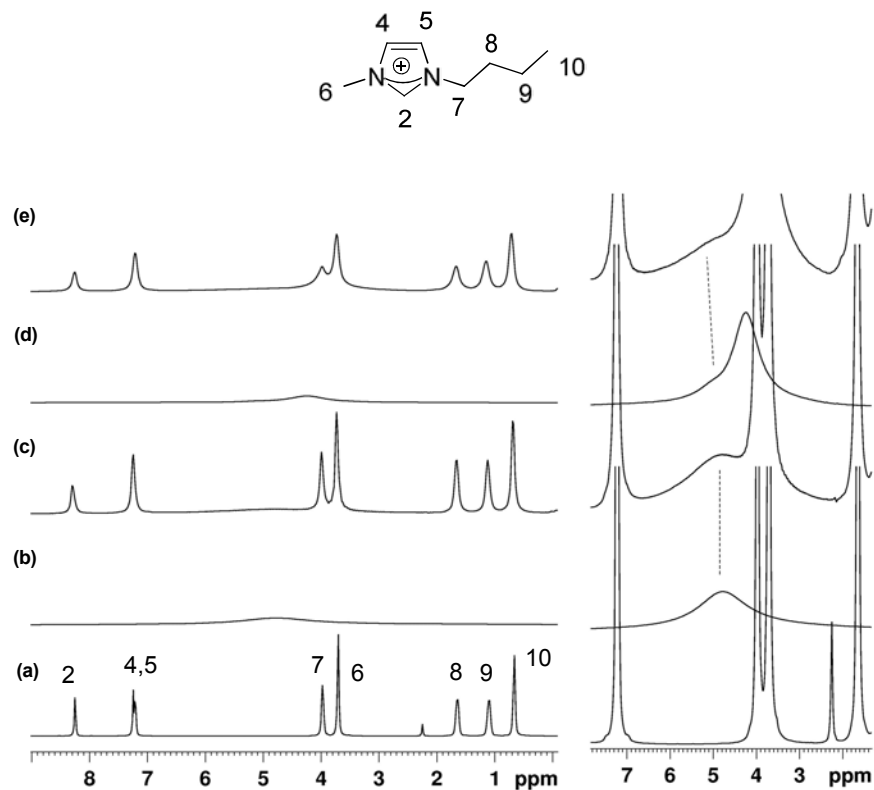


Figure 3.14: ¹H MAS NMR spectra (left) and expansion plots of the NMR peak of hydroxyl protons (right): a) pure [bmim][PF₆], b) Al₂O₃, c) Al₂O₃-SIL, d) SiO₂ and (e) SiO₂-SIL.

Direct polarization and cross polarization experiments were carried out by direct polarization ¹³C{¹H} DP MAS NMR spectra did not show differences between both composites in relation to pure [bmim][PF₆], except some signal broadening for SiO₂-SIL in particular for the methyl of the butyl group (Figure 3.15, signal 9).

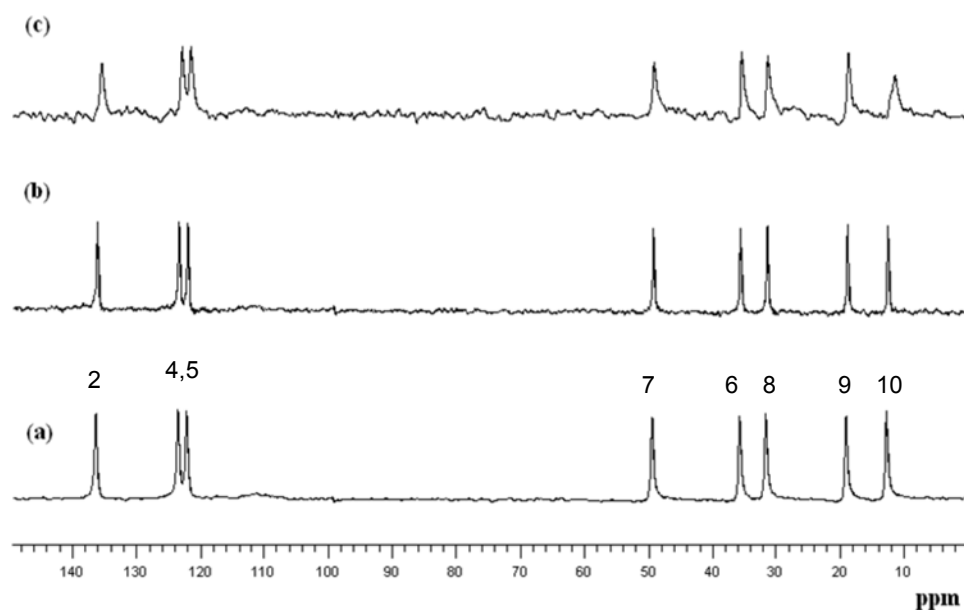


Figure 3.15: $^{13}\text{C}\{^1\text{H}\}$ DP MAS NMR spectra (for labeling; see Figure 3.16): a) pure [bmim][PF₆], b) Al₂O₃-SIL and c) SiO₂-SIL.

On the contrary, the corresponding $^1\text{H}/^{13}\text{C}$ CP MAS NMR spectra revealed notable differences (Figure 3.16). For Al₂O₃-SIL composites, any carbon atom could be distinguished (Figure 3.16b), in contrast to pure ILs where all the carbon atoms were observed (Figure 3.16a). This fact can be related to the higher mobility (^1H - ^{13}C dipolar couplings average to zero) of the protons for the ionic liquid supported on the alumina than that displayed by the pure ionic liquid, in agreement with the supramolecular arrangement showed by imidazolium-based ILs.⁸⁰ It can be concluded that the interaction between Al₂O₃ and the ionic liquid destroys the polymeric structure of the ILs favouring the mobility of the protons. However, for SiO₂-SIL, only the signals corresponding to both methyl groups disappeared (Figure 3.16c, carbon atoms 9 and 10), probably due to a dynamic behaviour of the cations close to the solid surface.

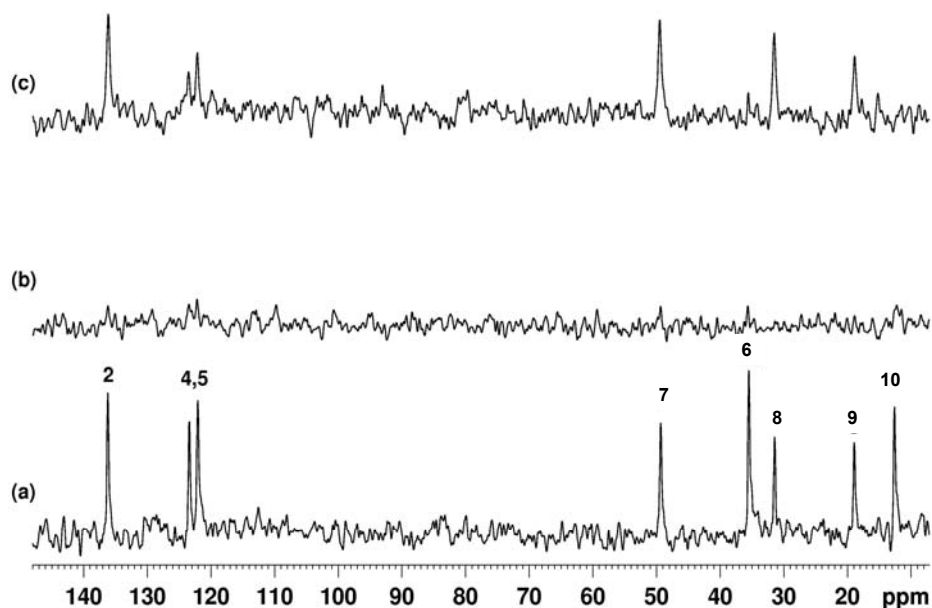


Figure 3.16: ^{13}C CP/MAS NMR spectra (for labeling; see Figure 3.16): a) pure [BMI][PF₆], b) Al₂O₃-SIL and c) SiO₂-SIL.

Concerning the hexafluorophosphate anion, $^{31}\text{P}\{^1\text{H}\}$ and $^{31}\text{P}\{^1\text{H},^{19}\text{F}\}$ MAS NMR spectra did not show differences between the pure ionic liquid and both composites (Figure 3.17).

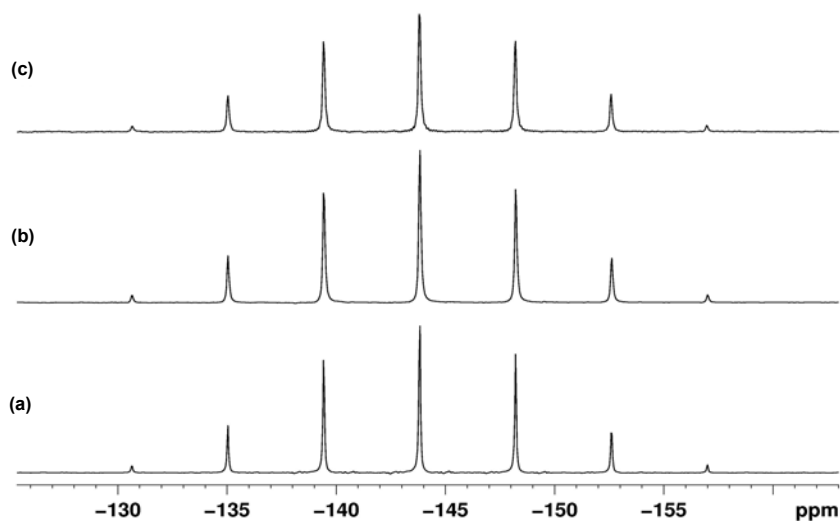


Figure 3.17: $^{31}\text{P}\{^1\text{H}\}$ MAS NMR spectra of: a) pure [bmim][PF₆], b) Al₂O₃-SIL and c) SiO₂-SIL

While ^{19}F MAS NMR spectra for [bmim][PF₆] and Al₂O₃-SIL composite are identical, SiO₂-SIL shows three kinds of different fluor atoms coupled to phosphorous ($^1J_{31\text{P}-19\text{F}} = 710.6$

Hz) (Figure 3.18). This complex signal is probably due to the interactions of PF_6^- with silica and/or the imidazolium cation by hydrogen-bond links. No data of the probable interaction with the silica surface via hydrogen-bond could be obtained. But, its deconvolution evidences four different fluor atoms coupled to phosphorus (Figure 3.19)

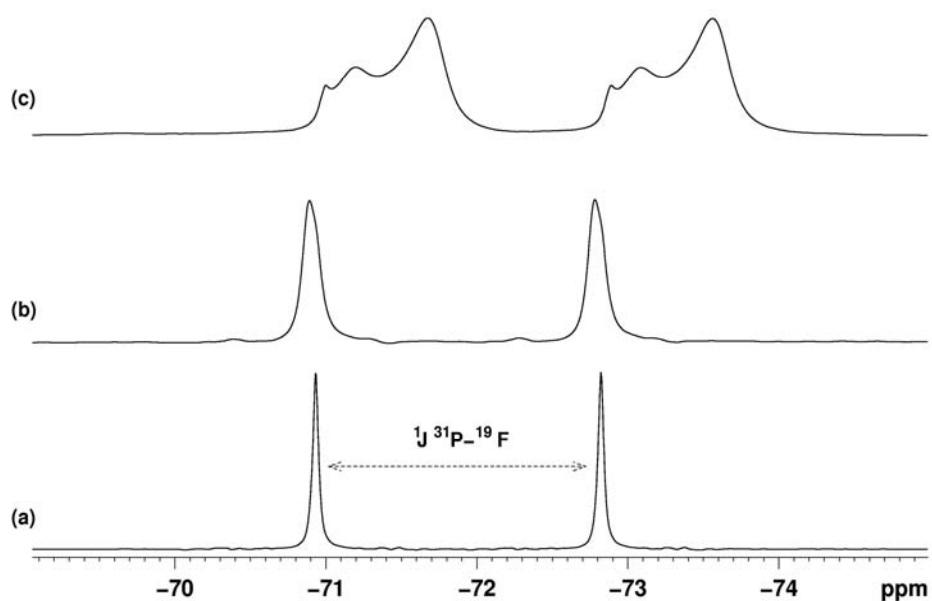


Figure 3.18: ^{19}F MAS NMR spectra of a) $[\text{bmim}][\text{PF}_6]$, b) $\text{Al}_2\text{O}_3\text{-SIL}$ and c) $\text{SiO}_2\text{-SIL}$

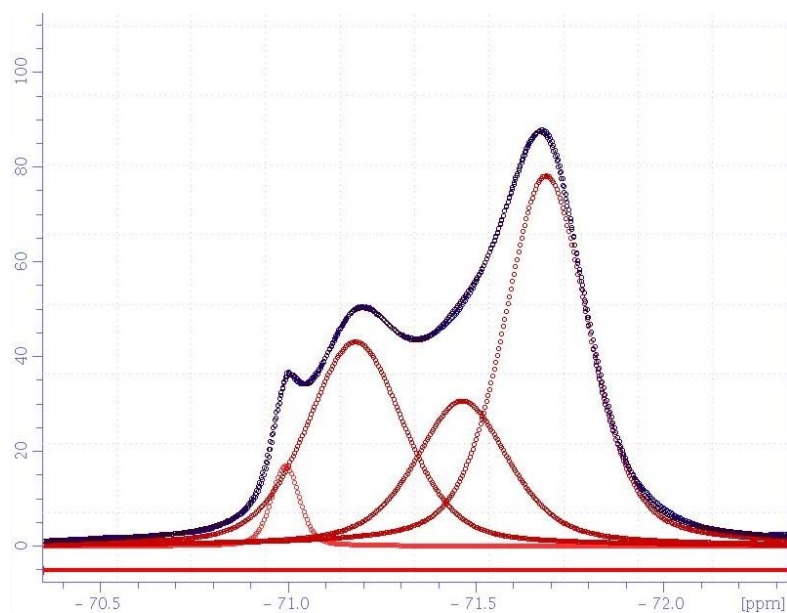


Figure 3.19: ^{19}F MAS NMR spectrum of $\text{SiO}_2\text{-SIL}$ (only showing the signal at ca. -71.5 ppm). Spectrum was fully deconvoluted by Topspin software. Black trace corresponds to the experimental spectrum

In relation to the supports, ^{29}Si and ^{27}Al CPMAS NMR spectra did not exhibit differences between SiO_2 or Al_2O_3 and their corresponding composites (Figure 3.20). In ^{29}Si MAS NMR, three signals corresponding to the different silicon environments are observed: $\text{Q}_2 = \text{Si}(\text{OSi})_2(\text{OH})_2$, $\text{Q}_3 = \text{Si}(\text{OSi})_3(\text{OH})$ and $\text{Q}_4 = \text{Si}(\text{OSi})_4$. Those different OH groups at the SiO_2 surface probably interacts with the fluor atoms of hexafluorophosphate anion leading to different fluor atoms coupled to phosphorous as observed in Figure 3.18.

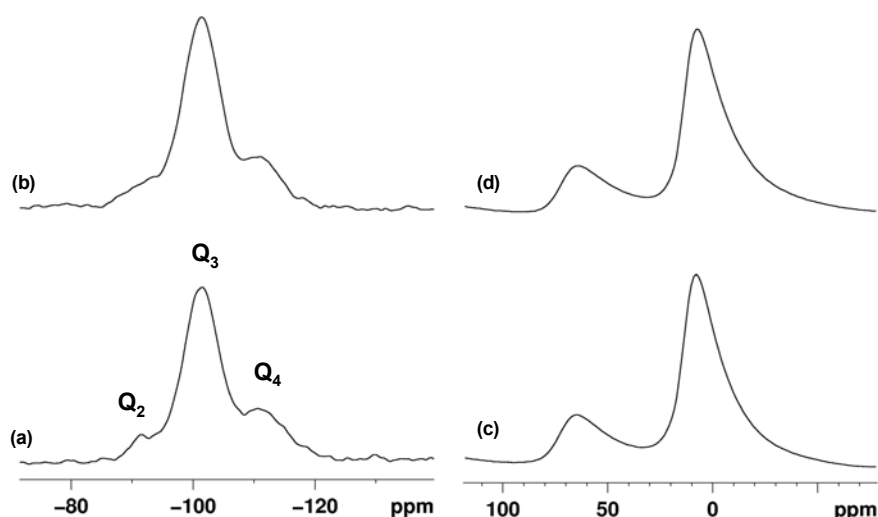


Figure 3.20. ^{29}Si CPMAS NMR spectra (left): (a) SiO_2 and (b) $\text{SiO}_2\text{-SIL}$. ^{27}Al MAS NMR spectra (right) (c) Al_2O_3 and (d) $\text{Al}_2\text{O}_3\text{-SIL}$

Concerning the interactions of the anion with the support, cross polarization $^{19}\text{F}\text{-}^{29}\text{Si}$ experiments could not evidence any correlation of proximity between fluor and silicon atoms. The analogous experiments with ^{27}Al could not be carried out due to its quadrupolar moment.

The different affinity of the ionic liquid for both surfaces reminds the point of zero charge (PZC) in surface science. The point of zero charge, a physico chemical concept in relation to the adsorption phenomenon, describes the conditions when the electrical charge density on a surface is zero and it is usually determined in relation to the pH of an electrolyte only for systems in which H^+ and OH^- are the potential-determining ions (the common case). For SiO_2 the theoretical PZC is around $\text{pH} = 3$ and for Al_2O_3 around $\text{pH} = 8$. When the pH is lower than the PZC value, the system is "below the PZC." Below the PZC, the acidic water donates more protons than hydroxide groups, and in consequence the adsorbent surface is positively charged and attracts the anions. On the contrary, the surface is negatively charged "above PZC" and attracts cations or repels the anions. Maybe the different adsorption of the ionic

liquid onto both supports is related to the PZC, thus further studies considering this parameter should be a new pathway to explore.

In relation to the interactions between anion and cation, cross polarization ^{19}F - ^{13}C experiments were carried out, but any close interaction could be observed (broad signals), probably due to the dipolar decoupling with ^1H .

In summary, the NMR study reveals a loss of structural order of the ionic liquid when supported on alumina, increasing the protons mobility of the imidazolium moiety, in agreement with previous research works concerning the interaction of ammonium surfactants with disordered materials⁸⁴ without showing any interaction neither with the anion nor with the surface. On the other hand, SiO_2 -SIL presents a strong interaction between the ionic liquid and the silica evidenced for imidazolium cation and hexafluorophosphate anion, probably by means of hydrogen bonds between silica, the anion and the cation, analogously to the physisorption proposed for N-methylimidazolium chloride adsorbed on silica.⁸⁵

We have inferred that the different thermal decomposition temperature exhibited in the TGA for SiO_2 -SIL (315 °C) and Al_2O_3 -SIL (434 °C) compared to pure ILs (425 °C) and the supramolecular destructure observed by the structural study (NMR, DRX and DSC) could have an influence on the vapour pressure of $[\text{bmim}][\text{PF}_6]$. A surface mediated distillation was thus performed with both composites SiO_2 -SIL and Al_2O_3 -SIL.

3.4.4 Ionic Liquid surface mediated distillation

Taking into account TGA results, the distillation process was carried out under reduced pressure (0.5 mbar) at 240 °C. The distilled product was recovered by cooling the gas phase.

The composite SiO_2 -SIL(10 %) was chosen because of a 10% of ionic liquid loading corresponds to a thin film of ca. 1.7 layers, considering a triclinic symmetry for the $[\text{bmim}][\text{PF}_6]$.⁸⁶ This thin ILs film on silica signifies strong interactions between the solid surface and the ionic liquid.

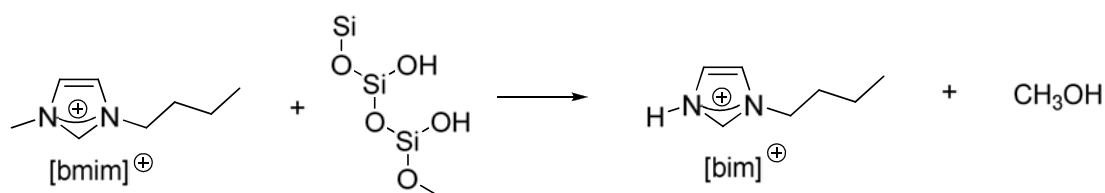
Decomposition of the ionic liquid was observed when the reaction was performed for 24 hours increasing the temperature from 180 to 250. The product obtained was characterized by multi-nuclear (^1H , ^{13}C , ^{19}F and ^{31}P) NMR spectroscopy, showing a complete degradation of both anion (with disappearance of F and P signals) and cation probably due to a Hoffmann elimination promoted by hydroxyl groups of the SiO_2 surface.

At 250 °C for three hours, ^1H and ^{13}C NMR (in acetone- d_6) spectra of the distilled product mainly showed a signals pattern corresponding to butyl imidazole cation, $[\text{bim}]$. Other minor signals can be related to $[\text{bmim}]$ cation. In relation to the characterization of the anion, ^{31}P NMR spectrum mainly evidenced the presence of PF_6 , but signals at ca. 0 ppm also points to

the formation of phosphates. ^{19}F NMR spectrum exhibited in addition to the expected doublet at *ca.* -70 ppm attributed to hexafluorophosphate anion, another signal (singlet) at -140 ppm was also observed.

Mass spectrometry analysis (IS, positive mode) showed one peak at m/z 125 attributed to [bim] cation and another at 139 which corresponds to [bmim] cation. The PF_6 counter anion peak was also observed in the mass spectroscopy analysis (IS, negative mode) at m/z 145.

These results can be related to the surface reactivity represented in Scheme 3.5.



Scheme 3.5: Surface like reactivity between [bmim][PF₆] and silica gel.

These facts can be correlated to the NMR study at the solid state described in section 3.4.3. ^{13}C CP/MAS NMR (see Figure 3.16, section 3.4.3) spectra evidenced the disappearance of the two methyl groups, indicating a stronger interaction of them with the surface than that produced with the other protons of the cation.

As expected from TGA analyses, Al_2O_3 -SIL(10 %) composite did not distillate at 240 °C because of the high temperature decomposition of the ionic liquid layer, similar to that observed for neat ionic liquid. An orange liquid residue was obtained after distillation, mainly constituted by water. Similar treatment was applied for the distillation of pure ionic liquid. No distillation product under the same conditions was observed after 6 h of reaction. ^1H , ^{13}C , ^{19}F and ^{31}P NMR patterns of the undistilled ionic liquid showed no structural modifications.

In conclusion, the product distribution depends on the reaction time, avoiding a complete degradation when short times (3 h versus 24 h) were applied. Thus, a mixture of product was obtained: a [bmim][PF₆] distilled product and an imidazolium-based ionic liquid coming from the surface reactivity due to the surface destructure. Further studies should be realized in order to clarify the obtained results and determined the other unassigned minor species formed.

-
- ¹ C.P. Mehnert, *Chem. Eur. J.* **2005**, 11, 50.
- ² (a) M A. Gelesky, S S X. Chiaro F A. Pavan, J H Z. dos Santos, J. Dupont, *Dalton Trans.* **2007**, 5549; (b) U. Hintermair, G. Zhao, C. Santini, M J. Muldoon, D J. Cole-Hamilton, *Chem. Commun.* **2007**, 1462.
- ³ W A. Herrmann, *Applied Homogeneous Catalysis with Organometallic Compounds*, ed. B. Cornils Wiley-VCH, Weinheim, **2002**, pp. 600–699.
- ⁴ A. Riisager, B. Jørgensen, P. Wasserscheid, R. Fehrmann, *Chem. Commun.*, **2006**, 994.
- ⁵ H. Vu, F. Gonc alves, R. Philippe, E. Lamouroux, M. Corrias, Y. Kihn, D. Plee, P. Kalck, P. Serp, *J. Catal.*, **2006**, 240, 18.
- ⁶ X. Pan, Z. Fan, W. Chen, Y. Ding, H. Luo, X. Bao, *Nature Mater.* **2007**, 6, 507.
- ⁷ P. Serp, M. Corrias, P. Kalck, *Appl. Catal. A* **2003**, 253, 337.
- ⁸ M. Ruta, I. Yuranov, P. J. Dyson, G. Laurenczy, L. Kiwi-Minsker, *J. Catal.* **2007**, 247, 269.
- ⁹ R.R. Schrock, J.A. Osborn, *J. Am. Chem. Soc.* **1971**, 2397
- ¹⁰ *Nanoscale materials in chemistry*; K. J. Klabunde, (Eds) Wiley-Interscience: New York, **2001**
- ¹¹ A. Henglein, *Chem. Rev.* **1989**, 89, 1861.
- ¹² T. Vossmeier, E. DeIonno, J. R. Heath, *Angew. Chem. Int. Ed. Engl.* **1997**, 36, 1080.
- ¹³ W. Caseri, *Macromol. Rapid Commun.* **2000**, 21, 705.
- ¹⁴ M. Antonietti, C. Göltner, *Angew. Chem. Int. Ed. Engl.* **1997**, 36, 910.
- ¹⁵ G. Schmid, *Adv. Eng. Mater.* **2001**, 3, 737.
- ¹⁶ G. Schmid, U. Simon, *Chem. Commun.* **2005**, 697.
- ¹⁷ J. Glanz, *Science* **1995**, 269, 1363.
- ¹⁸ A. P. Alisivatos, K. P. Johnsson, X. Peng, T. E. Wilson, C. J. Loweth, M. P. Jr. Bruchez, P. G. Schultz, *Nature* **1996**, 382, 609.
- ¹⁹ R. Elghanian, J.J. Storhoff, R.C. Mucic, R.L. Letsinger, C.A. Mirkin, *Science* **1997**, 277, 1078.
- ²⁰ H. Bönemann, R.M. Richards, *Eur. J. Inorg. Chem.* **2001**, 2455.
- ²¹ J.D. Aiken III, R.G. Finke, *J. Mol. Catal. A: Chem.* **1999**, 145, 1.
- ²² A. Roucoux, J. Schulz, H. Patin, *Chem. Rev.* **2002**, 102, 3757.
- ²³ D. Astruc, F. Lu, A. Ruiz, *Angew. Chem. Int. Ed.* **2005**, 44, 7852.
- ²⁴ G. Schmid, *Chem. Rev.* **1992**, 92, 1709.

-
- ²⁵ Clusters and colloids: from theory to applications; J. S. Bradley, G. Schmid, (Eds.) VCH: Weinheim, **1994**.
- ²⁶ R.G. Finke, In Metal nanoparticles: synthesis, characterization, and applications; Feldheim, D. L., Foss, C. A., (Eds.), Marcel Dekker: New York, **2002**; chap. 2.
- ²⁷ B.L. Cushing, V.L. Kolesnichenko, C.J. O'Connor, Chem. Rev. **2004**, 104, 3893.
- ²⁸ M.S. Sibbald, G. Chumanov, T. M. Cotton, J. Phys. Chem. **1996**, 100, 4672.
- ²⁹ J. Zhang, J. Worley, S. Dénomée, C. Kingston, Z.J. Jakubek, Y. Deslandes, M. Post, B. Simard, J. Phys. Chem. B **2003**, 107, 6920.
- ³⁰ M.A. Watzky, R.G. Finke, J. Am. Chem. Soc. **1997**, 119, 10382.
- ³¹ J.A. Widegren, J.D. Aiken III, S. Özkar, R.G. Finke, Chem. Mater. **2001**, 13, 312.
- ³² J. Turkevich, P.C. Stevenson, J. Hillier, Discuss. Faraday Soc. **1961**, 11, 55-75
- ³³ K.J. Klabunde, H.F. Efner, T.O. Murdock, R. Ropple, J. Am. Chem. Soc. **1976**, 98, 1021.
- ³⁴ T.O. Murdock, K.J. Klabunde, J. Org. Chem. **1976**, 41, 1076.
- ³⁵ I. Willner, D. Mandler, J. Am. Chem. Soc. **1989**, 111, 1330.
- ³⁶ N. Toshima, T. Yonezawa, New J. Chem. **1998**, 22, 1179.
- ³⁷ M.T. Reetz, W. Helbig, J. Am. Chem. Soc. **1994**, 116, 7401.
- ³⁸ M.T. Reetz, G. Lohmer, Chem. Commun. **1996**, 1921
- ³⁹ C.W. Chen, M. Akashi, Langmuir, **1997**, 13, 6465.
- ⁴⁰ C.K. Tan, W. Newberry, T.R. Webb, C.A. McAuliffe, J. Chem. Soc., Dalton Trans. **1987**, 1299.
- ⁴¹ M.R. Mucalo, R.P. Cooney, J. Chem. Soc., Chem. Commun. **1989**, 94.
- ⁴² M. Zhao, L. Sun, R.M. Crooks, J. Am. Chem. Soc. **1998**, 120, 4877.
- ⁴³ K. Esumi, T. Tano, K. Meguro, Langmuir **1989**, 5, 268.
- ⁴⁴ J.L. Marignier, J. Belloni, M.O. Delcourt, J.P. Chevalier, Nature **1985**, 317, 344.
- ⁴⁵ K.S. Suslick, S.-B. Choe, A.A. Cichowlas, M.W. Grinstaff, Nature **1991**, 353, 414.
- ⁴⁶ N.A. Dhas, A. Gedanken, J. Mater. Chem. **1998**, 8, 445.
- ⁴⁷ N.A. Dhas, K.S. Suslick, J. Am. Chem. Soc. **2005**, 127, 2368.
- ⁴⁸ J.S. Bradley, E W. Hill, S. Behal, C. Klein, B. Chaudret, A. Duteil, Chem. Mater. **1992**, 4, 1234.
- ⁴⁹ A. Duteil, R. Quéau, B. Chaudret, R. Mazel, C. Roucau, J.S. Bradley, Chem. Mater. **1993**, 5, 341.

-
- ⁵⁰ L.S. Ott, R.G. Finke, *Coord. Chem. Rev.* **2007**, 251, 1075.
- ⁵¹ J. D. Aiken III, Y. Lin, R.G. Finke, *J. Mol. Catal. A: Chem.* **1996**, 114, 29.
- ⁵² K. Itoh, F. Ueda, K. Hirai, Y. Ishii, *Chem. Lett.* **1977**, 6, 877.
- ⁵³ N. Miyaura, A. Suzuki, *Chem. Rev.* **1995**, 95, 2457.
- ⁵⁴ D. Astruc, F. Lu, J.R. Aranzaes, *Angew. Chem.* **2005**, 117, 8062; *Angew. Chem. Int. Ed.* **2005**, 44, 7852.
- ⁵⁵ P. Migowski, J. Dupont, *Chem. Eur. J.* **2007**, 13, 32.
- ⁵⁶ J. Dupont, G.S. Fonseca, A.P. Umpierre, P.F.P. Fichtner, S.R. Teixeira, *J. Am. Chem. Soc.* **2002**, 124, 4228.
- ⁵⁷ F. Fernández, B. Cordero, J. Durand, G. Muller, F. Malbosc, Y. Kihn, E. Teuma, M. Gómez, *Dalton Trans.* **2007**, 5572.
- ⁵⁸ S. Jansat, J. Durand, I. Favier, F. Malbosc, C. Pradel, E. Teuma, M. Gomez, *ChemCatChem* **2009**, 1, 244.
- ⁵⁹ J. Durand, E. Teuma, F. Malbosc, Y. Kihn, M. Gómez, *Catal. Commun.* **2008**, 9, 273.
- ⁶⁰ R.M. Crooks, M. Zhao, L. Sun, V. Chechik, L.K. Yeung, *Acc. Chem. Res.* **2001**, 34, 181.
- ⁶¹ B.P.S. Chauhan, J.S. Rathore, M. Chauhan, A. Krawicz, *J. Am. Chem. Soc.* **2003**, 125, 2876.
- ⁶² C. Amiens, D. de Caro, B. Chaudret, J.S. Bradley, R.Mazel, C. Roucau, *J. Am. Chem. Soc.* **1993**, 115, 11638.
- ⁶³ C. Pan, K. Pelzer, K. Philippot, B. Chaudret, F. Dassenoy, P. Lecante, M.J. Casanove, *J. Am. Chem. Soc.* **2001**, 123, 7584.
- ⁶⁴ Y. Lin, R.G. Finke, *J. Am. Chem. Soc.* **1994**, 116, 8335.
- ⁶⁵ S. Özkar, R.G. Finke, *J. Am. Chem. Soc.* **2002**, 124, 5796.
- ⁶⁶ Y. Yin, A.P. Alisivatos, *Nature* **2005**, 437, 664.
- ⁶⁷ M.J. Earle, J.M.S.S. Esperança, M.A. Gilea, J.N. Canongia Lopes, L.P.N. Rebelo, J.W. Magee, K.R. Seddon, J.A. Widegren, *Nature* **2006**, 439, 831.
- ⁶⁸ K. Philippot, B. Chaudret, *C. R. Chimie* **2003**, 6, 1019.
- ⁶⁹ J. Durand, E. Teuma, M. Gómez, *C. R. Chimie* **2007**, 10, 152
- ⁷⁰ J. Durand, E. Teuma, M. Gómez, *Eur. J. Inorg. Chem.* **2008**, 3577
- ⁷¹ T.E. Ould, C. Amiens, B. Chaudret, E. Snoeck, M. Respaud, J.M. Broto, *Chem Mater* **1999**, 11, 526.
- ⁷² E. Ramirez, S. Jansat, K. Philippot, P. Lecante, M. Gómez, A.M. Masdeu-Bultó, B. Chaudret, *J. Organomet. Chem.* **2004**, 689, 4601.
- ⁷³ I. Favier, M. Gómez, G. Muller, D. Picurelli, A. Nowicki, A. Roucoux, J. Bou, *J. Appl. Polym. Sci.* **2007**, 105, 2772.

-
- ⁷⁴ I. Favier, S. Massou, E. Teuma, K. Philippot, B. Chaudret, M. Gómez, *Chem. Commun.* **2008**, 3296.
- ⁷⁵ D. Sanhes, Nouveaux ligands dihydroanthracène vers la formation de nanoparticules et de complexes de palladium. Etudes de leur comportement catalytique dans différents milieux. PhD thesis, Toulouse University, December **2008**.
- ⁷⁶ J. Huang, T. Jiang, H. Gao, B. Han, Z. Liu, W. Wu, Y. Chang, G. Zhao, *Angew. Chem. Int. Ed.* **2004**, 43, 1397
- ⁷⁷ S. Chen, G. Wu, M. Sha, S. Huang, *J. Am. Chem. Soc.* **2007**, 129, 2416.
- ⁷⁸ (a) T. Fukushima, A. Kosaka, Y. Ishimura, T. Yamamoto, T. Takigawa, N. Ishii, T. Aida, *Science* **2003**, 300, 2072; (b) Y. Zhao, H. Liu, Y. Kou, M. Li, Z. Zhu, Q. Zhuang, *Electrochem. Commun.* **2007**, 9, 2457.
- ⁷⁹ T. Fukushima, T. Aida, *Chem.–Eur. J.* **2007**, 13, 5048.
- ⁸⁰ (a) A. Karout, A.C. Pierre, *Catal. Commun.* **2009**, 10, 359. (b) K. Ueno, K. Hata, T. Katakabe, M. Kondoh, M. Watanabe, *J. Phys. Chem. B* **2008**, 112, 9013.
- ⁸¹ T. Fukushima, A. Kosaka, Y. Ishimura, T. Yamamoto, T. Takigawa, N. Ishii, T. Aida, *Science* **2003**, 300, 2072-2074.
- ⁸² J.G. Huddleston, A.E. Visser, W.M. Reichert, H.D. Willauer, G.A. Broker, R.D. Rogers, *Green Chem.* **2001**, 3, 156.
- ⁸³ A. Triolo, A. Mandanici, O. Russina, V. Rodriguez-Mora, M. Cutroni, C. Hardrace, M. Nieuwenhuyzen, H.-J. Bleif, L. Keller, M.A. Ramos, *J. Phys. Chem. B* **2006**, 110, 21357.
- ⁸⁴ (a) L.Q. Wang, J. Liu, G.J. Exarhos, B.C. Bunker, *Langmuir* **1996**, 12, 2663. (b) L.Q. Wang, G.J. Exarhos, J. Liu, *Adv. Mater.* **1999**, 11, 1331.
- ⁸⁵ R. Lungwitz, S. Spange, *J. Phys. Chem. C* **2008**, 112, 19443-19448.
- ⁸⁶ A.R. Choudhury, N. Winterton, A. Steiner, A.I. Cooper, K.A. Johnson, *J. Am. Chem. Soc.* **2005**, 127, 16792.

CHAPTER IV

Supported ionic liquid phase: applications in catalysis

4 SUPPORTED IONIC LIQUID PHASE: APPLICATIONS IN CATALYSIS

Over the last twenty years several homogeneous catalysts dissolved in ionic liquid medium have been used in liquid–liquid biphasic systems.^{1,2} Inspired by the work of Davis et al. on supported aqueous-phase catalysis,³ Mehnert and co-workers in 2002 combined the advantages of ionic liquid phase with solid supported materials.^{4,5} The supported ionic liquid phase catalysis has attracted much attention in recent years, being applied for both metallic complexes and metal nanoparticles in several catalytic processes such as hydrogenation, hydroformylation, hydroamination or methanol carbonilations (see section 1.2).

In the present work, the behaviour of two different catalytic supported ionic liquid systems on functionalized multi-walled carbon nanotubes has been studied. Rhodium complex $[\text{Rh}(\text{nbd})(\text{PPh}_3)_2]\text{PF}_6$ immobilized as supported homogeneous catalyst, has been applied in hydrogenation reaction of 1-hexene and palladium nanoparticles have been used as supported heterogeneous catalyst in selective hydrogenation, Heck C-C coupling and also sequential process (Heck coupling followed by hydrogenation).

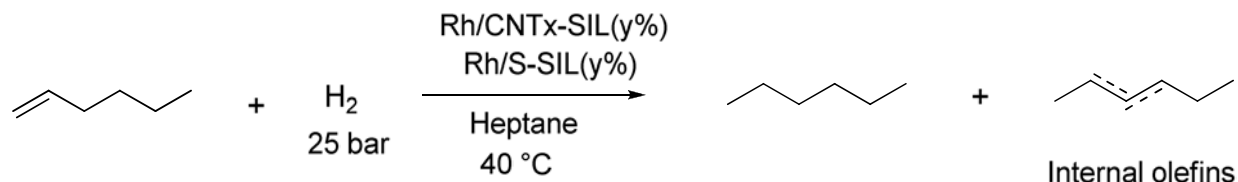
4.1 HOMOGENEOUS SUPPORTED IONIC LIQUID PHASE CATALYSIS: APPLICATIONS IN HYDROGENATION

SILP containing metal complexes (Ru and Rh) immobilized over classical supports (SiO_2 , Al_2O_3 , MgO and AC) have been largely studied in olefin hydrogenation reactions.^{5,6} Usually, these systems present two main advantages compared to homogeneous and biphasic systems: higher activities and better recycling.

Carbon nanotubes can offer significant advantages compared to other classical supports due to their mesoporous nature,⁷ avoiding mass transfer limitations, the possibility to operate in the inner cavity arising high activities and/or selectivities,⁸ and their tunable structure by chemical functionalization.⁹ In this section, we highlight the functionalized MWCNTs catalytic efficiency as support in SILP catalysis for 1-hexene hydrogenation compared to SILPC prepared on oxide supports and active carbon.

4.1.1 Results and discussion

The catalytic activity of the homogeneous SILCP described in section 3.1 was studied for the hydrogenation of 1-hexene. The reaction was carried out in a batch autoclave using heptane as solvent at 40 °C under 25 bar of hydrogen (Scheme 4.1).



$x = 0 - 7$ CNT-[C₈N₃OH₁₁]₁PF₆

S = SiO₂, Al₂O₃, ZrO₂, ZnO, AC, MgO, TiO₂

y = 20, 37, 55, 64% see chapter 3

Scheme 4.1: Rh/SILP-catalyzed 1-hexene hydrogenation.

Purified, oxidized and functionalized multi-walled carbon nanotubes were used as supports. The ratio between the rhodium catalyst [Rh(nbd)(PPh₃)₂]₁PF₆ immobilized in the ionic liquid [bmim]₁[PF₆] phase and the substrate was 1/2900. The yield was determined by GC (gas chromatography) analysis.

In a first study, we have studied the influence of MWCNTs functionalization on the catalytic behaviour of SILPC. After 2 h reaction, Rh/CNT0-SIL(y%) (y = 20 to 55%) (Table 4.1, entries 1-3) and Rh/CNT2-SIL(55%) (Table 4.1, entry 9) led to a complete conversion. However, for Rh/CNT0-SIL(y%) (y = 20 to 55%) a severe ILs and Rh leaching was observed, in contrast to Rh/CNT2-SIL system. For Rh/CNT1-SIL, the conversion was not complete at any ionic liquid loading (20, 37, 55%), and ILs and Rh leaching was noticed (determined by ICP). These results evidence the importance of the appropriate functionalization of MWCNTs for the design of stable and recyclable catalysts. Thus only the MWCNTs containing ionic imidazolium moieties (CNT2) avoid the ionic liquid catalytic phase leaching. The non-supported homogeneous catalytic system presented higher catalytic activity than the analogous SILPC one, but the catalyst could not be recuperated at the end of the reaction (Table 4.1, entry 10).

Entry	Catalyst	Conversion (%) ^a	Selectivity (%) ^{a,b}	TOF (h ⁻¹) ^c
1	Rh/CNT0-SIL(20%)	100	80	959
2	Rh/CNT0-SIL(37%)	100	79	959
3	Rh/CNT0-SIL(55%)	100	78	959
4	Rh/CNT1-SIL(20%)	85	47	815
5	Rh/CNT1-SIL(37%)	66	52	633
6	Rh/CNT1-SIL(55%)	69	73	662
7	Rh/CNT2-SIL(20%)	20	69	192
8	Rh/CNT2-SIL(37%)	45	66	432
9	Rh/CNT2-SIL(55%)	100	79	959
10	Rh/Non-supported ^d	100	100	3597

Table 4.1: Influence of multi-walled carbon nanotubes nature and ionic liquid loading on catalytic hydrogenation. Reaction conditions: Rh/Substrate = 1/2900; Rh = 1.39 10⁻⁵ mol, 0.04 mol of 1-hexene in 55 ml of heptane at 40 °C and 25 bar for 2 hours. ^aDetermined by GC.

^bSelectivity = (mol of hexane x 100)/mol converted. ^cTOF = mol of substrate converted/(mol of catalyst x time (hours)). ^d Substrate = 0.1 mol.

The optimum amount of grafted imidazolium groups on the MWCNTs surface was also evaluated (CNT2<CNT3<<CNT4). For CNT2-SIL (Table 4.1 entries 7-9) and CNT3-SIL (Table 4.2, entries 1-4), the activity was markedly better than that for CNT4-SIL (Table 4.2, entries 5-7), this latter giving low activity whatever the amount of added ILs (20 to 55% w/w). This fact should be related to the poor dispersibility of CNT4-SIL, leading to a low surface of contact (gel formation). Thus, the carbon nanotubes functionalization should be controlled in order to obtain performant catalytic supports favouring the interaction between the supported ionic liquid phase and the surface, but avoiding the gel formation. The catalyst Rh/CNT3-SIL was used in order to evaluate the ionic liquid loading influence on the catalytic phase. The optimum value was clearly reached between 37 and 55% of ILs w/w, achieving TOF of 2880 and 2550 h⁻¹ respectively (Table 4.2, entries 2 and 3).

Entry	Catalyst	Conversion (%) ^a	Selectivity (%) ^{a,b}	TOF (h ⁻¹) ^c
1	Rh/CNT3-SIL(20%)	79	81	1270
2	Rh/CNT3-SIL(37%)	100	90	2880
3	Rh/CNT3-SIL(55%)	100	92	2550
4	Rh/CNT3-SIL(64%)	88	84	1140
5	Rh/CNT4-SIL(20%)	26	72	417
6	Rh/CNT4-SIL(37%)	20	80	321
7	Rh/CNT4-SIL(55%)	11	100	176

Table 4.2: Influence of the amount of grafted ionic functionalities on the CNT surface and the ionic liquid loading. Reaction conditions: Rh/Substrate = 1/2900; Rh = $1.39 \cdot 10^{-5}$ mol, 0.04 mol of 1-hexene in 55 ml of heptane at 40 °C and 25 bar for the specific time. ^aDetermined by GC. ^bSelectivity = (mol of hexane x 100)/mol converted. ^cTOF (turn over frequencies) = mol of substrate converted/(mol of catalyst x time (h)).

With the aim of studying the influence of the support nature on SILP catalysis, we compared the catalytic activity of the Rh/CNT3–SIL(55%) catalyst with that of SILPC (see section 3.1) on a large variety of supports S-SIL(y%) (S = γ -Al₂O₃, ZrO₂, TiO₂, SiO₂, ZnO, MgO and Active Carbon (AC)); these supported ionic liquid catalytic phases were prepared as described in the experimental section 5.5.1. Table 4.3 summarizes the results obtained with these supports at different ionic liquid loading. For Al₂O₃, TiO₂, ZrO₂, MgO and ZnO, the optimal ILs concentration was 20% (Table 4.3, entries 4, 7, 10, 13, 19). Beyond this value, the formation of soft pastes induces a drastic decrease of the catalytic activity or even the impossibility to use the catalyst to as occurred with ZnO-SIL(>20%) due to several technical hitches during work up. For silica and activated carbon, similar conversions were obtained whatever the ILs loading (20 to 55% w/w) (Table 4.3, for SiO₂ entries 1-3, for AC entries 16-18).

Entry	Catalyst	Conversion (%) ^a	Selectivity (%) ^{a,b}	TOF (h ⁻¹)
1	Rh/SiO ₂ -SIL(20%)	96	97	1381
2	Rh/SiO ₂ -SIL(37%)	99	100	1425
3	Rh/SiO ₂ -SIL(55%)	100	100	1599
4	Rh/Al ₂ O ₃ -SIL(20%)	72	86	1036
5	Rh/ Al ₂ O ₃ -SIL(37%)	58	83	835
6	Rh/ Al ₂ O ₃ -SIL(55%)	45	85	645
7	Rh/TiO ₂ -SIL(20%)	52	73	748
8	Rh/TiO ₂ -SIL(37%)	44	64	633
9	Rh/TiO ₂ -SIL(55%)	25	67	360
10	Rh/ZrO ₂ -SIL(20%)	20	88	289
11	Rh/ZrO ₂ -SIL(37%)	21	80	302
12	Rh/ZrO ₂ -SIL(55%)	23	81	331
13	Rh/MgO-SIL(20%)	49	77	705
14	Rh/MgO-SIL(37%)	40	79	576
15	Rh/MgO-SIL(55%)	67	74	964
16	Rh/AC-SIL(20%)	68	73	978
17	Rh/AC-SIL(37%)	69	78	993
18	Rh/AC-SIL(55%)	70	85	1007
19	Rh/ZnO-SIL(20%)	75	84	1079

Table 4.3: Influence of the nature of the support and the ionic liquid loading in the Rh/SILP-catalyzed hydrogenation. Reaction conditions: Rh/Substrate = 1/2900; Rh = 1.39·10⁻⁵ mol, 0.04 mol of 1-hexene in 55 ml of heptane at 40 °C and 25 bar the specific time. ^aDetermined by GC. ^bSelectivity = (mol of hexane x 100)/mol converted

As noticed in Figure 4.1, Rh/SILPCs prepared with CNT3 showed better performances than SILPC supported on oxide supports, including SiO₂ or activated carbon. Indeed, Rh/CNT3–SIL(55%) showed almost twice the catalytic activity of Rh/SiO₂–SIL. This result is probably related to the open structure of MWCNTs aggregates that facilitates mass transport and improves the kinetics avoiding the trapping of catalysts inside the pores as happens for other supports. The highest selectivity towards n-hexane was obtained on SiO₂, followed by Rh/CNT2–SIL(55%). Significant isomerization was observed for activated carbon and TiO₂ supports.

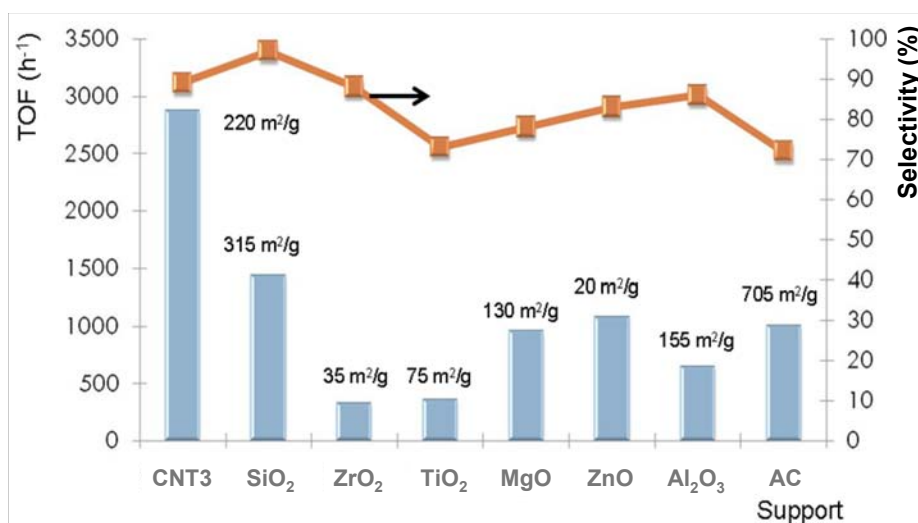


Figure 4.1: Activity and selectivity of Rh-catalyzed hydrogenation of 1-hexene using different supports. Specific surface area values are indicated for each support.

The reaction kinetics was monitored by the hydrogen pressure consumption for the silica gel and CNT3 rhodium supported catalysts. It should be noted (Figure 4.2) that a significant induction period was required for Rh/SiO₂-SIL(55%), in contrast to Rh/CNT3-SIL(55%) catalyst. This fact could be probably related to the complex accessibility. Strong interactions between the hydroxyl groups of the SiO₂ surface and the rhodium complex could take place, giving stable species. In this case, the ionic liquid might surround the [Rh(nbd)(PPh₃)₂]PF₆ complex making difficult the substrate access. Even more, the SiO₂ support has lesser open mesoporous structure than that exhibited by MWCNTs, making more difficult the interaction of the substrate with the catalyst.

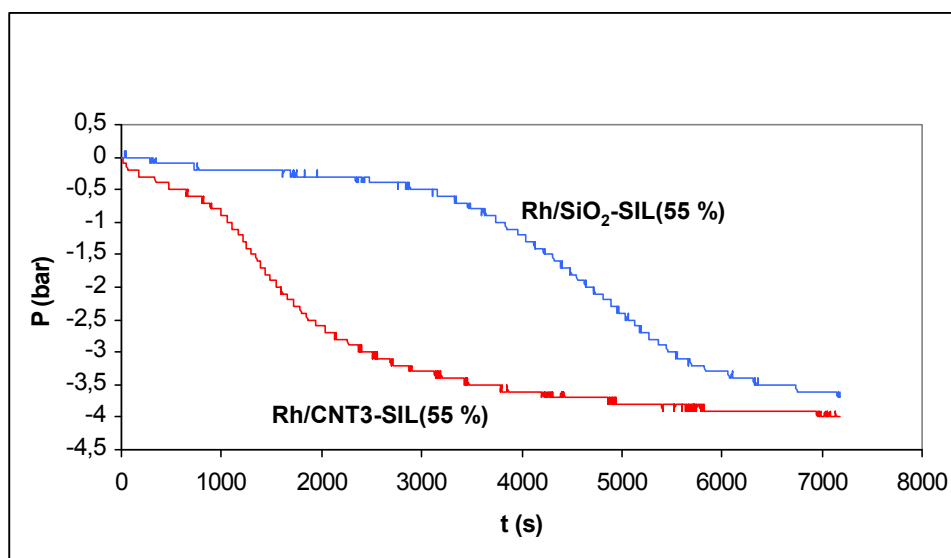


Figure 4.2: Kinetics profile for Rh catalyst supported on silica and functionalized MWCNTs. Reaction conditions: Rh/Substrate = 1/2900; Rh = $1.39 \cdot 10^{-5}$ mol, 0.04 mol of 1-hexene in 55 ml of heptane at 40 °C and 25.

The effective performances in the recycling process was studied using Rh/CNT2–SIL(55%) as catalyst. The supported catalytic system was separated from the reaction medium by filtration and reused five times without any loss of catalytic activity; the selectivity towards hexane in relation to the olefin isomerization was found to increase up to 100% after the second cycle (Figure 4.3). This increase in selectivity could be probably related to the formation of a catalytic species that favours the selectivity towards hexane after the first run. A study of the selectivity evolution with the reaction time could be interesting to understand this behaviour and the relation with the kinetics profile. After the reaction, the extraction of the ionic liquid phase with acetone evidenced the presence of the Rh precursor by ^1H and ^{31}P NMR spectroscopy.

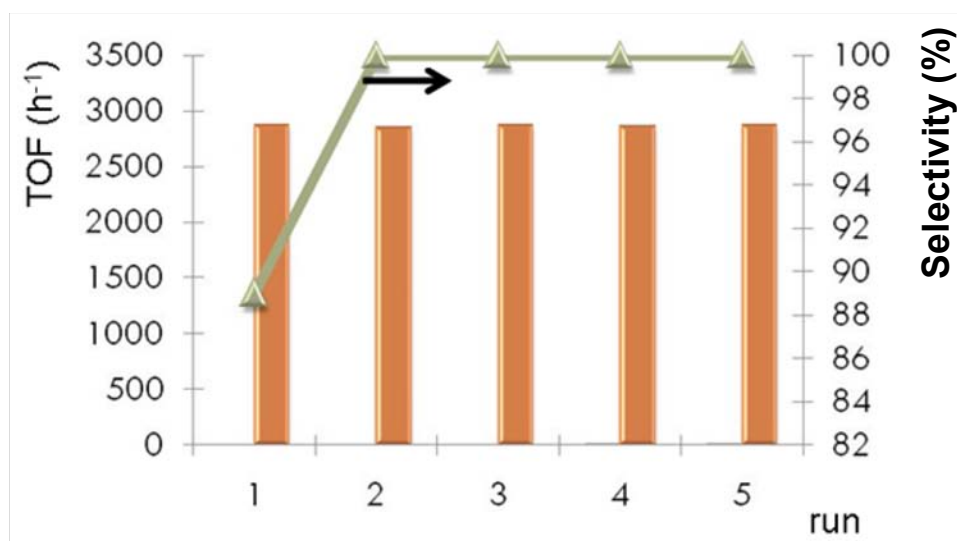


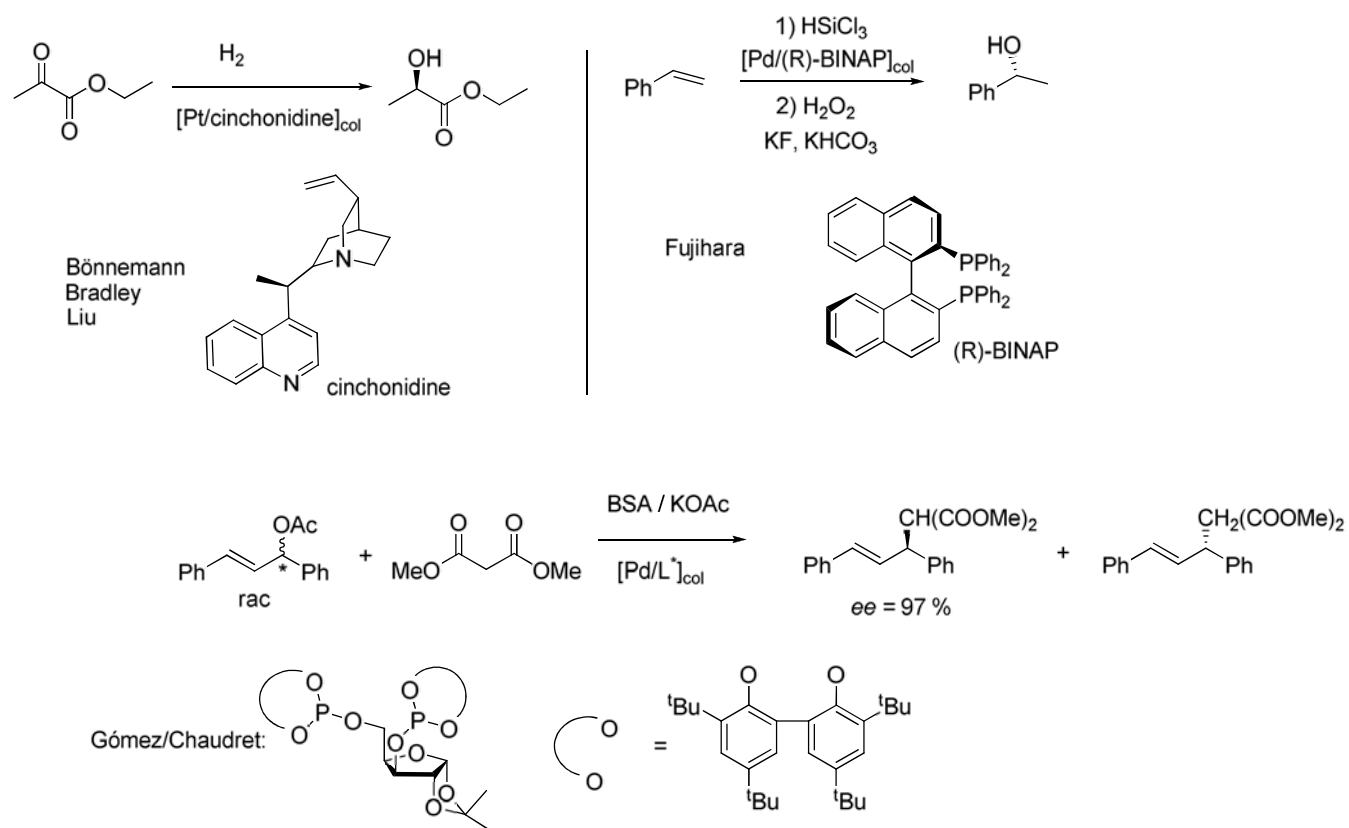
Figure 4.3: Recycling experiments for 1-hexene hydrogenation catalyzed by Rh/CNT2-SIL(55 %). Reaction conditions: Rh/Substrate = 1/2900; Rh = $1.39 \cdot 10^{-5}$ mol, 0.04 mol of 1-hexene in 55 ml of heptane at 40 °C and 25 bar for 2 hours.

4.2 HETEROGENEOUS SUPPORTED IONIC LIQUID PHASE CATALYSIS: APPLICATIONS IN HECK C-C COUPLING AND SELECTIVE HYDROGENATION.

The first reports with metallic entities showing nanometric scale size come from the XIX century. Michael Faraday was the first scientist to work with this kind of systems,¹⁰ although the name of colloid for those entities was introduced later by T. Graham.¹¹ Soon after, many other authors worked in this field,¹² some of them using colloids for catalytic purposes,¹³ until J. Turkevitch et al. synthesized the first known real metallic nanoparticles in 1970 (see section 3.2.).¹⁴

These new systems, mainly gold nanoparticles, were immediately used as catalysts in a variety of reactions such as hydrogen¹⁵ and oxygen¹⁶ transfers and olefin hydrogenation.^{17,18} Nowadays, metallic nanoparticles are applied in almost any catalytic process known.¹⁹ Some selected examples concerns their use in hydrogenation,^{20,21} hydrosilylation,²² oxidation²³ and allylic alkylation^{24,25} reactions. In relation to selective catalytic applications, very few nanoparticle-catalyzed processes have been reported (Scheme 4.2). One of the most interesting applications is the piruvate hydrogenation catalyzed by Pt or Pd nanoparticles using cinchonidine as chiral auxiliary, leading to excellent enantioselectivities (up to 98 % *ee*) in.^{26,27,28} Good enantioselectivities have been also found for hydrosilylation of styrene with

Pd/BINAP colloidal systems.²⁹ It is also remarkable the kinetic resolution of substrate induced by palladium nanoparticles stabilized by chiral phosphites in allylic alkylation.²⁴



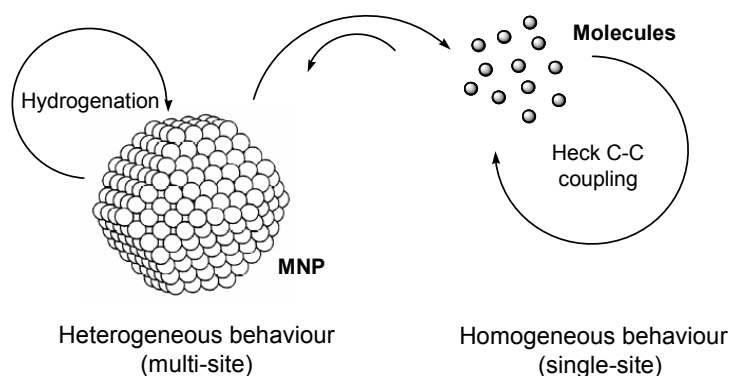
Scheme 4.2: Examples of enantio selective processes catalyzed by metallic nanoparticles stabilized by chiral ligands.

Another type of process where nanoclusters have been widely used as catalysts are C-C bond formation reactions,^{30,31} especially Heck³² and Suzuki³³ couplings. These reactions include some examples where the particles are formed without the addition of any extra stabilizing agent apart from the solvent or the ligands that the metallic precursor could contain (ligand-free system).^{34,35,36,37}

Some of these ligand-free systems have taken advantage of the use of ionic liquids as solvents,³⁸ since the ionic liquid itself can act as stabilizing agent for metallic nanoparticles, especially in the case of imidazolium-based ILs.³⁹ The use of ILs permits the immobilization of the metallic nanoparticles and, therefore, the recycling of the catalyst.^{40,41} In spite of good results obtained in ionic liquid biphasic catalysis, the use of solid catalysts is still preferred from a point of view of practical work-up. In this respect, a new strategy was developed in this area: the preparation of solid-supported metal nanoparticles using ILs. In this case, the ionic liquid plays two important roles acting as metal nanoparticles stabilizer and

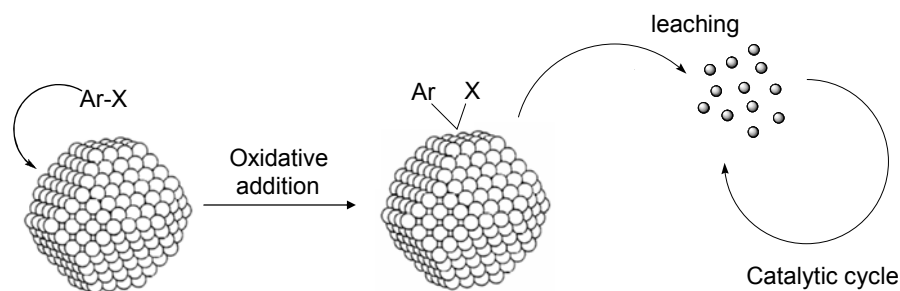
immobilizing agent on the support. This strategy has been in particular applied with Pd, Pt, Ru and Rh metal nanoparticles, in different ionic liquids and mainly supported onto silica gel or carbonaceous supports (see section 1.1.3.3). In these instances, metallic nanoparticles are prepared in situ by reduction of the metallic precursor and further applied in hydrogenation^{42,43} or C-C cross coupling reactions.^{44,45}

It should be noted that, because of their properties between classical homogeneous and heterogeneous catalysts, metallic nanoparticles used as catalytic precursors in wet medium can behave as reservoir of active molecular species and can also have their own surface-like reactivity, depending on the reaction conditions (Scheme 4.3).^{40,46,47,48}



Scheme 4.3: Representation of nanoparticles as heterogeneous (multi-site) catalysts or reservoir of homogeneous species.

Actually, nanoparticles dispersed in solution can leach molecular species coming from low coordination positions (vertex or edge atoms) promoted by solvation, the presence of Lewis bases or other effects related to the specific reaction conditions.^{49,50} Therefore, the detection of nanoparticles during the catalytic process does not necessarily imply that a surface-like catalytic behaviour takes place. Not even their detection at the end of the reaction is enough to assure the heterogeneity of the catalyst, because leached species coming from small nanoparticles tend to re-agglomerate around large ones to diminish the global energy of the system, in an effect known as Ostwald ripening that makes small particles shrink and large ones grow.^{51,52} Dupont and co-workers postulate that palladium nanoparticles act as a reservoir of molecular complexes in the case of Heck C-C coupling reactions, where leached species are the true homogeneous catalyst.⁵³ Even a mechanism for this coupling is proposed,^{37,54} starting with an oxidative addition on the particles surface and followed by leaching of molecular species that enter the catalytic cycle and re-form nanoparticles at the end of the reaction (Scheme 4.4).



Scheme 4.4: Mechanism proposed for the Heck reaction using palladium nanoparticles as catalytic precursors.

TEM analyses after catalysis shows that nanoparticles have grown in size, from 1.7 nm before to 6.1 nm after catalysis.⁴⁹ Moreover, analysis of the organic phase at low substrate conversion has permitted to detect Pd molecular species.^{37,54,55} ¹³C NMR spectroscopy has evidenced the formation of molecular species in the reaction between Pd colloids and iodobenzene.⁵⁵

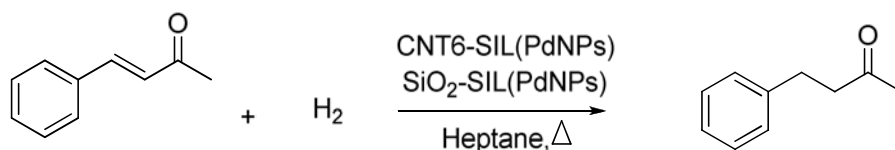
In this section, we have taken advantage of this dual catalytic behaviour with palladium nanoparticles preformed in ionic liquid and further supported on ionic functionalized multi-walled carbon nanotubes. The surface-like reactivity of the supported ionic liquid catalytic phase was evidenced in hydrogenation and its behaviour as reservoir of molecular species in the Heck C-C coupling reactions. The application of this dual catalytic behaviour in sequential process (Heck coupling followed by hydrogenation) was also studied.

4.2.1 Hydrogenation reactions

Transition metal nanoparticles stabilized in ionic liquid medium,^{56,57} have been largely used as catalyst in biphasic hydrogenation reactions given the proven hydrogen solubility in several ionic liquids reported by Dyson et al.⁵⁸ The fact to support them onto a solid support has led to highly active catalytic systems for this type of reactions (see section 1.2.4).

4.2.1.1 Results and discussion

We have studied the benzylidenacetone (α,β -unsaturated carbonyl compound) hydrogenation reaction using palladium nanoparticles as supported ionic catalytic phase (Scheme 4.5).

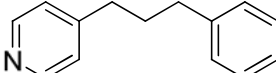


CNT6 = CNT-([C₈N₃OH₁₁])PF₆

PdNPs = Pd_a/IL₁, Pd_b/IL₁, Pd_b/L/IL₁, Pd_b/L/IL₂

a = [PdCl₂(cod)] as PdNPs precursor

b = [Pd₂(dba)₃] as PdNPs precursor

L = 4-(3-phenylpropyl) pyridine 

IL : IL₁ = [bmim][PF₆]

IL₂ = [emim][HPO(OMe)O]

Scheme 4.5: Benzylideneacetone hydrogenation reaction catalyzed by palladium SILP catalysts.

The reaction was carried out in a batch autoclave. The nature of palladium precursor, the presence of extra stabilizing ligand, and the influence of the ionic liquid and support nature are some of the main evaluated parameters.

The process optimization was carried out using SiO₂ as reference support used largely in the literature, before starting the catalytic study with functionalized multi-walled carbon nanotubes. Unless stated otherwise, the benzylideneacetone hydrogenation was done using heptane as solvent and a Pd/L ratio of 1/0.3.

Unless stated otherwise, the benzylideneacetone hydrogenation reaction was done using heptane as solvent and a Pd/L ratio of 1/0.3; conversion was determined by GC analysis.

In order to study the influence of the nature of the palladium precursor and the influence of the ligand, palladium nanoparticles synthesized in [bmim][PF₆] (see section 3.2.2.1), were used to obtain the heterogeneous supported ionic liquid catalytic phases SiO₂-SIL(Pd_a/IL₁), SiO₂-SIL(Pd_b/IL₁) and SiO₂-SIL(Pd_b/L/IL₁) (see section 3.2.3).

Firstly, 80 °C and 50 bar of hydrogen pressure were chosen with a Pd/substrate ratio of 1/220. Two different reaction times have been studied, 3 or 18 h. Conversions were determined by GC analysis. Hydrogenation results are presented in Table 4.4

entry	Catalyst	PdNPs size (nm)	Pd/Substrate ratio	P (bar)	T (°C)	Time (h)	Conversion (%) ^a	TOF (h ⁻¹) ^b
1	SiO ₂ -SIL(Pd _a /IL ₁)	2.15 ± 0.72	1/220	50	80	18	70	9
2	SiO ₂ -SIL(Pd _b /IL ₁)	5.25 ± 2.31	1/220	50	80	3	90	65
3	SiO ₂ -SIL(Pd _b /L/IL ₁)	4.34 ± 1.33	1/220	50	80	3	100	61
4	SiO ₂ -SIL(Pd _a /IL ₁)	2.15 ± 0.72	1/220	20	80	3	65	47
5	SiO ₂ -SIL(Pd _b /IL ₁)	5.25 ± 2.31	1/220	20	80	3	93	62
6	SiO ₂ -SIL(Pd _b /L/IL ₁)	4.34 ± 1.33	1/220	20	80	3	100	65
7	SiO ₂ -SIL(Pd _a /IL ₁)	2.15 ± 0.72	1/220	20	40	3	12	10
8	SiO ₂ -SIL(Pd _b /IL ₁)	5.25 ± 2.31	1/220	20	40	3	18	17
9	SiO ₂ -SIL(Pd _b /L/IL ₁)	4.34 ± 1.33	1/220	20	40	3	100	65
10	SiO ₂ -SIL(Pd _b /IL ₁)	5.25 ± 2.31	1/550	40	80	3	58	55
11	SiO ₂ -SIL(Pd _b /L/IL ₁)	4.34 ± 1.33	1/550	40	80	3	100	94

Table 4.4: Influence of the precursor of metallic nanoparticles and ligand in the benzylidenacetone hydrogenation reaction. Reaction conditions: 1 ml of heptane with:

- Pd/Substrate = 1/220; Pd = 1.08 10⁻⁶ mol, Pd/L = 1/0.3; Substrate = 2.37 10⁻⁴ mol (for SiO₂-SIL(Pd_b/IL₁) and SiO₂-SIL(Pd_b/L/IL₁)) or substrate = 9.46 10⁻⁴ mol, (for SiO₂-SIL(Pd_a/IL₁)).
- Pd/Substrate = 1/550; Pd = 4.33 10⁻⁶ mol; Pd/L = 1/0.3; Substrate = 2.37 10⁻⁴ mol (for SiO₂-SIL(Pd_b/IL₁) and SiO₂-SIL(Pd_b/L/IL₁)).

^a determined by GC. ^bTOF = mol of substrate converted/(mol of catalyst x time (h)).

According to the results presented on Table 4.4, SiO₂-SIL(Pd_b/IL₁) and SiO₂-SIL(Pd_b/L/IL₁) catalysts (entries 2 and 3 respectively) obtained from [Pd₂(dba)₃] palladium precursor exhibited the best catalytic activities. The lower conversion of SiO₂-SIL(Pd_a/IL₁) could be related to the low dispersion of those nanoparticles as well as their non homogeneity in size (section 3.2.2.2, Figure 3.1). Actually, when [PdCl₂(cod)] was used as PdNPs precursor, chloride anions could remain bounded to the palladium surface, acting as poison for the hydrogenation reaction. On the contrary, when [Pd₂(dba)₃] was used, the dba ligand could remain anchored on the nanoparticles surface after reduction, acting as stabilizer and protecting NPs from oxidation. Similar results were observed when the reaction was carried out at the same Pd/substrate ratio (1/220) but decreasing the pressure (20 bar) (Table 4.4, entries 4, 5 and 6), indicating that the hydrogen solubility in the ionic liquid layer is not the

rate determining step. Surprisingly, the results obtained at both pressures (50 and 20 bar) with SiO₂-SIL(Pd_a/IL) are almost equal (table 4.4, entries 1 and 4). Nanoparticles obtained from [PdCl₂(cod)] precursor showed lower activity, only achieving 70% conversion.

Decreasing the reaction temperature from 80 °C to 40 °C at constant pressure (20 bar) and Pd/substrate ratio, led to a conversion decrease, not only with SiO₂-SIL(Pd_a/IL₁), but also using SiO₂-SIL(Pd_b/IL₁) as catalyst (entries 7 and 8, Table 4.4). These results can be related to the formation of nanoparticles agglomerates from [Pd₂(dba)₃] stabilized only by the ionic liquid, in the absence of ligand, as revealed the TEM analysis (section 3.2.2.3).

SiO₂-SIL(Pd_b/L/IL₁) exhibited the best catalytic activity (entry 9, Table 4.4). The ligand 4-(3-phenylpropyl)pyridine acting as stabilizer has a positive influence concerning the dispersion of palladium nanoparticles, as could be observed by the TEM analysis (see section 3.2.2.3). The good dispersion of those nanoparticles with no agglomeration zones should be the responsible of the high conversion achieved. Moreover, decreasing the Pd/substrate ratio up to 1/550, SiO₂-SIL(Pd_b/L/IL₁) induced higher conversion (almost twice) compared to SiO₂-SIL(Pd_b/IL₁) (entries 10 and 11, Table 4.4).

In view of these results, [Pd₂(dba)₃] has been chosen as the only palladium precursor to be used hereafter stabilized by 4-(3-phenylpropyl)pyridine in a ratio 1/0.3.

After setting the best catalytic conditions using silica as support, a comparative study using functionalized multi-walled carbon nanotubes as a support for the ionic liquid catalytic phase has been carried out.

In this comparative study, the preparation way of the supported catalyst strongly influences the catalytic behaviour. Actually, two different solvents acetone and pentane were used for the catalyst preparation (see section 3.2.3). The catalyst was then tested in the benzylidenacetone hydrogenation reaction at 30 °C and 20 bar of hydrogen pressure for 3 h (Table 4.5).

entry	Catalyst	P/S	Conversion (%) ^a	TOF (h ⁻¹) ^d
1	SiO ₂ -SIL(Pd _b /L/IL ₁) ^b	1/313	51	35
2	SiO ₂ -SIL(Pd _b /L/IL ₁) ^b	1/628	14	39
3	CNT6-SIL(Pd _b /L/IL ₁) ^b	1/628	16	42
4	CNT6-SIL(Pd _b /L/IL ₁) ^c	1/313	76	52
5	CNT6-SIL(Pd _b /L/IL ₁) ^c	1/628	31	76

Table 4.5. Influence of the solvent used in the synthesis of the catalyst. ^b acetone, ^c pentane. Reaction conditions: 1 ml of heptane at 30 °C, 20 bar for 3 h with

- Pd/substrate = 1/313; Pd = 7.59 10⁻⁷ mol, Pd/L = 1/0.3; Substrate = 2.37 10⁻⁴ mol.
- Pd/Substrate = 1/628; Pd = 3.77 10⁻⁷ mol; Pd/L = 1/0.3; Substrate = 2.37 10⁻⁴ mol.

^a determined by GC. ^bTOF = mol substrate converted/(mol of catalyst x time (h))

When silica was used as catalytic support, acetone was the solvent of choice because in pentane the system was not well dispersed (entries 1 and 2, Table 4.5). On the contrary, the best solvent for CNT6 was pentane (entries 3-5, Table 4.5). In both cases, the good dispersion overcomes the mass transfer limitations.

Thus, we can conclude that CNT6 is the best support for the hydrogenation reaction of benzylidenacetone using palladium nanoparticles (Pd_b/L/IL₁) as supported ionic liquid catalytic phase. This result can be related to the carbon nanotubes open structure which avoids mass transfer limitations.

Until now, only the catalytic behaviour of nanoparticles synthesized in [bmim][PF₆] was studied. In section 3.2.2.3, TEM microphotographs of palladium nanoparticles synthesized from [Pd₂(dba)₃] with 4-(3-phenylpropyl)pyridine in [emim][HPO(OMe)O] revealed a good dispersion and narrow particle size distribution. Those nanoparticles were also applied as supported ionic liquid catalytic phase using CNT6. A comparative study between CNT6-SIL(Pd_b/L/IL₁) and CNT6-SIL(Pd_b/L/IL₂) (IL₁ = [bmim][PF₆]; IL₂ = [emim][HPO(OMe)O]) has been done at 20 bar, 30 °C for 3 h with a Pd/Substrate ratio of 1/313. Indeed, as it could be expected, CNT6-SIL(Pd_b/L/IL₂) exhibited low catalytic activity (33% conversion) compared to CNT6-SIL(Pd_b/L/IL₁) (76% conversion) probably related to the different hydrogen solubility in both ionic liquids.

CNT6-SIL(Pd_b/L/IL₁) catalytic system was recycled. The catalyst was separated from the reaction medium by filtration and reused four times without significant loss of activity up to four cycles, decreasing the activity in the fifth cycle.

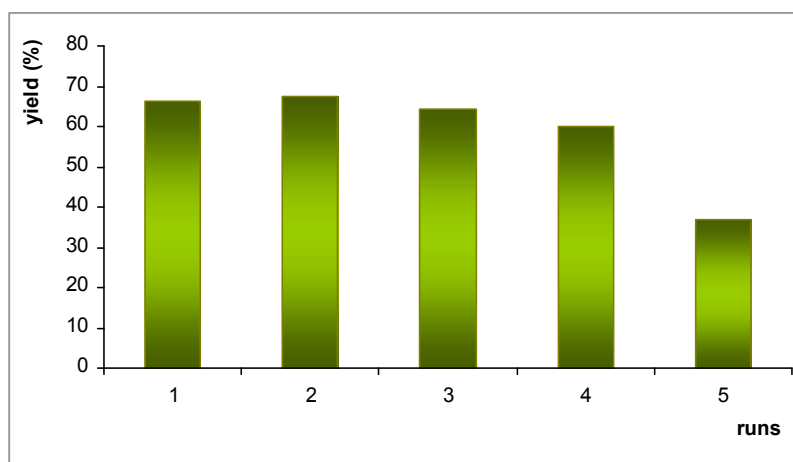


Figure 4.4: Recycling experiments using CNT6-SIL(Pd_b/L/IL₂) as catalyst. Reaction conditions: Pd/substrate = 1/313, Pd/L = 1/0.3, [Pd] = $7.59 \cdot 10^{-7}$ mol/l, $2.37 \cdot 10^{-4}$ mol of benzylidenacetone in 1 ml of heptane at 30 °C, 20 bar of hydrogen pressure, for 3 h.

4.2.2 C-C cross coupling reactions

4.2.2.1 Introduction

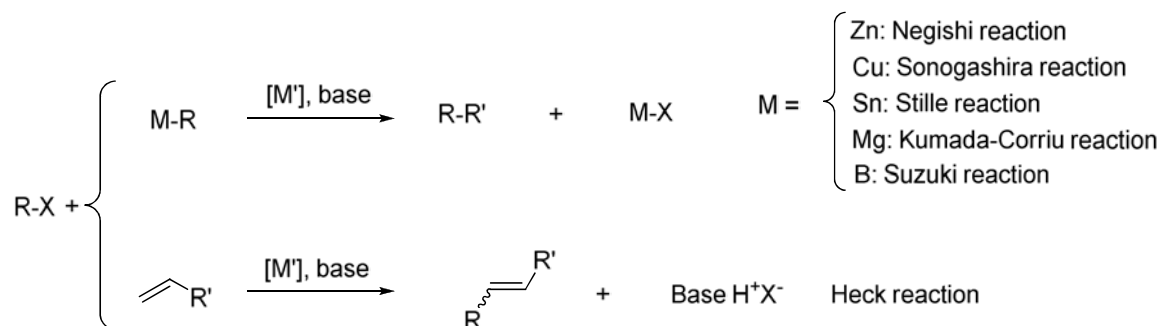
C-C cross-coupling reactions constitute a very important field for fine chemistry. This is due to their high versatility and the great interest of the products that can be obtained to produce fine chemicals.⁵⁹ For this reason, an extensive study of these reactions has been carried out to find new catalysts able to give the desired products with good activities and selectivities.⁶⁰

In the last decades, new methodologies have been developed in order to permit the reuse of the homogeneous catalysts, due to the elevated cost of metal and sometimes ligands involved, and to anticipate environmental-friendly processes. C-C coupling reactions are found among the first reactions studied using ionic liquids.^{2,61,62} Even more, the immobilization and reuse of the catalyst, recovering the products by distillation or extraction, are one of the subjects of great interest since they permit to minimize costs.

4.2.2.2 General remarks

A C-C cross-coupling is defined as a reaction between an organic halide (or involving other leaving groups such as trifluoromethylsulfonate) with an olefin or an organometallic reagent catalyzed by a transition metal to yield a new C-C bond.⁶³ When an olefin is used as

reagent, the process is named Heck reaction. In addition, diverse organometallic reagents can be also used in this type of processes, giving rise to a number of reactions, such as Kumada-Corriu (from an organomagnesium reagent),^{64,65} Sonogashira (using copper organometallic compounds),^{66,67} Negishi (from an organozinc compound),^{68,69} Stille (from an organotin reagent)^{70,71} and Suzuki (from an organoboron compound) couplings (Scheme 4.6).



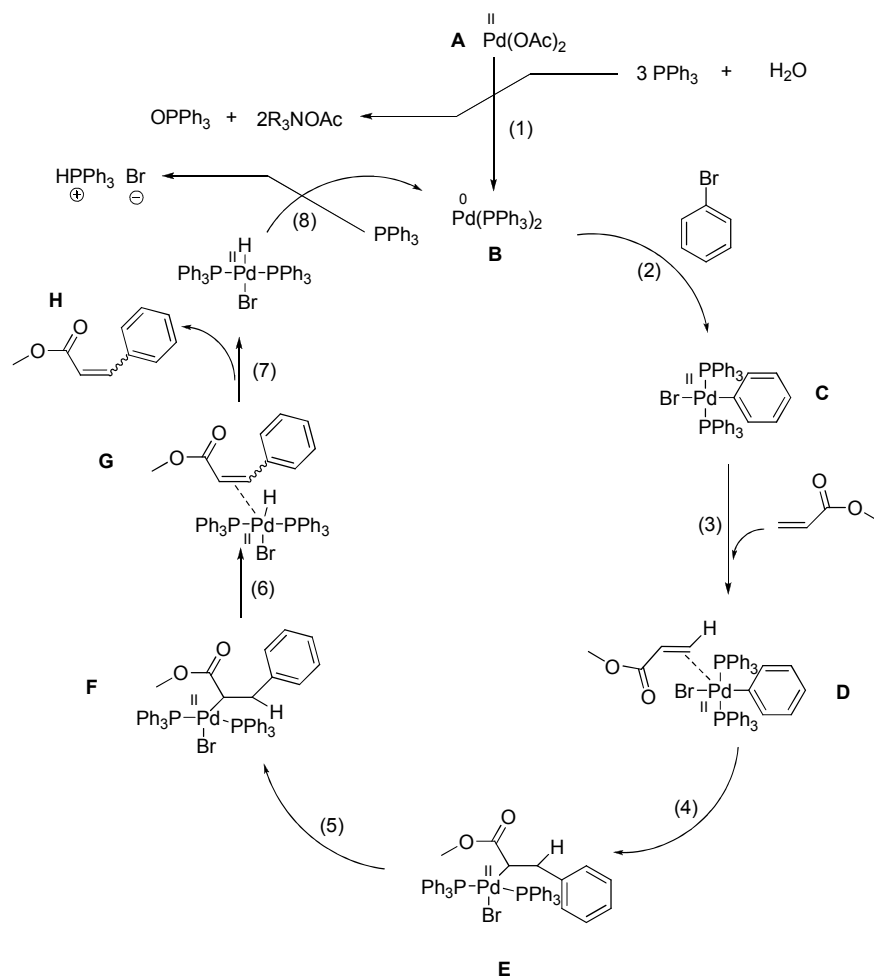
R, R' = aryl, vinyl or alkyl groups

X = Cl, Br, I, OTf

M = Pd, Ni

Scheme 4.6: The most common C-C coupling reactions catalyzed by transition metal species.

Among these couplings, the most studied processes undoubtedly have been Heck^{72,73,74,75} and Suzuki^{76,77,78,79,80,81} reactions. From the so called Heck reactions, palladium salts as palladium acetate containing phosphines like triphenylphosphine, are the most common used catalytic systems. Scheme 4.7 shows a representative reaction mechanism based on Pd(0)-Pd(II) catalytic species applied a one specific reaction. Palladium acetate is reduced by triphenylphosphine to di(triphenylphosphine)palladium(0) and triphenylphosphine is oxidized to triphenylphosphine oxide in step 1. After oxidative addition of aryl bromide (step 2), palladium forms a π complex with the alkene (step 3) and the alkene inserts itself in the palladium-carbon bond in a syn addition; after a β -hydride elimination, the coupling product is formed (step 7) regenerating the active catalytic species B by means of a base (step 8). The presence of a base has been found to be mandatory for the cross-coupling reactions. For this reason a wide range of organic (mainly amines) and inorganic bases have been employed.⁸² In spite of this, the real role played by the base both in Heck and Suzuki coupling reactions remains still controversial.⁸³



Scheme 4.7: Text book Heck catalytic cycle based on Pd(0)-Pd(II) catalytic species.

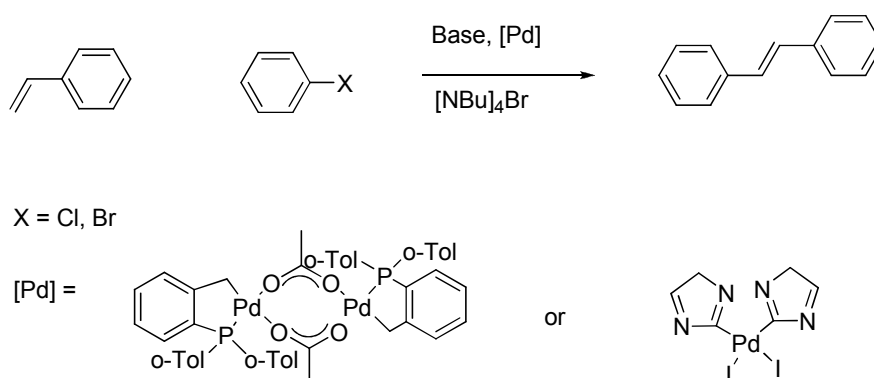
Even if palladium complexes are the most commonly used catalysts, in the last twenty years catalytic systems based on palladium colloids are also reported in the literature. Hermann's group was one of the pioneers in using palladium colloids as catalyst in the Heck C-C coupling reaction.⁸⁴ The reaction between different substituted bromoarenes containing electro-withdrawing groups (CHO, MeCO) and styrene or butyl acrylate led to higher conversions than those obtained using classical molecular systems. Simultaneously, Reetz et al. showed similar results from the same reaction using Pd colloids stabilized by propylene carbonate.⁸⁵ Many other examples are reported in the literature using palladium nanoparticles such as palladium colloids in block copolymer micelles for the reaction between aryl halides and alkenes⁸⁶ and the poly(vinylpyrrolidone)-stabilized colloidal palladium in the coupling of p-bromobenzaldehyde with butyl acrylate.⁸⁷

4.2.2.2.1 C-C cross-coupling reactions in ionic liquids and in supported catalytic liquid phase

Carbon-carbon coupling processes are among the most widely studied reactions in ionic liquid medium. Therefore, the immobilization and reuse of the catalyst, recovering the products by distillation (in biphasic reactions) or filtration (in SILP catalytic reactions), is a subject of great interest.

Thus, examples of Negishi,⁸⁸ Stille,⁸⁹ and Sonogashira⁹⁰ couplings, and also of other C-C bond formation processes like allylic alkylation,^{91,92,93} performed in ILs can be found in the literature. However, the largest volume of work in this field has been devoted to Suzuki and, especially, Heck coupling reactions.

The first example of Heck coupling performed in an ionic liquid was carried out by Kaufmann et al., achieving high yields in the reaction between bromobenzene and butyl acrylate in ammonium and phosphonium-based ionic liquids.⁹⁴ Also using tetraalkylammonium ILs, Herrmann and Böhm described the activation of aryl chlorides and greatly enhanced the activity of their palladacycle and N-heterocyclic carbene catalysts compared to common organic solvents like DMF in the formation of styrene (Scheme 4.8).^{95,96} Seddon et al. successfully worked on a three-phase system ILs/H₂O/hexane to favour the extraction of the products in the organic phase and the residual salts in water, finding an activity enhancement in imidazolium-based compared to the results in pyridinium-based ILs.⁹⁷ Xiao and co-workers demonstrated that this rate enhancement is due to the in situ formation of palladium carbene complexes under basic conditions.⁹⁸ Since these pioneering contributions, many other examples of the use of ionic liquids as solvents for the Heck reaction have been reported, claiming enhanced activities or selectivities either with molecular or with colloidal systems.^{99,100,101}



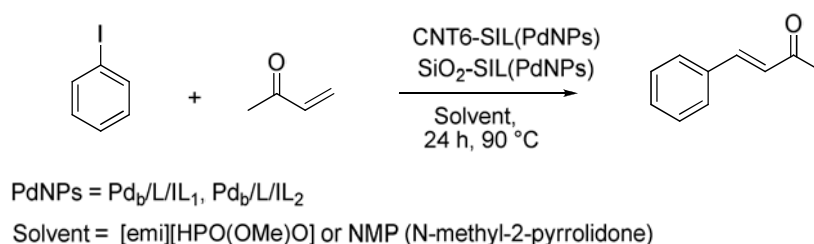
Scheme 4.8: Pioneering work of Herrmann and Böhm on the Heck C-C coupling reaction in ILs.^{95,96}

SILP catalysis favours the catalyst recovery and recycling due to the solid nature of the catalyst. Indeed, Hagiwara et al.⁴⁵ first reported the use of silica based SILP catalysis with palladium compounds ($\text{Pd}(\text{OAc})_2$, $[\text{Pd}(\text{PPh}_3)_4]$) and $[\text{bmim}][\text{PF}_6]$ as ionic liquid leading to high activities compared to those obtained using heterogeneous Pd/SiO_2 catalyst. Other studies using palladium nanoparticles as supported ionic liquid catalytic phase have been reported with tetramethyl guaridine ionic liquid over molecular sieves or SBA-15 silica, showing high activity and selectivity for the reaction of iodobenzene and methyl acrylate.¹⁰²

The use of functionalized carbon nanotubes as support for the SILP catalysis of Heck C-C coupling reaction is described for the first time in the next section.

4.2.2.3 Results and discussion

Palladium nanoparticles supported on functionalized MWCNTs and silica ionic liquid catalytic phase systems were used in Heck C-C coupling reaction between iodobenzene and methyl vinyl ketone (Scheme 4.9). Both the support and the ionic liquid nature strongly influence the catalytic process.



Scheme 4.9: Heck C-C coupling reaction between iodobenzene and methyl vinyl ketone catalyzed by SILP palladium systems.

Based on the studies developed in our group with biphasic palladium systems on Heck C-C coupling reactions,¹⁰³ $[\text{emim}][\text{HPO}(\text{OMe})\text{O}]$ has been chosen as ionic liquid to synthesize palladium nanoparticles from $[\text{Pd}_2(\text{dba})_3]$ precursor with 4-(3-phenylpropyl)pyridine as stabilizer. CNT6 have revealed good performances as support for hydrogenation reactions (see section 4.2.1.1). Thus, the catalyst $\text{CNT6-SIL}(\text{Pd}_b/\text{L}/\text{IL}_2)$ was used for the preliminary tests.

A conversion of 96% (entry 1, Table 4.6) was achieved using $[\text{emim}][\text{HPO}(\text{OMe})\text{O}]$ as solvent at 90 °C for 24 h without addition of extra base (the basicity was supplied by the basic methyl hydrogenphosphonate anion of the ionic liquid).

But the aim of the SILP catalysis is to economize the ionic liquid used; therefore, the dispersibility of the catalyst was tested in several solvents (heptane, toluene) in order to have the best performances of the catalyst. NMP (N-methyl-2-pyrrolidone) was chosen as solvent due to its physical properties (polarity and high boiling point) and low toxicity.

The two criteria studied to decide the best SILP catalytic system for this reaction was the support and the ionic liquid used. In this context, four different catalysts were studied, (Table 4.6).

entry	Catalyst	Pd/substrate	Time (h)	Conversion (%) ^a	TOF (h ⁻¹)
1	CNT6-SIL(Pd _b /L/IL ₂) ^b	1/336	24	96	14
2	CNT6-SIL(Pd _b /L/IL ₂) ^b	1/672	6	24	27
3	CNT6-SIL(Pd _b /L/IL ₂) ^b	1/672	24	28	8
4	CNT6-SIL(Pd _b /L/IL ₁) ^c	1/672	24	-	-
5	CNT6-SIL(Pd _b /L/IL ₂) ^c	1/672	6	69	77
6	CNT6-SIL(Pd _b /L/IL ₂) ^c	1/672	24	72	20
7	SiO ₂ -SIL(Pd _b /L/IL ₁) ^c	1/672	24	-	-
8	SiO ₂ -SIL(Pd _b /L/IL ₂) ^c	1/672	6	48	54
9	SiO ₂ -SIL(Pd _b /L/IL ₂) ^c	1/672	24	48	14

Table 4.6: Influence of the support and ionic liquid used. Reaction conditions: 1 ml of heptane under argon with

- Pd/substrate = 1/336; Pd/L = 1/0.3; Pd = 5.95 10⁻⁶ mol; Substrate = 2 10⁻³ mol.
- Pd/Substrate = 1/672; Pd/L = 1/0.3; Pd = 2.97 10⁻⁶ mol; substrate = 2 10⁻³ mol.

^a Determined by GC. ^b The reaction was carried out without extra base addition. ^c Extra base was added in a ratio iodobenzene/Na₂CO₃ = 1/2.5.

When the reaction was carried out in NMP without addition of extra base, the catalytic activity decreased to 28% (Table 4.6, entry 3). Effectively the amount of ionic liquid present on the supported ionic liquid phase is not enough to provide the basic character. On the contrary, good conversions were achieved for the same system, adding extra Na₂CO₃ (in a water solution) in a ratio 1/2.5 for iodobenzene/Na₂CO₃ after 6 or 24 h of reaction (Table 4.6, entries 5 and 6 respectively). Functionalized multi-walled carbon nanotubes as support for SILP catalysis showed better catalytic activity than silica (Table 4.6, entries 7 and 8). Moreover, nanoparticles synthesized in [emim][HPO(OMe)O] present higher catalytic activities than the corresponding PdNPs synthesized in [bmim][PF₆] which were inactive either with CNT6 or with SiO₂ (Table 4.6, entries 4 and 7). The well-dispersed nanoparticles with narrow size distribution obtained in [emim][HPO(OMe)O] (Figure 3.4, section 3.2.2.3) should be the responsible of this high catalytic activity.

TEM analysis indicate the agglomeration of the nanoparticles after C-C coupling reaction for both systems CNT6-SIL(Pd_b/L/IL₁) and CNT6-SIL(Pd_b/L/IL₂) (Figure 4.5)

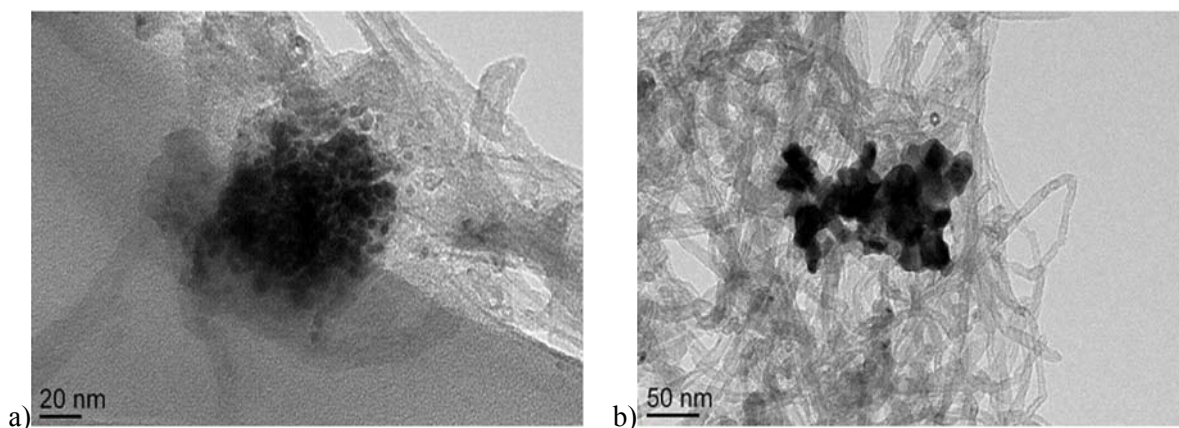
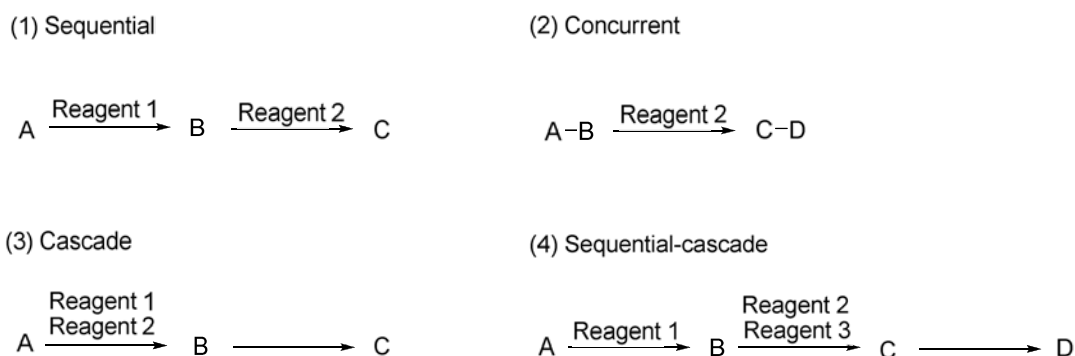


Figure 4.5: TEM photograph after reaction of a) CNT6-SIL(Pd_b/L/IL₁) and b) CNT6-SIL(Pd_b/L/IL₂).

4.2.3 Sequential reactions

The design of synthetic strategies involving multi-step processes in one-pot procedure is a key challenge for the fine chemical industry, in order to achieve an economical and sustainable production.^{104,105} The concept may be taken from nature, where multienzymatic systems provide ample evidence of multi-step catalysis in an aqueous environment.¹⁰⁶ Thus, multi-step processes can be defined as a sequence of reactions that are performed in one process without isolation or purification of any intermediate.¹⁰⁷ These processes can be divided in three principal types (Scheme 4.10): (1) Sequential, consecutive or iterative reactions, in which reagents are added and/or the conditions are altered to initiate subsequent reactions; this process is the most straightforward when incompatible reagents are employed in the different steps, avoiding cross-reactivity problems; (2) Cascade or domino process, in which one reaction initiates an entire sequence, and the formation of the product in the first transformation reveals functionality that then allows a second transformation to occur; this transformation reveals functionality that then allows a third transformation to occur, and so on; (3) Concurrent process, in which all the reagents are present at once and in which the first reaction is not necessary for the second to occur. A multi-step process may also combine aspects of these three types (Scheme 4.10, 4).¹⁰⁸

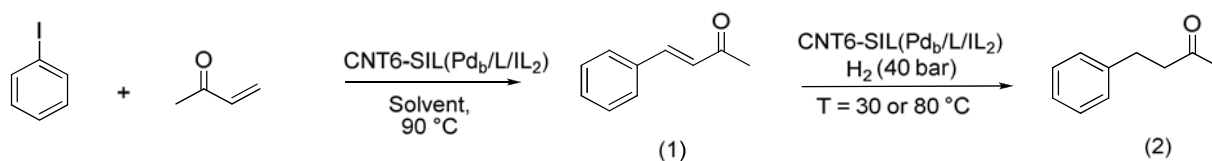


Scheme 4.10: Representation of different multi-step reaction processes.¹⁰⁸

The use of a single catalyst for different kinds of reactions is especially attractive for metal catalyzed process. The dual catalytic behaviour plausible exhibited by metallic nanoparticles, acting as homogeneous (reservoir of molecular species) or heterogeneous (surface-like reactivity) catalysts,^{40,46,47,48} shows an enormous potential in complex transformations for economizing purification steps. Our group has studied for the first time a sequential catalytic process involving metal nanoparticles demonstrating their dual homogeneous and heterogeneous behaviour, using ionic liquids as solvent due to the enhanced stability of the nanoclusters in this medium.¹⁰³ The influence of supporting the catalytic phase over a solid support is developed in the following section.

4.2.3.1 Results and discussion

In this section, we are going to apply the best SILP catalytic system for the Heck and selective hydrogenation, CNT6-SIL(Pd_b/L/IL₂), in the sequential process (Scheme 4.11) involving C-C coupling and hydrogenation steps, analogously to the work described by Corma and co-workers concerning palladium-supported catalysts on zeolites.¹⁰⁹



Solvent = [emim][HPO(OMe)O] or NMP

Scheme 4.11: Sequential Heck coupling and hydrogenation process catalyzed by PdNPs supported on CNT6.

Under optimal conditions for Heck (90 °C, 24 h) and hydrogenation (40 bar H₂, 30°C, 6 h) reactions, CNT6-SIL(Pd_b/L/IL₂) was applied in the sequential reaction using [emim][HPO(OMe)O] as solvent. An iodobenzene conversion of 95% was observed for the

C-C coupling in agreement with the previous results. The catalytic system was then pressurised with hydrogen without further treatment of separation, giving a coupling product (1)/hydrogenation product (2) ratio of 51/44. Therefore the dual catalytic behavior of metallic nanoparticles is a great advantage for sequential processes allowing the use of the same catalytic system for two different reactions avoiding an intermediate step of separation and purification.

On the contrary, when the sequential reaction was carried in NMP organic solvent in the presence of base (Na_2CO_3) is mandatory in order to obtain the Heck coupling product (see section 4.2.2.3). More over, the low H_2 solubility in NMP suggests the use of slightly harder conditions (40 bar H_2 , 80 °C during 18 h) compared to the conditions studied in section 4.2.1.1. Under these conditions, an iodobenzene conversion of 71% which further gives a coupling product (1)/hydrogenation product (2) ratio of 53/17. The low conversion of the hydrogenation reaction compared with the results obtained in section 4.2.1.1 is probably due to the formation of Pd-NHC (NHC=N-heterocyclic carbene) molecular species during the Heck reaction under basic conditions,^{110, 111} which cannot be easily reduced under hydrogen pressure and consequently the catalytic system becomes inactive for further hydrogenation reactions.

To sum up, the use of metallic nanoparticles for the sequential reaction of the C-C coupling followed by the hydrogenation reactions is only possible using [emim][HPO(OMe)O] as solvent without addition of supplementary base, thanks to the methyl hydrogenphosphonate basicity. The absence of extra base permits the regeneration of palladium nanoparticles after the coupling reaction, active for the further hydrogenation. Thus one single catalytic precursor could be used for the C-C coupling/hydrogenation sequential process.

-
- ¹ J. Dupont, R.F. de Souza, P.A.Z. Suarez, *Chem. Rev.* **2002**, 102, 3667.
- ² P.J. Dyson, T.J. Geldbach, (Eds.) *Metal catalyzed reactions in ionic liquids*, Series: *Catalysis by Metal Complexes*, Vol. 9, Springer, Dordrecht, **2005**
- ³ J.P. Arhancet, M.E. Davis, J.S. Merola, B.E. Hanson, *Nature* **1989**, 339, 454.
- ⁴ C.P. Mehnert, R.A. Cook, N.C. Dispenziere, M. Afeworki, *J. Am. Chem. Soc.* **2002**, 124, 12932. b) ExxonMobil (C. P. Mehnert, R. A. Cook), US 6673 737, **2004**.
- ⁵ C.P. Mehnert, E.J. Mozeleski, R.A. Cook, *Chem. Commun.* **2002**, 3010.
- ⁶ L. Lou, X. Peng, K. Yu, S. Liu, *Catal. Commun.* **2008**, 9, 1891.
- ⁷ H. Vu, F. Gonçalves, R. Philippe, E. Lamouroux, M. Corrias, Y. Kihn, D. Plee, P. Kalck, P. Serp, *J. Catal.* **2006**, 240, 18.
- ⁸ X. Pan, Z. Fan, W. Chen, Y. Ding, H. Luo, X. Bao, *Nature Mater.* **2007**, 6, 507.
- ⁹ P. Serp, M. Corrias, P. Kalck, *Appl. Catal. A* **2003**, 253, 337.
- ¹⁰ M. Faraday, *Philos. Trans. R. Soc. London* **1857**, 147, 145.
- ¹¹ T. Graham, *Philos. Trans. R. Soc.* **1861**, 151, 183.
- ¹² J. Turkevitch, *Disc. Faraday Soc.* **1951**, 11, 55.
- ¹³ L.D. Rampino, F.F. Nord, *J. Am. Chem. Soc.* **1941**, 63, 2745.
- ¹⁴ J. Turkevitch, G. Kim, *Science* **1970**, 169, 873.
- ¹⁵ G. Parravano, *J. Catal.* **1970**, 18, 320.
- ¹⁶ D.Y. Cha, G.J. Parravano, *Catal.* **1970**, 18, 200.
- ¹⁷ G.C. Bond, P.A. Sermon, *Gold Bull.* **1973**, 6, 102.
- ¹⁸ H. Hirai, Y. Nakao, N.J. Toshima, *Macromol. Sci. Chem. A* **1978**, 12, 1117.
- ¹⁹ D. Astruc (Eds.) *Nanoparticles and catalysis*, VCH-Wiley, Houston, **2007**.
- ²⁰ W. Yu, H. Liu, X. An, X. Ma, Z. Liu, L. Qiang, *J. Mol. Catal. A: Chem.* **1999**, 147, 73.
- ²¹ J.A. Widegren, R.G. Finke, *J. Mol. Catal. A: Chem.* **2003**, 191, 187.
- ²² G. Schmid, H. West, H. Mehles, A. Lehnert, *Inorg. Chem.* **1997**, 36, 891.
- ²³ Y. Shiraishi, N. Toshima, *J. Mol. Catal. A: Chem.* **1999**, 141, 187.

-
- ²⁴ S. Jansat, M. Gómez, K. Philippot, G. Muller, E. Guiu, C. Claver, S. Castellón, B. Chaudret, J. Am. Chem. Soc. **2004**, 126, 1592.
- ²⁵ I. Favier, M. Gomez, G. Muller, M.R. Axet, S. Castillon, C. Claver, S. Jansat, B. Chaudret, K. Philippot, Adv. Synth. Catal. **2007**, 349, 2459.
- ²⁶ (a) H. Bönemann, G.A. Braun, Angew. Chem. Int. Ed. Engl. **1996**, 35, 1992. (b) H. Bönemann, G. A. Braun, Chem. Eur. J. **1997**, 3, 1200.
- ²⁷ (a) J.U. Köhler, J.S. Bradley, Catal. Lett. **1997**, 45, 203. (b) J.U. Köhler, J.S. Bradley, Langmuir **1998**, 14, 2730.
- ²⁸ X. Zuo, H. Liu, M. Liu, Tetrahedron Lett. **1998**, 39, 1941.
- ²⁹ M. Tamura, H. Fujihara, J. Am. Chem. Soc. **2003**, 125, 15742.
- ³⁰ M. Moreno-Mañas, R. Pleixats, Acc. Chem. Res. **2003**, 36, 638.
- ³¹ D. Astruc, Inorg. Chem. **2007**, 46, 1884.
- ³² M. Beller, H. Fischer, K. Kühlein, C.P. Reisinger, W.A. Herrmann, J. Organomet. Chem. **1996**, 520, 257.
- ³³ R. Narayanan, M.A. El-Sayed, J. Am. Chem. Soc. **2003**, 125, 8340.
- ³⁴ M.T. Reetz, E. Westermann, R. Lohmer, G. Lohmer, Tetrahedron Lett. **1998**, 39, 8449.
- ³⁵ A.H.M. de Vries, J.M.C.A. Mulders, J.H.M. Mommers, H.J.W. Henderckx, J.G. de Vries, Org. Lett. **2003**, 5, 3285.
- ³⁶ J.G. de Vries, A.H.M. de Vries, Eur. J. Org. Chem. **2003**, 799.
- ³⁷ M.T. Reetz, J.G. de Vries, Chem. Commun. **2004**, 1559.
- ³⁸ P. Migowski, J. Dupont, Chem. Eur. J. **2007**, 13, 32.
- ³⁹ L.S. Ott, M.L. Cline, M. Deetlefs, K.R. Seddon, R.G. Finke, J. Am. Chem. Soc. **2005**, 127, 5758.
- ⁴⁰ J. Durand, E. Teuma, F. Malbosc, Y. Kihn, M. Gómez, Catal. Commun. **2008**, 9, 273.
- ⁴¹ J. Huang, T. Jiang, B. Han, H. Gao, Y. Chang, G. Zhao, W. Wu, Chem. Commun. **2003**, 1654.
- ⁴² M.A. Gelesky, S.S.X. Chiaro, F.A. Pavan, J.H.Z. dos Santos, J. Dupont, Dalton Trans. **2007**, 5549.
- ⁴³ M. Ruta, G. Laurency, P.J. Dyson, L. Kiwi-Minsker, J. Phys. Chem. C **2008**, 112, 17814 .
- ⁴⁴ H. Hagiwara, K.H. Ko, T. Hoshi, T. Suzuki, Chem. Commun. **2007**, 2838 .
- ⁴⁵ H. Hagiwara, Y. Sugawara, K. Isobe, T. Hoshi and T. Suzuki, Org. Lett. **2004**, 6, 2325
- ⁴⁶ N.T.S. Phan, M. Van Der Sluys, C.W. Jones, Adv. Synth. Catal. **2006**, 348, 609.
- ⁴⁷ J. Durand, E. Teuma, M. Gómez, Eur. J. Inorg. Chem. **2008**, 3577.

-
- ⁴⁸ F. Fernandez, B. Cordero, J. Durand, G. Muller, F. Malbosc, Y. Kihn, E. Teuma, M. Gomez, *Dalton Trans.* **2007**, 5572.
- ⁴⁹ C.C. Cassol, A.P. Umpierre, G. Machado, S.I. Wolke, J. Dupont, *J. Am. Chem. Soc.* **2005**, 127, 3298.
- ⁵⁰ M.B. Thathagar, P.J. Kooyman, R. Boerleider, E. Jansen, C.J. Elsevier, G. Rothenberg, *Adv. Synth. Catal.* **2005**, 347, 1965.
- ⁵¹ Á. Imre, D.L. Beke, E. Gontier-Moya, I.A. Szabó, E. Gillet, *Appl. Phys. A* **2000**, 71, 19.
- ⁵² A. Howard, C.E.J. Mitchell, R.G. Egdell, *Surf. Sci.* **2002**, 515, 504.
- ⁵³ C.S. Consorti, F.R. Flores, J. Dupont, *J. Am. Chem. Soc.* **2005**, 127, 12054.
- ⁵⁴ J.G. de Vries, *Dalton Trans.* **2006**, 421.
- ⁵⁵ M.T. Reetz, E. Westermann, *Angew. Chem. Int. Ed.* **2000**, 39, 165.
- ⁵⁶ (a) G.S. Fonseca, A.P. Umpierre, P.F.P. Fichtner, S.R. Teixeira, J. Dupont, *Chem. Eur. J.* **2003**, 9, 3263. (b) J. Dupont, G.S. Fonseca, A.P. Umpierre, P.F.P. Fichtner, S.R. Teixeira, *J. Am. Chem. Soc.* **2002**, 124, 4228. (c) E.T. Silveira, A.P. Umpierre, L.M. Rossi, G. Machado, J. Morais, G.V. Soares, I.J.R. Baumvol, S.R. Teixeira, P.F.P. Fichtner, J. Dupont, *Chem. Eur. J.* **2004**, 10, 3734. (d) C.W. Scheeren, G. Machado, J. Dupont, P.F.P. Fichtner, S.R. Teixeira, *Inorg. Chem.* **2003**, 42, 4738. (e) P. Migowski, G. Machado, S.R. Teixeira, M.C.M. Alves, J. Morais, A. Traverse, J. Dupont, *Phys. Chem. Chem. Phys.* **2007**, 9, 4814. (f) H.S. Schrekker, M.A. Gelesky, M.P. Stracke, C.M.L. Schrekker, G. Machado, S.R. Teixeira, J.C. Rubim, J. Dupont, *J. Colloid Interface Sci.* **2007**, 316, 189.
- ⁵⁷ A.P. Umpierre, G. Machado, G.H. Fecher, J. Morais, J. Dupont, *Adv. Synth. Catal.* **2005**, 347, 1404.
- ⁵⁸ P.J. Dyson, G. Laurencyzy, C.A. Ohlin, J. Vallance, T. Welton, *Chem. Commun.* **2003**, 2418.
- ⁵⁹ H.U. Blaser, A. Indolese, F. Naud, U. Nettekoven, A. Schnyder, *Adv. Synth. Catal.* **2004**, 346, 1583.
- ⁶⁰ A. de Meijere, F. Diederich, (Eds.) *Metal-catalyzed cross-coupling reactions*; Wiley- VCH: Weinheim, **2004**.
- ⁶¹ F. Alonso, I.P. Beletskaya, M. Yus, *Tetrahedron* **2005**, 61, 11771.
- ⁶² F. Alonso, I.P. Beletskaya, M. Yus, *Tetrahedron* **2008**, 64, 3047.
- ⁶³ B. Cornils, W.A. Herrmann, (Eds.) *Applied homogeneous catalysis with organometallic compounds: a comprehensive handbook in three volumes*; 2nd ed.; Wiley-VCH: New York, **2002**.
- ⁶⁴ K. Tamao, K. Sumitani, M. Kumada, *J. Am. Chem. Soc.* **1972**, 94, 4374.
- ⁶⁵ R.J.P. Corriu, J.P. Masse, *J. Chem. Soc., Chem. Commun.* **1972**, 144.
- ⁶⁶ K. Sonogashira, Y. Tohda, N. Hagihara, *Tetrahedron Lett.* **1975**, 16, 4467.
- ⁶⁷ D.J. Keddie, K.E. Fairfull-Smith, S.E. Bottle, *Org. Biomol. Chem.* **2008**, 6, 3135.

-
- ⁶⁸ E. Negishi, A.O. King, N. Okukado, *J. Org. Chem.* **1977**, 42, 1821.
- ⁶⁹ E. Negishi, *Acc. Chem. Res.* **1982**, 15, 340.
- ⁷⁰ D. Milstein, J.K. Stille, *J. Am. Chem. Soc.* **1978**, 100, 3636.
- ⁷¹ J.K. Stille, *Angew. Chem. Int. Ed. Engl.* **1986**, 25, 508.
- ⁷² R.F. Heck, J.P. Nolley Jr., *J. Org. Chem.* **1972**, 37, 2320.
- ⁷³ R.F. Heck, *Acc. Chem. Res.* **1979**, 12, 146.
- ⁷⁴ W. Cabri, I. Candiani, *Acc. Chem. Res.* **1995**, 28, 2.
- ⁷⁵ I.P. Beletskaya, A.V. Cheprakov, *Chem. Rev.* **2000**, 100, 3009.
- ⁷⁶ N. Miyaura, A. Suzuki, *Chem. Rev.* **1995**, 95, 2457.
- ⁷⁷ A. Suzuki, *J. Organomet. Chem.* **1999**, 576, 147.
- ⁷⁸ A. Suzuki, *J. Organomet. Chem.* **2002**, 653, 83.
- ⁷⁹ S.R. Chemler, D. Trauner, S.J. Danishefsky, *Angew. Chem. Int. Ed.* **2001**, 40, 4544.
- ⁸⁰ S. Kotha, K. Lahiri, D. Kashinath, *Tetrahedron* **2002**, 58, 9633.
- ⁸¹ A.F. Littke, G.C. Fu, *Angew. Chem. Int. Ed.* **2002**, 41, 4176.
- ⁸² J.P. Wolfe, R.A. Singer, B.H. Yang, S.L. Buchwald, *J. Am. Chem. Soc.* **1999**, 121, 9550.
- ⁸³ J.M. Brown, K.K. Hii, *Angew. Chem. Int. Ed. Engl.* **1996**, 35, 657.
- ⁸⁴ M. Beller, H. Fischer, K. Kühlein, C.P. Reisinger, W.A. Herrmann, *J. Organomet. Chem.* **1996**, 520, 257.
- ⁸⁵ M.T. Reetz, G. Lohmer, *Chem. Commun.* **1996**, 1921.
- ⁸⁶ S. Klingelhöfer, W. Heitz, A. Greiner, S. Oestreich, S. Förster, M. Antonietti, *J. Am. Chem. Soc.* **1997**, 119, 10116.
- ⁸⁷ J. Le Bars, U. Specht, J.S. Bradley, D.G. Blackmond, *Langmuir*, **1999**, 15, 7621.
- ⁸⁸ J. Sirieix, M. Ossberger, B. Betzemeier, P. Knochel, *Synlett* **2000**, 1613.
- ⁸⁹ S.T. Handy, X. Zhang, *Org. Lett.* **2001**, 3, 233.
- ⁹⁰ T. Fukuyama, M. Shinmen, S. Nishitani, M. Sato, I. Ryu, *Org. Lett.* **2002**, 4, 1691.
- ⁹¹ W. Chen, L. Xu, C. Chatterton, J. Xiao, *Chem. Commun.* **1999**, 1247.
- ⁹² Š. Toma, B. Gotov, I. Kmentová, E. Solčániová, *Green Chem.* **2000**, 2, 149.
- ⁹³ J. Ross, W. Chen, L. Xu, J. Xiao, *Organometallics* **2001**, 20, 138.
- ⁹⁴ D.E. Kaufmann, M. Nouroozian, H. Henze, *Synlett* **1996**, 1091.

-
- ⁹⁵ W.A. Herrmann, V.P.W. Böhm, *J. Organomet. Chem.* **1999**, 572, 141.
- ⁹⁶ V.P.W. Böhm, W.A. Herrmann, *Chem. Eur. J.* **2000**, 6, 1017.
- ⁹⁷ A.J. Carmichael, M. J. Earle, J.D. Holbrey, P.B. McCormac, K.R. Seddon, *Org. Lett.* **1999**, 1, 997.
- ⁹⁸ L. Xu, W. Chen, J. Xiao, *Organometallics* **2000**, 19, 1123.
- ⁹⁹ V. Caló, A. Nacci, A. Monopoli, S. Laera, N. Cioffi, *J. Org. Chem.* **2003**, 68, 2929.
- ¹⁰⁰ J.C. Xiao, B. Twamley, J.M. Shreeve, *Org. Lett.* **2004**, 6, 3845.
- ¹⁰¹ V. Calò, A. Nacci, A. Monopoli, *Eur. J. Org. Chem.* **2006**, 3791.
- ¹⁰² X. Ma, Y. Zhou, J. Zhang, A. Zhu, T. Jiang, B. Han, *Green Chem.* **2008**, 10, 59.
- ¹⁰³ S. Jansat, J. Durand, I. Favier, F. Malbosc, C. Pradel, E. Teuma, M. Gomez, *ChemCatChem* **2009**, 1, 244.
- ¹⁰⁴ J.C. Wasilke, S.J. Obrey, R.T. Baker, G.C. Bazan, *Chem. Rev.* **2005**, 105, 1001.
- ¹⁰⁵ J. M. Lee, Y. Na, H. Han, S. Chang, *Chem. Soc. Rev.* **2004**, 33, 302.
- ¹⁰⁶ (a) C.A. Townsend, *Chem. Biol.* **1997**, 4, 721. (b) P.F. Leadlay, *Curr. Opin. Chem. Biol.* **1997**, 1, 162. (c) J. Staunton, B. Wilkinson, *Chem. Rev.* **1997**, 97, 2611. (d) C. Khosla, *Chem. Rev.* **1997**, 97, 2577.
- ¹⁰⁷ P.A. Wender, *Chem. Rev.* **1996**, 96, 1.
- ¹⁰⁸ P.J. Walsh, M.C. Kozlowski, *Fundamentals of Asymmetric Catalysis*, J. Murdzek (Eds.), University Science Books, Sausalito, California, **2009**.
- ¹⁰⁹ M. J. Climent, A. Corma, S. Iborra, M. Mifsud, *Adv. Synth. Catal.* **2007**, 349, 1949.
- ¹¹⁰ (a) N.D. Clement, K.J. Cavell, C. Jones, C. J. Elsevier, *Angew. Chem.* **2004**, 116, 3933; *Angew. Chem. Int. Ed.* **2004**, 43, 3845; (b) D.S. McGuinness, K.J. Cavell, B.F. Yates, B.W. Skeleton, A.H. White, *J. Am. Chem. Soc.* **2001**, 123, 8317.
- ¹¹¹ (a) L. Starkey Ott, M.L. Cline, M. Deetlefs, K.R. Seddon, R.G. Finke, *J. Am. Chem. Soc.* **2005**, 127, 5758. (b) J. Dupont, J. Spencer, *Angew. Chem.* **2004**, 116, 5408; *Angew. Chem. Int. Ed.* **2004**, 43, 5296.

CHAPTER V

Experimental section

5 EXPERIMENTAL SECTION

5.1 GENERAL ASPECTS

Reactions involving water-sensible intermediates (like multi-walled carbon nanotubes functionalized with acid chloride), as well as reactions in the presence of organometallic complexes (synthesis of coordination compounds and catalytic processes), and syntheses of metallic nanoparticles were conducted under argon or nitrogen inert atmosphere, using standard Schlenk and vacuum-line techniques. For the synthesis of metallic nanoparticles, Fisher-Porter bottles were also used.

Multi-walled carbon nanotubes were prepared by C-CVD¹ (catalytic chemical vapour deposition) in the "Laboratoire de Genie Chimie" of the Université de Toulouse (purity >95 %, <5 % remaining iron particles; active surface = 227 cm²/g; pore volume = 0.66 cm³/g; average pore diameter = 6-20 nm; external diameter = 21-8 nm; internal diameter = 12-4 nm). Al₂O₃ (Brockmann I, standard grade, neutral, 150 mesh), TiO₂ (purum, catalyst grade, specific surface 35-65 m²/g), AC (specific surface >100 m²/g) purchase from Aldrich. ZrO₂ (catalyst grade, specific surface 15-35 m²) and MgO (99+ %, catalyst grade, specific surface 130 m²/g) were purchase from Alfa Aesar. Mesoporous silica (EP10X amorphous silica, Crosfield Ltd., pore volume = 1.81 cm³/g, particle size ≈ 100 μm) was purchase from INEOS Silicas. ZnO was synthesized in our laboratory by CVD (specific surface 20 m²/g).

Tris(dibenzylideneacetone)dipalladium(0), [Pd₂(dba)₃], was purchased from Aldrich as well as 4-(3-phenylpropyl)pyridine. [Rh(nbd)(PPh₃)₂PF₆ and dichloro(1,5-cyclooctadiene)palladium(II) ([PdCl₂(cod)]) were prepared according to literature method.^{2,3}

1-hexene used in the hydrogenation catalytic reaction was purchase from Panreac (99.9 %). Benzylidenacetone and the iodobenzene were purchased from Acros Organics (98.5 %) and methyl vinyl ketone (99 %) from Aldrich.

Organic solvents used in the functionalization of multi-walled carbon nanotubes and catalysts preparation were previously purified by means of distillation under nitrogen atmosphere in a "MBraun solvent purification system" and with the appropriate drying agents (sodium/benzophenone for tetrahydrofuran; calcium oxide: calcium chloride (1:1) for dichloromethane). Other solvents and reagents were used as received, unless stated otherwise.

Ionic liquids employed in this work were purchased from Solvionic ([bmim][PF₆] at 98 %; [bmim][PF₆] and [emim][HPO(OMe)O] 99.5+%; chloride contents certified to <1 ppm) and treated overnight under reduced pressure at 70 °C prior to use.).

5.2 CHARACTERIZATION TECHNIQUES

The techniques applied to the product characterization are following listed: nuclear magnetic resonance spectroscopy (NMR), infrared spectroscopy (IR), Raman spectroscopy, X-ray Photoelectron Spectroscopy (XPS), mass spectrometry (MS), elemental analysis (EA), differential scanning calorimetry (DSC), thermogravimetical analysis (ATG), X-ray diffraction (XRD), transmission electron microscopy (TEM), gas chromatography (GC) and specific surface area BET.

5.2.1 Nuclear magnetic resonance spectroscopy

NMR spectra were recorded on a Bruker Avance 300 (^1H , ^{13}C , standard SiMe_4) and Bruker Avance 500 (^{31}P -NMR and ^{19}F -NMR, standards phosphoric acid H_3PO_4 and trifluoroacetic acid CF_3COOH , respectively). All chemical shifts are reported in ppm. Magnetic field, acquisition temperature and deuterated solvent are indicated in brackets for each product. ^{13}C -NMR and ^{31}P -NMR spectra were ^1H -decoupled, indicated as $^{13}\text{C}\{^1\text{H}\}$ or $^{31}\text{P}\{^1\text{H}\}$.

Solid state NMR experiments were recorded on a Bruker Avance 400 spectrometer equipped with a 4 mm probe operating at 399.60 MHz for ^1H , 376.00 MHz for ^{19}F , 161.76 MHz for ^{31}P , 104.12 MHz for ^{27}Al , 100.48 MHz for ^{13}C , and 79.39 MHz for ^{29}Si . Samples were spun at 12 kHz at the magic angle using ZrO_2 rotors. All chemical shifts for ^1H , ^{13}C and ^{29}Si are relative to TMS. ^{19}F , ^{27}Al and ^{31}P were referenced to CFCl_3 , $[\text{Al}(\text{H}_2\text{O})_6]^{3+}$ and 85% H_3PO_4 , respectively. For ^1H MAS, ^{13}C MAS, ^{19}F MAS, ^{27}Al MAS, ^{29}Si MAS and ^{31}P MAS single pulse experiments, small flip angle ($\sim 30^\circ$) were used with recycle delays of 5 s, 10 s, 10 s, 3 s, 200 s and 20 s, respectively. ^{13}C -CP/MAS and ^{29}Si -CP/MAS spectra were recorded with a recycle delay of 5 s and contact times of 2 ms and 3 ms respectively.

5.2.2 Infrared spectroscopy

Infrared spectra were carried out using pellets of dispersed samples of the corresponding compounds in dried KBr for solid products. The instrument used was a Perkin Elmer Spectrum One FT-IR. The spectral range was $4000\text{-}400\text{ cm}^{-1}$.

5.2.3 Mass spectrometry

Mass chromatograms were carried out by the "Service commun de spectrométrie de masse de la Structure Fédérative de Toulouse de l'Université Paul Sabatier": Electronic Impact (EI) and Chemical Ionization (CI using methane or ammonia as reactant gas), on a TSQ 7000

Thermo Electron apparatus and electrospray (ES) on a API-365 MS/MS Spectrometer (Perkin Elmer Sciex).

5.2.4 Elemental analysis

Elemental analyses were carried out by the “Service Inter-Universitaire d’Analyse Élémentaire” at the ENSIACET of Toulouse (using a Thermo Electron Corporation, CE instruments EA 1110 analyzer) (C, H, O and N) and by the “Service de microanalyse du Laboratoire de Chimie de Coordination (LCC)” of Toulouse (using a Perkin Elmer 2400 series II microanalyser) (C, H, O and N).

5.2.5 Differential scanning calorimetry

DSC thermograms (second cooling and heating) were performed under argon on a DSC 204 NETZSCH at heat flow between -120 to 600 °C with a 10 Kmin⁻¹ ramp. The samples were introduced inside an aluminum crucible.

5.2.6 Thermogravimetric analysis

Thermogravimetric analyses were carried out under air in a Setaram apparatus. The sample (~ 5 mg) was introduced inside an aluminium or platinum crucible and heated with a 10 °Cmin⁻¹ ramp between 25 and 1000 °C, followed by an isotherm at 1000 °C for 30 minutes.

5.2.7 X-ray diffraction

XRD was performed on a Seifert XRD 3000 spectrometer at room temperature for multi-walled carbon nanotubes and in a MPD-Pro de Panalytical at -20 °C on cooling at a rate of 10 °Cmin⁻¹ and at room temperature for S-SIL composites (S = Al₂O₃, ZrO₂, TiO₂, SiO₂, ZnO, MgO, AC) and the pure ILs, using Cu K α radiation ($\lambda = 0.15406$ nm).

5.2.8 Transmission electron microscopy

TEM micrographs were obtained using a Philips CM12 microscope operating at 120 kV. The CNTs samples were dispersed in ethanol, sonicated for 5 minutes and the resulting suspension was dropped onto a holey carbon copper grid and the solvent was allowed to evaporate.

The images of particles dispersed in ILs were obtained in the “Service commun TEMSCAN” of Toulouse from: a transmission electron Philips CM12 microscope running at 120 kV; a JEOL JEM 1011 running at 100 kV for routine images (resolution 4, 5 Å), acquisition by camera slow scans SIS (Megaview III) and a JEOL JEM 2100F running at 100 kV with high resolution images (resolution 2,3 Å), X-ray analysis PGT (light elements detection, resolution 135 eV), images acquisition by camera slow scan Gatan 1K x 1K. A drop of solution was deposited on a holey carbon grid and the excess of ILs was removed in order to obtain a film as thin as possible. Images were recorded on the film of ILs lying on the holes of the grid. The nanoparticles size distribution and average diameter were directly determined from TEM images by Image-J software associated to a Microsoft excel macro developed by Christian Pradel.

5.2.9 Gas chromatography

Products obtained in the hydrogenation of 1-hexene were analyzed using a Perkin Elmer Clarus 500 chromatograph fitted with a FID detector, using anisole as internal standard. The column employed was an Elite 5 (PerkinElmer, 60 meter x 0.53 mm x 1.5 µm; temperature range from -60 to 325/350°C). The injector temperature was 150 °C and the split 0.02 µL. The column head pressure of the carrier gas (hydrogen) during the analysis was maintained at 6 psi. Temperature programme (A): 35 °C for 6 min, 15 °C/min ramp to 75 °C hold for 5 min, 30 °C/min to 200 °C hold for 1 min. was maintained at 60 °C for min followed by a 20 °Cmin⁻¹ ramp until 200 °C.

Products obtained in the hydrogenation of benzylidenacetone and the C-C Heck coupling reactions were analyzed using a Perkin Elmer Clarus 500 chromatograph fitted with a FID detector, using anisole as internal standard. The column employed was Stabilawax-DA (Restec, 30 meter x 0.25 mm x 0.25 µm; temperature range from 40 to 240/250°C). The injector temperature was 150 °C and the split 0.02 µL. The column head pressure of the carrier gas (Helium) during the analysis was maintained at 23 psi. Temperature programme (B): 80 °C for 2 min, 20 °C/min to 200 °C hold for 7 min.

5.2.10 X-ray Photoelectron Spectroscopy

XPS analyses were performed on a VG Escalab model MK2 spectrophotometer with pass energy of 20 eV and with Al Ka (1486.6eV, 300W) photons as an excitation source. The semi-quantitative analysis were performed from the C1s (284.3 eV) signal.

5.2.11 Raman spectroscopy

Raman spectra were recorded on a Labram HR800 of Jobin et Yvon (632.82 cm^{-1}).

5.2.12 Porosimetry and specific surface area

Nitrogen adsorption-desorption analyses at $-196 \text{ }^\circ\text{C}$ were performed using either a Micrometrics Asap 2010 equipment or a Coulter Omnisorp 100CX, to measure BET specific surface areas and to get information concerning the porosity of the powders. The analyses were carried out by the “Centre d’Elaboration de Matériaux et d’Études Structurales (CEMES)” in Toulouse.

5.2.13 Thermal programme desorption

Temperature programmed desorption (TPD) spectra of CO and CO₂ were performed in an AMI-200 (Altamira Instruments) apparatus at Toulouse University. In a typical experiment, 100 mg sample was subjected to a $5 \text{ }^\circ\text{C}/\text{min}$ linear temperature rise up to $1100 \text{ }^\circ\text{C}$ under helium flow of 25 sccm (mln/min). The amounts of CO ($m/z = 28$) and CO₂ ($m/z = 44$) desorbed from the samples were monitored with a mass spectrometer (Dymaxion 200 amu, Ametek).

5.3 MULTI-WALLED CARBON NANOTUBES FUNCTIONALIZATION

5.3.1 MWCNTs purification

CNT0: CNTs were purified with a H₂SO₄ treatment followed a published procedure.⁴

IR (KBr pellet), XPS and Elemental analyse see section 2.2.1.2.

ATG: weight loss and temperature decomposition 98 %, $640 \text{ }^\circ\text{C}$

5.3.2 MWCNTs activation

CNT1: CNT0 were treated with HNO₃ following a published procedure⁴ during 0.5, 1, 3 or 8 hours giving CNT1a, CNT1b, CNT1c, CNT1d.

IR (KBr pellet), XPS and Elemental analyse see section 2.2.1.2.

ATG: weight loss and temperature decomposition 98 %, $680 \text{ }^\circ\text{C}$

Chemical titration of carboxylic groups:

Samples of 200 mg of untreated and oxidized CNTs were stirred in polyethylene bottles with 25 ml of a solution containing 0.1 M NaCl (supporting electrolyte) and 0.1 mM oxalic acid in demineralised-water, acidified to pH = 3 with HCl (conc). The bottle was sealed. The acidic functionalities on the CNTs surfaces were determined by neutralization with aqueous sodium hydroxide. 0.08 M NaOH solution was prepared with boiled distilled water (to remove dissolved carbon dioxide). The number of μ moles of NaOH was calculated based on the change in the pH value and the volume of the sample and the original NaOH concentration **Data obtained** = 0.85 COOH/nm²

5.3.3 Ionic functionalization of the MWCNTs surface: CNT2-CNT9

5.3.3.1 Covalent approach (CNT2-CNT8)

CNT2a, CNT3a: Oxidized CNTs, CNT1d, (1 g) were further refluxed in a solution of thionyl chloride (90 ml) for 24 hours at 70 °C under nitrogen; the solvent was then evaporated under vacuum. The solid was separated by filtration, washed with anhydrous THF and dried under vacuum giving samples CNTxa (x = 2, 3).

CNT4a: Oxidized CNTs, CNT1d, (3 g) were further refluxed in a solution of thionyl chloride (90 ml) for 24 hours at 70 °C under nitrogen; the solvent was then evaporated under vacuum.

CNT5a: Oxidized CNTs, CNT1a, (3 g) were further refluxed in a solution of thionyl chloride (90 ml) for 24 hours at 70 °C under nitrogen; the solvent was then evaporated under vacuum.

CNT6a: Oxidized CNTs, CNT1b, (3 g) were further refluxed in a solution of thionyl chloride (90 ml) for 24 hours at 70 °C under nitrogen; the solvent was then evaporated under vacuum.

CNT7a: Oxidized CNTs, CNT1c, (3 g) were further refluxed in a solution of thionyl chloride (90 ml) for 24 hours at 70 °C under nitrogen; the solvent was then evaporated under vacuum.

CNT8a: Oxidized CNTs, CNT1d, (0.250 mg) were mixed methane sulfonyl acid (0.3 ml) in presence of 1 ml of triethylamine in dichloromethane. The reaction was carried out under nitrogen at room temperature during 24 h. The solid was separated by filtration and washed with dichloromethane followed by NH₄Cl and ending with dichloromethane again. The sample was dried under vacuum for 24 h.

IR (KBr pellet) ν (cm⁻¹) (CNT8a): 2900 (C-H stretching), 1725 (C=O, acid), no band from the C-S stretching between 720-570 was detected.

XPS and Elemental analyse see section 2.2.2.1.2.

CNT2b-CNT8b: Chlorinated CNT2a-CNT7a and mesylate (CNT8a) samples were reacted with 1-(3-aminopropyl)imidazole (50 ml) 120 °C for 24 hours under nitrogen atmosphere. The solid was separated by filtration through a 0.2- μ m poly(tetrafluoroethylene) (PTFE) membrane and washed successively with anhydrous THF followed by consecutive washings with 1 M aqueous HCl solution, saturated aqueous NaHCO₃ solution and water until the pH of the filtrate was 7.0. The resulting solid was finally washed with ethanol and dried overnight undervacuum to obtain CNTxb (x = 1-8).

IR (KBr pellet) ν (cm⁻¹): 2900 (C-H stretching), 1725 (C=O, acid), 1648 (C=O, amide), 1575 (C-H vibration in plane) for CNTxb (x = 2-7); 2900 (C-H stretching), 1725 (C=O, acid), 1575 (C-H vibration in plane) for CNT8b

CNT2c-CNT8c: 1-bromobutane (50 ml) was added to imidazolium functionalized CNTxb (x = 1-8) carbon nanotubes and stirred at 80 °C for 24 h under nitrogen atmosphere. The solid was separated by filtration through 0.2- μ m PTFE membrane and thoroughly washed with anhydrous THF several times to remove the excess of bromobutane. The resulting solid was dried under vacuum at room temperature for 24 h giving CNTxc (x = 1-8).

IR (KBr pellet) ν (cm⁻¹): 2900 (C-H stretching), 1725 (C=O, acid), 1648 (C=O, amide), 1575 (C-H vibration in plane), 601 (C-Br stretching) for CNTxc (x = 2-7); 2900 (C-H stretching), 1725 (C=O, acid), 1575 (C-H vibration in plane) for CNT8c.

CNT2-CNT8: The anion exchange of Br⁻ by PF₆⁻ was obtained mixing the resulting solid CNTxc (x = 1-8) with an aqueous solution of KPF₆⁻ (1 g in 150 ml of purified water). The mixture was stirred at room temperature for 24 h. The solid was separated by filtration and washed with water to remove the water soluble species such as KBr. After several washings with water, the resulting solid was dried overnight under vacuum giving CNTx (x = 2-8)

IR (KBr pellet) ν (cm⁻¹): 2900 (C-H stretching), 1725 (C=O, acid), 1648 (C=O, amide), 1575 (C-H vibration in plane) and 870 (P-F stretching) for CNTx (x = 2-7); 2900 (C-H stretching), 1725 (C=O, acid), 1575 (C-H vibration in plane) for CNT8

ATG: weight loss and temperature decomposition: 3.5 %, 310 °C (ionic functionalities thermal decomposition); 98 %, 750 °C (multi-walled carbon nanotubes thermal decomposition) for CNT2-7.

XPS and Elemental analyses see section 2.2.2.1.2.

5.3.3.2 Ionic approach

CNT9: Oxydized carbon nanotubes (1 g) were mixed with a solution of sodium hydroxide (50 ml, 0.05 M) for 24 h at room temperature in order to produce the sodium salt of the acidified nanotubes. The solid was filtered and washed with water until pH 7. The resulting solid was treated with an excess of [bmim][Cl] (0.500 g) at 55 °C for 24 h, followed by a filtration step and washed with water to give CNT9.

XPS and Elemental analyse see section 2.2.2.1.2

5.4 SYNTHESIS OF METALLIC NANOPARTICLES IN IONIC LIQUID

Synthesis of Pd_a/IL₁, Pd_b/IL₁, Pd_b/L/IL₁ and Pd_b/L/IL₂ (a = palladium precursor [Pd₂(dba)₃]; b = palladium precursor [PdCl₂(cod)]; L = 4-(3-phenylpropyl)pyridine) in ionic liquid (IL₁ = [bmim][PF₆] 99.5 % and IL₂ = [emim][HPO(OMe)O], 99.5 %): The appropriate palladium precursor (0.94 mmol (270 mg) for [PdCl₂(cod)]; 0.23 mmol (109 mg) for [Pd₂(dba)₃]) and 4-(3-phenylpropyl)pyridine ligand (0.07 mmol, 14.1 mg) in ILs (2 ml of [bmim][PF₆] or [emim][HPO(OMe)O]) was stirred at room temperature under argon in a Fischer–Porter bottle until complete dissolution (30 min). The system was then pressurized with hydrogen (3 bar) and stirred at room temperature for 24 h, leading to a black solution. In the case of [Pd₂(dba)₃], heating at 60 °C was necessary to decompose the palladium precursor. The residual gas was then released and volatiles removed under reduced pressure.

Pd_a/IL₁: synthesized in the absence of ligand. **TEM**: Ø_m = 2.15 ± 0.72 nm.

Pd_b/IL₁: synthesized in the absence of ligand. **TEM**: Ø_m = 5.25 ± 2.31 nm.

Pd_b/L/IL₁: **TEM**: Ø_m = 4.34 ± 1.33 nm.

Pd_b/L/IL₂: **TEM**: Ø_m = 4.47 ± 0.78 nm.

5.5 SYNTHESIS OF SUPPORTED IONIC LIQUID PHASE

Synthesis of [bmim]PF₆/support systems: supports (MWCNTs = CNT0, CNT1, CNT2, CNT3, CNT4, CNT5, CNT6, CNT7; SiO₂, Al₂O₃, MgO, ZrO₂, TiO₂, ZnO, AC) (200 mg), were contacted for 15 min at room temperature with [bmim]PF₆ (98 % purity) (250, 150 and 50 mg corresponding to 55, 37 and 20% w/w, respectively), in the presence of a small amount of acetone (ca. 15 ml). Acetone was removed under vacuum and the mixture was dried for 18 h under vacuum.

ATG: weight loss and temperature decomposition for ionic liquid film and carbon nanotubes see section 3.3

XRD and TEM: CNT3-SIL see section 3.3.

XPS and Elemental analyses:

Entry	MWCNTs	% wt elemental analyze				% atomic XPS			
		C	H	N	O	C	O	N	F
1	CNT0-SIL(55%)	59.1	3.2	6.1	-	74.9	2.3	5.5	17.3
2	CNT4-SIL(55%)	53.1	3.4	7.1	-	70.5	10.8	4.6	14.1

Note: [bmim]PF₆/support used in the structural study by solid NMR, XRD and DSC, were synthesised with Al₂O₃ or mesoporous silica (10 g), and [bmim]PF₆ (99,5 % purity) (7.5, 2.5, 1.25 and 0.5 g corresponding to 37, 20, 11 and 5% w/w, respectively) contacted for 1 h.

5.5.1 Immobilization of [Rh(nbd)(PPh₃)₂]PF₆ over a SILPC

Supports (MWCNTs = CNT0, CNT1, CNT2, CNT3, CNT4, CNT5, CNT6, CNT7; SiO₂, Al₂O₃, MgO, ZrO₂, TiO₂, ZnO, AC) (200 mg), were contacted for 15 min at room temperature with a solution of [Rh(nbd)(PPh₃)₂][PF₆] (10 mg, 1.39 · 10⁻² mmol) in [bmim][PF₆] (50, 150, 250 or 350 mg, corresponding to 20, 37, 55 or 64% w/w, respectively) (98 % purity) in 15 ml of acetone; acetone was then removed under vacuum. The catalysts prepared following this procedure were used in the hydrogenation reaction of 1-hexene.

5.5.2 Immobilization of PdNPs over a SILPC

Supports (MWCNTs = CNT6, SiO₂) (100 or 50 mg), were contacted for 15 min a solution of preformed PdNPs in ionic liquid (Pd_a/IL₁, Pd_b/IL₁, Pd_b/L/IL₁ and Pd_b/L/IL₂) (0.1, 0.5 or 0.25 ml, 0.472 M for Pd_a and 0.119 M for Pd_b) corresponding to 34 % w/w of ILs loading and 2, 0.5 or 0.25 % of palladium contained in the catalyst) in 15 ml of solvent (acetone or pentane) at 20 °C; acetone was then removed under vacuum. The catalysts prepared following this procedure were used in the hydrogenation of benzylidenacetone, in the C-C coupling Heck reaction and in the sequential process.

TEM and EDX: see section 3.2.3

5.6 DISTILLATION PROCEDURES

Distillation of SiO₂-SIL(11%): 10 g of SiO₂ impregnated with [bmim][PF₆] as explained in section 5.4 was tested for distillation. The sample was introduced in a two-necked flask (which was heated at 240 °C), connected to another two-necked flask (cooled with liquid nitrogen), under vacuum for 3 h. The condensed products were analysed by ¹H and ¹³C NMR.

Distillation of Al₂O₃ (11%): 10 g of Al₂O₃ impregnated with [bmim][PF₆] as explained in section 5.4 was tested for distillation. The sample was introduced inside a two-necked flask (which was heated at 240 °C), connected to another two-necked flask (cooled with liquid nitrogen), under vacuum for 3 h. After 3 hour under vacuum no evaporation has been observed.

Distillation of [bmim]PF₆: A sample (5 g) was heated at 240 °C in a two-necked flask connected to another two-necked flask cooled with liquid nitrogen. After 3 hour under vacuum, no condensed products were observed. The distillation residue showed no sign of decomposition as evidence by NMR.

5.7 CATALYTIC PROCEDURES

Two different batch autoclaves were used for the catalytic procedures.

TOP Industrie autoclave (1809.1000): Inox autoclave with a cuve of 100 ml and mechanical stirring with counterpales. Oven heating (temperature from 40 to 120 °C) controlled with a thermocoupling and rapid cooling with compressed air. The autoclave is connected to a gas reservoir (3 l, bursting disc maximum pressure 200 ± 10 % bar) with the pressure controlled by a pressure sensor; a manometer for low pressure 42 ± 0.5 bar. Two fitting valves and one purge valve arrive at the inox cuve (bursting disc maximum pressure 50 ± 5 %) by the autoclaves head. The pressure in the gas recipient is controlled by a pressure sensor. The autoclave has a bleed valve connected to the inox recipient. The sealing of the reactor is achieved with a teflon joint. The autoclave is connected to a PC with a software LOG 100 that allows the monitoring of different parameters during the reaction.

TOP Industrie autoclave (ref 1919 1000): Inox autoclave of 50 or 100 ml and magnetic stirring. Glass buckets were used to carry out the reactions. Oven heating (temperature from 40 to 120 °C) controlled with a thermocoupling. The autoclave has a gas reservoir (2 l, bursting disc maximum pressure 200 ± 10 % bar) controlled by a manometer (200 ± 0.5 bar). The autoclaves head has two fitting bands, one connected to the reservoir of hydrogen, and one connected to a vacuum-line in order to work under vacuum or argon. The gas pressure in the reactor is controlled by a pressure sensor. The autoclave has sample valve connected to

the inox cuve. The sealing of the reactor is achieved with a teflon joint. The autoclave is connected to a PC with a software associated to a Microsoft excel macro that allows the monitoring of different parameters during the reaction.

5.7.1 General procedure for hydrogenation reaction using the complex

[Rh(nbd)(PPh₃)₂]PF₆ as catalytic precursor

1-hexene (0.04 mol) was dissolved in heptane (55 ml) and SILPC (Rh/CNTx-SIL (y %) or Rh/S-SIL(y %) (450, 350, 250 g depending on the ionic liquid loading 55 %, 37 % and 20 % respectively) was then added. The reaction was carried out at the autoclave TOP Industry (1809.1000). The mixture was purged with hydrogen (five times). At 40 °C, the system was pressurized under 25 bar of hydrogen and maintained constant during the reaction. After due time, the catalyst was recovery by filtration and the product was analyzed by GC with Elite5 column and program A (see above).

GC: $t_{\text{retention}}$ (retention time)(min) = 2.97 (1-hexene), 3.06(hexane), 3.15 and 3.27(internal olefins of hexane).

Note: Recycling experiments were done reusing the filtrated catalyst following the general procedure described.

5.7.2 General procedure for hydrogenation reaction using preformed nanoparticles as SILPC

Benzylidenacetone (0.138 g, $9.46 \cdot 10^{-4}$ mol (for SiO₂-SIL(Pd_a/IL₁); 0.035 g, $2.37 \cdot 10^{-4}$ mol (for SiO₂-SIL(Pd_b/IL₁), SiO₂-SIL(Pd_b/L/IL₁), CNT6-SIL(Pd_b/L/IL₁)) was dissolved in heptane (1 ml). The SILP Catalyst (SiO₂-SIL(Pd_a/IL₁), SIL(Pd_b/IL₁), SiO₂-SIL(Pd_b/L/IL₁), CNT6-SIL(Pd_b/L/IL₁) or CNT6-SIL(Pd_b/L/IL₂)) (23 mg or 8 mg depending on the experiment) was added to the solution. The reaction was carried out in a TOP Industry (ref 1919 1000). Five glass buckets were introduced in the autoclave (two reactions, and one known reaction as reference). The air was removed under vacuum and the system was purged three times with argon followed by three times with hydrogen. At the appropriate reaction temperature (30, 40, 50 or 80 °C, depending on the experiment), the system was pressurized under hydrogen pressure (20 or 40 bar). After due time, the catalyst was recovered by filtration and the product was analyzed by GC with stabilwax column and the program B (see above).

GC: $t_{\text{retention}}$ (min) = 8.82 (benzylidenacetone), 11.40 (4-phenyl-2-butanone).

Note: Recycling experiments were done reusing the filtrate catalyst following the general procedure described.

5.7.3 General procedure for Heck coupling reaction using preformed nanoparticles as SILPC

Iodobenzene (0.408 g, $2 \cdot 10^{-3}$ mol), methylvinylketone (0.2 ml, $2.4 \cdot 10^{-3}$ mol, 1.2 eq.) and Na_2CO_3 (0.530 g, $5 \cdot 10^{-3}$ mmol, 2.5 eq.) dissolved in 1 ml of water (previously degassed) were mixed under argon in N-methyl pyrrolidone (NMP). The SILP catalyst ($\text{SiO}_2\text{-SIL}(\text{Pd}_b/\text{L}/\text{IL}_1)$, $\text{SiO}_2\text{-SIL}(\text{Pd}_b/\text{L}/\text{IL}_2)$, $\text{CNT6-SIL}(\text{Pd}_b/\text{L}/\text{IL}_1)$ or $\text{CNT6-SIL}(\text{Pd}_b/\text{L}/\text{IL}_2)$) (0.1 g) was then added to the solution under argon. The mixture was stirred for 24 h at 90 °C. After 18 h, the system was cooled at room temperature and the product was recovery by filtration. The solution was then analyzed by GC with stabilwax column and the program B (see above).

GC: $t_{\text{retention}}$ (min) = 1.51 (metyl vynil ketone), 6.39 (iodobenzene), 8.78 (benzylidenacetone), 11.32 (4-phenyl-2-butanone).

Note: When [emim][HPO(OMe)O] was used as solven, the reaction was carried out without base addition and the amount of added catalyst was 0.2 g in 5 ml of ionic liquid.

5.7.4 General procedure for catalytic sequential Heck/hydrogenation procedure using preformed nanoparticles as SILPC

Iodobenzene (0.408 g, $2 \cdot 10^{-3}$ mol), methylvinylketone (0.2 ml, $2.4 \cdot 10^{-3}$ mol, 1.2 eq.) and Na_2CO_3 (0.530 g, $5 \cdot 10^{-3}$ mmol, 2.5 eq.) dissolved in 1 ml of water (previously degassed) were dissolved under argon in N-methyl pyrrolidone (NMP). The SILP catalyst ($\text{CNT6-SIL}(\text{Pd}_b/\text{L}/\text{IL}_2)$) (0.1 g) was added to the solution under argon. The mixture was then stirred for 24 h at 90 °C. After the specific time, the system was allowed to cool to room temperature. The catalytic mixture was then introduced in the autoclave TOP Industry (ref 1919 1000) and pressurized at 40 bar of hydrogen during 18 hours at 80 °C. The product was recovery by filtration. The solutions were then analyzed by GC with stabilwax column and the program B (see above).

When [emim][HPO(OMe)O] was used as solvent, the reaction was carried out without base addition. The amount of added catalyst was 0.2 g in 5 ml of [emim][HPO(OMe)O]. The hydrogenation reaction was carried out at the same pressure but for 6 hours at 30 °C. The final product was extracted using cyclohexane (5 x 5 ml) and analyzed by GC with stabilwax column and the program B (see above).

¹ M. Corrias, B. Causat, A. Ayrat, J. Durand, Y. Kihn, P. Kalck, P. Serp, Chem. Eng. Sci. **2003**, 58, 4475.

² R.R. Schrock, J.A. Osborn, J. Am. Chem. Soc. **1971**, 2397.

³ D. Drew, J.R. Doyle, Inorg. Synth. **1990**, 28, 346.

⁴ A. Solhy, B.F. Machado, J. Beausoleil, Y. Kihn, F. Gonçalves, M.F.R. Pereira, J.J.M. Orfão, J.L. Figueiredo, J.L. Faria, P. Serp, Carbon **2008**, 46, 1194.

CHAPTER VI

Conclusions

6 CONCLUSIONS

During this work new supported ionic liquid catalytic phase systems based on functionalized multi-walled carbon nanotubes have been developed and employed in different catalytic reactions.

The multi-walled carbon nanotubes functionalization with ionic moieties has been synthesized and fully characterized. The activation treatment by oxidation with nitric acid induces the formation of oxygen groups on the surface, mainly carboxylic acid groups (CNT1), opening the possibility to further functionalization. Moreover, varying the activation time treatment, the amount of the surface functionalities can be controlled.

Two different ways of controlling the amounts of surface functionalities were observed: (i) the variation of the activation time (nitric acid treatment) and further reaction with thioly chloride without organic solvent and (ii) a washing step after treatment maintaining constant the activation time. Subsequent reactions with amine (3-(aminopropyl)imidazole) to give the corresponding amide, bromobutane to give the cationic imidazolium moieties and potassium hexafluorophosphate to exchange the anion, led to the formation of functionalized MWCNTs. Therefore, six ionic functionalized multi-walled carbon nanotubes, CNT_x (x = 2-7), could be prepared showing different functionalization degree.

Alternative reaction with methane sulfonyl acid to activate the carboxylic acid functions led to low degree of sulfonate functionalities with the consequent inefficiency of the subsequent reaction with the amine. Poor efficiency was also observed with the ionic functionalization approach.

The ionic covalent functionalization allowed good interactions between ionic liquid and the carbon nanotubes surface as proved by their good dispersibility on this medium compared to activated carbon nanotubes CNT1 or purified carbon nanotubes CNT0. Hence, ionic functionalized MWCNTs were applied as support for SILPC applications.

In order to prepare the SILP homogeneous and heterogeneous catalyst, a rhodium complex and preformed palladium nanoparticles were immobilized as ionic liquid catalytic phase.

Palladium nanoparticles were synthesized in ionic liquid from organometallic precursors, in the absence and in the presence of additional stabilizer. The use of the ligand 4-(3-phenylpropyl)pyridine in the nanoparticles formation in [bmim][PF₆] from [Pd₂(dba)₃] avoids the formation of aggregates leading to well-dispersed nanoparticles, showing spherical shape and quite narrow size distribution. Besides the positive influence of the ligand in the stabilization of PdNPs, the ionic liquid [emim][HPO(OMe)O] conferred a special stabilization

probably due to [HPO(OMe)O] counter anion forming nanoparticles with a Gaussian like particles size distribution also in the presence of ligand. Nanoparticles synthesized from [PdCl₂(cod)] in [bmim][PF₆] in absence of ligand are smaller because of the high precursor concentration used which favours a fast nucleation process avoiding the formation of special atoms arrangement.

TEM analysis of the supported ionic liquid phase, [bmim][PF₆], on functionalized multi-walled carbon nanotubes (CNT3-SIL) composites showed an increase on the average internal size diameter from 10 nm (CNT0) to 17 nm (CNT3-SIL) and a change in their thermostability for both the ionic liquid phase and the support.

The thermostability of the ionic liquid film on analogous composites, but based on classical supports (Al₂O₃, SiO₂, MgO, TiO₂, AC, ZrO₂ and ZnO), was also studied. The existence of different interactions between support and ILs that may have an impact on catalytic reactions. Two composites SiO₂-SIL and Al₂O₃-SIL were chosen to carry out a structural study in order to evidence the surface influence on the ionic liquid film by means of DSC, RDX and NMR at the solid state. The analogous NMR study using multi-walled carbon nanotubes was not faisable because of the presence of remaining iron nanoparticles from the synthetic catalyst encapsulated inside the tubes.

DSC at low temperatures showed similar patterns between [bmim][PF₆] and Al₂O₃-SIL while SiO₂-SIL revealed remarkably differences with both. The same trend was observed in XRD at -100 °C and -20°C were the ionic liquid film anchored on silica gel remains amorphous at both temperatures compared to the crystalline structure obtained for pure [bmim][PF₆] and Al₂O₃-SIL. These results suggest a strong interaction between the silica and the [bmim][PF₆]. Solid NMR studies confirmed this hypothesis and highlight a loss of structural order of the ionic liquid film on the Al₂O₃-SIL composite, exhibited by the protons mobility increase. Non-equivalent fluor atoms were evidenced for hexafluorophosphate anion (³¹P and ¹⁹F MAS NMR spectra) for SiO₂-SIL probably due to the different interactions of the anion PF₆ with the different OH sites on the silica surface.

The supported ionic liquid phase catalyst was prepared immobilizing the active catalyst in the ionic liquid phase and supporting it subsequently onto the CNTx by a simple and efficient method. Different amounts of ionic liquid loading (20, 37, 55 and 64 % w/w) were used, combined with each functionalized MWCNTs. The appropriate combination of both parameters led to free flowing powders catalysts and avoided gel formation (CNT4-SIL (64%)).

TEM analysis of the catalyst CNT6-SIL(Pd_b/L/IL₂), synthesized using preformed palladium nanoparticles (Pd_b/L/IL₂) and supported them on CNT6, showed the effective presence of palladium nanoparticles. FFT calculations shows the crystallographic planes of

the fcc palladium metal and two other planes probably related to a crystalline ionic liquid form placed around the nanoparticles.

Rh/SILPC system was applied in the hydrogenation reaction of 1-hexene. The positive effect of the MWCNTs functionalization was highlighted by the excellent catalytic conversions and selectivities obtained with Rh/CNT2-SIL(55 %), without leaching compared to Rh/CNT0-SIL(20, 37 or 55 %) and Rh/CNT1-SIL(20, 37, or 55 %). A comparative study with other Rh/SILPC based on classical supports (Al_2O_3 , SiO_2 , MgO , TiO_2 , AC, ZrO_2 and ZnO) revealed that functionalized MWCNTs as support (Rh/CNT3-SIL(37 %) showed almost twice catalytic activity compared to silica gel (2880 and 1425 h^{-1} respectively), probably due to the open structure of CNTs which avoids mass transfer limitations; this fact can also justify the differences in kinetics observed for both supports. The system Rh/CNT2-SIL(55 %) could be recycled without loss of activity up to 5 runs.

Palladium nanoparticles supported ionic liquid catalytic phase was applied in three different reactions: hydrogenation of benzylidenacetone, C-C Heck coupling of iodobenzene and methyl vinyl ketone and the sequential process Heck coupling/hydrogenation.

High activities in the hydrogenation reaction of benzylidenacetone were achieved using supported $\text{Pd}_b/\text{L}/\text{IL}_1$ as supported ionic liquid catalytic phase compared to those obtained using Pd_b/IL_1 and Pd_a/IL_1 , because of their well dispersion and the absence of remaining impurities, such as chloride anions, in the nanoparticles surface. The use of $\text{Pd}_b/\text{L}/\text{IL}_2$ as supported ionic liquid catalytic phase led to low conversions probably due to the low solubility of hydrogen in $[\text{emim}][\text{HPO}(\text{OMe})\text{O}]$. A comparative study of the support influence using CNT6-SIL($\text{Pd}_b/\text{L}/\text{IL}_1$) and SiO_2 -SIL($\text{Pd}_b/\text{L}/\text{IL}_1$) supported systems, showed the best performances when CNT6 was used as support. Recycling experiments using this catalyst were carried out without significant loss of activity up to 4 cycles.

CNT6-SIL($\text{Pd}_b/\text{L}/\text{IL}_2$) catalyst showed good activities compared to SiO_2 -SIL($\text{Pd}_b/\text{L}/\text{IL}_2$) in the C-C coupling reaction in the presence of a base (Na_2CO_3) in NMP as organic solvent. On the contrary, the same catalytic systems were inactive without base addition. When the reaction was carried out in $[\text{emim}][\text{HPO}(\text{OMe})\text{O}]$ using CNT6-SIL($\text{Pd}_b/\text{L}/\text{IL}_2$) in the absence of base, good activities were obtained because of the basic character of the $[\text{HPO}(\text{OMe})\text{O}]$ counter anion.

The Heck coupling/hydrogenation sequential process presented good performances only when CNT6-SIL($\text{Pd}_b/\text{L}/\text{IL}_2$) was applied using $[\text{emim}][\text{HPO}(\text{OMe})\text{O}]$ as solvent. This behaviour could be explained by the formation of molecular palladium-carbene species during

the Heck coupling in the presence of an additional base, being difficult to further reduce under hydrogen to regenerate the formation of catalytically active palladium nanoparticles.

The application of this SILP catalytic system using MWCNTs as support in further catalytic reaction (for example asymmetric hydrogenation or in other sequential reactions) could be interesting due to the higher catalytic activity obtained compared with other studied classical supports.

In order to understand the special interactions between the ionic liquids and the different support materials further studies should be done. These studies may help the catalytic scientific community to synthesized high performing catalys.

Nouveaux systèmes catalytiques en phase liquide ionique supportée sur nanotubes de carbone

AUTEUR: RODRIGUEZ PEREZ Laura

DIRECTEURS DE THESE: SERP Philippe and GOMEZ Montserrat.

7 FRENCH SUMMARY

7.1 INTRODUCTION ET OBJECTIFS

La recherche de procédés catalytiques de faible coût et respectueux de l'environnement est devenue l'un des principaux sujets de la chimie synthétique moderne. Dans ce contexte, le développement de catalyseur hautement actifs et sélectifs présente une importance primordiale. Dans les procédés industriels, la catalyse hétérogène est préférée à la catalyse homogène, car l'extraction du produit et la récupération du catalyseur sont relativement plus faciles. Cependant, les contraintes de transfert de masse et/ou de chaleur, conduisent à une diminution de l'activité catalytique ainsi qu'à une chimio- et stéréo-sélectivité moins efficace par rapport à la catalyse homogène. En conséquence, un système catalytique comportant en même temps les avantages de la catalyse homogène et ceux de la catalyse hétérogène (une bonne activité, une haute sélectivité et une extraction aisée du produit suivi de la récupération du catalyseur) renforcerait considérablement l'intérêt pour les applications catalytiques industrielles.

D'autre part, les liquides ioniques (ILs) désignés sous le nom de sels fondus sont des électrolytes (composés uniquement d'ions) liquides à une température inférieure à 100 °C et possédant une tension de vapeur négligeable et une excellente ainsi qu'une stabilité thermique et chimique.^{1,2} Les propriétés physico-chimiques de ces sels permettent de les considérer comme une alternative « verte » aux composés organiques volatiles (COVs), notamment les solvants chlorés.^{3,4} Les ILs sont de bons solvants pour des synthèses organiques et inorganiques, et en particulier pour des applications en catalyse.^{5,6}

Les ILs possèdent en général une faible miscibilité avec les solvants organiques et les substrats polaires et apolaires, mais ils permettent de dissoudre certains gaz à différentes concentrations (CO₂, éthane, méthane, argon, dioxygène, dihydrogène) ainsi que les précurseurs organométalliques.^{1,7} Ainsi, ces sels sont utilisés en catalyse bi-phasique pour immobiliser le catalyseur et faciliter son recyclage et la récupération des produits organiques par simple décantation ou extraction. Ces systèmes bi-phasiques présentent à la fois les avantages de la catalyse homogène (meilleure efficacité du catalyseur sous des conditions de réaction douces) et de la catalyse hétérogène (récupération du catalyseur et séparation aisée des produits).^{8,9} D'un point de vue structurale, ces solvants non conventionnels sont considérés comme de superstructures polymériques, formées par une association de liaisons hydrogène entre les cations et les anions.¹⁰ Ils peuvent alors induire des réactivités chimiques particulières dans des procédés catalytiques (énantio)sélectifs.¹¹

Par contre, ces solvants présentent différents inconvénients lorsqu'ils sont appliqués dans la catalyse en tant que milieu réactionnel, comme leur coût élevé, leur relative haute viscosité, leur pureté et l'utilisation de solvants organiques volatiles pour la séparation et le recyclage du catalyseur. Le fait de les supporter sur différents types de solides peut permettre à la fois de réduire de façon significative les quantités de ILs utilisées et de récupérer facilement le catalyseur immobilisé dans la phase liquide ionique. Cette phase liquide ionique supportée (SILP) a déjà été appliquée dans l'électrochimie,¹² la chromatographie¹³ et l'élaboration de matériaux comme les membranes comme procédés de séparation.¹⁴ Une grande variété de supports a été utilisée pour ces applications. Dans le domaine de la catalyse, ce concept est nommé catalyse en phase liquide ionique supportée (SILPC) et il est basé sur la catalyse en phase aqueuse supportée (SAPC) décrite en 1989 par Davis et al.,¹⁵ dans laquelle un catalyseur soluble dans l'eau est immobilisé sur une couche mince d'eau supporté sur silice. Dans ce système, les composés organiques se trouvent dans la phase organique tandis que la réaction a lieu à l'inter-phase eau-solvant organique. La grande surface inter-faciale du catalyseur SAPC combinée avec le fait que le catalyseur reste sur le support, conduit à des systèmes catalytiques hautement performants. Par contre, ces catalyseurs n'ont pas pu être appliqués avec succès dans des procédés industriels. Les deux principaux inconvénients sont l'extraction de la phase catalytique supportée par des forces mécaniques et l'évaporation de la couche d'eau supportée dans des réacteurs en phase gazeuse. Ces difficultés conduisent à des catalyseurs à courte durée de vie.

Dans ce contexte, l'utilisation de catalyseurs en phase liquide ionique supportée présente de nombreux avantages en raison de leur faible pression de vapeur et de leurs polarités adéquates (Figure 7.1). La possibilité d'immobiliser de faibles quantités de liquide ionique sur un support pour des applications en catalyse a attiré beaucoup d'attention dans ces dernières années,^{16,17} car ce concept semble unifier les avantages de la catalyse homogène et hétérogène. De plus, le solvant peut subsister à l'état fluide sur le support, même à des températures élevées. Cela fait que le SILPC peut être approprié pour des procédés industriels en continu. La phase liquide ionique peut être fixée soit par liaison chimique entre le cation ou l'anion du liquide ionique et le support, soit par physisorption du liquide ionique sur le support. SILPC a été étudié sur une large variété de supports solides principalement des oxydes inorganiques. Les ILs immobilisés peuvent comporter comme précurseurs catalytiques soit des complexes organométalliques soit des nanoparticules métalliques. Les matériaux préparés présentent l'avantage d'être sous forme solide qui facilite la séparation du catalyseur et des produits de la réaction catalytique.

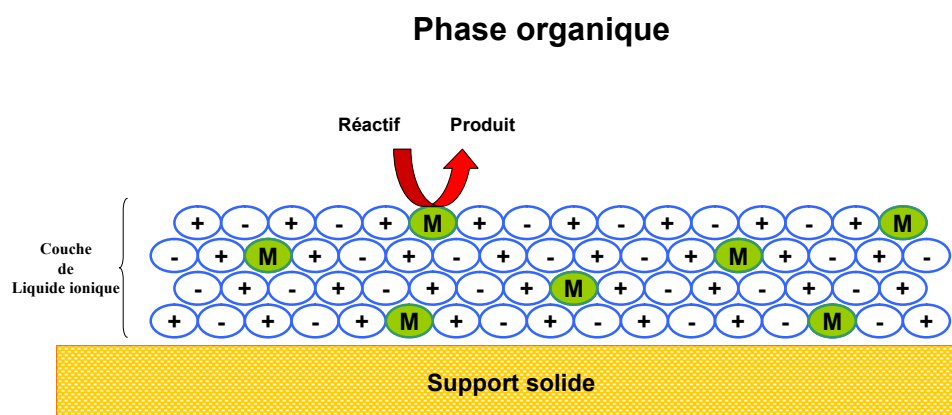


Figure 7.1: Représentation schématisée de la catalyse en phase liquide ionique supportée (SILPC).

Au cours de cette thèse, des catalyseurs en phase liquide ionique supportée sur nanotubes de carbone multi-parois fonctionnalisés ont été synthétisés et utilisés postérieurement en catalyse. La structure très ouverte des nanotubes de carbone avec une haute porosité favorise le transfert de masse et en conséquence augmente la cinétique de la réaction. Par contre la surface des nanotubes de carbone est inerte d'un point de vue chimique et une première étape de fonctionnalisation peut permettre d'améliorer la compatibilité avec la phase liquide ionique supportée.

Jusqu'à présent, la catalyse supportée en phase liquide ionique a mis en jeu des supports mésoporeux d'oxydes inorganiques classiques comme la silice. De cet fait, une étude comparative entre ces types de supports et les nanotubes de carbone multi-parois a été réalisée pour différentes réactions catalytiques modèles : l'hydrogénation, le couplage C-C de Heck et le processus séquentiel Heck/hydrogénation.

En particulier, les objectifs de cette thèse ont été décrits ci-après :

- Fonctionnalisation efficace et caractérisation des nanotubes de carbone multi-parois (MWCNTs) contenant des unités ioniques, ainsi que l'étude de leur affinité pour le milieu liquide ionique.
- Etude structurale des interactions entre le support solide et les liquides ioniques par différentes techniques du solide.
- Synthèse et caractérisation de nanoparticules de palladium à partir de précurseurs métalliques.
- Synthèse et caractérisation de catalyseurs supportés en phase liquide ionique sur MWCNTs fonctionnalisés, en utilisant soit un complexe de Rh soit des nanoparticules de palladium comme phase catalytiquement active.

- Utilisation du catalyseur en phase liquide ionique supportée dans des réactions d'hydrogénation, de couplage C-C de Heck et des réactions séquentielles.

7.2 MODIFICATION DE LA SURFACE DES NANOTUBES DE CARBONE MULTI-PAROIS

Les nanotubes de carbone sont des structures cylindriques constituées par des plans de graphène où les atomes de carbone présentent une hybridation sp^2 .¹⁸ Ils ont été découverts en 1991 par S. Iijima lors de ses travaux sur les fullerènes.¹⁹ Plusieurs types de nanotubes de carbone existent suivant leurs dimensions et l'arrangement des plans de graphène. Ils sont classiquement classés en trois grandes familles : les nanotubes de carbone mono-paroi (Single Wall Carbon NanoTubes, SWCNTs), les nanotubes de carbone multi-parois (Multi Wall Carbon NanoTubes, MWCNTs) et les nanofibres de carbone (Graphite NanoFibers, GNFs) (Figure 7.2).

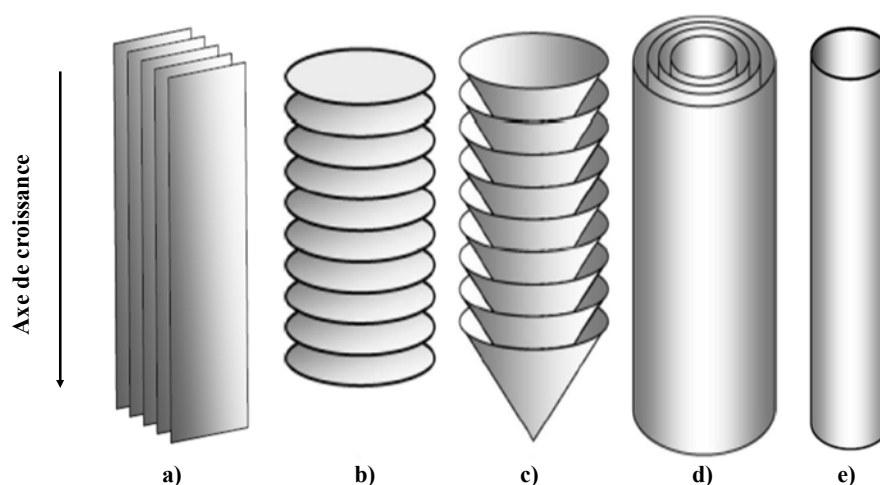


Figure 7.2: Représentation schématique du CNTs et CNF. (a) CNF-R (type « ruban »), (b) CNF-P (type « plateau »), (c) CNF-H (type « arêtes de poisson »), (d) MWCNTs, (e) SWCNTs

Les nanotubes de carbone multi-parois (Figure 7.2, d) sont constitués d'au moins deux cylindres concentriques, parallèles à l'axe de croissance avec des interactions inter-tubes de type « lip-lip » qui contribuent à stabiliser la structure globale.

En ce qui concerne la synthèse, les nanotubes sont en général préparés selon deux approches : i) par voie physique selon des méthodologies à haute température (comme l'ablation laser et la méthode à arc électrique)^{20,21} et ii) par voie chimique en utilisant de plus basses températures (comme le dépôt chimique en phase vapeur catalytique (CCVD))²².

Bien que d'un point de vue structural les nanotubes de carbone peuvent être considérés proches du graphite, ils présentent des propriétés intrinsèques bien différentes et parfois beaucoup plus intéressantes que celles du graphite. Les principales propriétés mises en avant sont leur résistance mécanique²³ et leur conductivité électronique,²⁴ mais d'autres propriétés telles que leurs capacités d'adsorption,²⁵ leur conductivité thermique²⁶ ou encore leur réactivité chimique,²⁷ ont été étudiées, ouvrant des applications potentielles pour ces matériaux.

En ce qui concerne la fonctionnalisation chimique de ces MWCNTs, l'absence de liaisons ouvertes rend les nanotubes de carbone relativement inertes. Néanmoins, leurs défauts structuraux et leurs extrémités plus réactives sont de sites potentiels de réactivité permettant d'envisager toute une chimie de surface par fonctionnalisation, sans modification de la structure de base du matériau.²⁸ Les traitements acides utilisés pour purifier les MWCNTs ou pour les fonctionnaliser, introduisent principalement des groupements oxydés (carbonyles et acides carboxyliques).

L'amidation ou l'estérification des nanotubes de carbone oxydés est une méthode efficace pour la production de matériaux solubles dans différents solvants organiques ou dans l'eau.^{29,30} De plus, la fonctionnalisation avec des unités ioniques augmente la solubilité des MWCNTs dans les liquides ioniques.^{31,32}

Compte tenu de leurs propriétés, de nombreux efforts de recherche sont menés visant au développement de ces matériaux. Dans le cadre des applications chimiques et plus concrètement de la catalyse, leurs propriétés d'adsorption, conjuguées à leur relative inertie chimique et à leur conduction thermique, leur confèrent un avenir intéressant en tant que supports de catalyseurs. Des performances déjà remarquables ont été obtenues grâce aux interactions électroniques, à la bonne affinité entre particules métalliques et nanotubes de carbone, à la suppression des limitations de transfert de matière par l'absence de microporosité et au maintien d'une surface de contact élevée (grande surface spécifique).³³ De nombreux résultats ont été déjà publiés, démontrant des améliorations certaines en termes d'activité et de sélectivité catalytiques.³⁴

Nous nous sommes intéressés à la modification chimique de la surface des MWCNTs comportant des unités ioniques afin d'améliorer la compatibilité avec la phase catalytique dans le liquide ionique.

7.2.1 Discussion des résultats

Dans notre étude, des nanotubes de carbone multi-parois synthétisés par dépôt chimique en phase vapeur catalytique ont été utilisés.

Même si ces nanotubes présentent une haute pureté, une première étape de purification avec de l'acide sulfurique à 140 °C est nécessaire pour éliminer le carbone amorphe et le catalyseur restant (particules de fer). Cet échantillon est nommé CNT0. Les analyses ATG montrent une pureté de 98% (subsistent 2% de Fe dû au catalyseur de synthèse). Ces CNTs sont mésoporeux avec un volume poreux de 0.66 cm³/g et un diamètre de pores de 6-20 nm ; leur surface spécifique est de 227 m²/g. Ils peuvent atteindre 10 nm de longueur et la plupart d'entre eux montre des extrémités fermées. Comme il peut être observé par analyse TEM, le diamètre interne est compris entre 4 et 12 nm, tandis que le diamètre extérieur va de 8 à 21 nm. L'étude par spectroscopie Raman montre deux bandes caractéristiques des MWCNTs correspondant aux liaisons C-C: le mode D (carbone sp³) à des fréquences situées entre 1330 et 1360 cm⁻¹, et le mode G ou MT-mode tangentiel, (carbone sp²) à 1580 cm⁻¹ (le rapport des intensités est : I_D/I_G = 1.45).

Afin d'introduire des fonctionnalités covalentes sur les MWCNTs, une étape d'activation de surface est nécessaire. La méthode la plus commune pour introduire des groupements acides carboxyliques de surface est l'oxydation chimique utilisant l'acide nitrique comme agent oxydant. Les CNT0 ont été oxydés avec de l'acide nitrique concentré à différents temps de réaction (0.5, 1, 3 et 8 heures), donnant lieu à différentes fonctionnalisations de surface (échantillons nommés respectivement CNT1a, CNT1b, CNT1c et CNT1d).

L'acide réagit principalement avec les défauts structuraux de surface situés de façon majoritaire aux extrémités des CNTs, en les fermant. Une analyse BET après le traitement d'activation révèle, une augmentation de la surface spécifique de 227 à 244 m²/g, en raison de l'ouverture de certains nanotubes.

L'efficacité du traitement a été mise en évidence par spectroscopie infrarouge. En plus des bandes caractéristiques de la structure des nanotubes, vibration C-C dans le plan à 1570 cm⁻¹ et élongation C-H à 2910 cm⁻¹, sont observées d'autres nouvelles bandes à 1717 cm⁻¹ (élongation C = O) et à 1200 cm⁻¹ (élongation C-O), associées aux fonctions acides carboxyliques. La bande large à 3300 cm⁻¹ est attribuée à des groupes hydroxyles.

La composition des MWCNTs préparés (CNT0 et CNT1d) a été déterminée par XPS (X-ray Photoelectron Spectroscopy) et par analyse élémentaire (Tableau 7.1). Comme prévu, la teneur en oxygène des nanotubes de carbone oxydés augmente jusqu'à 5.3% (valeur déterminée par analyse élémentaire) ; d'ailleurs l'analyse XPS de ces tubes activés montre un pourcentage d'atomes d'oxygène de 7.6%, ce qui démontre l'efficacité du greffage des

groupes oxygénés à la surface. La concentration des fonctions acides sur la surface MWCNTs est de 0.85 groupement COOH/nm² pour CNT1d (traitement d'activation pour 8 h), déterminée par dosage chimique.³⁵

MWCNTs	% wt analyse elementaire				% atomique (XPS)	
	C	H	N	O	C	O
CNT0	95	0.16	-	0.64	100	-
CNT1d	87.3	0.3	0.15	5.3	92.4	7.6

Tableau 7.1: Analyse XPS et analyse élémentaire des MWCNTs purifiés (CNT0) et MWCNTs oxydés (CNT1d).

Dans le but d'améliorer l'affinité entre les nanotubes de carbone et les liquides ioniques, les MWCNTs oxydés (CNT1a, b, c et d) ont été fonctionnalisés avec des unités ioniques de type imidazolium pour obtenir les nanotubes de carbone multi-parois fonctionnalisés CNT2-CNT9. Deux différentes approches ont été utilisées: la méthodologie covalente et la méthodologie ionique.

De bons résultats ont été obtenus par voie covalente en formant comme intermédiaire le chlorure d'acyle correspondant. Les fonctionnalités acides carboxyliques ont été modifiées en quatre étapes, comme indiqué dans le Schéma 7.1 pour donner lieu aux matériaux CNT2-CNT7 qui correspondent à une fonctionnalisation CNT-([C₈N₃OH₁₁]₁PF₆).

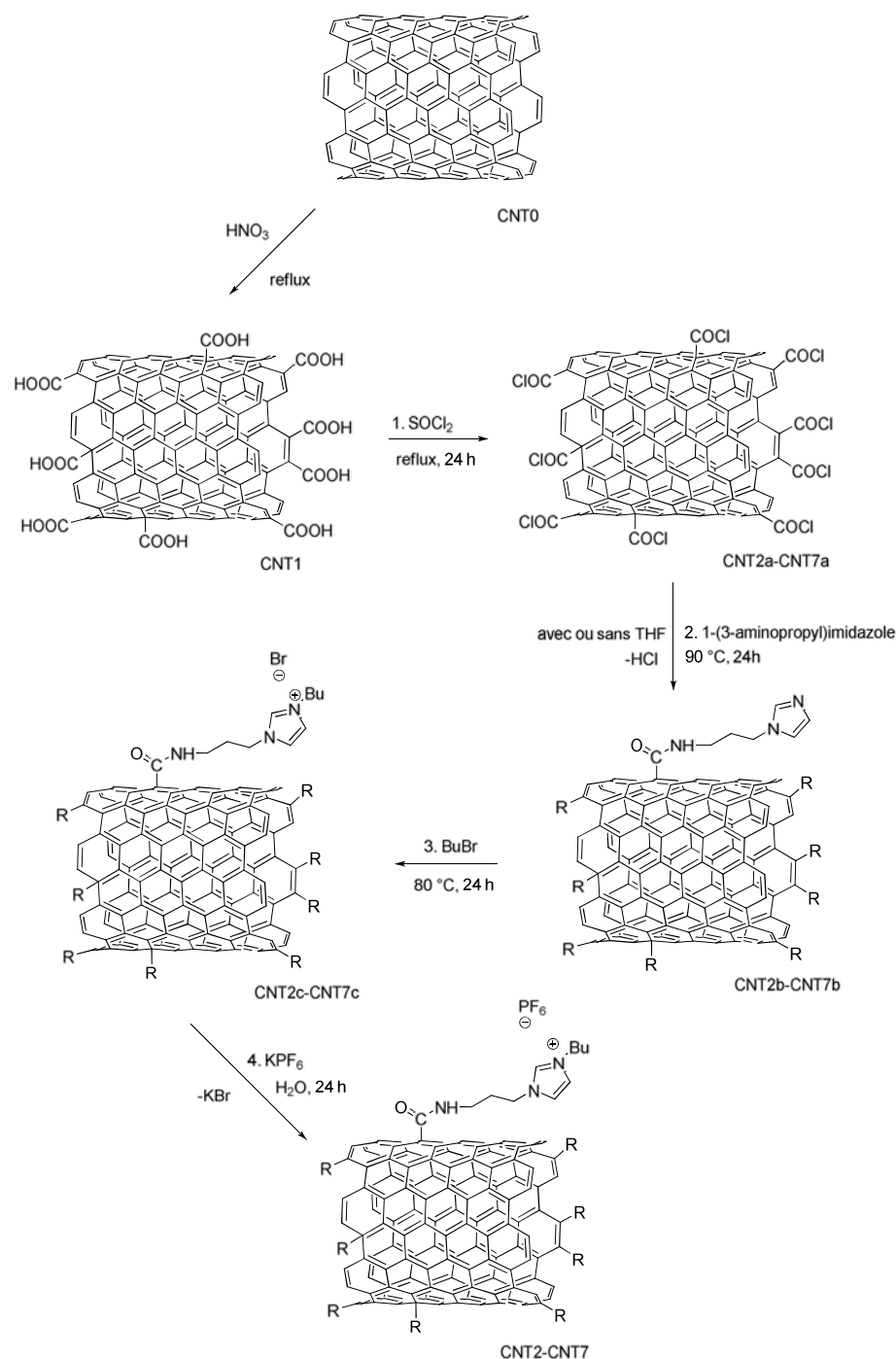


Schéma 7.1: Activation de CNT0 pour donner CNT1 (a, b, c, d) suivi de la fonctionnalisation par approche covalente pour donner CNT2-CNT7 (CNT-([C₈N₃OH₁₁]⁺PF₆⁻))

L'efficacité de la fonctionnalisation de surface a été mise en évidence par spectroscopie IR (infra-rouge), XPS, analyse élémentaire et ATG (analyse thermogravimétrique).

Le spectre IR des MWCNTs fonctionnalisés avec des unités imidazolium (CNT2-CNT7), montre une bande correspondant au groupement C=O amide à 1641 cm⁻¹, les bandes C-H aliphatiques d'élongation sont situées entre 2850 et 2950 cm⁻¹ et les bandes à 1250-1500 cm⁻¹

sont attribuées à des torsions C-H. L'apparition d'une bande intense correspondante à l'élongation de la liaison P-F de l'anion PF_6^- à 830 cm^{-1} confirme le greffage des fonctions ioniques.

L'analyse élémentaire et l'analyse semi-quantitative XPS de surface ont confirmé la fonctionnalisation des CNT (Table 7.1). Différents temps d'oxydation dans l'activation de la surface conduisent à différents degrés de fonctionnalisation. Comme on devait s'y attendre, on peut observer une augmentation du nombre de fonctions greffés à la surface des MWCNTs de surface suivant le temps d'activation. (Table 7.1, entrées 6 et 8). En effet, pour une activation de 8 h, lorsque le 1-(3-aminopropyl)imidazole a été utilisé en grand excès et en l'absence de solvants, on a obtenu le plus grand nombre de fonctionnalités de surface (7.3% du fluor en pourcentage atomique obtenu par XPS, entrée 5). Par contre, l'utilisation du THF dans la deuxième étape de la fonctionnalisation entraîne une baisse de quantité des groupes fonctionnels greffés (entrées 3 et 4).

Entrée	MWCNTs	% wt analyse élémentaire				% atomique XPS			
		C	H	N	O	C	O	N	F
1	CNT0	95	0.16	-	0.64	100	-	-	-
2	CNT1	87.03	0.3	0.15	5.3	92.4	7.6	-	-
3	CNT2	88.66	0.7	1.51	-	89.5	4.2	1.8	4.9
4	CNT3	82.6	1.5	1.85	7.5	82.7	10.3	1.8	5.2
5	CNT4	80.85	1.26	2.69	-	82.5	7.2	3.0	7.3
6	CNT5	70.37	0.68	1.53	-	80.8	14.2	-	5.0
7	CNT6	85.70	0.16	1.85	-	88.8	3.5	2	5.8
8	CNT7	79.70	0.65	2.31	-	84.1	6.8	3.1	6.0
9	CNT9 ^a	88.42	0.52	0.62	-	93.6	6.4	-	-

Table 7.1: Différents degrés de fonctionnalisation de surface des MWCNTs analysés par analyse élémentaire et XPS.

Les analyses ATG sous air montrent que les fonctionnalités ioniques de type imidazolium sont moins stables que le liquide ionique pur [bmim][PF_6] : la température de décomposition pour le ILs pur est de 425 °C et de 310 °C pour les matériaux modifiés. De plus, la

fonctionnalisation de surface a un effet sur la thermostabilité des MWCNTs : pour les MWCNTs fonctionnalisés avec le 1-(3-aminopropyl)imidazole (CNT2-CNT7) la température de décomposition est de 750 °C (CNT2) alors que pour les MWCNTs purifiés (CNT0) elle est de 640 °C.

La compatibilité entre les MWCNTs fonctionnalisés et le liquide ionique, nettement améliorée par le greffage des fonction ioniques peut être mis en évidence par leur dispersabilité dans le [bmim][PF₆] suivent la tendance: MWCNTs fonctionnalisés (CNT2) > MWCNTs activés (CNT1) >> MWCNTs purifiés (CNT0).

7.3 CATALYSEUR EN PHASE LIQUIDE IONIQUE SUPPORTEE : PREPARATION ET CARACTERISATION

Le SILPC est un concept très attractif dans lequel une couche mince de liquide ionique est immobilisée dans les pores d'un support solide combinant ainsi les avantages des deux matériaux.¹⁷ Un précurseur catalytique homogène (par exemple un complexe organométallique) ou hétérogène (par exemple des nanoparticules métalliques) pourrait être dispersé dans le liquide ionique et par la suite immobilisé sur un support solide pour constituer le catalyseur SILP.

Au cours de cette thèse, le hexafluorophosphate de 1-butyl-3-methylimidazolium, [bmim][PF₆], et des nanotubes de carbone multi-parois ont été utilisés pour préparer les catalyseurs en phase liquide ionique supportée.

Le complexe de rhodium [Rh(nbd)(PPh₃)₂]PF₆ (nbd = norbornadiène) et des nanoparticules de palladium préformées ont été immobilisés dans la phase liquide ionique en tant que précurseurs catalytiques pour les différentes réactions catalytiques étudiées

7.3.1 Immobilisation d'un catalyseur homogène

L'immobilisation des complexes organométalliques en phase liquide ionique supportée constitue une méthode appropriée en raison de la facilité de séparation des différents réactifs et du recyclage du catalyseur. Un catalyseur ionique de rhodium, [Rh(nbd)(PPh₃)₂]PF₆, a été immobilisé selon la méthodologie décrite dans le Schéma 7.2 sur différents supports : nanotubes de carbone multi-parois purifiés (CNT0), nanotubes de carbone multi-parois oxydés (CNT1d), nanotubes de carbone multi-parois fonctionnalisés (CNT2-CNT4), γ -Al₂O₃, ZrO₂, TiO₂, SiO₂, ZnO, MgO et charbon actif (CA). Différentes quantités de liquide ionique ont été utilisées pour avoir des teneurs de 20, 37, 55 ou 64 % en poids. Les catalyseurs obtenus sont nommés Rh/CNT_x-SIL(y %), (x = 0-4) pour les nanotubes de carbone et Rh/S-

SIL(y %) (S = γ -Al₂O₃, ZrO₂, TiO₂, SiO₂, ZnO, MgO et CA) pour les autres supports, y étant la charge en liquide ionique.

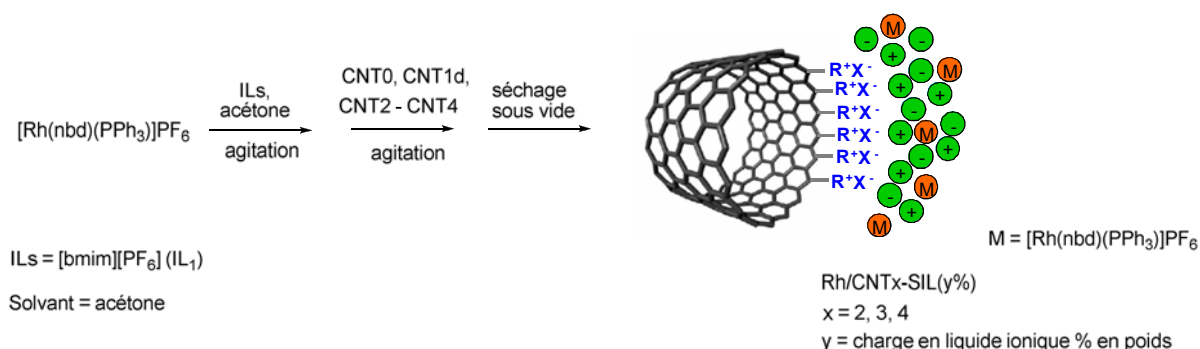


Schéma 7.2: Immobilisation du [Rh(nbd)(PPh₃)₂]PF₆ dans le [bmim][PF₆] sur MWCNTs fonctionnalisés.

Différents solides, pâtes ou poudres fines, ont été obtenus en fonction du support utilisé et de la quantité de liquide ionique utilisée.

7.3.2 Immobilisation d'un catalyseur hétérogène

Afin de synthétiser des composites en phase liquide ionique supportée avec un catalyseur hétérogène immobilisé, des nanoparticules de palladium ont été préformées en milieu liquide ionique.

Au cours de ces vingt dernières années, les nanomatériaux ont suscité un intérêt croissant dans le domaine de la catalyse de part leurs propriétés intermédiaires entre les catalyseurs homogènes (état moléculaire) et hétérogènes classiques (état massif). En effet, leur taille comprise entre 1 et 10 nm leur confère une surface spécifique très importante et donc potentiellement un nombre de sites actifs élevé pour la transformation de substrats. Aussi, les nanoparticules de métaux de transition en fonction de la nature de stabilisants utilisés peuvent être solubles en milieu organique et également en milieux non conventionnels comme l'eau, les liquides ioniques ou le CO₂ supercritique. Plus récemment, il a été montré que ces nanocatalyseurs possédaient non seulement une réactivité de surface, mais aussi un comportement moléculaire donc ils peuvent être considérés comme des réservoirs d'espèces moléculaires.^{36,37,38,39}

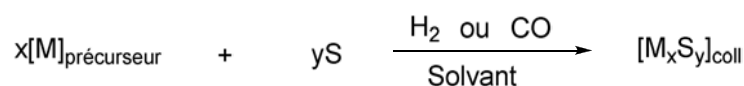
Concernant la formation des nanoparticules métalliques, il existe deux approches de synthèse. D'une part, la méthode physique de dissociation dite « top-down » consiste à fragmenter un métal massif en espèces de taille nanométrique. D'autre part, la méthode

chimique d'association, « bottom-up », est une réduction chimique de précurseur moléculaire aboutissant à la formation de nanoparticules métalliques.^{40,41} Parmi les deux approches de synthèse des nanoparticules, nous nous intéresserons uniquement à la voie chimique « bottom-up ». Celle-ci permet un meilleur contrôle de la taille, de la forme et de la composition chimique de la surface des nanoclusters.

Les particules nanométriques sont uniquement stables d'un point de vue cinétique et tendent à s'agglomérer vers la formation de métal massif. Afin d'éviter cette aggrégation l'utilisation d'un agent stabilisant s'impose.⁴² Le choix de ces stabilisants, présents à la surface métallique, permet d'une part de contrôler la taille, la forme et la composition de surface, et d'autre part de moduler la sélectivité chimique de ces nanoparticules dans les réactions catalytiques.

D'autre part, les liquides ioniques jouent le rôle de solvant dans de nombreuses réactions catalytiques ainsi que d'agents stabilisants des nanoparticules métalliques. Bien que le mode de stabilisation n'ait jamais été clairement mis en évidence, il est fortement suggéré que les liquides ioniques agissent comme des superstructures polymériques créant à la fois une barrière électrostatique et stérique entre les particules.⁴³

Dans notre étude nous nous sommes intéressés à la synthèse de nanoparticules de palladium basée sur la méthode développée par le groupe Chaudret. Elle consiste en la décomposition d'un précurseur organométallique sous atmosphère réductrice (dihydrogène ou monoxyde de carbone) et en présence d'agents stabilisants (Schéma 7.3).^{44,45} Les principaux agents stabilisants sont des ligands organiques ou des polymères. Nous nous sommes intéressés à des particules de palladium préparées sous atmosphère réductrice de dihydrogène à partir de deux précurseurs différents $[Pd_2(dba)_3]$ et $[PdCl_2(cod)]$, et stabilisées soit par un liquide ionique ($[bmim][PF_6]$ ou $[emim][HPO(OMe)O]$), soit par un mélange de liquide ionique et ligand (4-(3-phenylpropyl)pyridine).



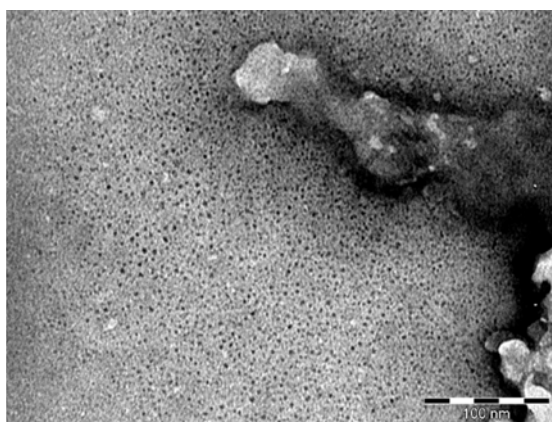
M = métal

S = stabilisant

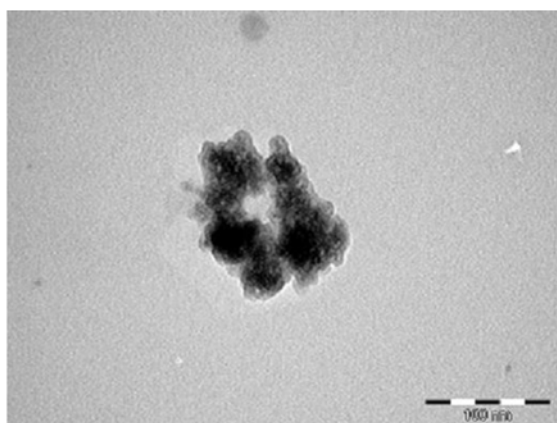
Schéma 7.3: Synthèse de nanoparticules métalliques par décomposition d'un précurseur organométallique.

Des nanoparticules différentes en taille ont été observées par analyse MET (Microscopie Electronique en Transmission) en fonction du précurseur métallique, du liquide ionique utilisé et de la présence ou non du ligand.

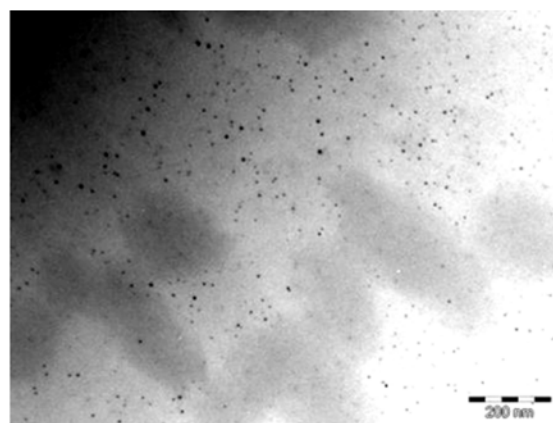
La décomposition du précurseur $[\text{PdCl}_2(\text{cod})]$ réalisée dans $[\text{bmim}][\text{PF}_6]$ conduit à des nanoparticules nommées Pd_a/IL_1 avec une distribution de taille de 2.15 ± 0.72 nm (Figure 7.3, a). Quand la réaction a été réalisée à partir de $[\text{Pd}_2(\text{dba})_3]$ dans $[\text{bmim}][\text{PF}_6]$ et en absence de ligand, les micrographes MET montrent la formation de grosses particules agglomérées (Figure 7.3, b) avec des régions où les particules restent dispersées et présentent un diamètre moyen de $5.25 \text{ nm} \pm 2.31$ (Figure 7.3, c), et une distribution de taille hétérogène (Pd_b/LI_1). L'utilisation de 0.3 équivalent de ligand 4-(3-phenylpropyl)pyridine par rapport au précurseur métallique évite la formation de grands agglomérats et conduit à la formation de nanoparticules de palladium ($\text{Pd}_b/\text{L}/\text{IL}_1$) hétérogènes en distribution de taille avec un diamètre moyen de 4.34 ± 1.33 (Figure 7.3, d). Par contre, l'utilisation de $[\text{emim}][\text{HPO}(\text{OMe})\text{O}]$ comme liquide ionique en combinaison avec le ligand 4-(3-phenylpropyl)pyridine favorise la formation de nanoparticules ($\text{Pd}_b/\text{L}/\text{IL}_2$) homogènes en taille avec un diamètre moyen de 4.47 ± 0.78 (Figure 7.3, e). L'organisation particulière observée peut être reliée à des effets du contre ion du liquide ionique.



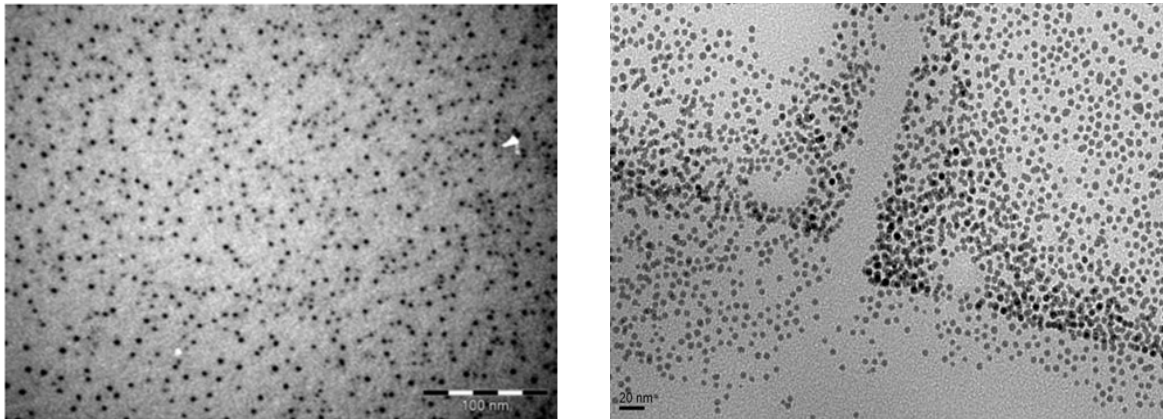
a)



b)



c)



d)

e)

Figure 7.3: Micrographes MET de: a) Pd_a/IL₁, b) Pd_b/IL₁ agglomérées, c) Pd_b/IL₁, d) Pd_b/L/IL₁, e) Pd_b/L/IL₂

Ces nanoparticules préformées ont été ultérieurement utilisées pour synthétiser le catalyseur en phase liquide ionique supportée sur des nanotubes de carbone fonctionnalisés (CNT3, CNT6) et sur silice en suivant la méthodologie présentée au Schéma 7.4 avec un chargement en liquide ionique de 34 % en poids. Les catalyseurs obtenus sont nommés CNT6-SIL(PdNPs) ou SiO₂-SIL(PdNPs) (PdNPs = Pd_a/IL₁, Pd_b/IL₁, Pd_b/L/IL₁, Pd_b/L/IL₂).

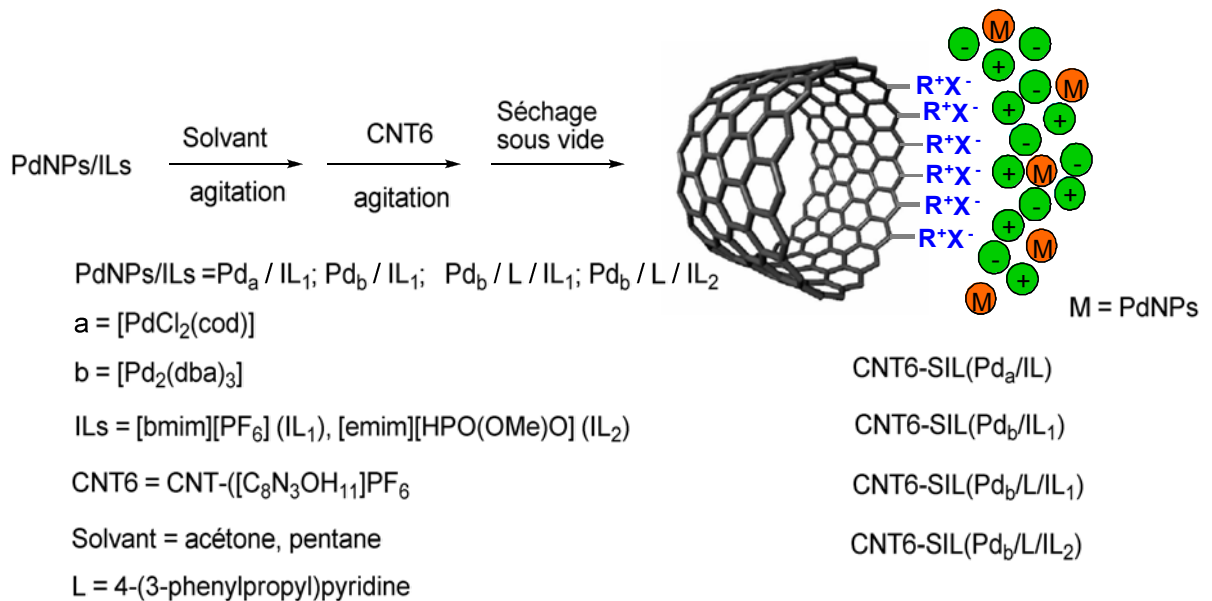


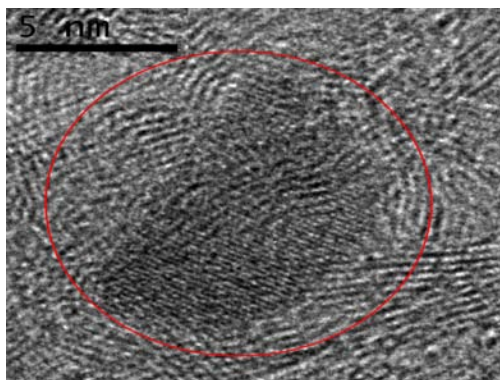
Schéma 7.4: Immobilisation des nanoparticules de palladium préformées en milieu liquide ionique sur CNT6.

Les analyses EDX (Energy Dispersive X-ray spectroscopy) sur le catalyseur CNT6-SIL (Pd_b/L/IL₂) ont montré la présence de nanoparticules de Pd dans le catalyseur, ainsi que la

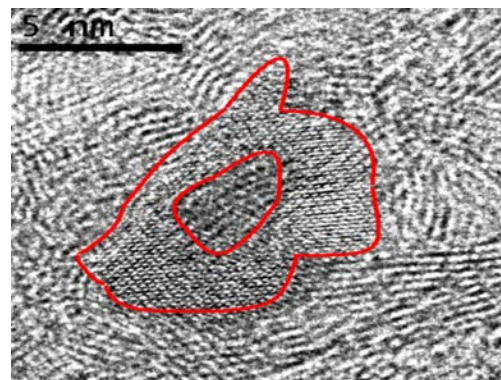
présence de C, O, N et P. En raison des impuretés provenant de la synthèse de nanotubes de carbone Fe, Al et Cr ont également été observés. Les analyse MET ont montré des nanoparticules de palladium entourées de nanotubes de carbone (Figure 7.4). L'image FFT (Fast Fourier Transform) correspondant à une nanoparticule isolée (Figure 7.4, b) présente au-delà des plans caractéristiques de la structure fcc du palladium (Figure 7.4, c), deux autres plans qui peuvent correspondre au liquide ionique cristallin qui entoure les nanoparticules (Figure 7.4, d).



a)



b)



d)

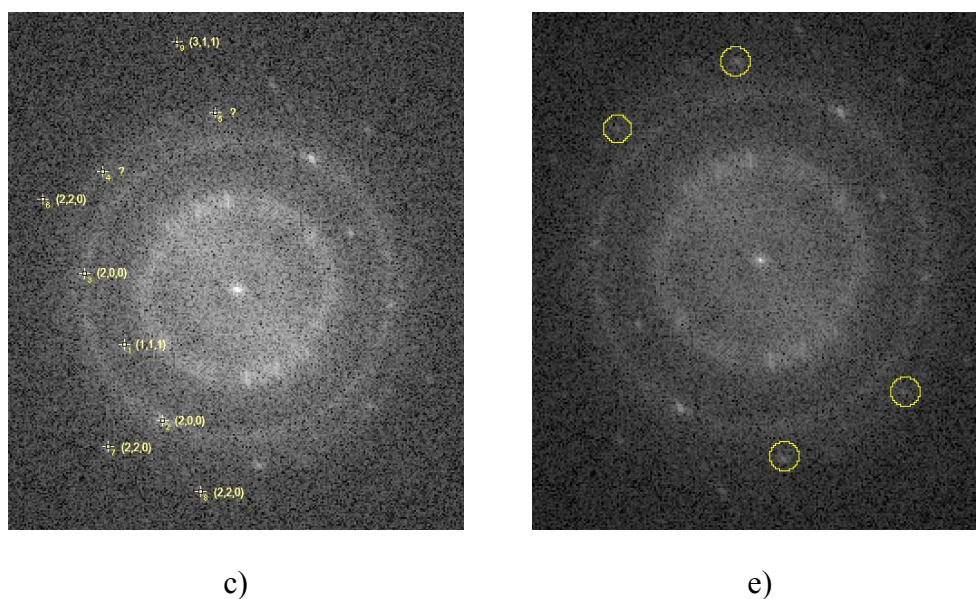


Figure 7.4: a) Micrographe MET de CNT6-SIL(Pd/L/IL₂) (échelle 10 nm), b) nanoparticule de palladium isolée (échelle de 5 nm); c) FFT de la nanoparticule avec les plans correspondants du palladium fcc; d) FFT inverse montrant les plans inconnus; e) image TEM calculée provenant de la FFT de l'image d).

7.3.3 Caractérisation des composites liquide ionique supportée

Des composites en phase liquide ionique ([bmim][PF₆]) le supportée sur des nanotubes de carbone fonctionnalisés (CNT_x-SIL(y% w/w)), préparés comme décrit précédemment mais en absence de espèces métalliques, ont été caractérisés par MET, ATG (analyse thermogravimétrique) et DRX (Diffraction des rayons X).

L'analyse MET a permis d'identifier l'immobilisation du liquide ionique sur des nanotubes de carbone fonctionnalisés. L'épaisseur du film de [bmim][PF₆] est fortement dépendant du chargement en liquide ionique. Des épaisseurs de couche de 3.3 nm en liquide ionique ont pu être observées avec CNT3-SIL(55%) (Figure 7.5).

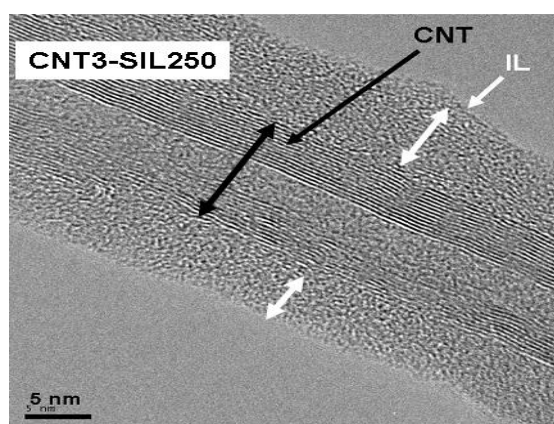


Figure 7.5: Micrographe MET de CNT3-SIL(55 %)

Le degré de fonctionnalisation de la surface MWCNTs a une influence sur la texture du composite CNT-SIL formé. En effet, CNT2 et CNT3 sont toujours obtenus sous forme de poudres indépendamment du chargement en liquide ionique. En revanche, CNT4, qui présente la plus forte concentration en groupements ioniques de surface, avec une charge en ILs de 55 % en poids (CNT4-SIL (55%)), est un gel. Ce phénomène a déjà été décrit pour des MWCNTs mélangés avec des liquides ioniques de type imidazolium et souvent appelés « bucky gels ». ⁴⁶

L'analyse ATG a confirmé la présence d'une couche de [bmim][PF₆] sur la surface des MWCNTs. La stabilité thermique du ILs supporté est inférieure à celle du ILs pur car les températures de décomposition du [bmim][PF₆] supporté sont de 340 ° C ou 360 ° C, en fonction de l'épaisseur du film, contrairement à la température de décomposition du ILs pur qui est de 425 ° C.

Les composites S-SIL (37%) (S = Al₂O₃, ZrO₂, TiO₂, SiO₂, ZnO, MgO, CA) ont également été analysés par ATG. La Figure 7.6 indique une forte influence du support dans la décomposition thermique du liquide ionique. Ainsi, les composites SiO₂-SIL(37%), MgO-SIL(37%), CA-SIL(37%), ZnO-SIL(37%) et CNTx-SIL(37%) présentent des températures de décomposition du ILs supporté inférieures à celle du [bmim][PF₆] pur. Par contre, Al₂O₃-SIL(37%), TiO₂-SIL (37%) et ZrO₂-SIL (37%) ont une thermostabilité égale ou supérieur que celle observée pour le ILs pur.

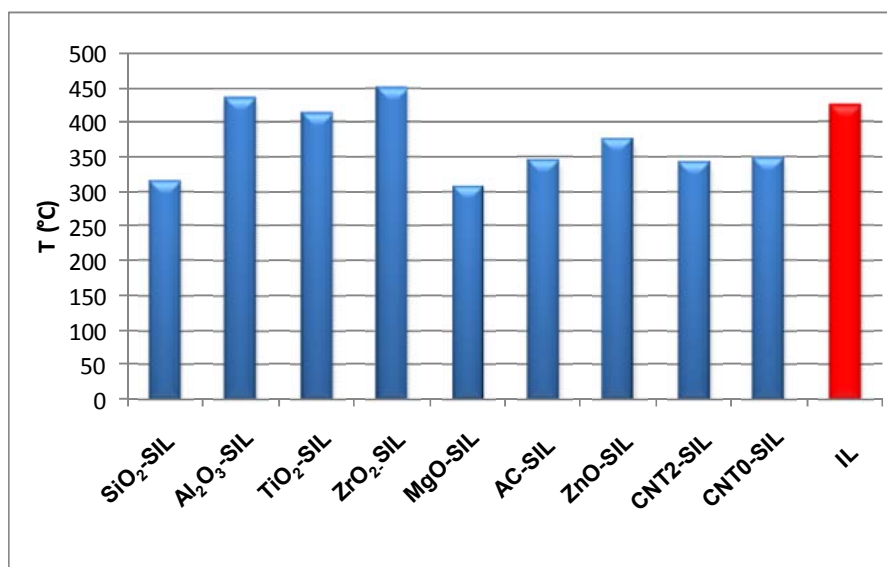


Figure 7.6: Décomposition thermique (analyse ATG) des composites S-SIL (37%), correspondant à la couche de liquide ionique

7.3.4 Etude structurale des interactions entre le support et le liquide ionique

Dans le but d'étudier les interactions des liquides ioniques avec les supports, nous nous sommes intéressés à réaliser une étude structurale comparative entre liquide ionique, SiO₂-SIL et Al₂O₃-SIL, essentiellement par RMN, DSC (calorimètre différentiel à balayage) et DRX.

Les analyses DSC ont montrés des profils complètement différents entre les composites SiO₂-SIL et Al₂O₃-SIL. Le composite Al₂O₃-SIL présente des pics exothermiques et endothermiques proches de ceux observés pour le [bmim][PF₆] pur, tandis que SiO₂-SIL ne présente aucun pic significatif.

Des résultats conformes à ceux du DSC ont été obtenus par DRX. Les analyses enregistrées à -100 °C et à -20 °C montrent des structures polycristallines pour le liquide ionique pur et pour le composite Al₂O₃-SIL. En ce qui concerne SiO₂-SIL, elles montrent des signaux larges pour les deux températures étudiées.

Des analyses RMN à l'état solide ont été effectuées par ¹H MAS NMR, ¹H/¹³C CP MAS NMR, ¹³C{¹H} DP MAS NMR, ¹⁹F MAS NMR, ³¹P{¹H,¹⁹F} MAS NMR, ²⁹Si et ²⁷Al CP MAS NMR. Cet étude révèle une perte de l'ordre structural du liquide ionique lorsqu'il est supporté sur de l'alumine en raison de la mobilité des protons du cation (Figure 7.7), sans montrer aucune interaction avec l'anion ni avec la surface. D'autre part, SiO₂-SIL présente une forte interaction entre le liquide ionique et la silice grâce aux cations imidazolium et aux

anions hexafluorophosphate, vraisemblablement par liaisons d'hydrogène entre la silice, l'anion et le cation.

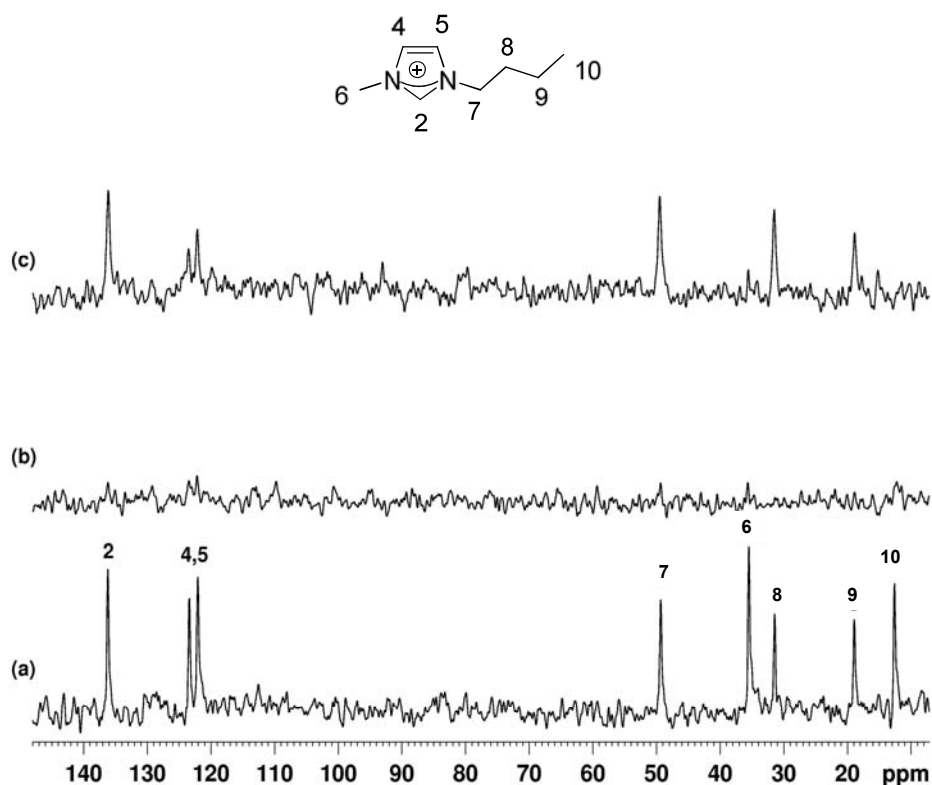
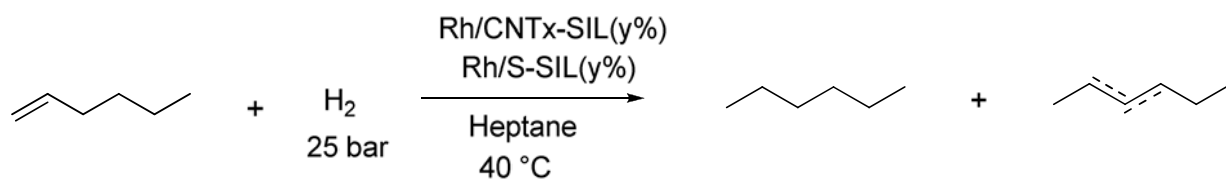


Figure 7.7: Spectres ^{13}C CP/MAS NMR: a) pur [bmim][PF₆], b) Al₂O₃-SIL et c) SiO₂-SIL.

7.4 PHASE LIQUIDE IONIQUE SUPPORTEE : APPLICATION EN CATALYSE

Le comportement de deux systèmes catalytiques différents basés sur la SILPC sur des nanotubes de carbones fonctionnalisés, l'un homogène comportant un complexe organométallique et l'autre hétérogène comportant des nanoparticules de palladium, a été étudié.

Le complexe de rhodium [Rh(nbd)(PPh₃)₂]PF₆ dissous dans le [bmim][PF₆] a été immobilisé pour son application dans l'hydrogénation du 1-hexène (Schéma 7.5).



$x = 0 - 7$, CNT-[C₈N₃OH₁₁]PF₆
 $S = \text{SiO}_2, \text{Al}_2\text{O}_3, \text{ZrO}_2, \text{ZnO}, \text{AC}, \text{MgO}, \text{TiO}_2$
 $y = 20, 37, 55, 64\%$

Schéma 7.5: Rh/SILPC pour l'hydrogénation du 1-hexène.

Dans une première étude, l'influence de la fonctionnalisation sur les performances catalytiques de nanotubes de carbone multi-parois utilisés comme support a été évaluée. Des bonnes conversions ont été observées avec des nanotubes purifiés (TOF = 959 h⁻¹), oxydés (TOF = 662 h⁻¹) et fonctionnalisés (TOF = 959 h⁻¹). Par contre, un forte leaching de la phase liquide ionique a pu être constaté après réaction en absence de fonctionnalisation de surface. En conséquence, la fonctionnalisation améliore la compatibilité entre la surface des nanotubes et le liquide ionique tout en évitant le leaching.

Une étude comparative avec d'autres supports classiques a montré que les nanotubes de carbones fonctionnalisés présentent une activité catalytique deux fois plus importante que la silice (Figure 7.8).

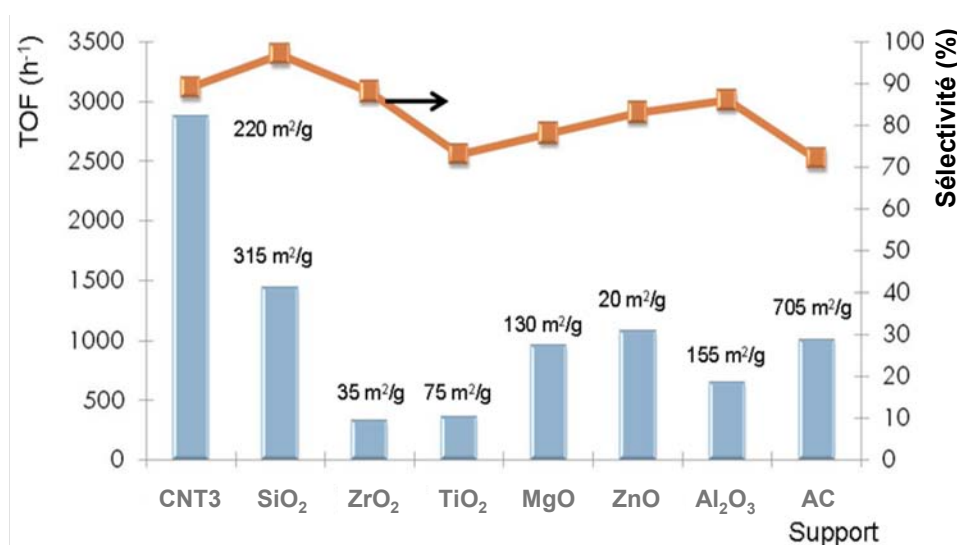


Figure 7.8: Activité et sélectivité du catalyseur de Rh/SILPC sur différents supports pour la réaction d'hydrogénation du 1-hexène. Les valeurs de la surface spécifique sont indiquées pour chaque support.

Le système Rh/CNT2-SIL(55 %) a été recyclé 5 fois sans perte d'activité catalytique.

Des nanoparticules de palladium préformées en liquide ionique ont été utilisées comme phase catalytique supportée sur des nanotubes de carbone fonctionnalisés pour deux réactions différentes: l'hydrogénation et le couplage C-C de Heck.

Le benzylidène cétone (composé carbonyle α,β -insaturé) a été choisi pour étudier l'hydrogénation sélective de la double liaison C=C avec les nanoparticules de palladium supportées (Schéma 7.6)

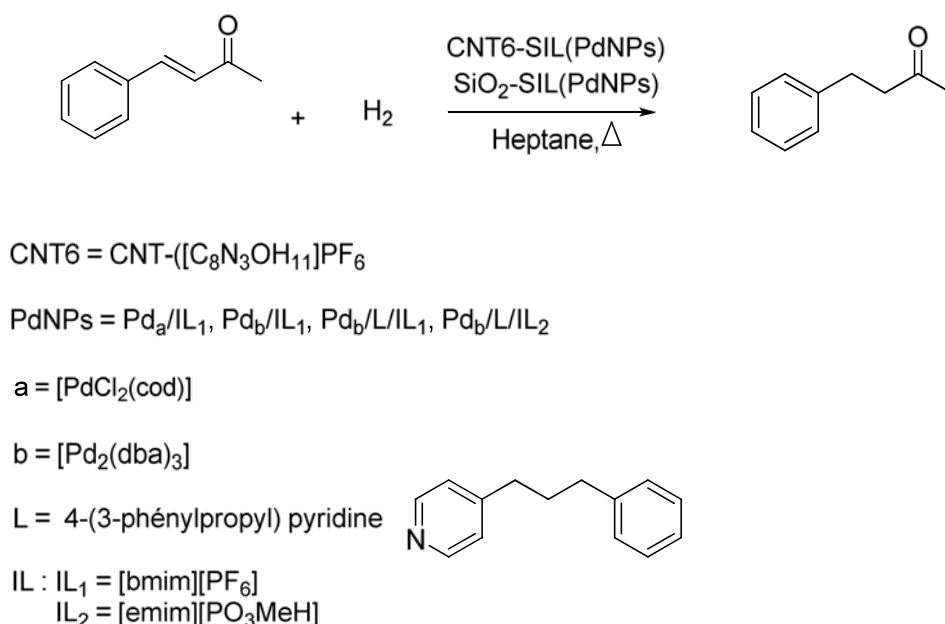


Schéma 7.6: Réaction d'hydrogénation du benzylidène cétone.

La nature des précurseurs du palladium, la présence de ligand comme agent stabilisant, l'influence du liquide ionique et la nature du support sont les principaux paramètres évalués.

De bonnes performances catalytiques ont été obtenues avec les nanoparticules (Pd_b/L/IL₁). La Table 7.2 montre l'influence positive des nanotubes de carbone fonctionnalisés dans les performances catalytiques de ces nanoparticules.

Entrée	Catalyseur	P/S	Conversion (%) ^a	TOF (h ⁻¹) ^b
1	SiO ₂ -SIL(Pd _b /L/IL ₁)	1/313	51	35
2	CNT6-SIL(Pd _b /L/IL ₁)	1/313	76	52

Table 7.2: Influence du support utilisé pour la synthèse du SILPC. Conditions de réaction: 1 ml d'heptane à 30 °C, 20 bar pendant 3 h avec Pd/substrat = 1/313; Pd = 7.59 10⁻⁷ mol, Pd/L = 1/0.3; Substrat = 2.37 10⁻⁴ mol.^a Déterminé par GC. ^bTOF = mole de substrat convertie/(mole de catalyseur x temps (h))

Les nanoparticules de palladium ont été aussi utilisées comme phase catalytique supportée sur MWCNTs fonctionnalisés dans la réaction de Heck entre l'iodobenzène et le méthyl vinyl cétone (Schéma 7.7).

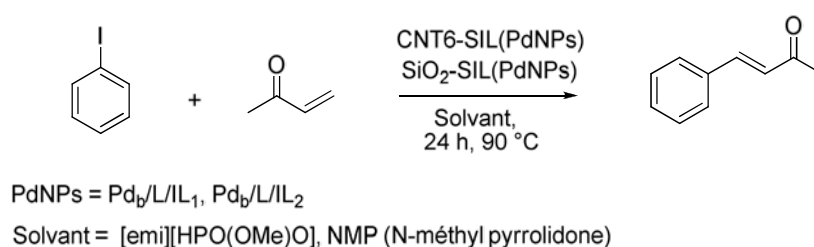


Schéma 7.7: Réaction de couplage de Heck catalysée par des systèmes Pd/SILPC.

Les nanoparticules de palladium (Pd_b/L/IL₂) synthétisées dans le [emim][HPO(OMe)O] ont présenté les meilleures performances catalytiques (Tableau 7.3, entrées 2, 4) par rapport aux nanoparticules synthétisées dans les mêmes conditions mais avec le liquide ionique [bmim][PF₆] (Tableau 7.3, entrées 1, 3). Par rapport aux supports utilisés, les nanotubes de carbone présentent une conversion plus haute que le SiO₂.

Entrée	Catalyseur	Pd/substrat	Temps (h)	Conversion (%) ^a	TOF (h ⁻¹)
1	CNT6-SIL(Pd _b /L/IL ₁)	1/672	24	-	-
2	CNT6-SIL(Pd _b /L/IL ₂)	1/672	24	72	20
3	SiO ₂ -SIL(Pd _b /L/IL ₁)	1/672	24	-	-
4	SiO ₂ -SIL(Pd _b /L/IL ₂)	1/672	24	48	14

Tableau 7.3: Influence du support et du liquide ionique utilisé dans la réaction de Heck. Conditions de réaction: 1 ml d'heptane sous argon avec Pd/Substrat = 1/672; Pd/L=1/0.3; Pd = 2.97 10⁻⁶ mol; substrat = 2 10⁻³ mol, iodobenzène/Na₂CO₃ = 1/2.5.^a Déterminée par GC.

On peut conclure que la structure très ouverte des nanotubes de carbone facilite le transfert et améliore la cinétique de la réaction en évitant le piégeage des catalyseurs à l'intérieur des pores comme cela se produit avec des supports classiques.

7.5 CONCLUSIONS

Au cours de cette étude des catalyseurs en phase liquide ionique supportée sur nanotubes de carbone multiparois ont été développés et employés dans différentes réactions catalytiques.

Des nanotubes de carbone multiparois fonctionnalisés avec des unités ioniques ont été synthétisés et entièrement caractérisés. Le traitement d'activation par oxydation à l'acide nitrique induit la formation de groupement oxygène à la surface, principalement acide carboxylique (CNT1), ouvrant la possibilité de fonctionnalisation supplémentaire.

Pour préparer des catalyseurs en phase liquide ionique supportée homogènes ou hétérogènes, un complexe de rhodium ou des nanoparticules de palladium préformées a été immobilisé dans la phase liquide ionique en constituant la phase catalytiquement active.

Des nanoparticules de palladium ont été synthétisées dans un liquide ionique à partir de précurseurs organométalliques, en absence ou en présence de stabilisant additionnel. L'utilisation du ligand 4 - (3-phénylpropyl) pyridine dans la formation des nanoparticules dans [bmim][PF₆] de [Pd₂(dba)₃], évite la formation d'agrégats conduisant à des nanoparticules bien dispersées. L'utilisation du liquide ionique [emim][HPO(OME)O] combiné avec le ligand confère une stabilisation spéciale.

Un analyse MET de la phase liquide ionique [bmim][PF₆] supportée sur nanotubes de carbone fonctionnalisés (CNT3-SIL) montre une couche de liquide ionique de 3.3 nm d'épaisseur. Des analyses ATG ont signalé un changement dans la thermostabilité de la couche de liquide ionique ainsi que dans celle nanotubes de carbone.

Deux composites SiO₂-SIL et Al₂O₃-SIL ont été choisis pour mener à bien une étude structurelle permettant de mettre en évidence l'influence de la surface sur le film liquide ionique à l'aide de DSC, le RDX et RMN à l'état solide. L'étude RMN utilisant des nanotubes de carbone multi-parois n'était pas faisable en raison de la présence de nanoparticules de fer restants dues au catalyseur synthétique encapsulé dans les tubes. Les résultats de ces analyses suggèrent une forte interaction entre la silice et le [bmim][PF₆].

Le catalyseur en phase liquide ionique supportée a été préparé par immobilisation de la phase catalytiquement active dans le ILs suivie d'une immobilisation sur le support.

Différents chargement en liquide ionique (20, 37, 55 et 64% w/w) ont été utilisés, combinés avec différents degrés de fonctionnalisations. La combinaison appropriée de ces deux paramètres a conduit à obtenir un catalyseur sous forme de poudre et à éviter ainsi la formation de gel (CNT4-SIL (64%)).

Une analyse MET du catalyseur CNT6-SIL (Pd_b/L/IL₂), synthétisé en utilisant des nanoparticules de palladium préformées (Pd_b/L/IL₂) et en les supportant sur CNT6, a révélé la présence effective des nanoparticules de palladium. Un calcul FFT montre les plans cristallographiques du métal palladium fcc et de deux autres plans probablement liés à une forme cristalline du liquide ionique placés autour des nanoparticules.

Rh/SILPC système a été appliqué dans la réaction d'hydrogénation du 1-hexène. L'effet positif de la fonctionnalisation des MWCNTs a été souligné par les excellentes conversions obtenues sans leaching. Une étude comparative avec d'autres Rh/SILPC sur des supports classiques (Al₂O₃, SiO₂, MgO, TiO₂, AC, ZrO₂ et ZnO) a révélé que les MWCNTs fonctionnalisés en tant que support (Rh/CNT3-SIL (37%)) ont une activité catalytique de presque doublée par rapport à celle du gel de silice (2880 et 1425 h⁻¹, respectivement). Ces résultats sont probablement dus à la structure ouverte qui évite les limitations de transfert de masse. Le système Rh/CNT2-SIL(55%) a pu être recyclé sans perte d'activité jusqu'à 5 cycles.

Des nanoparticules de palladium ont été utilisées avec succès dans deux réactions différentes: l'hydrogénation du benzylidène cétone et le couplage C-C de Heck entre le iodobenzène et la méthyl vinyl cétone.

Une plus haute activité a été obtenue dans la réaction d'hydrogénation du benzylidène cétone en utilisant comme phase catalytiquement active Pd_b/L/IL₁ par rapport à celle obtenue avec Pd_b/IL₁ et Pd_a/IL₁. Une étude comparative de l'influence du support en utilisant CNT6-SIL(Pd_b/L/IL₁) et SiO₂-SIL(Pd_b/L/IL₁) comme systèmes supportés a montré les meilleures performances lorsque CNT6 est utilisé.

Le catalyseur CNT6-SIL(Pd_b/L/IL₂) a montré une meilleure activité par rapport à SiO₂-SIL(Pd_b/L/IL₂) dans la réaction de couplage C-C.

-
- ¹ J. Dupont, P.A.Z. Suarez, *Phys. Chem. Chem. Phys.* **2006**, 8, 2441.
- ² P. Wasserscheid, W. Keim, *Angew. Chem. Int. Ed.* **2000**, 39, 3772.
- ³ J.G. Huddleston, H.D. Willauer, R.P. Swatloski, A.E. Visser, R.D. Rogers, *Chem. Commun.* **1998**, 1765.
- ⁴ C.C. Cassol, A.P. Umpierre, G. Ebeling, B. Ferrera, S.S.X. Chiaro, J. Dupont, *Int. J. Mol. Sci.* **2007**, 8, 593.
- ⁵ H. Olivier-Boutbigou, L. Mogna, *J. Mol. Catal. A: Chem.* **2002**, 419, 182.
- ⁶ P.J. Dyson, T.J. Geldbach, (Eds.) *Metal catalyzed reactions in ionic liquids*, Series: *Catalysis by Metal Complexes*, Vol. 9, Springer, Dordrecht **2005**.
- ⁷ J. Dupont, R.F. De Souza, P.A.Z. Suarez, *Chem. Rev.* **2002**, 102, 3667.
- ⁸ T. Welton, *Chem. Rev.* **1999**, 99, 2071.
- ⁹ V.I. Pârvulescu, C. Hardacre, *Chem. Rev.* **2007**, 107, 2615.
- ¹⁰ J. Dupont, *J. Braz. Chem. Soc.* **2004**, 15, 341.
- ¹¹ J. Durand, E. Teuma, M. Gómez, *C.R. Chimie* **2007**, 10, 152.
- ¹² *Electrochemical Aspects of Ionic Liquids*, Hiroyuki Ohno (Ed.), Wiley Interscience: Hoboken, NJ **2005**.
- ¹³ (a) C.F. Poole, *J. Chromatogr. A.* **2004**, 1037, 49; (b) S. Pandey, *Anal. Chim. Act.* **2006**, 556, 38.
- ¹⁴ A.P. de los Ríos, F.J. Hernández-Fernández, F. Tomás-Alonso, J.M. Palacios, D. Gómez, M. Rubio, G. Villora, *J. Membrane Sci.* **2007** 300, 88.
- ¹⁵ J.P. Arhancet, M.E. Davis, J.S. Merola, B.E. Hanson, *Nature*, **1989**, 339, 454
- ¹⁶ A. Riisager, R. Fehrmann, *Ionic Liquids in Synthesis*, 2nd edn., (Eds.: P. Wasserscheid, T. Welton), Wiley-VCH, Weinheim **2008**, Vol. 2, pp 527 – 558.
- ¹⁷ C.P. Mehnert, *Chem. Eur. J.* **2005**, 11, 50.
- ¹⁸ (a) *Science and Application of Nanotubes*, D. Tománek R.J. Enbody, (Eds.), Kluwer Academic/Plenum Publishers, New York, **2000**. (b) J.P. Issi, J.C. Charlier in *The Science and Technology of Carbon Nanotubes*, K. Fukui, K. Tanaka, T. Yamabe, (Eds.), Elsevier, **1999**. (c) M. Monthieux, P. Serp, E. Flahaut, C. Laurent, A. Peigney, M. Razafinimanana, W. Bacsa, J.M. Broto. Introduction to Carbon Nanotubes. In “Springer handbook of nanotechnology” Second revised and extended Edition B. Bhushan (eds.), Springer-Verlag, Heidelberg, Germany, **2007**, 43-112.
- ¹⁹ S. Iijima, *Nature*, **1991**, 354, 56.

-
- ²⁰ A. Thess, R. Lee, P. Nikolaev, H. Dai, P. Petit, J. Robert, C. Xu, Y.H. Lee, S.G. Kim, A.G. Rinzler, D.T. Colbert, G.E. Scuseria, D. Tomanek, J.E. Fischer, R.E. Smalley, *Science* **1996**, 273, 483.
- ²¹ W. Krätschmer, L.D. Lamb, K. Fostiropoulos, D.R. Huffman. *Nature* **1990**, 347, 353.
- ²² P.L. Walker Jr, *J. Phys. Chem.* **1959**, 63, 133.
- ²³ D.H. Robertson, D.W. Brenner, J.W. Mintmire, *Phys. Rev. B* **1992**, 45, 12592.
- ²⁴ T. White, T.N. Todorov, *Nature* **1998**, 393, 240.
- ²⁵ S. Talapatra, A.Z. Zambano, S.E. Weber, A.D. Migone, *Phys. Rev. Lett.* **2000**, 85, 138.
- ²⁶ M. Ouyang, J.L. Huang, C.M. Lieber, *Acc. Chem. Res.* **2002**, 35, 1018.
- ²⁷ A. Hirsch, *Angew. Chem. Int. Ed.* **2002**, 41, 1853.
- ²⁸ C.N.R Rao, A Govindaraj, B.C. Satishkumar. *Chem Commun* **1996**, 1525.
- ²⁹ B. Li, Z. Shi, Y. Lian, Z. Gu, *Chem. Lett.* **2001**, 30, 598.
- ³⁰ F. Pompeo, D.E. Resasco, *Nano Lett.* **2002**, 2, 369.
- ³¹ M.J. Park, J.K. Lee, B.S. Lee, Y.W. Lee, I.S. Choi, S.G. Lee, *Chem. Mater.* **2006**, 18, 1546.
- ³² B. Yu, F. Zhou, G. Liu, Y. Liang, W.T.S. Huck, W.Liu, *Chem. Commun* **2006**, 2356.
- ³³ H. Vu, F. Gonçalves, R. Philippe, E. Lamouroux, M. Corrias, Y. Kihn, D. Plee, P. Kalck and P. Serp, *J. Catal.* **2006**, 240, 18.
- ³⁴ P. Serp, M. Corrias, P. Kalck, *Appl. Catal. A* **2003**, 253, 337.
- ³⁵ M.L. Toebes, J.M.P. van Heeswijk, J.H. Bitter, A. Jos van Dillen, K.P. de Jong, *Carbon* **2004**, 42, 307.
- ³⁶ J. Durand, E. Teuma, F. Malbosc, Y. Kihn, M. Gómez, *Catal. Commun.* **2008**, 9, 273.
- ³⁷ N.T.S. Phan, M. Van Der Sluys, C.W. Jones, *Adv. Synth. Catal.* **2006**, 348, 609.
- ³⁸ J. Durand, E. Teuma, M. Gómez, *Eur. J. Inorg. Chem.* **2008**, 3577.
- ³⁹ F. Fernandez, B. Cordero, J. Durand, G. Muller, F. Malbosc, Y. Kihn, E. Teuma, M. Gomez, *Dalton Trans.* **2007**, 5572.
- ⁴⁰ K.J. Klabunde, H.F. Efnér, T.O. Murdock, R. Ropple, *J. Am. Chem. Soc.* **1976**, 98, 1021.
- ⁴¹ T.O. Murdock, K.J. Klabunde, *J. Org. Chem.* **1976**, 41, 1076.
- ⁴² R.G. Finke, In *Metal nanoparticles: synthesis, characterization, and applications*; Feldheim, D. L., Foss, C. A., (Eds.), Marcel Dekker: New York, **2002**; chap. 2.
- ⁴³ C.W. Scheeren, G. Machado, J. Dupont, P.F.P. Fichtner, S.R. Teixeira, *Inorg. Chem.* **2003**, 42, 4738.
- ⁴⁴ K. Philippot, B. Chaudret, *C.R. Chimie* **2003**, 6, 1019.

⁴⁵ B. Chaudret, C.R. Physique **2005**, 6, 117.

⁴⁶ (a) T. Fukushima, A. Kosaka, Y. Lshimura, T. Yamamoto, T. Takigawa, N. Ishii, T. Aida, Science **2003**, 300, 2072; (b) Y. Zhao, H. Liu, Y. Kou, M. Li, Z. Zhu, Q. Zhuang, Electrochem. Commun. **2007**, 9, 2457.